CONTENTS

Page

SUMMARY . . . 1 1/A14

INTRODUCTION . . . 1 1/A14

SYMBOLS . . . 3 1/B2

ANALYSIS . . . 8 1/B7
  Nonlinear Math Model for Vertical Drops . . . 8 1/B7
    Equations of Motion . . . 10 1/B9
    Pressure, Flow, and Volume Relationship . . . 14 1/B14
    Servovalve Dynamics . . . 16 1/C2
  Linear Math Model for Vertical Drops . . . 18 1/C5
  Energy Considerations . . . 27 1/D1
  Stability Analysis . . . 39 1/E2

ANALYTICAL RESULTS . . . 51 1/F11
  Vertical Drop Cases . . . 53 1/F14
  Land and Roll Cases . . . 53 1/F14

CONTROLLER FUNCTIONAL DESCRIPTION . . . 71 2/B11
  Associated Equipment . . . 71 2/B11
  Interface . . . 71 2/B11
  Performance Characteristics . . . 76 2/C7
  Operating-Mode Determination . . . 76 2/C7
    Landing Mode . . . 76 2/C7
    Takeoff Mode . . . 77 2/C8
  Limit-Force Command Determination . . . 78 2/C9
  Control Law Implementation . . . 78 2/C9
  Controller Design . . . 78 2/C9
    Functional Sections . . . 78 2/C9

CONTENTS (Contd.)

Page

TEST 89 2/E1

Test Fixture 89 2/E1

Test Conditions 93 2/E6

Test Results 93 2/E6

CONCLUSIONS 114 3/A9

APPENDIX

A Microprocessor Program Listing 115 3/A10

B Electronic Controller Detailed Description 131 3/B12

C Test Procedure 142 3/C11

D Oscillograph Recordings 148 3/D4

FIGURES

1 Illustration of variables used in nonlinear simulation of simplified vertical drop case 9 1/B8

2 Free body diagram of airplane mass 11 1/B10

3 Free body diagram of upper shock strut 11 1/B10

4 Free body diagram of lower shock strut 11 1/B10

5 Dynamic response of servovalve, ±10% input signal . . . 17 1/C3

6 Illustration of "Equivalent" system for the linear math model. 22 1/C9

7 Block diagram of linear math model 26 1/C13

8 Comparison of linear model and nonlinear model results, open loop, no compensation, no position feedback 28 1/D2

9 Various energy terms versus time, from the simplified nonlinear vertical drop simulation 33 1/D8

10 Illustration of the variation of limit force versus time and the various phases of operation following impact . . . 35 1/D11

11 Block diagram of linear system without compensation . . 40 1/E3

CONTENTS (Contd.)

Page

FIGURES

12 Nyquist plot of F_{wg}/F_{lim} with force loop opened, no position feedback, no compensation 41 1/E5

13 Electronic compensation network and its characteristics . . 42 1/E7

14 Nyquist plot of F_{wg}/F_{lim} with force loop opened, no position feedback, with compensation 43 1/E9

15 Nyquist plot of F_{wg}/F_{lim} with force loop opened, position loop closed, with compensation 45 1/E12

16 Nyquist plot of X_s/X_c with position loop opened, force loop closed, with compensation 46 1/F1

17 Frequency response of F_{wg}/F_{lim} with force and position loops closed, with compensation 47 1/F3

18 Frequency response of X_s/X_c with force and position loops closed, with compensation 48 1/F5

19 Nyquist plot of F_{wg}/F_{lim} with force loop opened, position loop closed, with compensation. 49 1/F7

20 Nyquist plot of F_{wg}/F_{lim} with force loop opened, position loop closed, with compensation. 50 1/F9

21 Wing/gear force transient, case A 54 1/G1

22 Wing/gear force transient, case B 55 1/G3

23 Strut position transient, case B 56 1/G5

24 Wing/gear force transient, case 1 . . . . 57 1/G7

25 Strut pressures, case 1 . . . . 58 1/G9

26 Strut position transient, case 1 . . . . 59 1/G11

27 Wing/gear force transient, case 2 . . . . 60 1/G13

28 Strut position transient, case 2 . . . . 61 2/A6

29 Wing/gear force transient, case 3 . . . . 63 2/A9

30 Wing/gear force transient, case 4 . . . . 64 2/A11

31 Servovalve flow rate, case A 65 2/A13

32 Servovalve flow rate, case B 66 2/B1

CONTENTS (Contd.)

Page

FIGURES

33 Servovalve flow rate, case 1 . . . . 67 2/B3
34 Servovalve flow rate, case 2 . . . . 68 2/B5
35 Servovalve flow rate, case 3 . . . . 69 2/B7
36 Servovalve flow rate, case 4 . . . . 70 2/B9
37 Input/Output Signal Schematic 72 2/B10
38 Control Law Functional Schematic 79 2/C10
39 Controller Functional Schematic 81 2/D1
40 Basic Functional Requirements 82 2/D3
41 Software Flow Chart 84 2/D6
42 Analog Section Schematic 85 2/D8
43 Analog Section - Front Panel Inputs 87 2/D11
44 Analog Section - Front Panel Outputs 88 2/D13
45 S-1C Test Fixture, Landing Gear Installed (View 1) . . . 90 2/E2
46 S-1C Test Fixture, Landing Gear Installed (View 2) . . . 91 2/E3
47 Net Force, Conditions 1, 4 (From W/G Accel #1) 95 2/E9
48 Net Force, Conditions 2, 5 (From W/G Accel #1) 96 2/E11
49 Net Force, Conditions 3, 6 (From W/G Accel #1) 97 2/E13
50 Net Force, Conditions 7, 10 (From W/G Accel #1) 98 2/F1
51 Net Force, Conditions 8, 11 (From W/G Accel #1) 99 2/F3
52 Net Force, Conditions 9, 12 (From W/G Accel #1) 100 2/F5
53 Gear Hydraulic Pressure, Conditions 1, 4 . . . . 101 2/F7
54 Gear Hydraulic Pressure, Conditions 2, 5 . . . . 102 2/F9
55 Gear Hydraulic Pressure, Conditions 3, 6 . . . . 103 2/F11
56 Gear Hydraulic Pressure, Conditions 7, 10 . . . . 104 2/F12
57 Gear Hydraulic Pressure, Conditions 8, 11 . . . . 105 2/G1
58 Gear Hydraulic Pressure, Conditions 9, 12 . . . . 106 2/G3

CONTENTS (Contd.)

Page

FIGURES

59 Strut Deflection, Conditions 1, 4 . . . . 107 2/G5

60 Strut Deflection, Conditions 2, 5 . . . . 108 2/G7

61 Strut Deflection, Conditions 3, 6 . . . . 109 2/G9

62 Strut Deflection, Conditions 7, 10 . . . . 110 2/G11

63 Strut Deflection, Conditions 8, 11 . . . . 111 2/G13

64 Strut Deflection, Conditions 9, 12 . . . . 112 3/A6

TABLES

I SUMMARY OF ACTIVE CONTROL LANDING CASES SIMULATED ON THE COMPUTER 52 1/F12

II PRIMARY INPUT SIGNAL SPECIFICATIONS 73 2/C1

III SECONDARY INPUT SPECIFICATIONS 74 2/C3

IV OUTPUT SPECIFICATIONS 75 2/C5

V CONTROL LAW TRANSFER FUNCTIONS 80 2/C12

VI PEAK FORCES AND PERCENTAGE REDUCTION 94 2/E7

REFERENCES 161 3/F1

N 15 1979

NASA Contractor Report 3113

ORIGINAL

COMPLETED

An Electronic Control for an Electrohydraulic Active Control Aircraft Landing Gear

MICROFILMED FROM
BEST AVAILABLE COPY

Irving Ross and Ralph Edson

CONTRACT NAS1-14459
APRIL 1979

NASA

170

NASA Contractor Report 3113

An Electronic Control for an Electrohydraulic Active Control Aircraft Landing Gear

Irving Ross and Ralph Edson
Hydraulic Research Textron
Valencia, California

Prepared for
Langley Research Center
under Contract NAS1-14459

National Aeronautics
and Space Administration

Scientific and Technical
Information Office

1979

Blank Page

CONTENTS

Page

SUMMARY 1

INTRODUCTION 1

SYMBOLS 3

ANALYSIS 8
  Nonlinear Math Model for Vertical Drops 8
    Equations of Motion 10
    Pressure, Flow, and Volume Relationship 14
    Servovalve Dynamics 16
  Linear Math Model for Vertical Drops 18
  Energy Considerations 27
  Stability Analysis 39

ANALYTICAL RESULTS 51
  Vertical Drop Cases 53
  Land and Roll Cases 53

CONTROLLER FUNCTIONAL DESCRIPTION 71
  Associated Equipment 71
  Interface 71
  Performance Characteristics 76
  Operating-Mode Determination 76
    Landing Mode 76
    Takeoff Mode 77
  Limit-Force Command Determination 78
  Control Law Implementation 78
  Controller Design 78
    Functional Sections 78

Page

TEST 89
Test Fixture 89
Test Conditions 93
Test Results 93

CONCLUSIONS 114

APPENDIX

A Microprocessor Program Listing 115
B Electronic Controller Detailed Description 131
C Test Procedure 142
D Oscillograph Recordings 148

FIGURES

1 Illustration of variables used in nonlinear simulation of simplified vertical drop case 9
2 Free body diagram of airplane mass 11
3 Free body diagram of upper shock strut 11
4 Free body diagram of lower shock strut 11
5 Dynamic response of servovalve, ±10% input signal . . . 17
6 Illustration of "Equivalent" system for the linear math model. 22
7 Block diagram of linear math model 26
8 Comparison of linear model and nonlinear model results, open loop, no compensation, no position feedback 28
9 Various energy terms versus time, from the simplified nonlinear vertical drop simulation 33
10 Illustration of the variation of limit force versus time and the various phases of operation following impact . . . 35
11 Block diagram of linear system without compensation . . 40

CONTENTS (Contd.)

Page

FIGURES

12 Nyquist plot of F_{wg}/F_{lim} with force loop opened, no position feedback, no compensation 41

13 Electronic compensation network and its characteristics . . 42

14 Nyquist plot of F_{wg}/F_{lim} with force loop opened, no position feedback, with compensation 43

15 Nyquist plot of F_{wg}/F_{lim} with force loop opened, position loop closed, with compensation 45

16 Nyquist plot of X_s/X_c with position loop opened, force loop closed, with compensation 46

17 Frequency response of F_{wg}/F_{lim} with force and position loops closed, with compensation 47

18 Frequency response of X_s/X_c with force and position loops closed, with compensation 48

19 Nyquist plot of F_{wg}/F_{lim} with force loop opened, position loop closed, with compensation. 49

20 Nyquist plot of F_{wg}/F_{lim} with force loop opened, position loop closed, with compensation. 50

21 Wing/gear force transient, case A 54

22 Wing/gear force transient, case B 55

23 Strut position transient, case B 56

24 Wing/gear force transient, case 1 57

25 Strut pressures, case 1 58

26 Strut position transient, case 1 59

27 Wing/gear force transient, case 2 60

28 Strut position transient, case 2 61

29 Wing/gear force transient, case 3 63

30 Wing/gear force transient, case 4 64

31 Servovalve flow rate, case A 65

32 Servovalve flow rate, case B 66

CONTENTS (Contd.)

Page

FIGURES

33 Servovalve flow rate, case 1 67

34 Servovalve flow rate, case 2 68

35 Servovalve flow rate, case 3 69

36 Servovalve flow rate, case 4 70

37 Input/Output Signal Schematic 72

38 Control Law Functional Schematic 79

39 Controller Functional Schematic 81

40 Basic Functional Requirements 82

41 Software Flow Chart 84

42 Analog Section Schematic 85

43 Analog Section - Front Panel Inputs 87

44 Analog Section - Front Panel Outputs 88

45 S-1C Test Fixture, Landing Gear Installed (View 1) . . . 90

46 S-1C Test Fixture, Landing Gear Installed (View 2) . . . 91

47 Net Force, Conditions 1, 4 (From W/G Accel #1) 95

48 Net Force, Conditions 2, 5 (From W/G Accel #1) 96

49 Net Force, Conditions 3, 6 (From W/G Accel #1) 97

50 Net Force, Conditions 7, 10 (From W/G Accel #1) 98

51 Net Force, Conditions 8, 11 (From W/G Accel #1) 99

52 Net Force, Conditions 9, 12 (From W/G Accel #1) 100

53 Gear Hydraulic Pressure, Conditions 1, 4 101

54 Gear Hydraulic Pressure, Conditions 2, 5 102

55 Gear Hydraulic Pressure, Conditions 3, 6 103

56 Gear Hydraulic Pressure, Conditions 7, 10 104

57 Gear Hydraulic Pressure, Conditions 8, 11 105

58 Gear Hydraulic Pressure, Conditions 9, 12 106

CONTENTS (Contd.)

Page

FIGURES

59 Strut Deflection, Conditions 1, 4 107
60 Strut Deflection, Conditions 2, 5 108
61 Strut Deflection, Conditions 3, 6 109
62 Strut Deflection, Conditions 7, 10 110
63 Strut Deflection, Conditions 8, 11 111
64 Strut Deflection, Conditions 9, 12 112

TABLES

I SUMMARY OF ACTIVE CONTROL LANDING CASES SIMULATED ON THE COMPUTER 52
II PRIMARY INPUT SIGNAL SPECIFICATIONS 73
III SECONDARY INPUT SPECIFICATIONS 74
IV OUTPUT SPECIFICATIONS 75
V CONTROL LAW TRANSFER FUNCTIONS. 80
VI PEAK FORCES AND PERCENTAGE REDUCTION. 94

REFERENCES. 161

SUMMARY

The electronic controller described in this report, together with an active control landing gear, are found to provide significant reductions in forces sustained by an aircraft during takeoff, landing impact and rollout. The degree of force reduction increases with the sink rate. These results were obtained analytically and confirmed experimentally by actual drop tests of a landing gear under active control.

The electronic controller continuously compares the kinetic energy of the aircraft with the work potential of the gear until the work potential exceeds the kinetic energy. The wing/gear interface force present at this condition becomes the command force to a servo loop which maintains the wing/gear interface force at this level by providing a signal to an electrohydraulic servovalve to port flow into or out of the landing gear.

INTRODUCTION

Hydraulic Research (HR) was retained under NASA Contract NAS 1-14459 to design, develop, fabricate and test an electronic controller for an electrohydraulic active control landing gear, as described in Reference 1. The primary function of the active control landing gear is to minimize the force to which the aircraft is subjected as a result of landing impact and rollout, takeoffs and taxi operations. As shown in Ref. 1, the resultant decrease in applied loads could be very beneficial in reducing structural fatigue design problems and increasing ride comfort for passengers and crew. The work was divided into two major phases: Phase 1 for the analytical development and design of the controller; and, Phase 2 for the fabrication and testing. This report summarizes the effort of both phases and provides the rationale for the controller design selected.

Phase 1 included the development and use of digital computer programs which simulated the dynamics of the landing gear/controller system. A nonlinear dynamic model and a simplified linear model for vertical drops were developed by HR and used extensively in the analysis. In addition, a computer program developed by NASA, which included aerodynamic simulation and landing gear dynamics, was supplied to HR in support of the program. The computer program was modified by HR to include the dynamics of the electrohydraulic servovalve and this program was incorporated into the study. The landing gear parameters, as described in the NASA computer program, were used as the basis for all analyses described herein. During this phase, the controller design was also developed. This design included analog circuitry for the control laws, compensation, summations and the signal to the servovalve driver while a digital microprocessor was used for the nonlinear computations and decision making.

During Phase 2, the controller, as defined in Phase 1, was fabricated and tested by actual drop tests of the gear.

SYMBOLS

A_o	area of orifice in shock strut orifice plate, 0.0000786 m^2 (0.1219 in^2)
A_1	shock strut hydraulic area (piston area), 0.00317 m^2 (4.909 in^2)
A_2	shock strut pneumatic area (cylinder area), 0.00535 m^2 (8.286 in^2)
A_3	annular area in shock strut between piston and cylinder walls, 0.00151 m^2 (2.34 in^2)
C_d	discharge coefficient for active control servovalve orifice, 0.62
C_{do}	discharge coefficient for shock strut orifice, 0.90
C_o	orifice coefficient for shock strut orifice - $C_{do} A_o \sqrt{2g_c/\rho}$, 3.45 (10^{-6}) $m^4 \, sec^{-1} \cdot N^{-1/2}$ (17.51 $in^3/sec/\sqrt{lb/in^2}$)
CP	linearized orifice coefficient for active control servovalve $= -\partial Q_{sv}/\partial P_1$ $= 3.16 \, (10^{-11}) \, m^5 \cdot N^{-1} \cdot sec^{-1}$ (0.01334 $in^3/sec/lb/in^2$)
CP_o	linearized orifice coefficient for shock strut orifice $= \partial Q_o/\partial P_1$ $= C_o/(2\sqrt{P_1 - P_2})$, $m^5 \cdot N^{-1} \cdot sec^{-1}$ ($in^3/sec/lb/in^2$)
CQ	linearized orifice coefficient for active control servovalve $= \partial Q_{sv}/\partial X_{sv}$ $= C_{sv} \sqrt{(P_S + P_R)/2}$, 8.61 m^2/sec (13 340 $\cdot$ $in^3/sec/in$)
C_{sv}	orifice coefficient for active control servovalve $= C_d W_{sv} \sqrt{2g_c/\rho}$, 0.00268 $m^3 \cdot sec^{-1} \cdot lb^{-1/2}$ (344.4 $in^3/sec/\sqrt{lb/in^2}$)
f	Coulomb friction between shock strut piston and cylinder, N (lb)
F_a	vertical force exerted on shock strut by the runway surface, N (lb)
F_{li}	impact phase limit force, N (lb)
F_{lim}	limit force, N (lb)
F_s	shock strut force, N (lb)
F_{wg}	wing/gear interface force, N (lb)

SYMBOLS (Continued)

g	acceleration due to gravity, 9.80 m/sec^2 (386 · in/sec^2)
g_c	gravitational acceleration constant, 1 kg · m · N^{-1} · sec^{-2} (12 slug · in · lb^{-1} · sec^{-2})
i_1	input signal to electronic compensation networks, A
i_2	output signal from electronic compensation networks, or input signal to active control servovalve, A ($\pm$0.040 A maximum)
K_a	amplifier gain in active control loop, 0.000040 A/V
K_f	position feedback gain in strut position control loop, 196.9 V/m (5.0 V/in)
K_{FDGE}	fraction of total strut stroke assumed available when computing impact phase force from equation 37
K_{sv}	position gain of servovalve in active control loop, 0.0635 m/A (2.50 in/A)
K_t	effective spring rate of tire, 245 000 · N/m (1400 lb/in)
K_x	gain in strut position control loop, 1.0 m/m (1.0 in/in)
L	total life force, N (lb)
M	mass of airplane per gear, 1456 kg (99.8 slugs)
M_C	mass of upper portion of landing gear (cylinder plus orifice plate attachment, kg (slug)
M_L	mass of lower portion of landing gear (piston plus tire), 32.1 kg (2.20 slugs)
M_U	upper mass, 1456 kg (99.8 slugs)
PE_t	potential energy stored in tire due to compression, N· m (ft· lb)
P_S	hydraulic supply pressure, 2.07 (10^7) N/m^2 (3000 lb/in^2)
P_R	hydraulic return pressure, 0.0 N/m^2 (0.0 lb/in^2)

SYMBOLS (Continued)

PROM	programmable read only memory
P_1	hydraulic pressure in shock strut piston, N/m^2 (lb/in^2)
P_2	pneumatic pressure in shock strut cylinder, N/m^2 (lb/in^2)
P_3	pressure in volume between walls of shock strut piston and cylinder, N/m^2 (lb/in^2)
Q_O	flow rate through shock strut orifice from piston to cylinder, m^3/sec (in^3/sec)
Q_{sv}	flow rate from active control servovalve to shock strut piston, linear mode, m^3/sec (in^3/sec)
Q_{sv_1}	flow rate through active control servovalve from supply pressure to the shock strut piston, m^3/sec (in^3/sec)
Q_{sv_2}	flow rate through active control servovalve from shock strut piston to return pressure, m^3/sec (in^3/sec)
RAM	random access memory
R_s	the slope of the limit force with respect to time during transition phase, 137 900 N/sec (31 000 lb/sec)
s	LaPlace operator, sec^{-1}
t	time, sec
V	velocity
V_1	hydraulic volume in shock strut piston and lines up to the active control servovalve, 0.00426 m^3 (260.0 in^3) for fully extended strut
V_2	pneumatic volume, 0.000624 m^3 (38.1 in^3) for fully extended strut
V_3	volume between shock strut piston and cylinder, 0.0 m^3 (0.0 in^3) for fully extended strut
Wsv	window width of orifices on third stage spool of active control servovalve, 0.0884 m (3.48 in)

SYMBOLS (Continued)

X	displacement, m (in)
X_c	commanded position of shock strut, 0.1016 m (4.0 in)
β	bulk modulus of hydraulic fluid, 6.89 (10^8) N/m^2 ($1 \cdot 10^5$ lb/in^2)
γ	ratio of specific heat of gas at constant pressure to that at constant volume, 1.1
ρ	mass density of hydraulic fluid, 838 kg/m^3 (0.000941 slugs/in^3)
τ_f	time constant in strut position feedback loop, 0.10 sec
τ_1	time constant in electronic compensation network, 0.0281 sec
τ_2	time constant in electronic compensation network, 0.0141 sec
τ_3	time constant in electronic compensation network, 0.0010 sec
τ_4	time constant in electronic compensation network, 0.0001 sec
ω_c	corner frequency in active control servovalve transfer function, 1263 sec^{-1}
ω_{sv}	natural frequency in active control servovalve transfer function, 655.5 sec^{-1}
ω_1	natural frequency in electronic compensation network, 251.3 sec^{-1}
ζ_{sv}	damping coefficient in active control servovalve transfer function, 0.436
ζ_1	damping coefficient in electronic compensation network, 5.10
ζ_2	damping coefficient in electronic compensation network, 0.10

SYMBOLS (Continued)

Subscripts:

a	lower mass of shock strut or axle
g	ground
i	initial conditions before impact
im	impact phase
L	lower mass
max	maximum value
min	minimum value
r	rollout phase
s	shock strut relative motion of the lower mass (piston) with respect to the upper mass (cylinder)
sv	servovalve
tr	transition phase
U	upper mass
wg	wing/gear interface

Miscellaneous:

d( )	indicates the differential of a variable
$\Delta(\ )$	indicates difference or change in a variable
$(\dot{\ }),(\ddot{\ }),(\dddot{\ })$	dots indicate differentiation with respect to time

ANALYSIS

Nonlinear Math Model for Vertical Drops

A simplified nonlinear dynamic model of an active control landing gear for vertical drops without aerodynamics and airplane dynamics was developed. The airplane mass is represented simply as a point mass located on top of the landing gear. This model proved to be of great value in this project for various reasons. First, it enhanced understanding of the basic equations of motion of the landing gear and the dynamic characteristics. This was very useful in the further development of an even more simplified linearized dynamic model, which was used extensively in the development of the electronic compensation networks that are required for stability. The linear model and its application are discussed in later sections. Secondly, it often was desirable to study the dynamic operation of the system without the complicating influences of the airplane dynamics, and the simplified nonlinear model provided a good tool to do this. Also, by neglecting airplane dynamics, the size of the computer simulation is greatly reduced and runs can be made in less computational time. Finally, the simplified model was used as a check with the more general computer program supplied by NASA, which required many programming changes in its application to this study.

Figure 1 shows a schematic of the simplified vertical drop case along with some of the variables used in modeling the system. The system basically consists of (1) an upper mass M_U, which is the mass M (per gear) of the airplane plus the mass M_C of the upper portion of the landing gear (i.e., the cylinder plus the orifice plate attachment), (2) a lower mass M_L, which consists of the tire mass plus the mass of the lower portion of the landing gear (i.e., the piston), (3) a three-way servovalve that ports fluid in the piston chamber to either supply or return pressure, and (4) an electronic controller. Note that the tire dynamics are simulated as a mass and linear

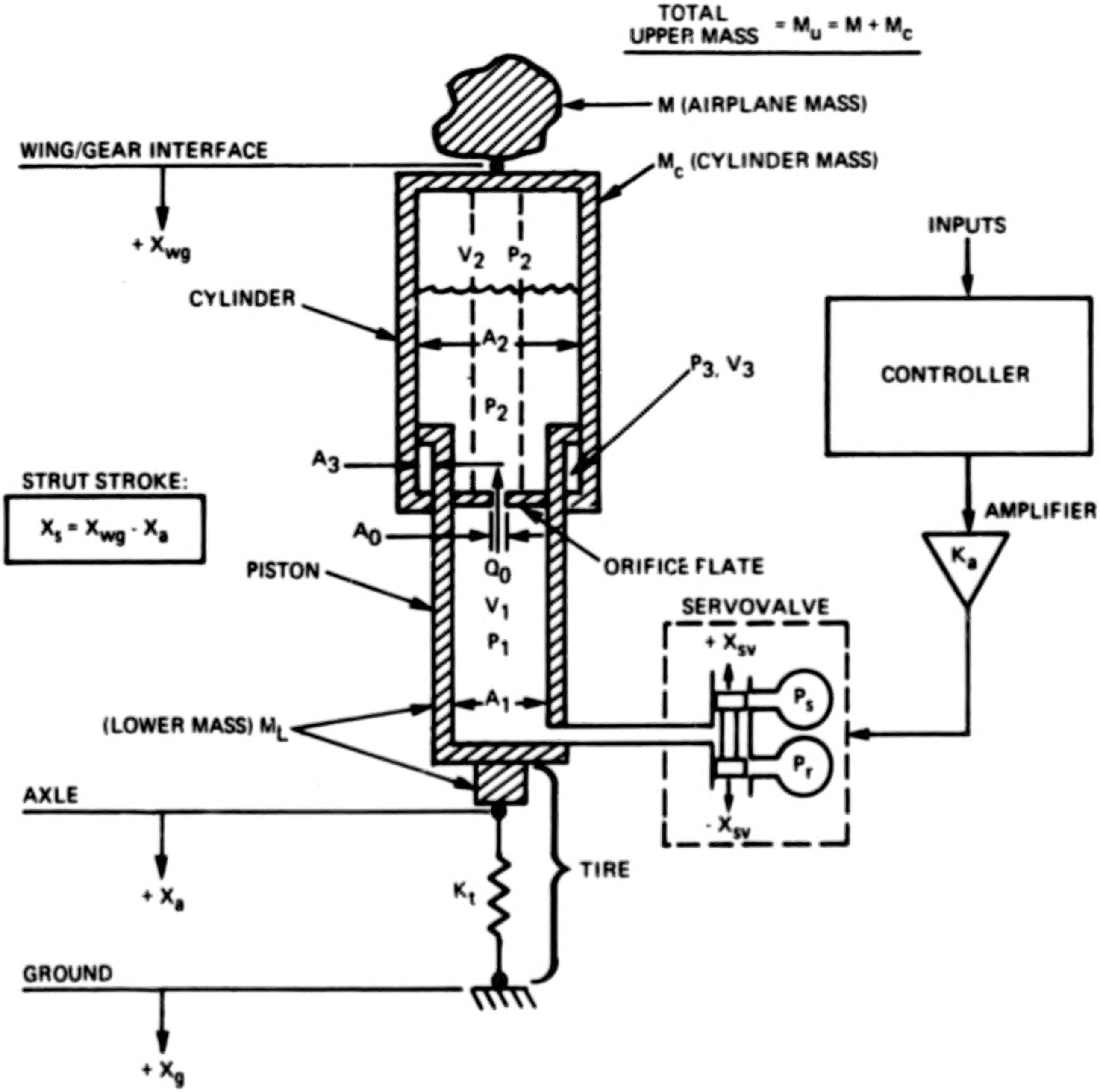
TOTAL UPPER MASS = $M_u = M + M_c$
M (AIRPLANE MASS)
WING/GEAR INTERFACE
M_c (CYLINDER MASS)
$+X_{wg}$
INPUTS
V_2 P_2
CYLINDER
A_2
P_3, V_3
CONTROLLER
P_2
A_3
STRUT STROKE:
$X_s = X_{wg} - X_a$
AMPLIFIER
A_0
K_a
PISTON
Q_0
ORIFICE PLATE
V_1
SERVOVALVE
P_1
$+X_{sv}$
P_s
A_1
(LOWER MASS) M_L
P_r
AXLE
$-X_{sv}$
TIRE
$+X_a$
K_t
GROUND
$+X_g$

Figure 1. - Illustration of variables used in nonlinear simulation of simplified vertical drop case.

spring K_t. The controller dynamics are presented later and will not be repeated here. Suffice it to say that at each instant in time the controller processes the input signals to provide a current to the servovalve.

Equations of Motion

The equations of motion of the landing gear in the vertical direction will now be derived, with down being defined as the positive direction. The two independent masses M_U and M_L give rise to two degrees of freedom, X_{wg} and X_a (See Figure 1). The final results, however, will be expressed in terms of the displacement variables X_{wg} and X_s, where X_s is the shock strut stroke, which ranges from zero for a fully extended strut to the maximum value for a fully contracted strut. The variable X_s is equal to $(X_{wg}-X_a)$.

Referring to Figure 2, a force balance on the airplane mass gives

$$M\ddot{X}_{wg} = Mg - L - F_s = -F_{wg} \qquad \ldots (1)$$

where F_s is the "shock strut force" and F_{wg} is the "wing gear interface force".

Referring to Figure 3, a force balance on the upper portion of the shock strut, which is assumed to be rigidly connected to the airplane mass, gives

$$M_c \ddot{X}_{wg} = M_c g + F_s - P_2A_2 + P_2(A_1-A_o) - P_1(A_1-A_o) + P_3A_3 \mp f$$

or

$$F_s = M_c \ddot{X}_{wg} - M_c g + (P_1-P_2)(A_1-A_o) + P_2A_2 - P_3A_3 \pm f \qquad \ldots (2)$$

Referring to Figure 4, a force balance on the lower portion of the shock strut, which includes the wheel and tire mass, gives

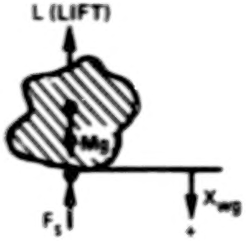
L (LIFT)
Mg
F_s
X_{wg}
+

Figure 2. - Free body diagram of airplane mass

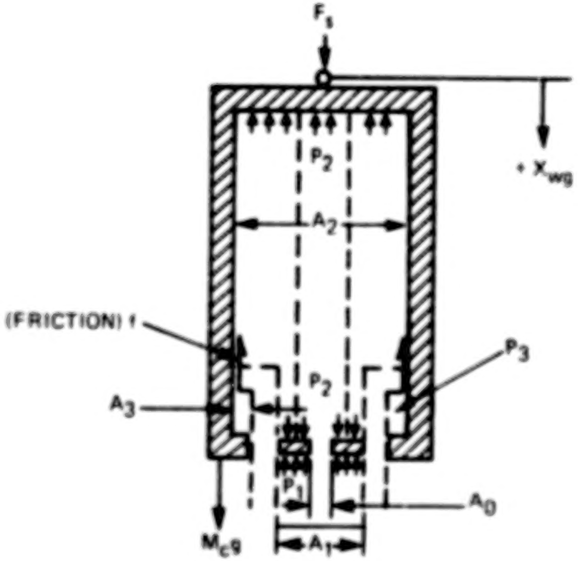
F_s
P_2
$+X_{wg}$
A_2
(FRICTION) f
P_3
A_3
P_2
P_1
A_0
M_cg
A_1

Figure 3. - Free body diagram of upper shock strut

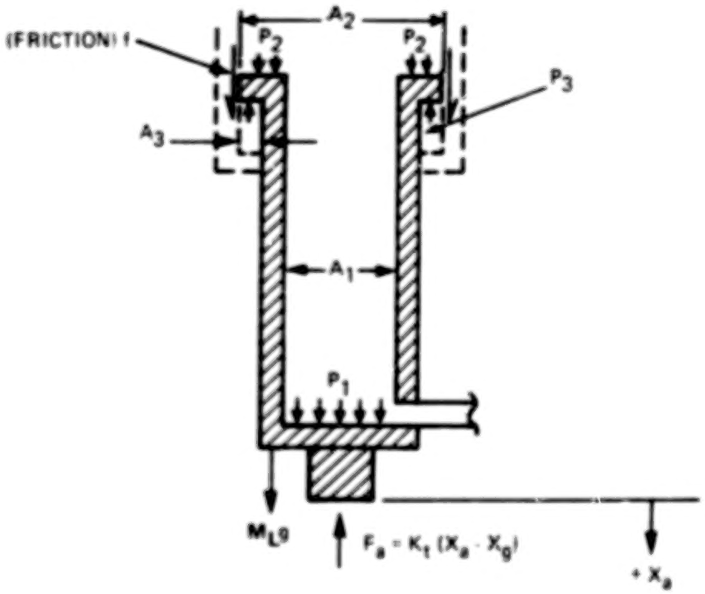
A_2
(FRICTION) f
P_2
P_2
P_3
A_3
A_1
P_1
M_Lg
$F_a = K_t (X_a - X_g)$
$+X_a$

Figure 4. - Free body diagram of lower shock strut

$$M_L\ddot{X}_a = M_Lg + P_2(A_2-A_1) + P_1A_1 - P_3A_3 - F_a \pm f \qquad \ldots (3)$$

substituting $(X_{wg}-X_s)$ for X_a

$$\left.\begin{aligned} M_L(\ddot{X}_{wg} - \ddot{X}_s) &= M_Lg + (P_1-P_2)A_1 + P_2A_2 - P_3A_3 - F_a \pm f \\ \text{where } F_a &= \begin{cases} K_t(X_{wg} - X_s - X_g) & \text{for } X_{wg} - X_s > X_g \\ 0 & \text{for } X_{wg} - X_s \leq X_g \end{cases} \end{aligned}\right\} \qquad \ldots (4)$$

Note that the tire force F_a is zero when the tire is not in contact with the runway surface.

Equations were developed for: (1) the case where the piston is in motion relative to the cylinder, or $V_s \neq 0$; and (2) the case where the piston is not in motion relative to the cylinder due to Coulomb stiction between the two, or $V_s = 0$. For the first case, the Coulomb friction f is simply the value of running friction that exists. But for the second case, the Coulomb friction is actually a stiction force that can vary over a range of absolute values from zero up to the breakaway friction value. Transition from case 1 to case 2 will occur whenever the relative velocity is zero or passes through zero throughout the digital integration process. Transition from case 2 to case 1 will occur whenever the absolute value of the friction force f exceeds the known breakaway friction value. The following equations express these relationships.

First, for the case when $V_s \neq 0$, equations 1 and 2 are combined to eliminate F_s.

$$M_u\ddot{X}_{wg} = M_ug - L - (P_1-P_2)(A_1-A_o) - P_2A_2 + P_3A_3 \mp f \qquad \ldots (5)$$

Substituting equation 5 for $\ddot{X}_{wg}$ into equation 4

$$\frac{M_L}{M_u}[M_u g - L - (P_1 - P_2)(A_1 - A_o) - P_2A_2 + P_3A_3 \mp f] - M_L\ddot{X}_s$$

$$= M_L g + (P_1 - P_2)A_1 + P_2A_2 - P_3A_3 - F_a \pm f$$

Solving for $\ddot{X}_s$

$$M_L\ddot{X}_s = \frac{M_L}{M_u}[(M_u + M_L)g - L] + (1 + \frac{M_L}{M_u})[-M_L g - (P_1 - P_2)A_1 - P_2A_2 + P_3A_3]$$

$$+ \frac{M_L}{M_u}(P_1 - P_2)A_o + F_a \mp (1 + \frac{M_L}{M_u})f$$

or

$$M_L\ddot{X}_s = (1 + \frac{M_L}{M_u})[\text{FORCE} \mp f] \qquad \ldots(6)$$

$$\text{FORCE} = \frac{\frac{M_L}{M_u}[(M_u + M_L)g - L] + (1 + \frac{M_L}{M_u})[-M_L g - (P_1 - P_2)A_1 - P_2A_2 + P_3A_3] + \frac{M_L}{M_u}(P_1 - P_2)A_o + F_a}{1 + \frac{M_L}{M_u}}$$

Equations 5 and 6 constitute the two inertial equations of motion when $V_s \neq 0$.

Next, for the case when $V_s = 0$, equations 4 and 5 are totaled to get

$$(M_u + M_L)\ddot{X}_{wg} = (M_u + M_L)g - L + (P_1 - P_2)A_o - F_a \qquad \ldots(7)$$

$$\ddot{X}_s = 0 \qquad \ldots(8)$$

Equations 7 and 8 are the two inertial equations of motion when $V_s = 0$. However, an expression must be derived to tell when the two masses break away from one another; i.e., when the break away stiction will be overcome causing relative motion between them. This required solving for the variable friction force f. Substituting equation 5 for $\ddot{X}_{wg}$ into equation 4

$$\frac{M_L}{M_u}\left[M_u\,g - L - (P_1 - P_2)(A_1 - A_o) - P_2A_2 + P_3A_3 \mp f\right]$$

$$= M_Lg + (P_1 - P_2)\,A_1 + P_2A_2 - P_3A_3 - F_a \pm f$$

Solving for f, gives

$$\pm f = \frac{\frac{M_L}{M_u}\left[(M_u + M_L)\,g - L\right] + \left(1 + \frac{M_L}{M_u}\right)\left[-M_Lg - (P_1 - P_2)\,A_1 - P_2A_2 + P_3A_3\right] + \frac{M_L}{M_u}\,(P_1 - P_2)\,A_o + F_a}{1 + \frac{M_L}{M_u}} \qquad \ldots(9)$$

If the value of f as calculated by equation 9 exceeds the breakaway stiction, then relative motion will result.

Pressure, Flow, and Volume Relationship

Referring to Figure 1, conservation of mass applied to the hydraulic fluid in volume V_1 gives

$$\frac{V_1}{\beta}\,\dot{P}_1 = A_1\,\dot{X}_s - Q_o + Q_{sv1} - Q_{sv2} \qquad \ldots(10)$$

where

$$Q_o = \begin{cases} A_o C_{do}\sqrt{\frac{2 g_c}{\rho}(P_1 - P_2)} & \text{for } P_1 > P_2 \\ -A_o C_{do}\sqrt{\frac{2 g_c}{\rho}(P_2 - P_1)} & \text{for } P_2 > P_1 \end{cases}$$

$$V_1 = V_{1_i} - A_1 X_s$$

The parameters Q_{sv1} and Q_{sv2} are the servovalve flows from supply pressure to P_1 and from P_1 to return pressure, respectively, and are a function of the spool displacement and valve geometry. These flows are calculated in a subroutine titled FLOZE2 in the nonlinear simulations. Note also that equation 10 considers the effect of fluid compressibility, which gives rise to the first derivative of pressure term.

The pressure/volume relationship for the pneumatic volume V_2 is

$$P_2 = P_{2_i} \left(\frac{V_{2_i}}{V_2}\right)^{\gamma} \qquad \ldots(11)$$

where

$$V_2 = V_{2_i} - (A_2 - A_1) X_s - V_{cum} + (V_3 - V_{3_i})$$

$V_{cum} = \Sigma (Q_o \Delta t) =$ the cumulative fluid flow through the orifice from V_1 to V_2

$$V_3 = V_{3_i} + A_3 X_s$$

The initial values of the pressure and volume variables referred to in the above equations are for the fully extended strut just prior to impact.

Servovalve Dynamics

The dynamic characteristics of the NASA-selected three-stage high response servovalve were supplied to HR by NASA. A mathematical representation of the servovalve dynamics was derived by the following procedure. The small signal frequency response characteristics obtained from NASA are shown reproduced in Figure 5 for reference. Amplitude and phase angle data at several discrete frequencies over the range of interest were taken from these curves and input to an HR-developed computer program that solves for an approximate linear transfer function by the method of least squares. The resultant transfer function is

$$\frac{X_{sv}}{i_2} = \frac{K_{sv}}{\left(\frac{s^2}{\omega^2_{sv}} + \frac{2\zeta_{sv}}{\omega_{sv}} s + 1\right)\left(\frac{s}{\omega_c} + 1\right)} \qquad \ldots(12)$$

where the values of the constants K_{sv}, ω_{sv}, ω_c, and ζ_{sv} are given in the SYMBOLS section and i_2 is input current and X_{sv} is output displacement of the third stage spool. For the nonlinear simulation this transfer function is represented in differential equation form as follows:

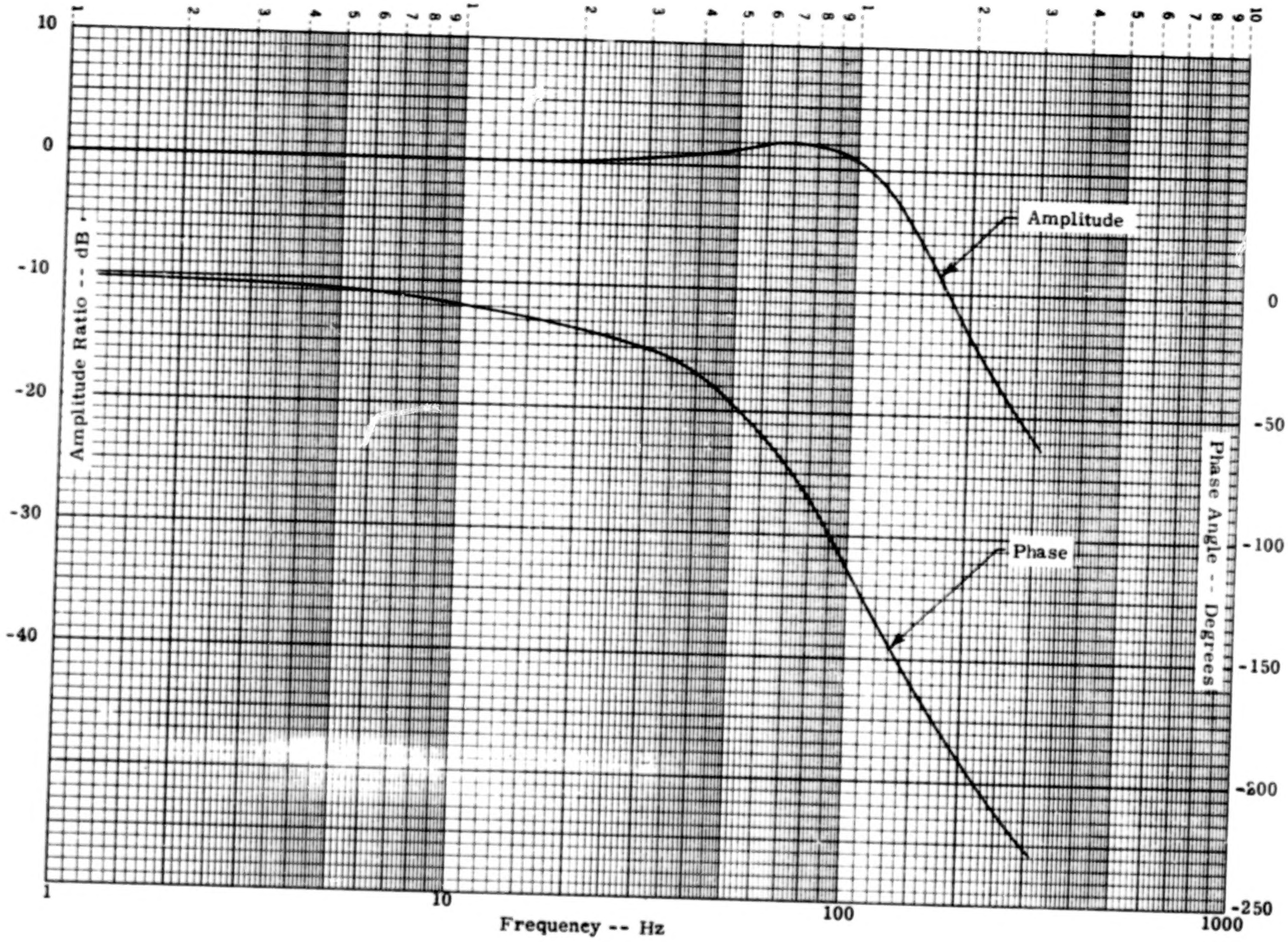

Figure 5. - Dynamic response of servovalve, ±10% input signal.

17

$$\left(\frac{1}{\omega^2_{sv}\,\omega_c}\right)\dddot{X}_{sv} + \left(\frac{1}{\omega^2_{sv}} + \frac{2\,\zeta_{sv}}{\omega_{sv}\,\omega_c}\right)\ddot{X}_{sv} + \left(\frac{2\,\zeta_{sv}}{\omega_{sv}} + \frac{1}{\omega_c}\right)\dot{X}_{sv} + X_{sv} = K_{sv}\, i_2 \quad \ldots(13)$$

Saturations in the various stages are treated as follows. Third stage spool saturation obviously places a limit on X_{sv} equal to $\pm X_{sv}$ max. Second stage saturation is assumed to place a limit on $d(X_{sv})/dt$ equal to $\pm$ (QSV2/ASV3), where QSV2 is the second stage saturation flow and ASV3 is the effective cross sectional area of the third stage spool connected to the lines from the second stage. First stage flapper saturation is assumed to place a limit on $d^2(X_{sv})/dt^2$ equal to $\pm (QSV1 \cdot CQ_2)/(ASV2 \cdot ASV3)$, where QSV1 is the first stage saturation flow, CQ_2 is the linearized flow gain of the second stage spool (flow rate per unit displacement of spool), ASV2 is the effective cross sectional area of the second stage spool connected to the flow lines from the first stage, and ASV3 is as already described.

Linear Math Model for Vertical Drops

This section describes the development of an approximate linear model of an active control landing gear for vertical drops, exclusive of aerodynamics and airplane dynamics. The linear model is a valuable tool since the effect of system modifications can be ascertained very rapidly. The study of system stability and the development of the electronic compensation networks, discussed in the following section, relied very heavily on the linear model. The results were then supported by analysis using the complete nonlinear model.

The equations for the actual landing gear and controller are inherently nonlinear, so some assumptions and simplifications must be made. The following list summarizes the assumptions that were made in the linearization process.

(1) The coulomb friction f between the piston and the cylinder is neglected.

(2) The pneumatic pressure P_2 is assumed constant.

(3) The pressure P_3 is identical to the pressure P_2.

(4) The lift and gravitational forces are constant.

(5) The cross sectional area of the piston wall is negligible with respect to the overall piston area.

(6) The area of the fixed orifice is negligible with respect to the overall piston area.

(7) The inertia of the upper part of the shock strut mass is negligible with respect to the airplane mass.

(8) Servovalve nonlinearities are neglected (i.e., constant flow gain and pressure gain partial derivative values are assumed).

The equations given in the previous section for the nonlinear math model can now be simplified as follows. Equations 5 and 6 become

$$M_u \ddot{X}_{wg} \approx M_u g - L - P_1 A_1$$

$$M_L \ddot{X}_s \approx \frac{M_L}{M_u} [(M_u + M_L) g - L] + (1 + \frac{M_L}{M_u}) [- M_L g - P_1 A_1] + K_t (X_{wg} - X_s)$$

If we let the variables X'_{wg}, X'_a, X'_s, and P'_1 represent the perturbation variables of X_{wg}, X_a, X_s, and P_1, (that is, they represent changes in those variables about some mean condition), then these two equations can be written

$$M_u \ddot{X}'_{wg} = -P'_1 A_1$$

$$M_L \ddot{X}'_s = (1 + \frac{M_L}{M_u})(-P'_1 A_1) + K_t (X'_{wg} - X'_s)$$

where the lift and gravitational terms have dropped out because they are assumed constant. Making use of the identity $X_s = X_{wg} - X_a$, these two equations can be solved for X_{wg} and X_a. Dropping the primes for simplicity, the results in LaPlace transform notation are

$$X_{wg} = -\frac{A_1 P_1}{M_u s^2} \qquad \ldots(14)$$

$$X_a = \frac{A_1 P_1}{M_L s^2 + K_t} \qquad \ldots(15)$$

Also, note from equations 1 and 2 that

$$F_{wg} = F_s \approx P_1 A_1 \qquad \ldots(16)$$

It is instructive to note that equations 14 and 15 are the linearized equations of motion that would result from a mass and piston driving into a sleeve connected to ground by a spring, with an orifice in the piston connecting the internal pressure P_1 with a constant pressure P_2 on the other side. This is illustrated schematically in Figure 6, along with a servovalve for active control. A force balance on the masses M_U and M_L will result exactly in equations 14 and 15.

A linearized expression for the pressure P_1 will now be derived. Referring to Figure 6, conservation of mass applied to the hydraulic fluid in volume V_1 gives

$$dQ_{sv} - dQ_o + A_1 \dot{X}_s = \frac{V_1}{\beta} \dot{P}_1 \qquad \ldots(17)$$

The flow from the servovalve is

$$Q_{sv} = \begin{cases} C_{sv} X_{sv} \sqrt{P_S - P_1} & \text{for } X_{sv} \geq 0 \\ C_{sv} X_{sv} \sqrt{P_1 - P_R} & \text{for } X_{sv} < 0 \end{cases}$$

Differentiating this, gives

$$dQ_{sv} = \begin{cases} C_{sv} \sqrt{P_S - P_1}\, dX_{sv} - \left(\dfrac{C_{sv} X_{sv}}{2\sqrt{P_S - P_1}} \right) dP_1 & \text{for } X_{sv} \geq 0 \\ C_{sv} \sqrt{P_1 - P_R}\, dX_{sv} + \left(\dfrac{C_{sv} X_{sv}}{2\sqrt{P_1 - P_R}} \right) dP_1 & \text{for } X_{sv} < 0 \end{cases}$$

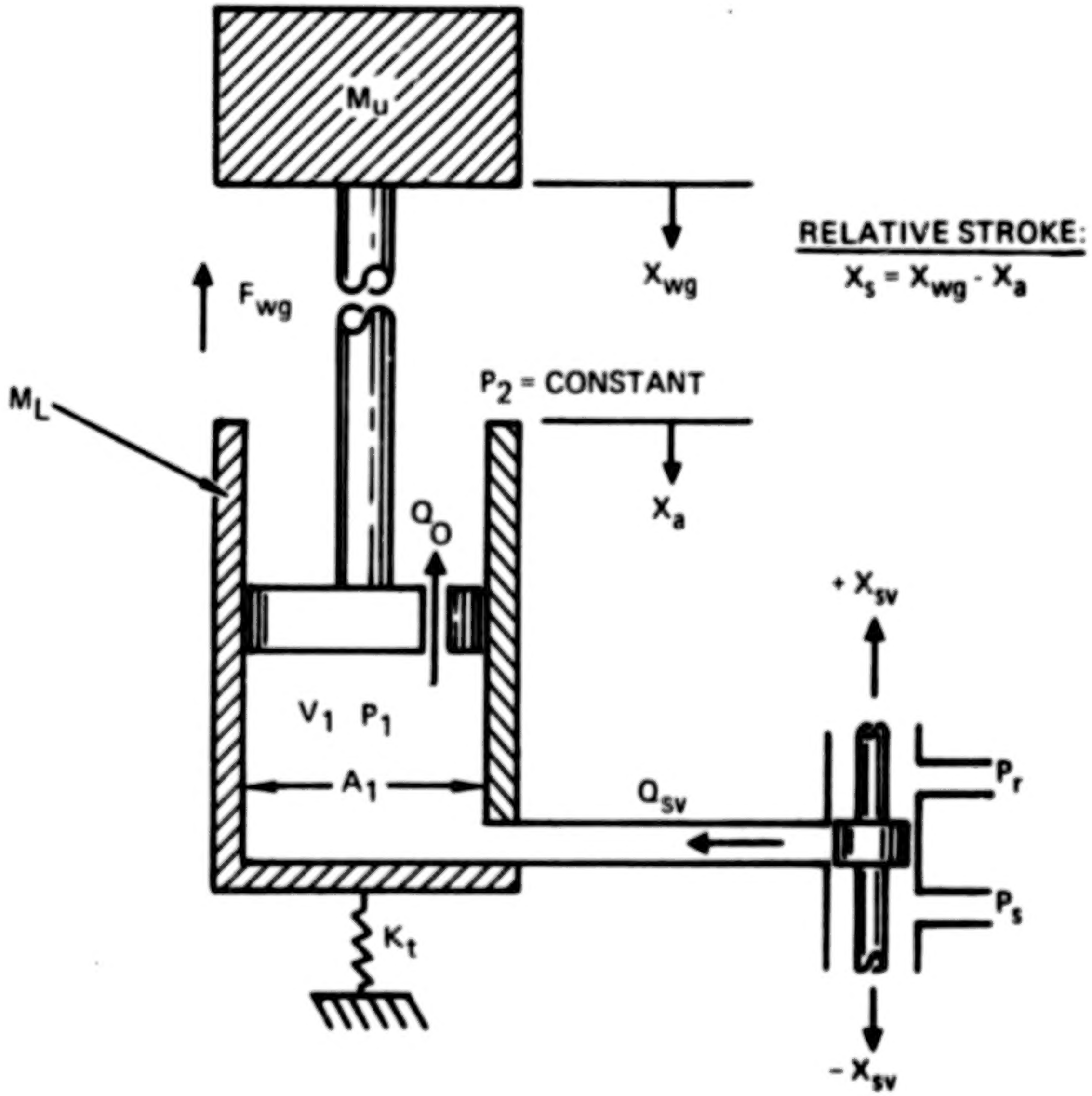
M_u
F_{wg}
X_{wg}
RELATIVE STROKE:
$X_s = X_{wg} - X_a$
M_L
P_2 = CONSTANT
X_a
Q_O
$+X_{sv}$
V_1 P_1
A_1
Q_{sv}
P_r
P_s
K_t
$-X_{sv}$

Figure 6. - Illustration of "equivalent" system for the linear math model.

Letting the mean value of the pressure P_1 equal $(P_S + P_R)/2$, and assuming small perturbations about this mean condition, the above relationships can be expressed as

$$dQ_{sv} = CQ \cdot dX_{sv} - CP \cdot dP_1 \qquad \ldots(18)$$

where

$$CQ = \frac{\partial Q_{sv}}{\partial X_{sv}} = C_{sv}\sqrt{(P_S + P_R)/2}$$

$$CP = -\frac{\partial Q_{sv}}{\partial P_1} = -CQ/PG$$

and where PG is the pressure gain of the spool in terms of pressure per spool displacement, at constant flow. In the linearized model the values of CQ and CP are assume constant.

The flow through the fixed orifice is

$$Q_o = K_o\sqrt{P_1 - P_2}$$

Differentiating this gives

$$dQ_o = \left(\frac{K_o}{2\sqrt{P_1 - P_2}}\right) dP_1 = CP_o\, dP_1 \qquad \ldots(19)$$

However, note that at the mean condition P_1 equals P_2, so the coefficient CP_o is undefined. In actuality, CP_o is a function of excitation amplitude and frequency. It is important to keep this fact in mind when applying the linearized model. The approach taken in this study was to vary CP_o over a reasonable range to determine its influence on the dynamic response of the system, and to proceed accordingly.

Substituting equations 18 and 19 into equation 17, solving for P_1, and expressing it in LaPlace transform notation gives

$$P_1 = \frac{CQ \cdot X_{sv} + A_1 s\, X_s}{\frac{V_1}{\beta} s + (CP_o + CP)} \qquad \ldots(20)$$

The transfer function of the servovalve dynamics in terms of output displacement of the third stage spool for input current was derived in the preceding section (equation 12) and is

$$\frac{X_{sv}}{i_2} = \frac{K_{sv}}{\left(\frac{s^2}{\omega^2_{sv}} + \frac{2\zeta_{sv}}{\omega_{sv}} s + 1\right)\left(\frac{s}{\omega_c} + 1\right)}$$

The transfer function for the electronic compensation network, which is derived in the next section, is

$$\frac{i_2}{i_1} = \left(\frac{s^2 + 2\zeta_2\, \omega_1 s + \omega_1{}^2}{s^2 + 2\zeta_1\, \omega_1 s + \omega_1{}^2}\right)\left(\frac{\tau_1 s + 1}{\tau_2 s + 1}\right)\left(\frac{\tau_3 s + 1}{\tau_4 s + 1}\right) \qquad \ldots(21)$$

The relationship describing the force feedback and the position loop feedback is

$$i_1 = K_a (F_{lim} - F_{wg}) - K_a \left(\frac{K_f}{\tau_f s + 1}\right) (X_c - K_x X_s) \qquad \ldots (22)$$

Equations 14, 15, 16, 20, 12, 21 and 22 make up the complete linarized model, and Figure 7 is a block diagram arrangement of these equations. The algebraic solution of transfer functions from this set of equations would be very tedious, so this practice was avoided. The following approach was taken. First, working from the block diagram, the system of equations is expressed in matrix form, where each element of the matrix is in general a polynomial in "s". A computer program is then used to solve for the coefficients of the numerator and denominator of the desired transfer function using Cramer's Rule. Frequency response characteristics are then calculated from the transfer function. Also, the roots of the numerator and denominator polynominals are easily determined using standard computer techniques. The linear model gives very rapid results, and thus is ideal for evaluating the effect of varying different parameters and for developing electronic compensation networks for stability.

The validity of the linear model was evaluated by comparing the open loop frequency response with results obtained from the nonlinear vertical drop model described in the preceding section. The loop was opened at the point of wing gear force (F_{wg}) feedback, and position feedback was not included. The conditions were for zero lift with the shock strut at a mean stroke equal to that required to balance the weight of the airplane, which was 67 percent of maximum stroke for this case. Also, no electronic compensation was used.

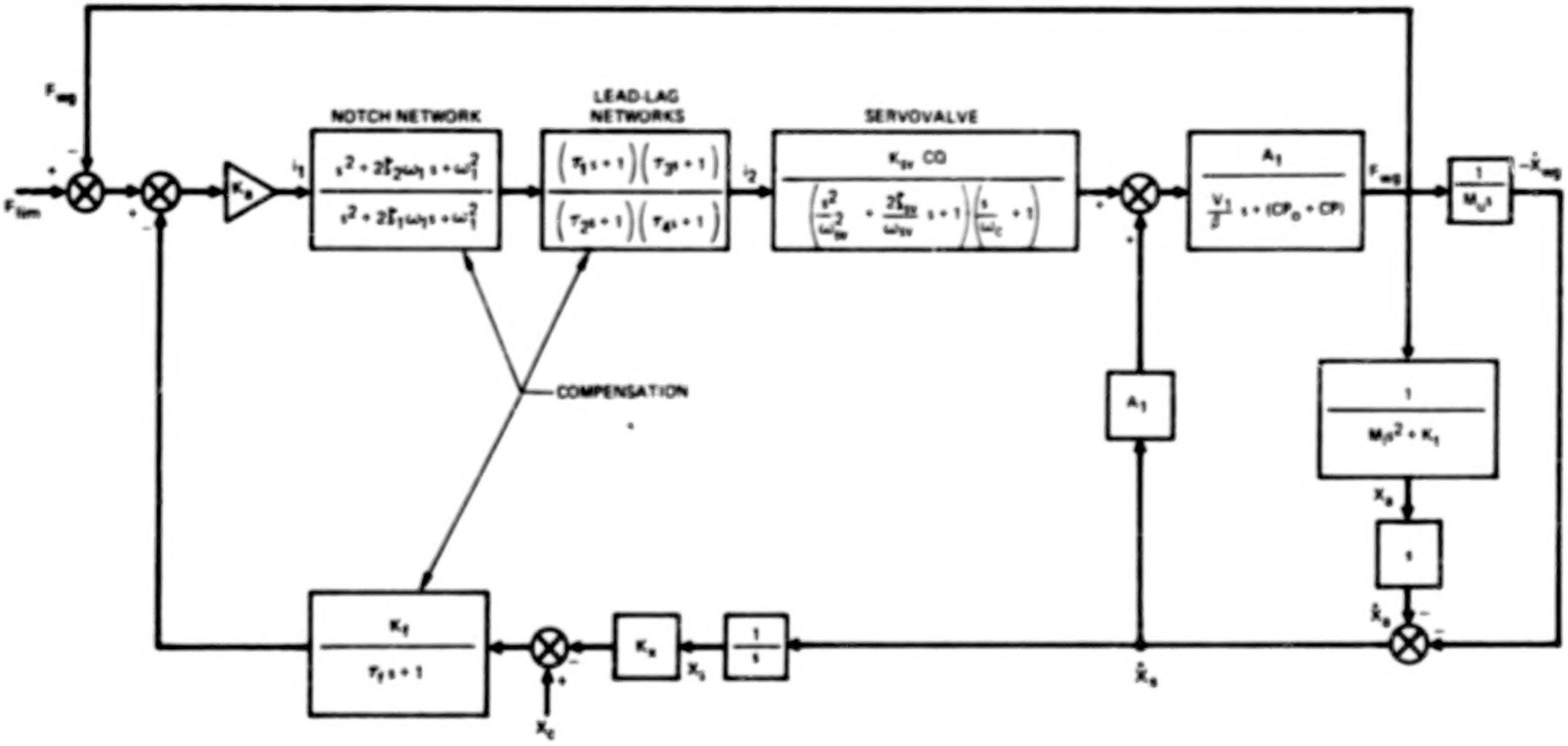
F_wg
F_lim
K_a
i_1
NOTCH NETWORK
s^2 + 2ζ_2ω_1 s + ω_1^2 / s^2 + 2ζ_1ω_1 s + ω_1^2
LEAD-LAG NETWORKS
(τ_1 s + 1)(τ_3 s + 1) / (τ_2 s + 1)(τ_4 s + 1)
i_2
SERVOVALVE
K_sv CQ / (s^2/ω_sv^2 + 2ζ_sv/ω_sv s + 1)(s/ω_c + 1)
A_1 / (V_1/β s + (CP_0 + CP))
F_wg
1 / M_U s
-Ẋ_wg
A_1
1 / M_B s^2 + K_1
X_B
s
Ẋ_B
Ẋ_s
1 / s
X_s
K_s
X_c
K_f / τ_f s + 1
COMPENSATION

Figure 7. - Block diagram of linear math model

The comparison of results is shown in Figure 8. Input is commanded limit force and output is wing gear force. Linear model results are shown for both a low and a high value of the fixed orifice parameter CP_o. The results for the low value of CP_o match the nonlinear results closest at low frequencies while the results for the high value of CP_o match closest at high frequencies. The basic trends are predicted reasonably well and it is concluded that the linear model is a valid tool for performing initial design and stability studies.

Energy Considerations

The primary function of the landing gear control system is to control the wing gear force at some commanded level. A secondary but necessary function of the controller is to set this commanded level such that the strut will not fully collapse, precluding structural damage. In order to do this, the controller must be able to monitor the energies present in the system during impact, and then set the limit force accordingly so that the work potential of the shock strut will be sufficient to absorb these energies. In order to study the feasibility of the controller performing this function, it is worthwhile to undergo an analytical development of the various energies present in the system and relate them to the work performed by the shock strut — the subject of this section. The equations will be developed from the equations of motion of the simplified vertical drop case, presented earlier; however, the results are almost directly applicable to the more general cases.

Equations 3 and 5 are the inertial equations of motion corresponding to the two independent masses M_U and M_L. These equations are rewritten in a form where each term represents the differential of an energy or work. This is done by multiplying equation 5 by dX_{wg} and equation 3 by dX_a, resulting in

$$M_u V_{wg} dV_{wg} = [M_u g - L - (P_1 - P_2)(A_1 - A_o) - P_2 A_2 + P_3 A_3 \mp f]\, dX_{wg} \qquad \ldots (23)$$

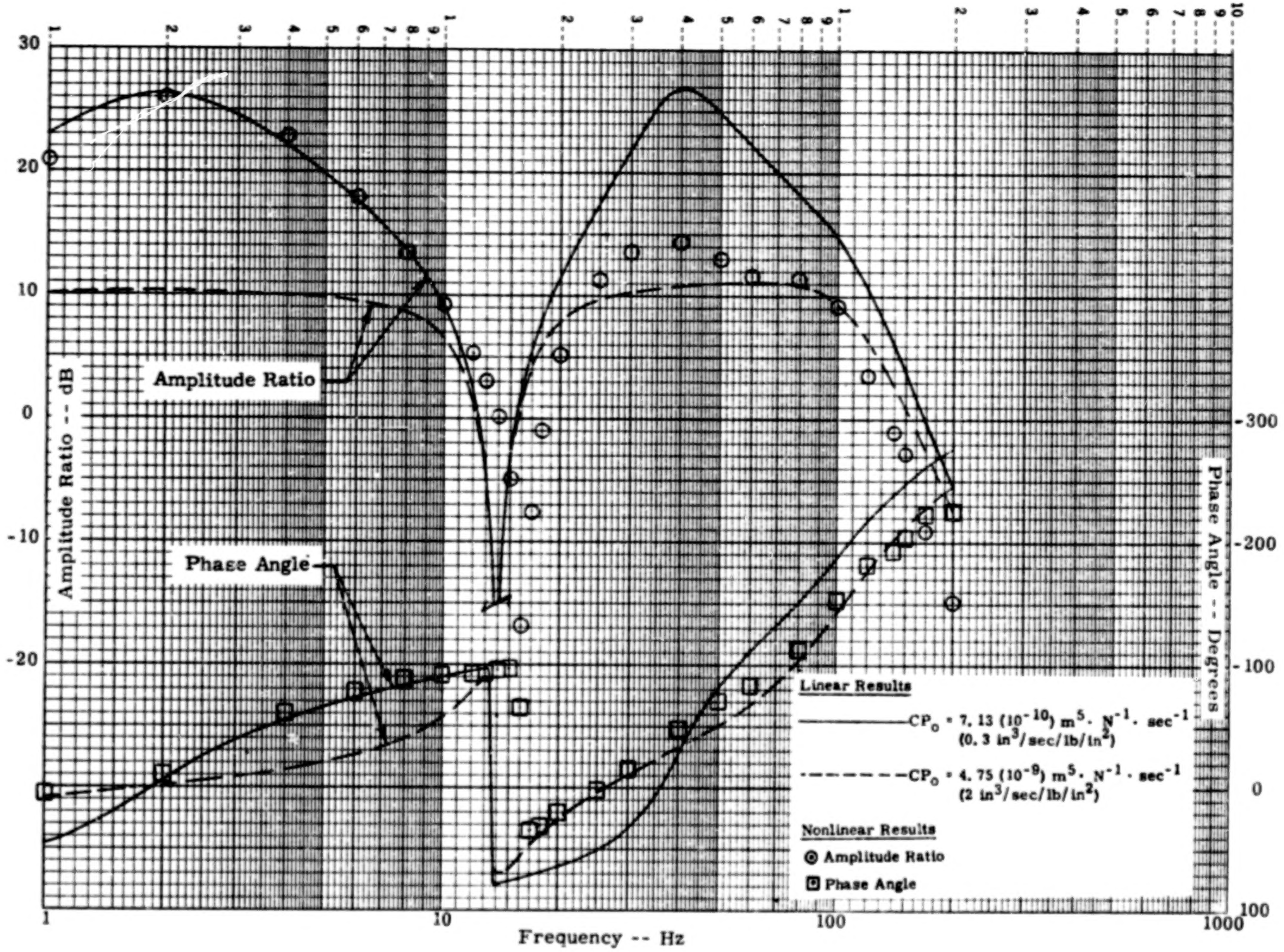

Figure 8. - Comparison of linear model and nonlinear model results, open loop, no compensation, no position feedback.

$$M_L V_a \, dV_a = [M_L g + P_2 (A_2 - A_1) + P_1 A_1 - P_3 A_3 - F_a \pm f] \, dX_a \qquad \ldots(24)$$

Note that if these equations are integrated from some initial condition to a final condition they express changes in energy that occur over that time interval. For example, the integral of the terms on the left side of the equations express the total change in kinetic energy of each mass. It is desired now to write an equation expressing the total change in kinetic energy of the system, which is assumed to consist entirely of the two masses M_U and M_L, as a function of the various other energy and work terms. This is done by adding equations 23 and 24, resulting in

$$\overbrace{M_u V_{wg} \, dV_{wg}}^{1} + \overbrace{M_L V_a \, dV_a}^{2} + [\overbrace{-M_u g}^{3} + \overbrace{L}^{4} \overbrace{-(P_1 - P_2) A_o}^{5}] \, dX_{wg}$$

$$+ [\overbrace{-M_L g}^{6} + \overbrace{F_a}^{7}] \, dX_a + [\overbrace{(P_1 - P_2) A_1}^{8} + \overbrace{P_2 A_2 - P_3 A_3}^{9} \overbrace{\pm f}^{10}] \, dX_s = 0 \qquad \ldots(25)$$

Equation 25 can be thought of as a statement of conservation of energy, since it essentially says that the sums of all changes in energy and work done in the system equals zero. Some of the terms in equation 25 are easily recognizable as to the type of energy they represent. For example, terms 1 and 2 represent changes in kinetic energy. Terms 3 and 6 represent changes in potential energy of the upper and lower masses due to height changes. Term 7 represents changes in potential energy stored in the tire spring. Term 10 represents energy dissipation due to Coulomb friction. Energy dissipation due to flow across the shock strut orifice also occurs, although this is not directly identifiable in equation 25 because of the complicating effects of fluid compressibility and flow to and from the active-control servovalve.

Equation 25 must be simplified to the point where it becomes a useful tool to the controller for monitoring the energies present in the system in terms of the available input signals; e.g., accelerometers, transducers, etc. First, term 5 was found to be negligible and can be immediately eliminated. Next, the combination of terms in the third bracket (terms 8, 9 and 10) are approximately equivalent to the shock strut force F_s. This can be seen by referring back to equation 2, neglecting the inertia and gravity forces on the shock strut portion of the upper mass, and neglecting the orifice area with respect to the piston area. With these simplifications, equation 25 is rewritten as

$$M_U V_{wg} dV_{wg} + M_L V_a dV_a + (-M_U g + L)\, dX_{wg} + (-M_L g + F_a)\, dX_a + F_s dX_s = 0 \qquad \ldots(26)$$

Note that the quantity $F_s dX_s$ represents the differential of the work performed by the shock strut. Integration of this equation over a given interval will thus yield an expression showing the net work performed by the shock strut as a function of the various other energy changes. The task of the controller is to monitor these energies and make sure that the remaining work potential of the shock strut is sufficient to dissipate them.

At this point, it is worthwhile summarizing the instrumentation that is available to the controller as originally proposed.

(1) Wing/gear acceleromters - measures $\ddot{X}_{wg}$
(2) Hub accelerometer - measures $\ddot{X}_a$
(3) LVDT on shock struct - measures X_s
(4) Upper cylinder pressure transducer - measures P_2 (pneumatic)
(5) Lower piston pressure transducer - measures P_1 (hydraulic).

With this instrumentation, it is not possible to apply equation 26 to the task at hand, because there is no way to monitor the lift L or the shock strut force F_s (note that by knowing one of these, the other may be obtained equation 1). It is therefore necessary to make further simplifications. Assuming that the total airplane weight equals the lift throughout impact, and neglecting the $M_L g$ term, then equation 26 becomes

$$M_U V_{wg} dV_{wg} + M_L V_a dV_a + F_a dX_a + F_s dX_s = 0 \qquad \ldots(27)$$

With the weight-equals-lift assumption, all of the parameters in equation 27 may be obtained. From equation 1,

$$F_s = -M_U \ddot{X}_{wg} \qquad \ldots(28)$$

It is possible to solve for F_a by first noting that equation 3 may be expressed as

$$M_L \ddot{X}_a \approx -F_a + F_s \qquad \ldots(29)$$

Substituting equation 28 for F_s into equation 29,

$$F_a \approx - M_U \ddot{X}_{wg} - M_L \ddot{X}_a \qquad \ldots(30)$$

The individual terms in equation 27 were integrated with respect to time throughout a typical vertical drop simulation using the simplified nonlinear vertical drop model described in a previous section to determine if the equation is indeed a valid representation of all the major energy changes that take place. The lift was set equal to the weight throughout the simulation, so this test case will say nothing regarding the validity of the "weight-equals-lift" simplification. The validity of that will be demonstrated later using actual land and roll simulations. The integrated variables are shown plotted in Figure 9. The sum of all the integrated variables is also shown, representing the total energy plus work done by the system. This should remain constant from the conservation of energy principle. It is indeed relatively constant, thus supporting the validity of equation 27, at least for vertical drop cases where weight equals lift. Note that the kinetic energy of the lower mass is negligible. Also, the potential energy stored in the tire, although not completely negligible, is a minor part of the total energy of the system. This raises the question whether it is worth the added complexity of including this term in the energy computations of the controller. The approach taken here is to neglect it and incorporate any errors into an empirical correction factor, if necessary. As a result, the only terms considered in the energy computations of the controller are the kinetic energy of the upper mass and the work of the shock strut.

The next step is to derive relationships that the controller can apply in setting the commanded limit force to a level such that bottoming of the strut will be prevented. There are various approximations or simplifications that can be made, some of which have already been mentioned in the preceding paragraph, which will introduce errors in the final result. In the interest of completeness and for reference, the more general derivation will be presented first, followed by the simplifications. The procedure is to integrate equation 27 from a time t_1 (controller initiation) to the end of transition; i.e., the start of rollout. The following assumptions are made.

(1) The actual wing/gear force is identical to the commanded limit force throughout the impact and transition phases.

(2) The velocity of the masses is zero at the end of transition (this also is the criterion used in calculating the wing/gear velocity at which transition begins).

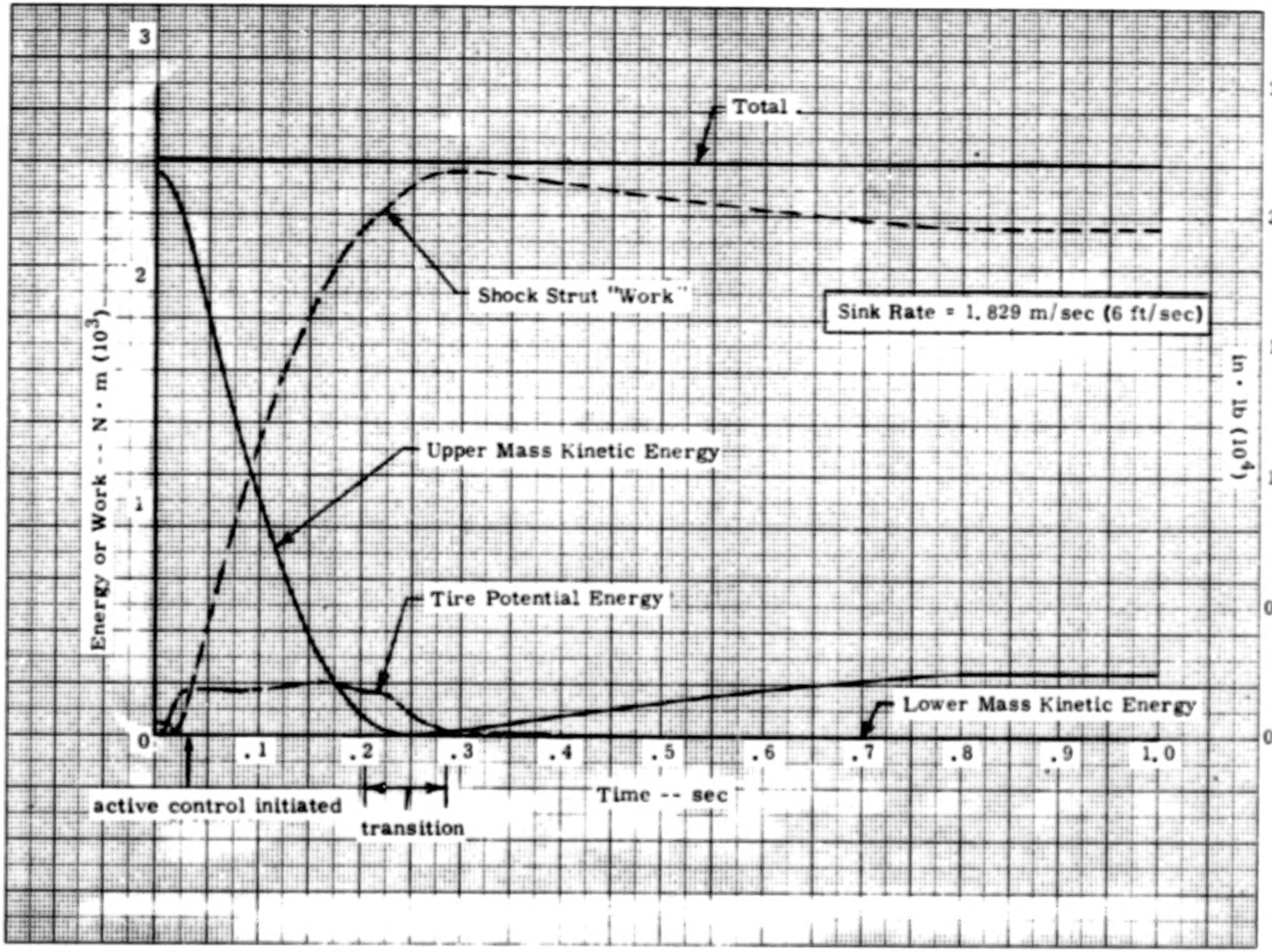

Figure 9. - Various energy terms versus time, from the simplified nonlinear vertical drop simulation.

(3) The commanded limit force is constant throughout the impact phase and linearly decreases during transition to zero limit force at the beginning of rollout. The slope in the transition phase is a known quantity.

A sketch of the variation of wing/gear force versus time for the above conditions is shown in Figure 10. Integration of equation 27 from t_1 to the start of transition t_{tr} gives

$$1/2\ M_u\,(V^2_{u_{tr}} - V^2_u) + 1/2\ M_L\,(V^2_{L_{tr}} - V^2_L) + \int_{t_1}^{t_{tr}} F_a\,dX_a + F_{li}\,\Delta X_{s_{im}} = 0$$

Integration from the start of transition t_{tr} to the end of transition t_r gives

$$1/2\ M_u\,(\cancelto{0}{V^2_{u_r}} - V^2_{u_{tr}}) + 1/2\ M_L\,(\cancelto{0}{V^2_{L_r}} - V^2_{L_{tr}}) + \int_{t_{tr}}^{t_r} F_a\,dX_a + \frac{F_{li}}{2}\,\Delta X_{s_{tr}} = 0$$

The quantities $\Delta X_{s_{im}}$ and $\Delta X_{s_{tr}}$ represent the shock strut stroke used in the impact and transition phases, respectively. The sum of these should be equal to or less than the total remaining available stroke, to prevent bottoming. Solving for ΔX_{s_i} and $\Delta X_{s_{tr}}$ in these equations and adding them together gives

$$\Delta X_s = \frac{1/2\ M_u(V^2_u - V^2_{u_{tr}}) + 1/2\ M_L\,V^2_{L_{tr}} - \int_{t_1}^{t_{tr}} F_a\,dX_a}{F_{li}} + \frac{1/2\ M_u\,V^2_{u_{tr}} + 1/2\ M_L\,V^2_{L_{tr}} - \int_{t_{tr}}^{t_r} F_a\,dX_a}{F_{li}/2} \quad \ldots(31)$$

Referring back to Figure 9, it is shown that any potential energy changes in the tire during the impact phase may be neglected. This is true because F_a and X_a remain relatively constant throughout this phase. Also, since the final

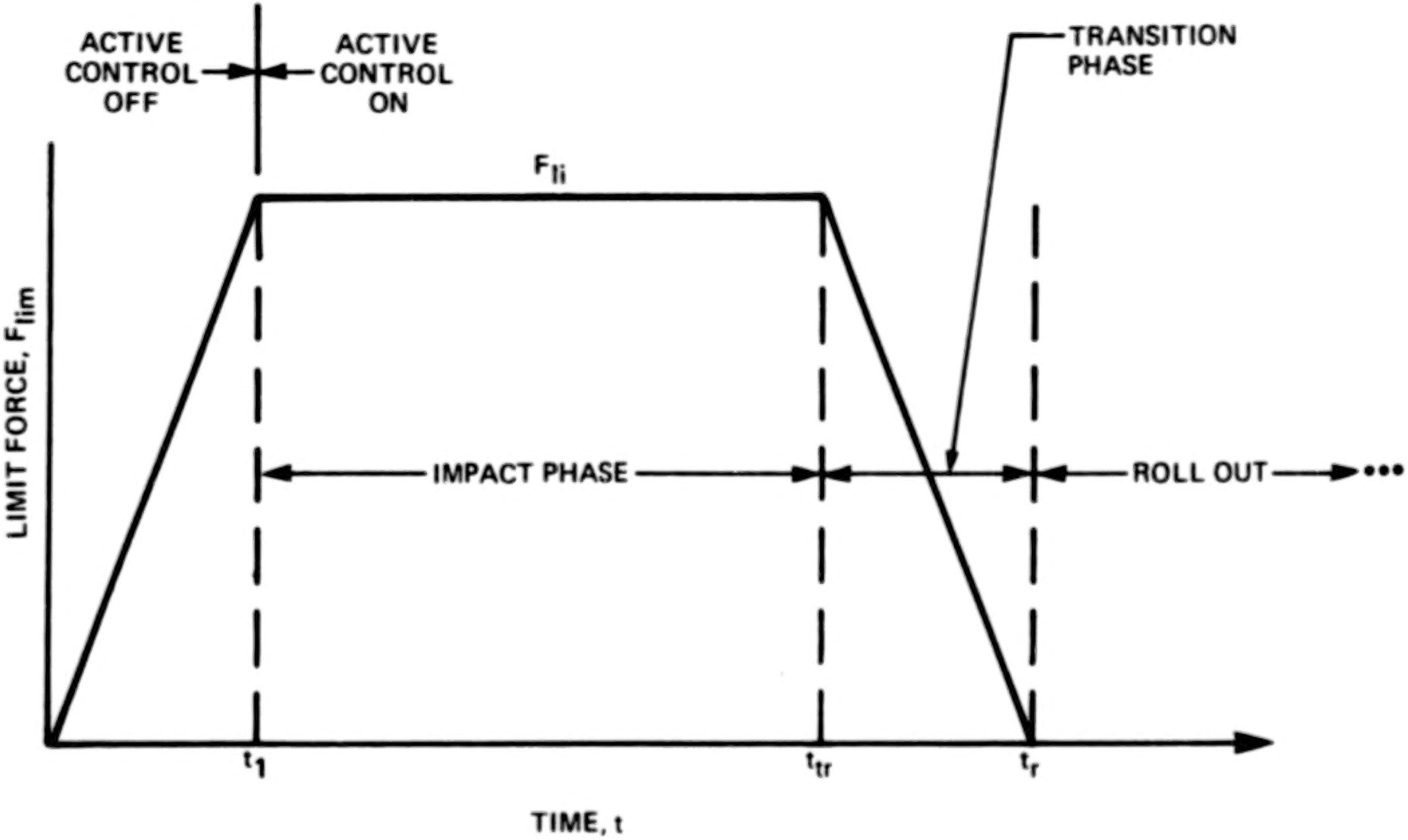
ACTIVE CONTROL OFF
ACTIVE CONTROL ON
TRANSITION PHASE
F_{li}
LIMIT FORCE, F_{lim}
IMPACT PHASE
ROLL OUT
t_1
t_{tr}
t_r
TIME, t

Figure 10. - Illustration of the variation of limit force versus time and the various phases of operation following impact.

rollout limit force is zero, F_a at that point will be approximately zero; and hence, roughly stated, that during transition the potential energy of the tire will go from its initial impact phase state to a zero energy state. This fact can be seen in Figure 9. Thus, in equation 31, the integral of $F_a dX_a$ over the interval t_1 to t_{tr} is approximately zero and the integral of $F_a dX_a$ over the interval t_{tr} to t_r is approximately equal to the negative of the potential energy stored in the tire at time t_1, the start of the integration interval. Signifying this energy level by the symbol PE_t, and neglecting the kinetic energy of the lower mass, equation 31 reduces to

$$F_{li}\,\Delta X_s = 1/2\, M_u V_u^2 + 1/2\, M_u \left(V_{u_{tr}}\right)^2 + 2 \cdot PE_t \qquad \ldots(32)$$

The upper mass velocity at the start of transition can be determined by equating the impulse to the change in momentum for the transition phase, resulting in

$$V_{u_{tr}} = \frac{F_{li}^2}{2 \cdot M_u \cdot R_s} \qquad \ldots(33)$$

where R_s is the slope of the limit force with respect to time during transition.

The application of equation 32 to the controller could be as follows: when the gear first impacts the runway surface the controller is in a passive mode; that is, no command is being initiated to the servovalve. Immediately after impact, at discrete intervals, the controller will compute the strut work ($F_{li}\Delta X_s$) required to absorb the energy using equations 32 and 33. In equation 33, the transition velocity is calculated using the current value of wing/gear interface force as the impact limit force (i.e., F_{li} is set equal to F_{wg}).

This calculated value of required strut work is continually compared to a signal representing the actual strut work currently available if the controller were to go into active control at that instant. This actual strut work is simply the current value of the wing gear force times the remaining shock strut stroke. When comparison of these signals indicates that the available shock strut work exceeds the value calculated by equation 32, then active control to the servovalve is initiated and the commanded impact phase limit force is set equal to that current value of wing gear force. The velocity of transition is also then set to the value computed from equation 33.

It may be desirable to further monitor the energy situation through the remainder of the impact phase to ensure that the strut will not bottom due to additional energy inputs. If so, equations 32 and 33 could be used to compute F_{1i} from the known remaining strut stroke (ΔX_s), and if the computed F_{1i} ever exceeded the original F_{1i} value, the controller would update F_{1i} to the newly-computed value; however, this would require the solution of a quartic equation.

A simplification in equation 32 can be made by neglecting the transition region. In other words, assume that in Figure 10 the constant impact limit force is continued throughout the transition region, and at the end of transition it drops abruptly to the rollout limit force of zero. It should also be stressed that it is not being proposed that the actual limit force commanded by the controller follow this pattern; this is only for the purpose of simplifying the energy relationships. Integration of equation 27 will then result in

$$1/2\ M_u\,(V^2_{u_r} - V^2_u) + 1/2\ M_L\,(V^2_{L_r} - V^2_L) + \int_{t_1}^{t_r} F_a\,dX_a + F_{1i}\,\Delta X_s = 0 \qquad \ldots(34)$$

Again, the integral of $F_a dX_a$ from t_1 to t_r is approximately equal to the negative of the potential energy stored in the tire at time t_1. Neglecting the kinetic energy of the lower mass, equation 34 becomes

$$F_{li}\,\Delta X_s = 1/2\, M_u V_u^2 + PE_t \qquad \ldots(35)$$

with equation 33 still applying for the velocity of transition. The use of equations 35 and 33 in the controller would be similar to that already described for equations 32 and 33.

A still further simplification, in addition to those already made, is to neglect the potential energy in the tire. Equation 35 then reduces to

$$F_{li}\,\Delta X_s = 1/2\, M_u\, V_u^2 \qquad \ldots(36)$$

with equation 33 still applying for the velocity of transition. This last approach is the one taken in the current design, and is the one programmed into the computer simulations.

To extend the use of equation 36 to actual land and roll cases, $\Delta X_s \cos \theta$ is substituted in place of ΔX_s, where θ is the angle the shock strut axis makes with the vertical (gravitational) direction. The angle θ is equal to the pitch angle of the airplane fuselage plus the angle of the wing with respect to the airplane fuselage. Also, the velocity and force in equation 36 are now the components in the vertical, or gravitational direction. The energy relationship used for land and roll cases is then

$$F_{li}\,\Delta X_s \cos \theta = 1/2\, M_u\, V^2{}_u \qquad \ldots(37)$$

For land and roll cases, the question of the validity of the "weight-equals-lift" simplification is raised. Whether or not this is valid is demonstrated by computer simulation of the actual landing roll cases provided by NASA. The simulation results are presented in the ANALYTICAL RESULTS section. Of interest to the present discussion, however, is the maximum resultant stroke that occurs in each case when the limit force is set according to equation 37 and the aforementioned procedure. Table I, presented in a later section, summarizes this information. As can be seen, the method is reasonably successful in setting the limit force so that a maximum amount of strut stroke is used in absorbing the impact energy.

Stability Analysis

The linear model discussed earlier was used to evaluate the frequency response and stability of the system. System parameters used were basically those given under SYMBOLS. The linearized orifice coefficient CP_o was given a value of 7.13 (10^{-7}) $m^3/sec/kPa$ (0.3 $in^3/sec/lb/in^2$) for frequencies less than 14 Hz and a value of 4.75 (10^{-6}) $m^3/sec/kPa$ (2.0 $in^3/sec/lb/in^2$) for frequencies greater than 14 Hz, providing a reasonable match with frequency responses generated with the nonlinear model.

Based on results from the nonlinear vertical drop model, it was determined that a force loop bandwidth of 10 Hz would be adequate to achieve desired performance. Using the uncompensated linear model shown in Figure 11, the Nyquist plot of Figure 12 was generated. The uncompensated system was unstable at a frequency (140 Hz) related to the servovalve dynamics and could not be stabilized by simply lowering loop gain without violating the 10-Hz bandwidth goal. It was evident that signal shaping was required.

Analysis of various forms of forward path electronic compensation ultimately yielded the filter configuration shown in Figure 13. It consists of a second-order notch and two lead lags. The resulting Nyquist plot is shown in Figure 14; and, it can be seen that stability margins are adequate.

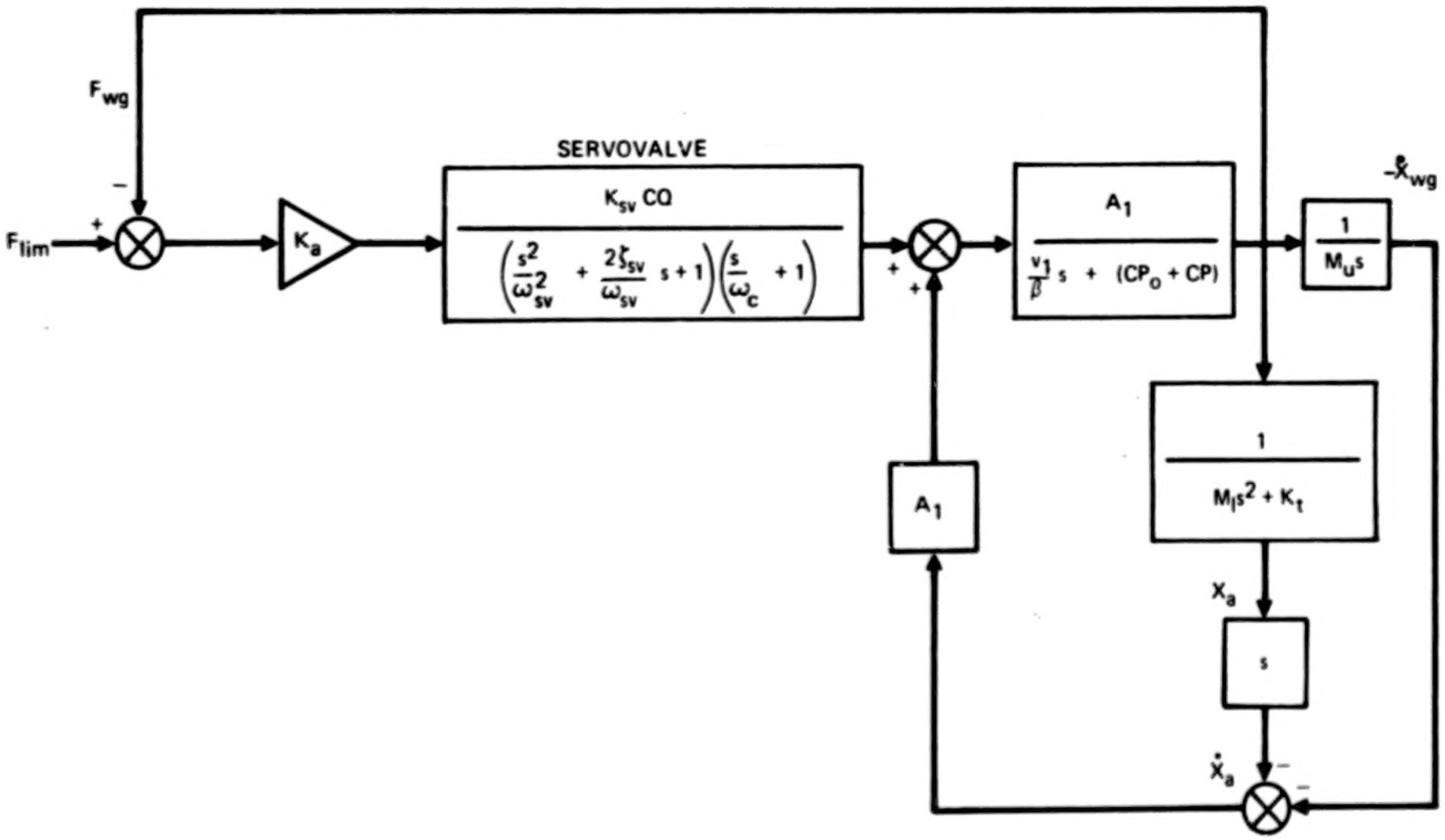

F_{wg}
$-$
$+$
F_{lim}
K_a
SERVOVALVE
$\dfrac{K_{sv}\,CQ}{\left(\dfrac{s^2}{\omega_{sv}^2} + \dfrac{2\zeta_{sv}}{\omega_{sv}}s + 1\right)\left(\dfrac{s}{\omega_c} + 1\right)}$
$+$
$+$
$\dfrac{A_1}{\dfrac{v_1}{\beta}s + (CP_o + CP)}$
$\dfrac{1}{M_u s}$
$-\dot{X}_{wg}$
$\dfrac{1}{M_l s^2 + K_t}$
A_1
X_a
s
$\dot{X}_a$
$-$
$-$

Figure 11. - Block diagram of linear system without compensation.

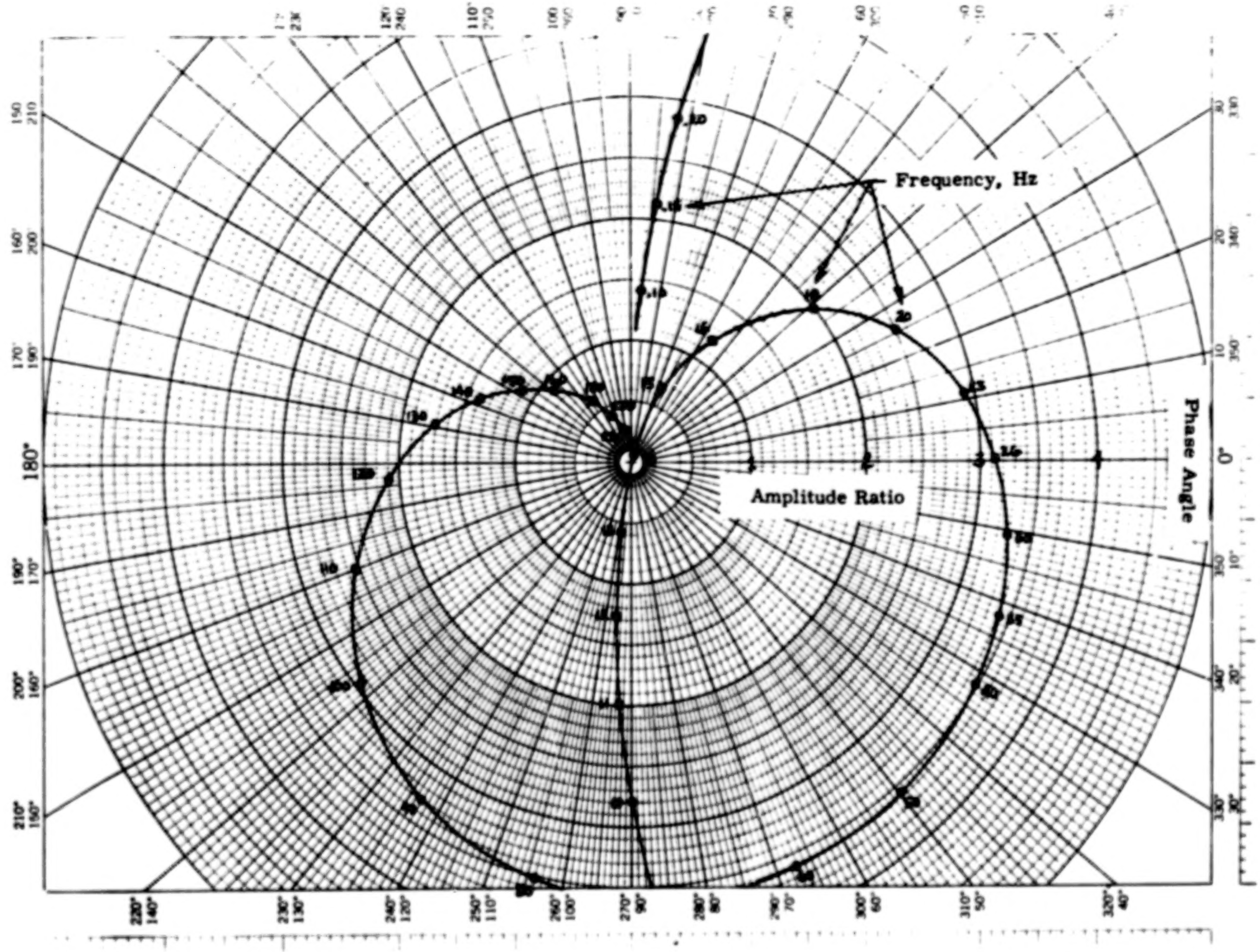

Figure 12. - Nyquist plot of F_{wg}/F_{lim} with force loop opened, no position feedback, no compensation.

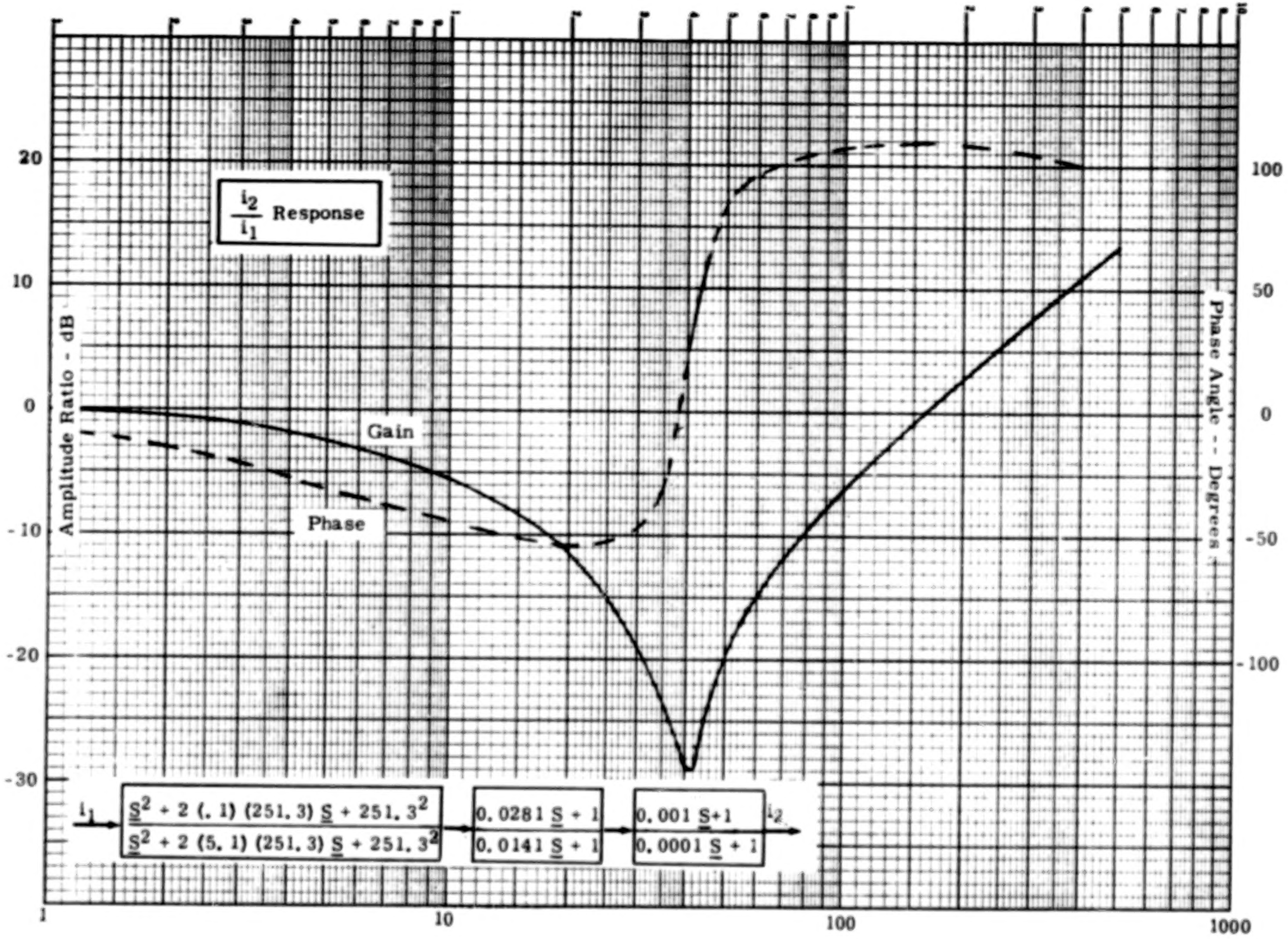

Figure 13. - Electronic compensation network and its characteristics.

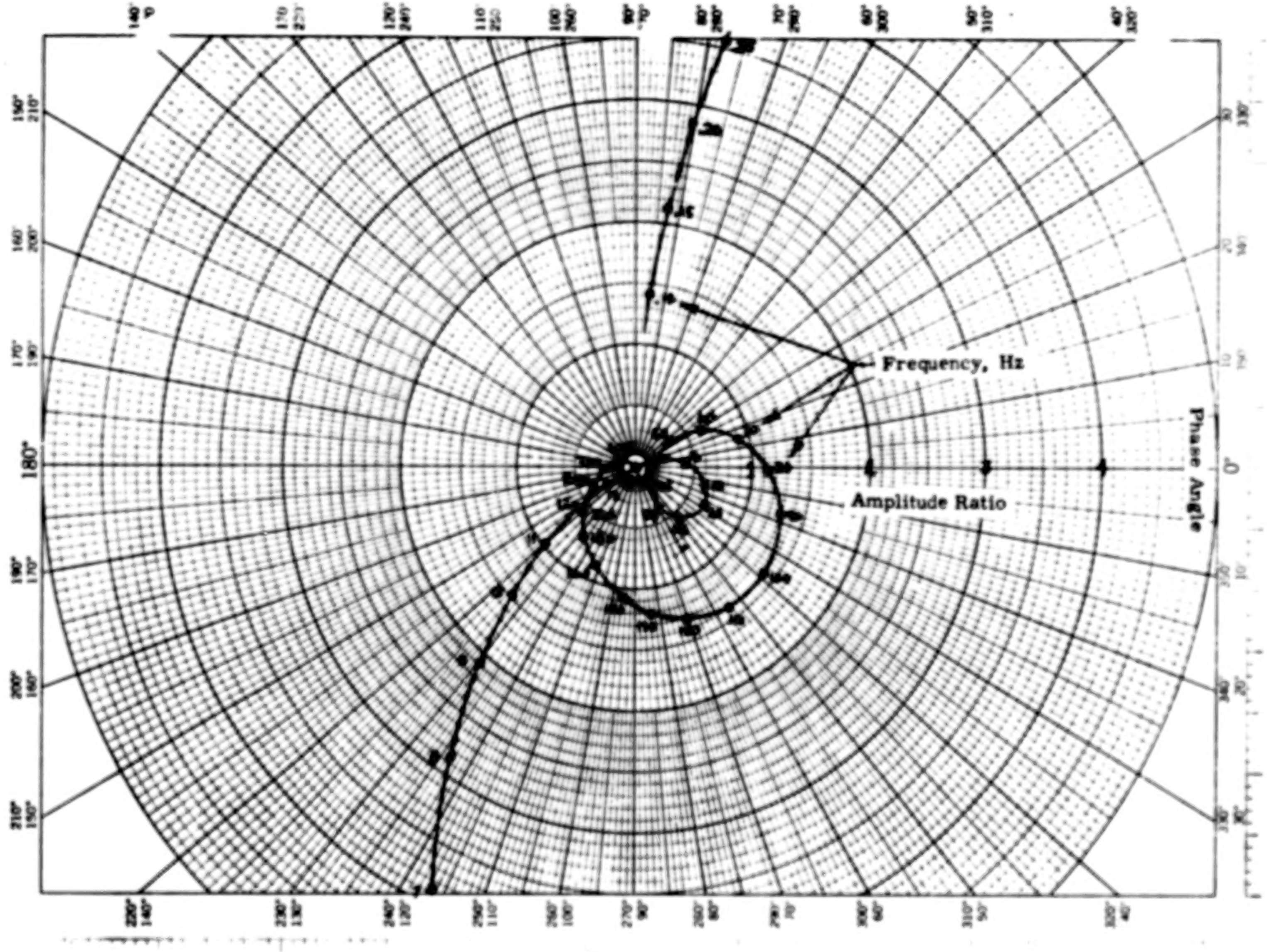

Figure 14. - Nyquist plot of F_{wg}/F_{lim} with force loop opened, no position feedback, with compensation.

The strut position feedback was next incorporated into the models. Its purpose is to ensure the return of the strut to its neutral position after landing impact. With no specific requirements on the time to return to neutral, it was assumed that a relatively gradual (approximately 10-sec) return would be acceptable. This assumption allowed a low bandwidth position loop which is essentially decoupled from the force loop. The resulting benefit is that the position loop can be continually active at all times during impact, transition, and rollout without degrading the performance of the force loop. A first-order lag in the position loop forward path yielded the desired results. The block diagram for the complete linearized system with position and force loops and compensation is shown in Figure 7.

Figure 15 shows the Nyquist plot of the F_{wg}/F_{lim} response for the complete system with the force loop opened and the position loop closed. Figure 16 shows the Nyquist plot of the X_s/X_c response with the position loop open and the force loop closed. Adequate stability margins are exhibited in these plots.

Figures 17 and 18 show the frequency response characteristics of the complete linearized system with the force and position loops closed, for F_{wg}/F_{lim} and X_s/X_c responses, respectively. Note that the bandwidth of the F_{wg}/F_{lim} response is about one hundred times greater than that for the X_s/X_c response.

The sensitivity of the system to hydraulic fluid compressibility was investigated because the effective bulk modulus of the air/oil mixture within the strut is relatively unknown. Throughout this study, a nominal bulk modulus of $6.89 (10^5)$ kPa (100 000 lb/in^2) was used based on past experience with hydraulic systems. Nyquist plots indicating system stability with bulk modulus values of $3.45 (10^5)$ kPa (50 000 lb/in^2) and $1.38 (10^6)$ kPa (200 000 lb/in^2) are shown in Figures 19 and 20. A linearized orifice coefficient of $7.13 (10^{-7})$ m^3/sec/kPa (0.3 in^3/sec/lb/in^2) was used at all frequencies for these cases. A high bulk modulus is destabilizing in the 200-Hz range and a

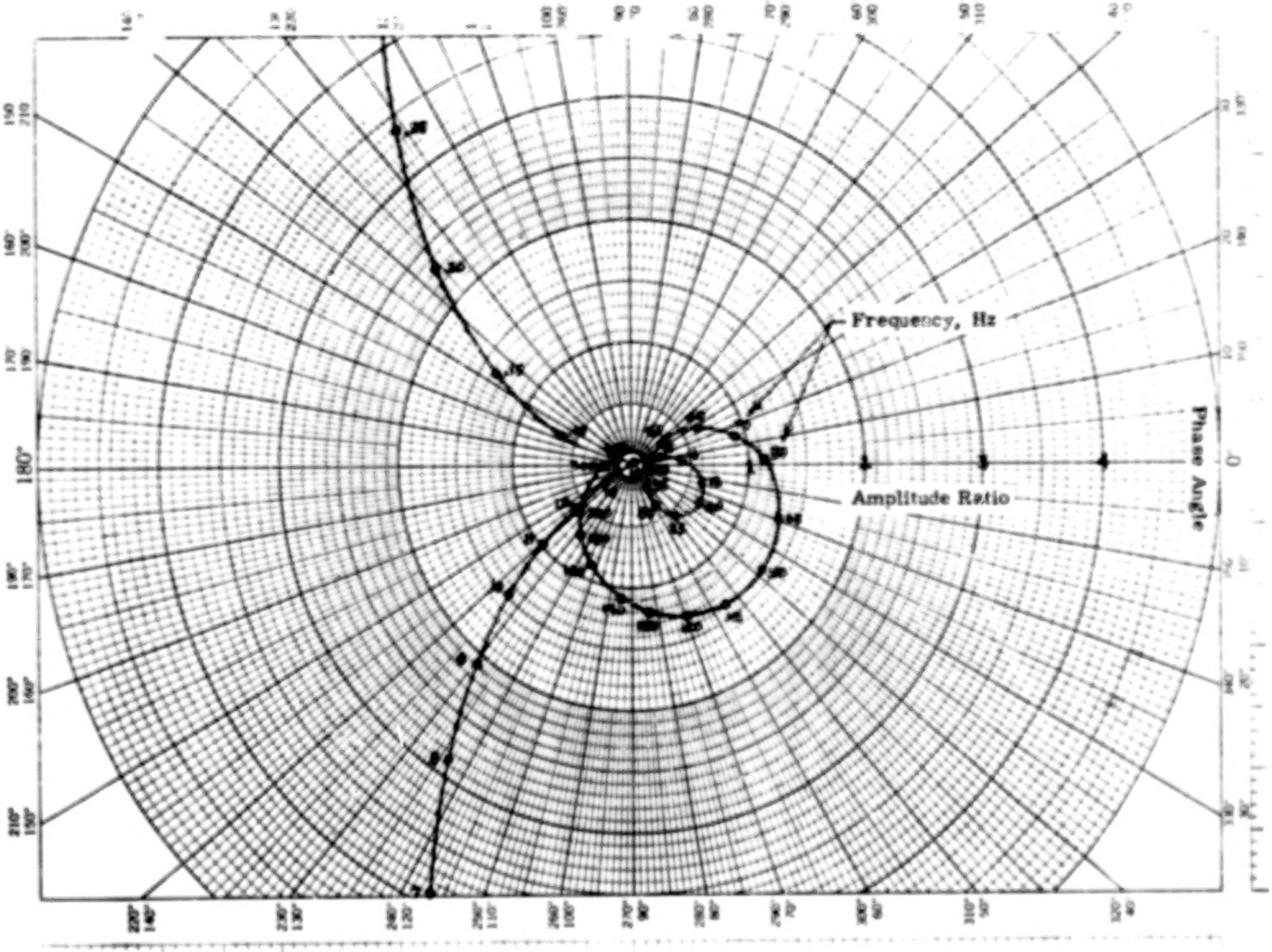

Figure 15. - Nyquist plot of F_{wg}/F_{lim} with force loop opened, position loop closed, with compensation.

BLANK PAGE

BLANK PAGE

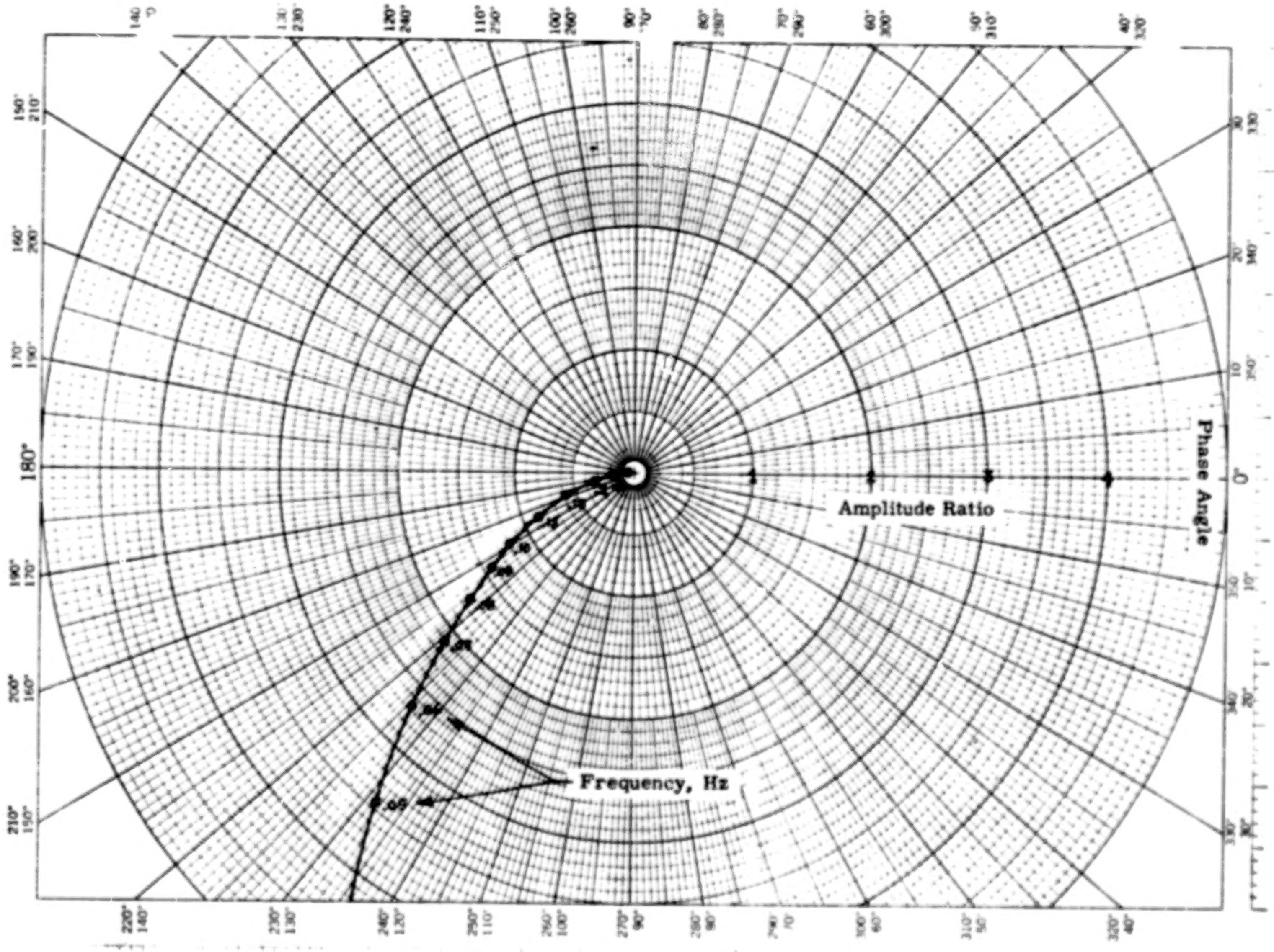

Figure 16. - Nyquist plot of X_s/X_c with position loop opened, force loop closed, with compensation.

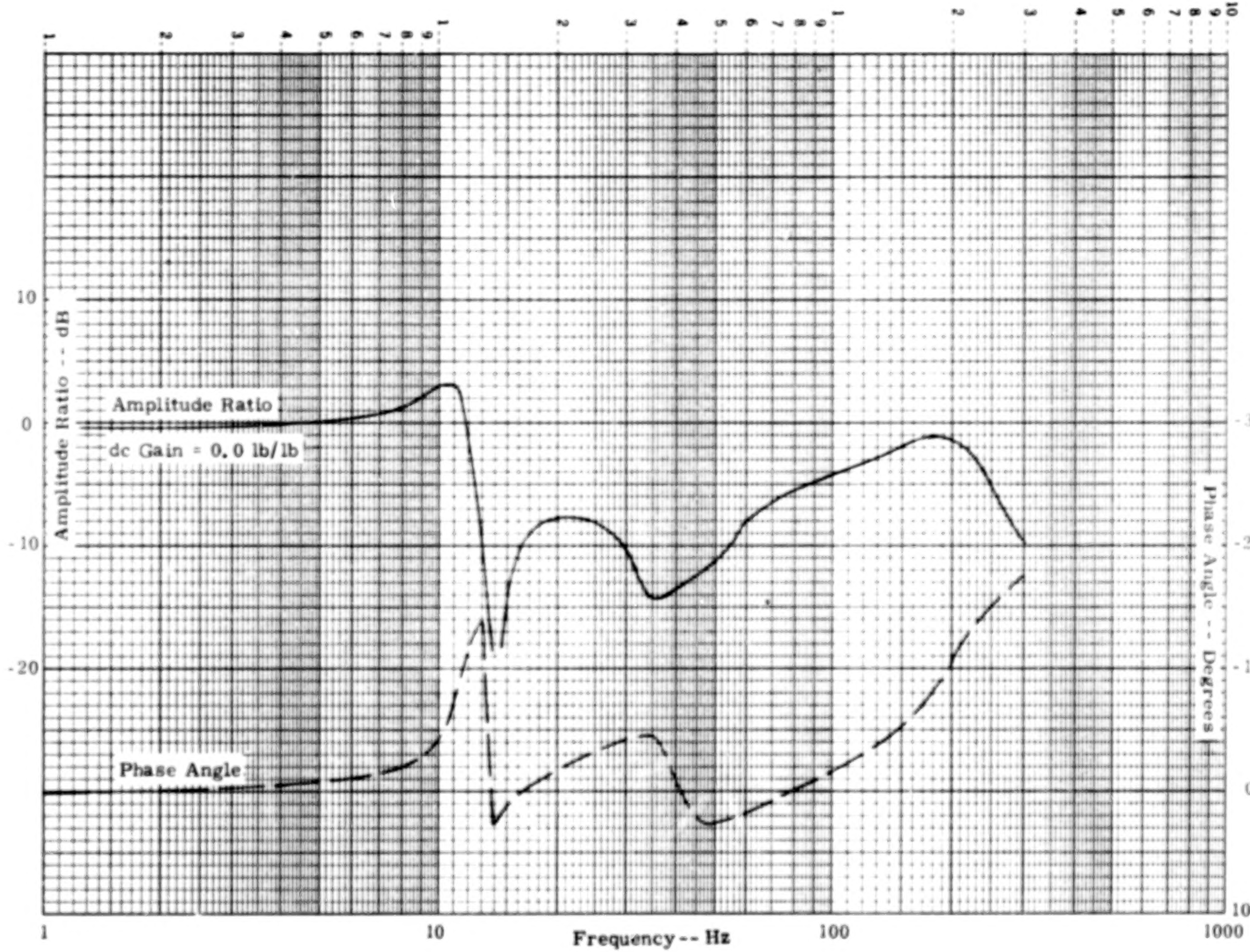

Figure 17. - Frequency response of F_{wg}/F_{lim} with force and position loops closed, with compensation.

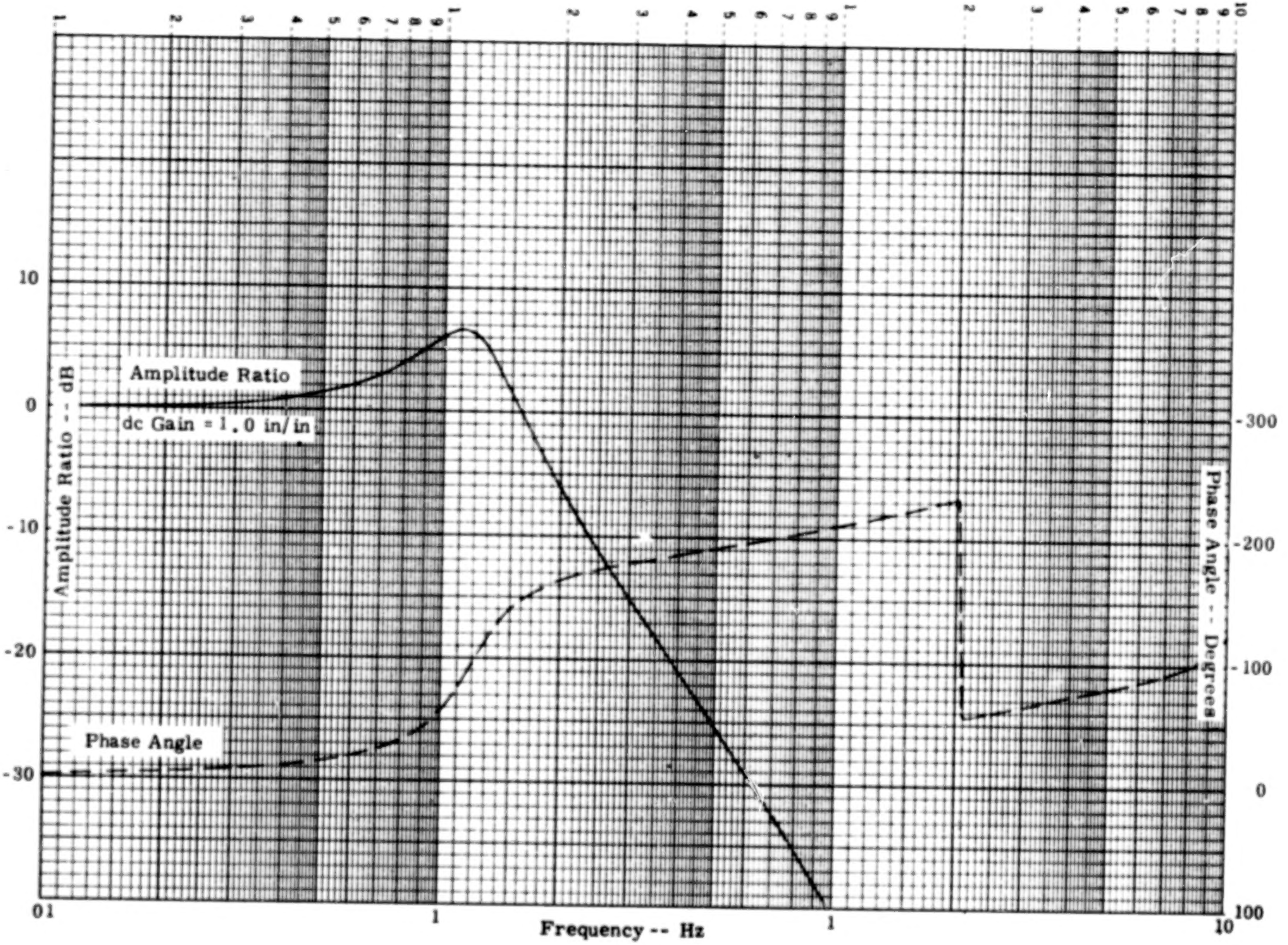

Figure 18. - Frequency response of X_s/X_c with force and position loops closed, with compensation.

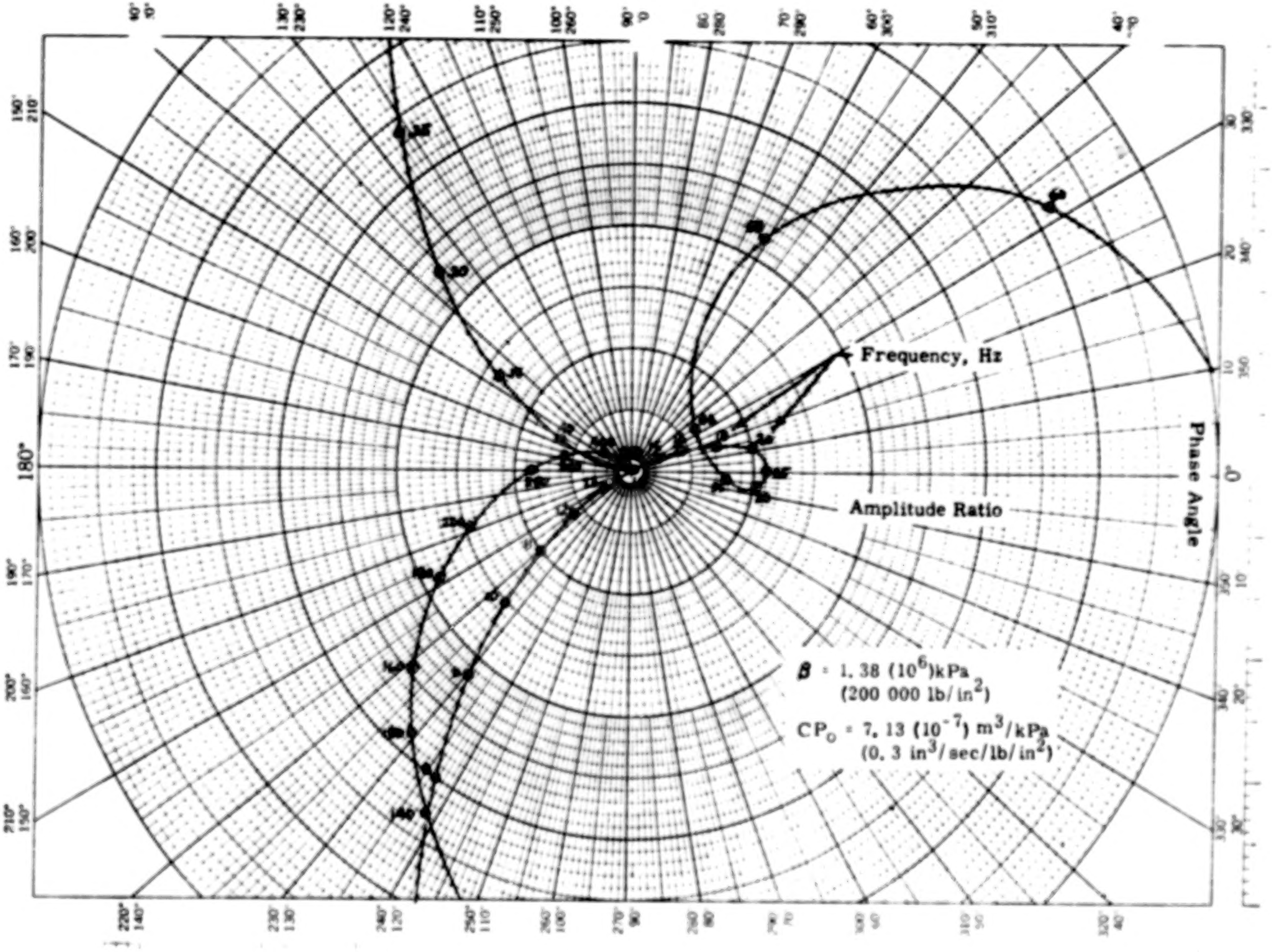

Figure 19. Nyquist plot of F_{wg}/F_{lim} with force loop opened, position loop closed, with compensation.

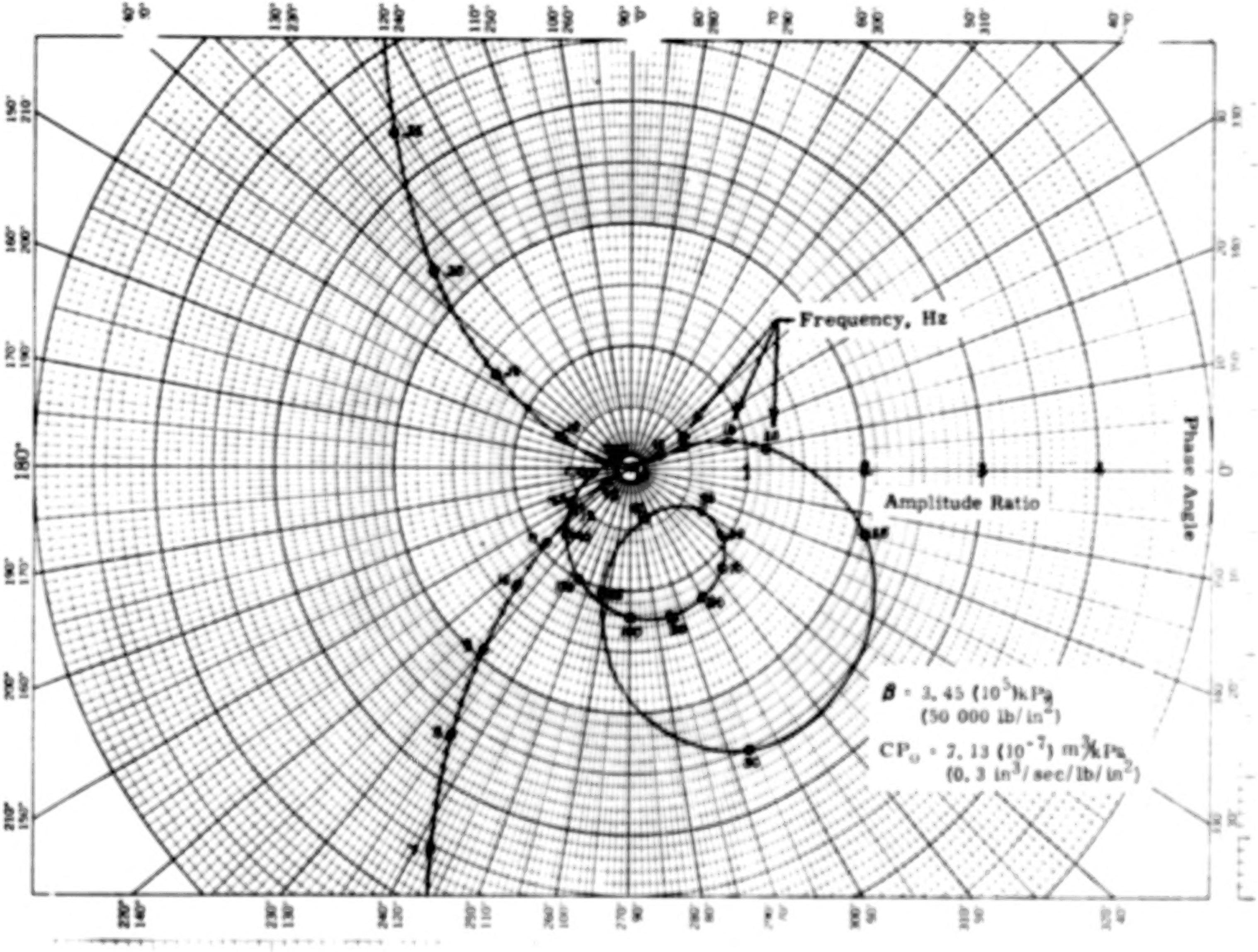

Figure 20. - Nyquist plot of F_{wg}/F_{lim} with force loop opened, position loop closed, with compensation.

low bulk modulus is destabilizing in the 100-Hz range. While these results show some sensitivity to bulk modulus, they are thought to be conservative in light of the model being used. It is expected that the bulk modulus in the actual strut will lie somewhere between 3.45 (10^5) and 1.38 $(10^6)\,m^3/sec/kPa$ (50 000 and 200 000 lb/in^2), and that the system, as configured, will exhibit the desired performance.

ANALYTICAL RESULTS

In this section, transient response results obtained from digital computer simulations are presented for: (1) vertical drop cases using the simplified nonlinear vertical drop model presented earlier, and (2) actual land and roll cases provided by NASA using a NASA-supplied computer program which was modified by HR for incorporation into this study. The purpose of these simulations is to demonstrate that the landing gear controller is developed and described in the previous sections performs the desired functions satisfactorily.

The NASA computer program includes detailed simulation of the aerodynamic and aircraft dynamics in two dimensions, as opposed to the one dimension for the simplified vertical drop model. However, the NASA program as supplied to HR did not contain control system and servovalve dynamics and did not include the effect of fluid compressibility. Therefore, it was modified to include all these items.

Table I lists all the cases which were simulated and reported in this section, along with a brief description of each. Cases will be referred to by the case number shown in the left column. For each case, two simulations were run — one using an active control landing gear and one using a passive gear — so that the performance of the active gear in reducing wing forces could be evaluated.

TABLE I
SUMMARY OF ACTIVE CONTROL LANDING CASES SIMULATED ON THE COMPUTER

Case No.	Type	Sink Rate m/sec(in/sec)	Forward Speed m/sec(in/sec)	Miscellaneous Comments	Peak Strut Stroke	Reduction in Peak F_{wg} due to Active Control
A*	Vertical	1.83 (72)	0	Lift=Weight	95%	28%
B*	Drop	1.83 (72)	0	Lift=Weight initially, linearly decreased by 50% over 0.4 sec interval	97%	23%
1	Land and Roll	1.83 (72)	42.7 (1680)	Sinusoidal runway (3Hz, ±0.0254 m (1 in)	91%	11%
2		1.83 (72)	42.7 (1680)	Flat runway, no braking	99%	23%
3		1.22 (48)	42.7 (1680)	Sinusoidal runway (.5 Hz, ±0.0254 m (1 in)	92%	18%
4		1.22 (48)	42.7 (1680)	Flat runway	83%	17%

* K_{FDGE} = 0.9 All other Cases K_{FDGE} = 1.0

Vertical Drop Cases

Figure 21 shows the commanded and actual wing gear forces occurring during the initial impact and transition phases for Case A. The total lift force is set equal to the total weight throughout this transient; and, as a consequence, the landing gear eventually lifts off the ground (or rebounds) after 0.754 seconds. At that time, the gear is fully extended and the system has some finite upward velocity which it continues to maintain as long as the lift stays equal to the weight. Figure 21 also shows the forces for the passive gear case. A 28% reduction in peak wing/gear force is obtained when using active control.

Figure 22 shows the forces for Case B. This is the same as Case A, except that starting from the instant of impact the lift force is linearly reduced to one half of its initial value. This reduction occurs over a time interval of 0.4 seconds. The gear does not leave the ground for this case. A 23% reduction in peak wing gear force from the passive gear case is obtained. The response of the strut stroke is shown in Figure 23. As the impact transients subside, the strut approaches the value commanded by the strut positioning loop.

Land and Roll Cases

Figure 24 shows the commanded and actual wing/gear forces occurring during the initial impact and transition phases for Case 1, which uses a 3-Hz, 0.0254 m (1-inch) amplitude sinusoidal runway for the first 3.083 seconds, then a flat runway. For this case, an 11% reduction in peak wing/gear force is obtained when using active control. Figure 25 shows the pressures in the strut as a function of time. Figure 26 shows the strut stroke transient. At a time of 1.86 seconds, the strut hits the stops in the fully extended position and remains there until 2.01 seconds. Figures 27 and 28 show the wing gear force

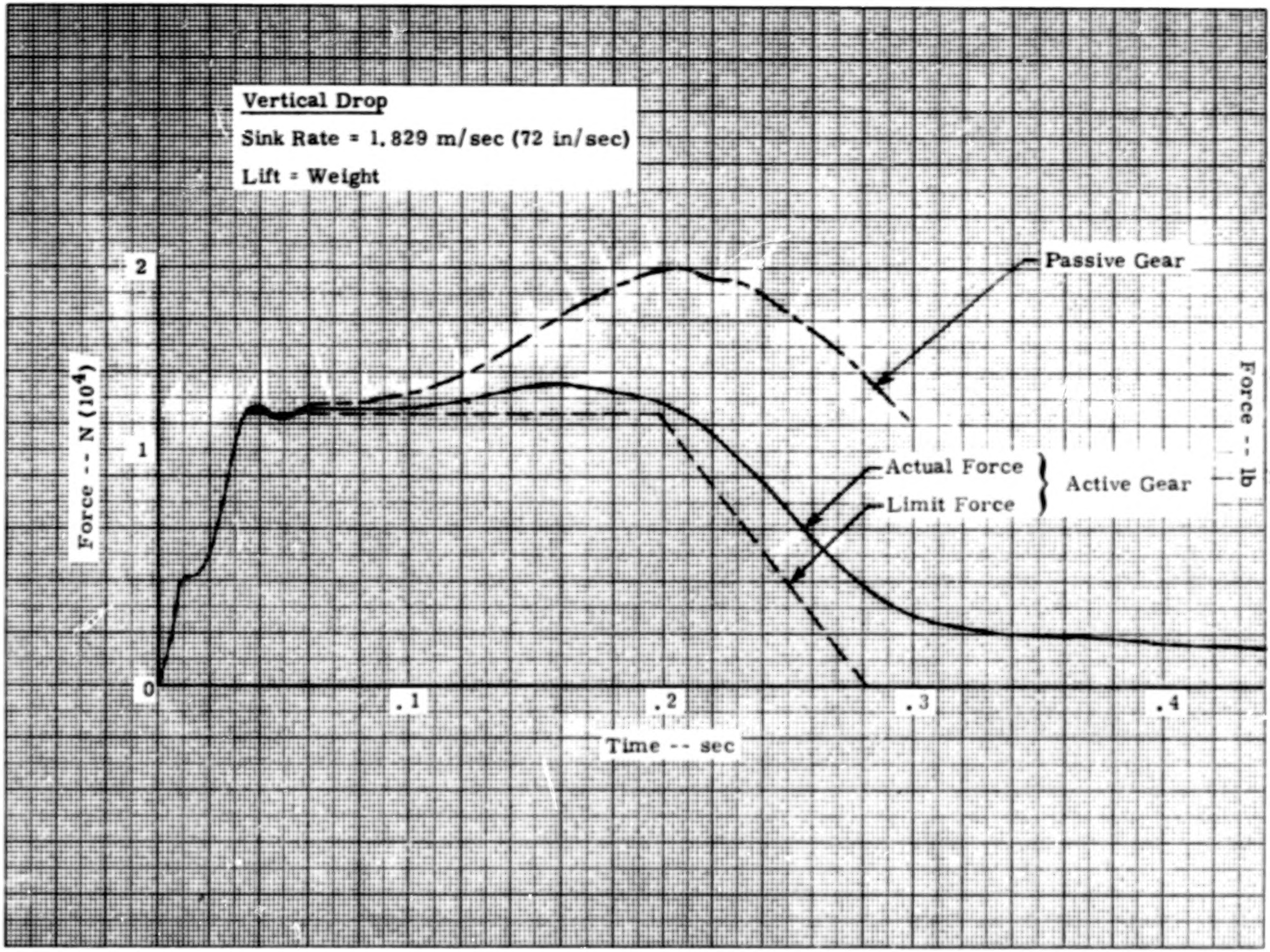

Figure 21. - Wing/gear force transient, case A.

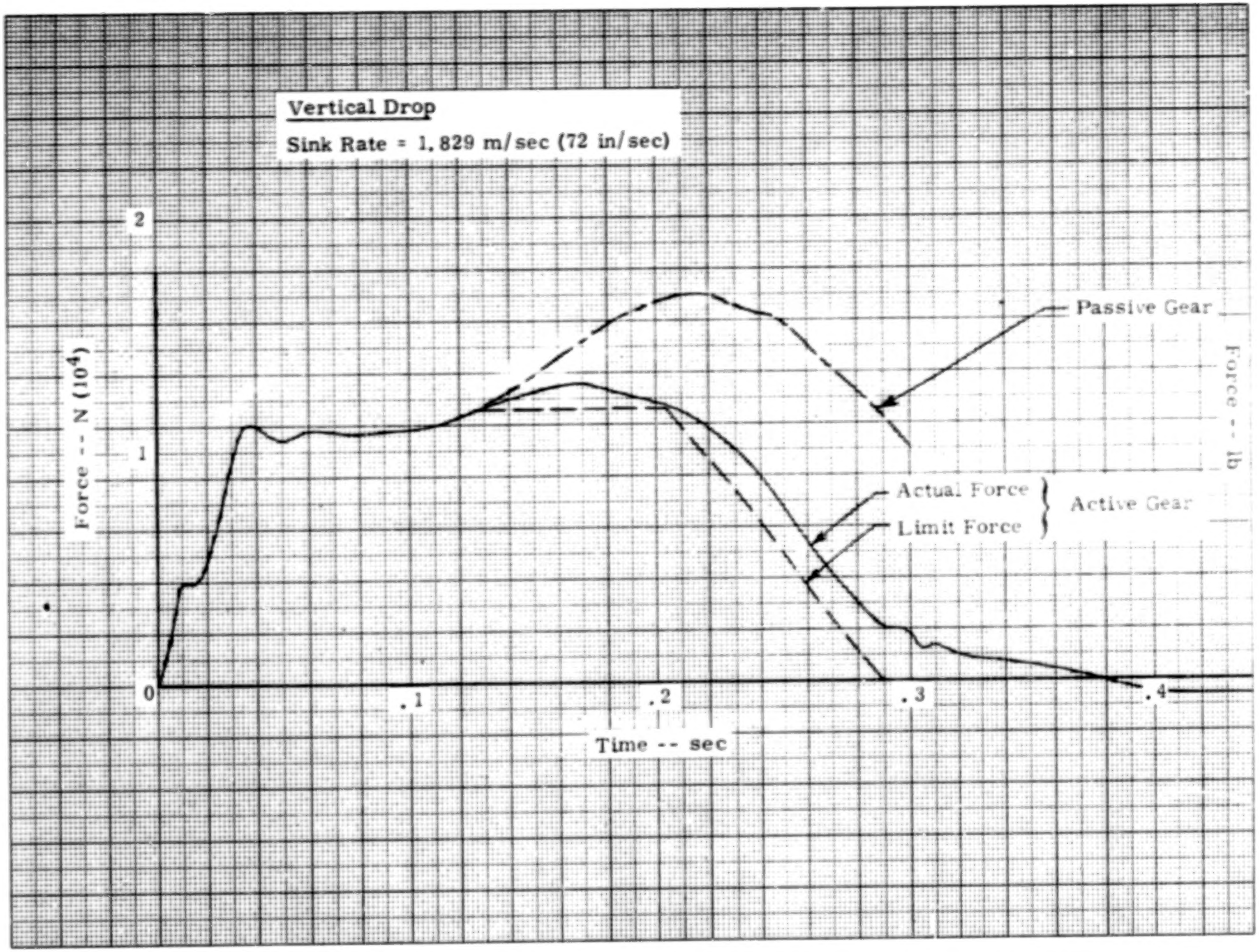

Figure 22. - Wing/gear force transient, case B.

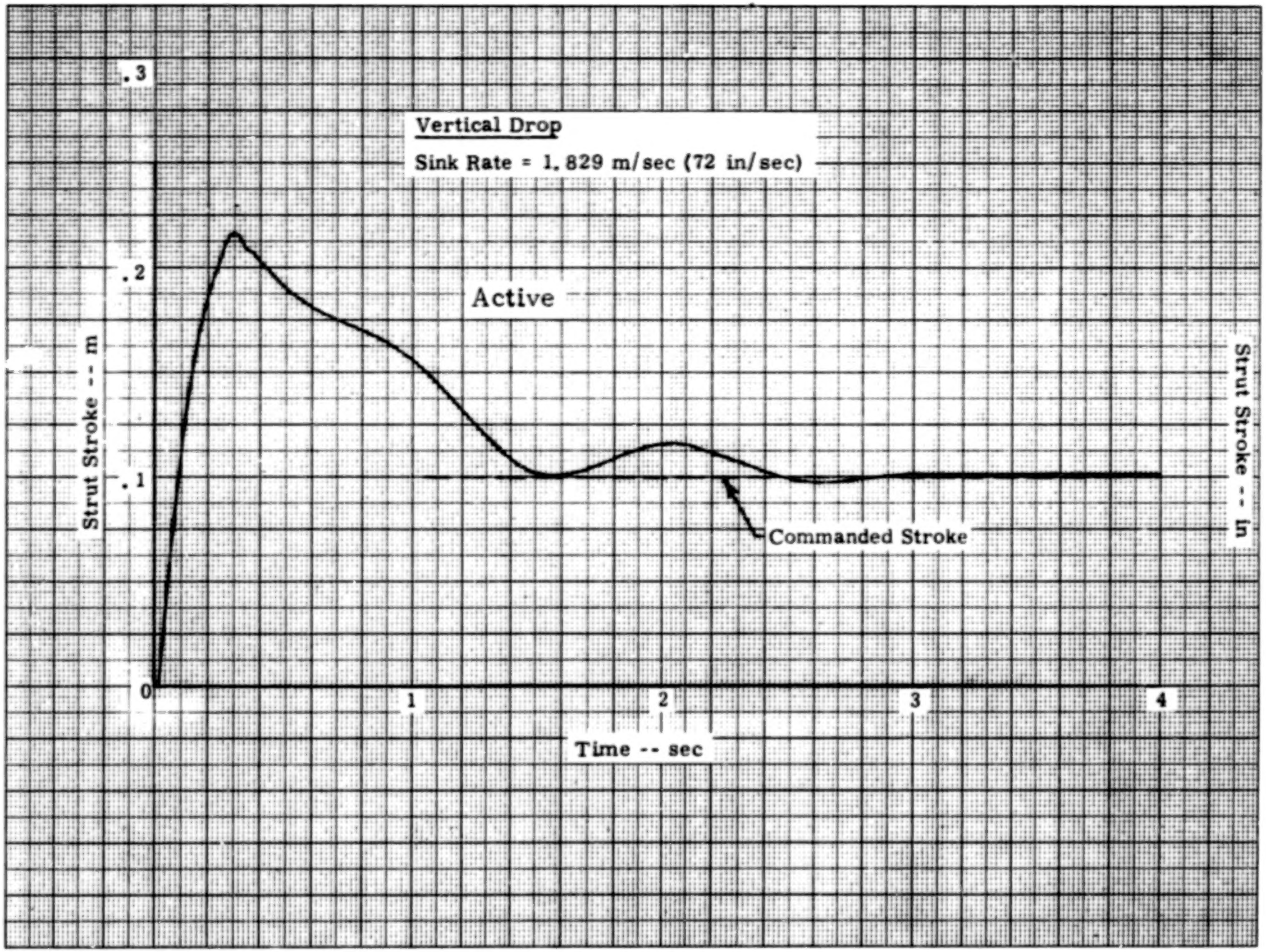

Figure 23. - Strut position transient, case B.

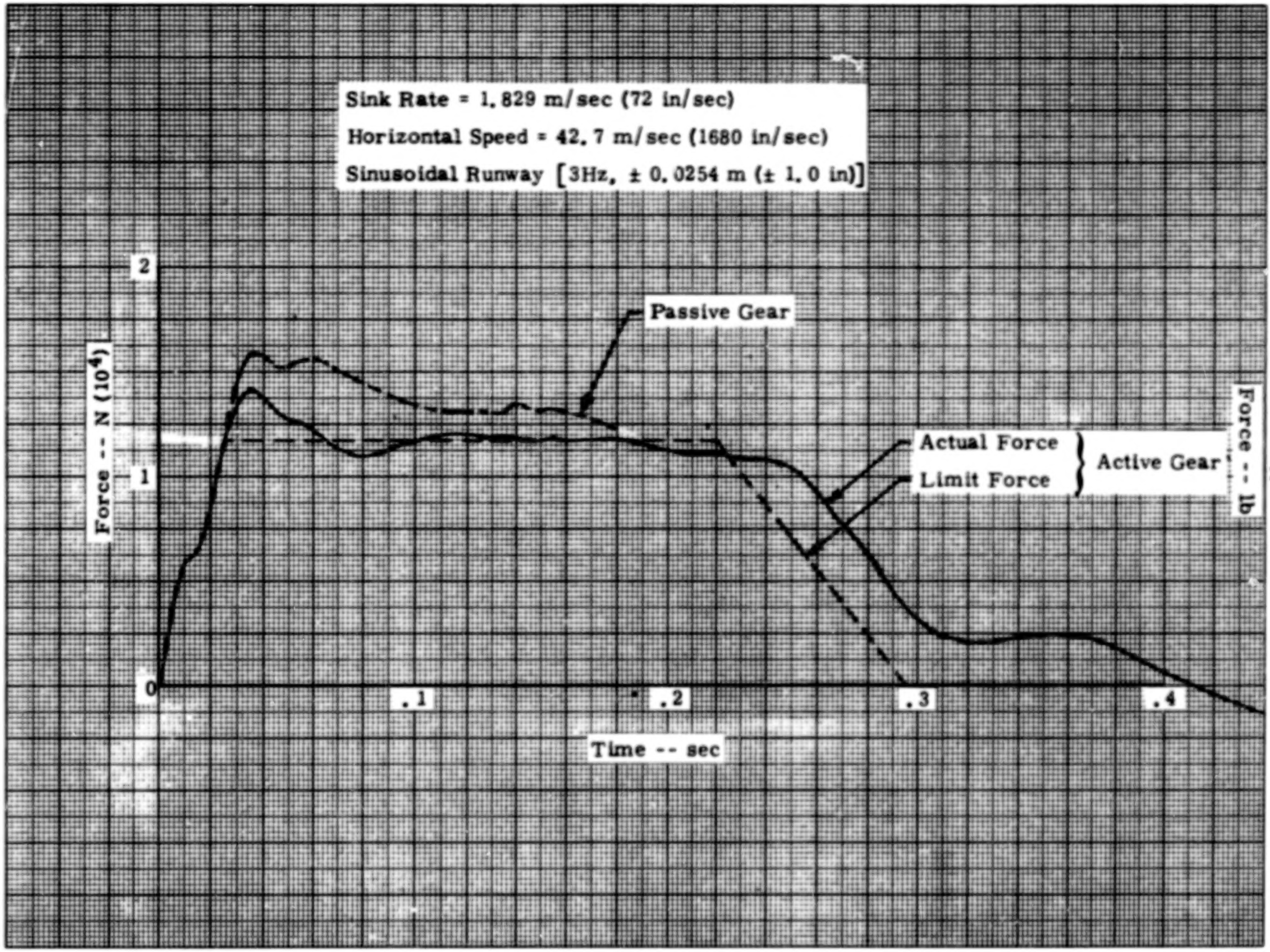

Figure 24. - Wing/gear force transient, case 1.

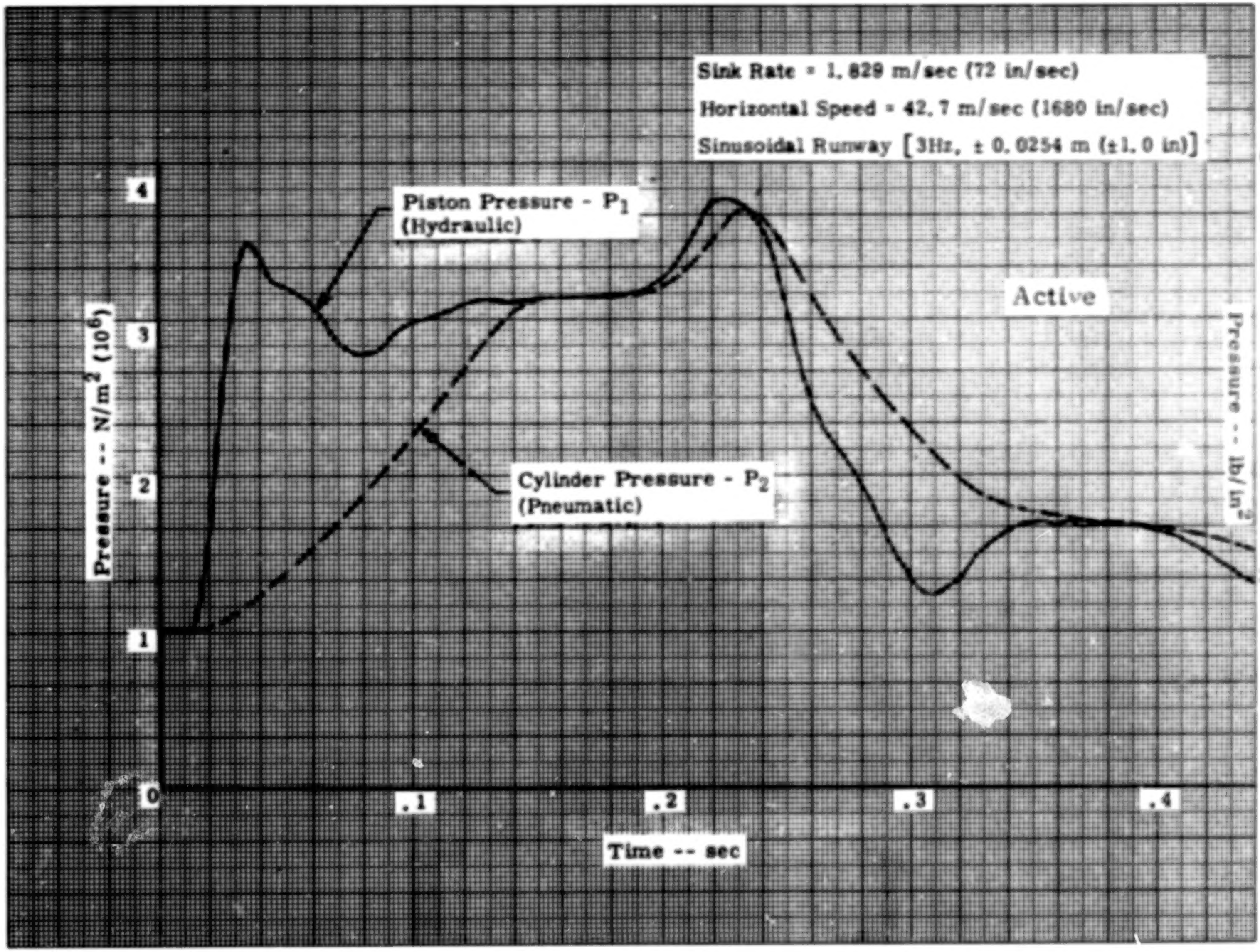

Figure 25. - Strut pres[illegible]res, case 1.

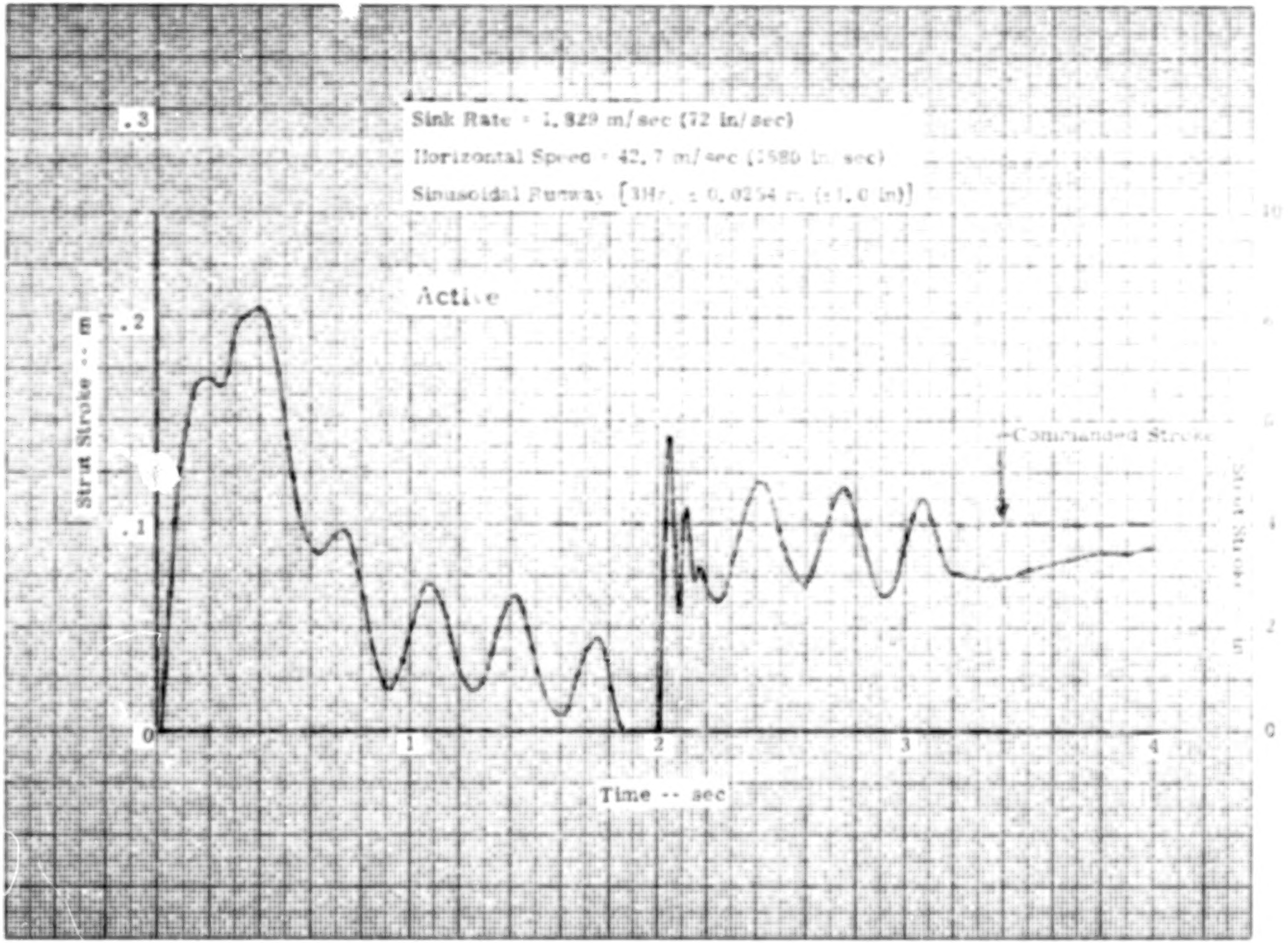

Figure 26. - Strut position transient, case 1.

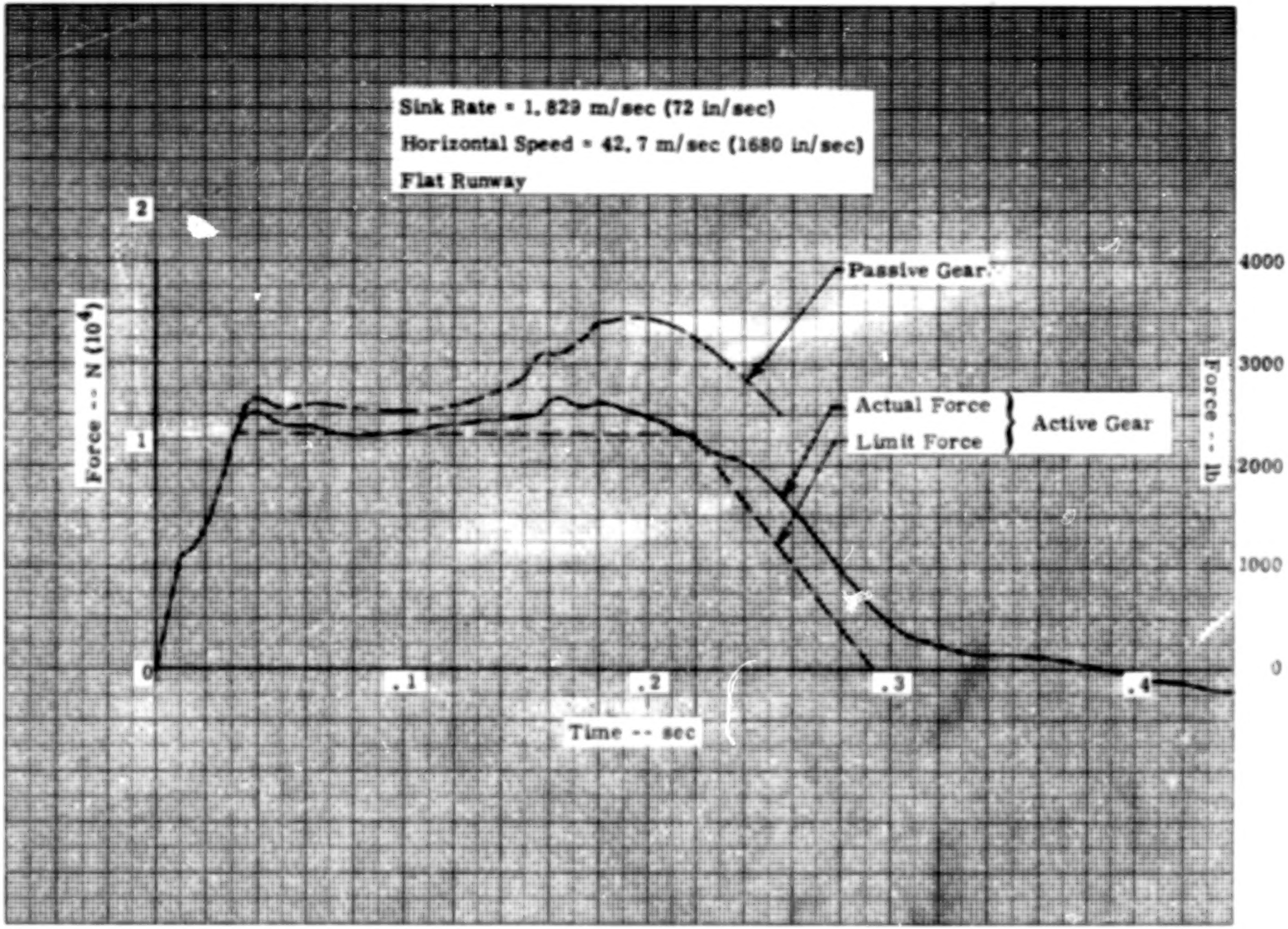

Figure 27. - Wing/gear force transient, case 2.

CONTENTS

Page

SUMMARY 1 1/A14

INTRODUCTION 1 1/A14

SYMBOLS. 3 1/B2

ANALYSIS 8 1/B7
- Nonlinear Math Model for Vertical Drops 8 1/B7
  - Equations of Motion 10 1/B9
  - Pressure, Flow, and Volume Relationship 14 1/B14
  - Servovalve Dynamics 16 1/C2
- Linear Math Model for Vertical Drops 18 1/C5
- Energy Considerations 27 1/D1
- Stability Analysis 39 1/E2

ANALYTICAL RESULTS 51 1/F11
- Vertical Drop Cases 53 1/F14
- Land and Roll Cases 53 1/F14

CONTROLLER FUNCTIONAL DESCRIPTION 71 2/B11
- Associated Equipment. 71 2/B11
- Interface 71 2/B11
- Performance Characteristics 76 2/C7
- Operating-Mode Determination. 76 2/C7
  - Landing Mode 76 2/C7
  - Takeoff Mode 77 2/C8
- Limit-Force Command Determination 78 2/C9
- Control Law Implementation 78 2/C9
- Controller Design 78 2/C9
  - Functional Sections 78 2/C9

CONTENTS (Contd.)

Page

TEST 89 2/E1

Test Fixture 89 2/E1

Test Conditions 93 2/E6

Test Results 93 2/E6

CONCLUSIONS 114 3/A9

APPENDIX

A Microprocessor Program Listing 115 3/A10

B Electronic Controller Detailed Description 131 3/B12

C Test Procedure 142 3/C11

D Oscillograph Recordings 148 3/D4

FIGURES

1 Illustration of variables used in nonlinear simulation of simplified vertical drop case 9 1/B8

2 Free body diagram of airplane mass 11 1/B10

3 Free body diagram of upper shock strut 11 1/B10

4 Free body diagram of lower shock strut 11 1/B10

5 Dynamic response of servovalve, ±10% input signal . . . 17 1/C3

6 Illustration of "Equivalent" system for the linear math model. 22 1/C9

7 Block diagram of linear math model 26 1/C13

8 Comparison of linear model and nonlinear model results, open loop, no compensation, no position feedback 28 1/D2

9 Various energy terms versus time, from the simplified nonlinear vertical drop simulation 33 1/D8

10 Illustration of the variation of limit force versus time and the various phases of operation following impact . . . 35 1/D11

11 Block diagram of linear system without compensation . . 40 1/E3

CONTENTS (Contd.)

Page

FIGURES

12 Nyquist plot of F_{wg}/F_{lim} with force loop opened, no position feedback, no compensation 41 1/E5

13 Electronic compensation network and its characteristics . . 42 1/E7

14 Nyquist plot of F_{wg}/F_{lim} with force loop opened, no position feedback, with compensation 43 1/E9

15 Nyquist plot of F_{wg}/F_{lim} with force loop opened, position loop closed, with compensation 45 1/E12

16 Nyquist plot of X_s/X_c with position loop opened, force loop closed, with compensation 46 1/F1

17 Frequency response of F_{wg}/F_{lim} with force and position loops closed, with compensation 47 1/F3

18 Frequency response of X_s/X_c with force and position loops closed, with compensation 48 1/F5

19 Nyquist plot of F_{wg}/F_{lim} with force loop opened, position loop closed, with compensation. 49 1/F7

20 Nyquist plot of F_{wg}/F_{lim} with force loop opened, position loop closed, with compensation. 50 1/F9

21 Wing/gear force transient, case A 54 1/G1

22 Wing/gear force transient, case B 55 1/G3

23 Strut position transient, case B 56 1/G5

24 Wing/gear force transient, case 1 . . . . 57 1/G7

25 Strut pressures, case 1 . . . . 58 1/G9

26 Strut position transient, case 1 . . . . 59 1/G11

27 Wing/gear force transient, case 2 . . . . 60 1/G13

28 Strut position transient, case 2 . . . . 61 2/A6

29 Wing/gear force transient, case 3 . . . . 63 2/A9

30 Wing/gear force transient, case 4 . . . . 64 2/A11

31 Servovalve flow rate, case A 65 2/A13

32 Servovalve flow rate, case B 66 2/B1

CONTENTS (Contd.)

Page

FIGURES

33 Servovalve flow rate, case 1 . . . . 67 2/B3

34 Servovalve flow rate, case 2 . . . . 68 2/B5

35 Servovalve flow rate, case 3 . . . . 69 2/B7

36 Servovalve flow rate, case 4 . . . . 70 2/B9

37 Input/Output Signal Schematic 72 2/B10

38 Control Law Functional Schematic 79 2/C10

39 Controller Functional Schematic 81 2/D1

40 Basic Functional Requirements 82 2/D3

41 Software Flow Chart 84 2/D6

42 Analog Section Schematic 85 2/D8

43 Analog Section - Front Panel Inputs 87 2/D11

44 Analog Section - Front Panel Outputs 88 2/D13

45 S-1C Test Fixture, Landing Gear Installed (View 1) . . . 90 2/E2

46 S-1C Test Fixture, Landing Gear Installed (View 2) . . . 91 2/E3

47 Net Force, Conditions 1, 4 (From W/G Accel #1) 95 2/E9

48 Net Force, Conditions 2, 5 (From W/G Accel #1) 96 2/E11

49 Net Force, Conditions 3, 6 (From W/G Accel #1) 97 2/E13

50 Net Force, Conditions 7, 10 (From W/G Accel #1) 98 2/F1

51 Net Force, Conditions 8, 11 (From W/G Accel #1) 99 2/F3

52 Net Force, Conditions 9, 12 (From W/G Accel #1) 100 2/F5

53 Gear Hydraulic Pressure, Conditions 1, 4 . . . . 101 2/F7

54 Gear Hydraulic Pressure, Conditions 2, 5 . . . . 102 2/F9

55 Gear Hydraulic Pressure, Conditions 3, 6 . . . . 103 2/F11

56 Gear Hydraulic Pressure, Conditions 7, 10 . . . . 104 2/F12

57 Gear Hydraulic Pressure, Conditions 8, 11 . . . . 105 2/G1

58 Gear Hydraulic Pressure, Conditions 9, 12 . . . . 106 2/G3

CONTENTS (Contd.)

Page

FIGURES

59 **Strut Deflection,** Conditions 1, 4 . . . . 107 2/G5

60 **Strut Deflection,** Conditions 2, 5 . . . . 108 2/G7

61 **Strut Deflection,** Conditions 3, 6 . . . . 109 2/G9

62 **Strut Deflection,** Conditions 7, 10 . . . . 110 2/G11

63 **Strut Deflection,** Conditions 8, 11 . . . . 111 2/G13

64 **Strut Deflection,** Conditions 9, 12 . . . . 112 3/A6

TABLES

I SUMMARY OF ACTIVE CONTROL LANDING CASES SIMULATED ON THE COMPUTER 52 1/F12

II PRIMARY INPUT SIGNAL SPECIFICATIONS 73 2/C1

III SECONDARY INPUT SPECIFICATIONS 74 2/C3

IV OUTPUT SPECIFICATIONS 75 2/C5

V CONTROL LAW TRANSFER FUNCTIONS. 80 2/C12

VI PEAK FORCES AND PERCENTAGE REDUCTION. 94 2/E7

REFERENCES. 161 3/F1

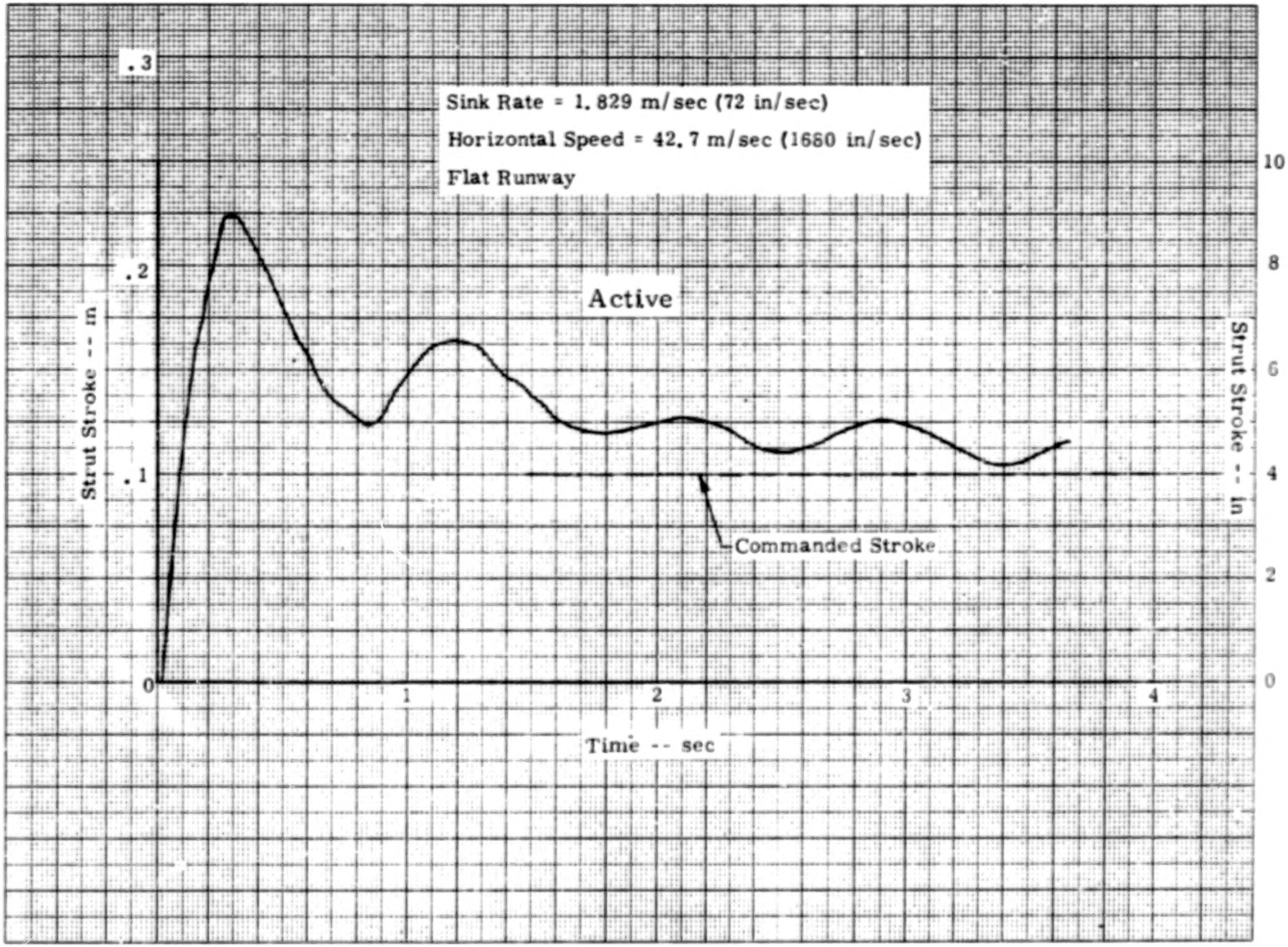

Figure 28. - Strut position transient, case 2.

and strut stroke transients for Case 2, which is the same as Case 1 except it uses a flat runway and has no wheel braking, while Figures 29 and 30 show the wing/gear force transients for Cases 3 and 4.

The flow rate through the servovalve of the active control landing gear during landing impacts is also of interest. Figures 31 through 36 show the time histories of the servovalve flow rates for each of the landings simulated herein. Positive flow is flow from supply to the piston chamber and negative flow is flow from the piston chamber to return.

Table I summarizes the amount of wing gear force reduction that was obtained from using active control for each of the cases reported in this section. From inspection of the force transients it appears that the reduction for some cases could be improved by increasing the bandwidth of the controller, which is presently about 10 Hz. This would reduce the magnitude of the initial overshoot. However, increasing the bandwidth would likely require more complex electronic compensation than that presently being used. In the absence of specific requirements, the results presented herein are judged satisfactory. The analyses indicate that the basic concept is workable.

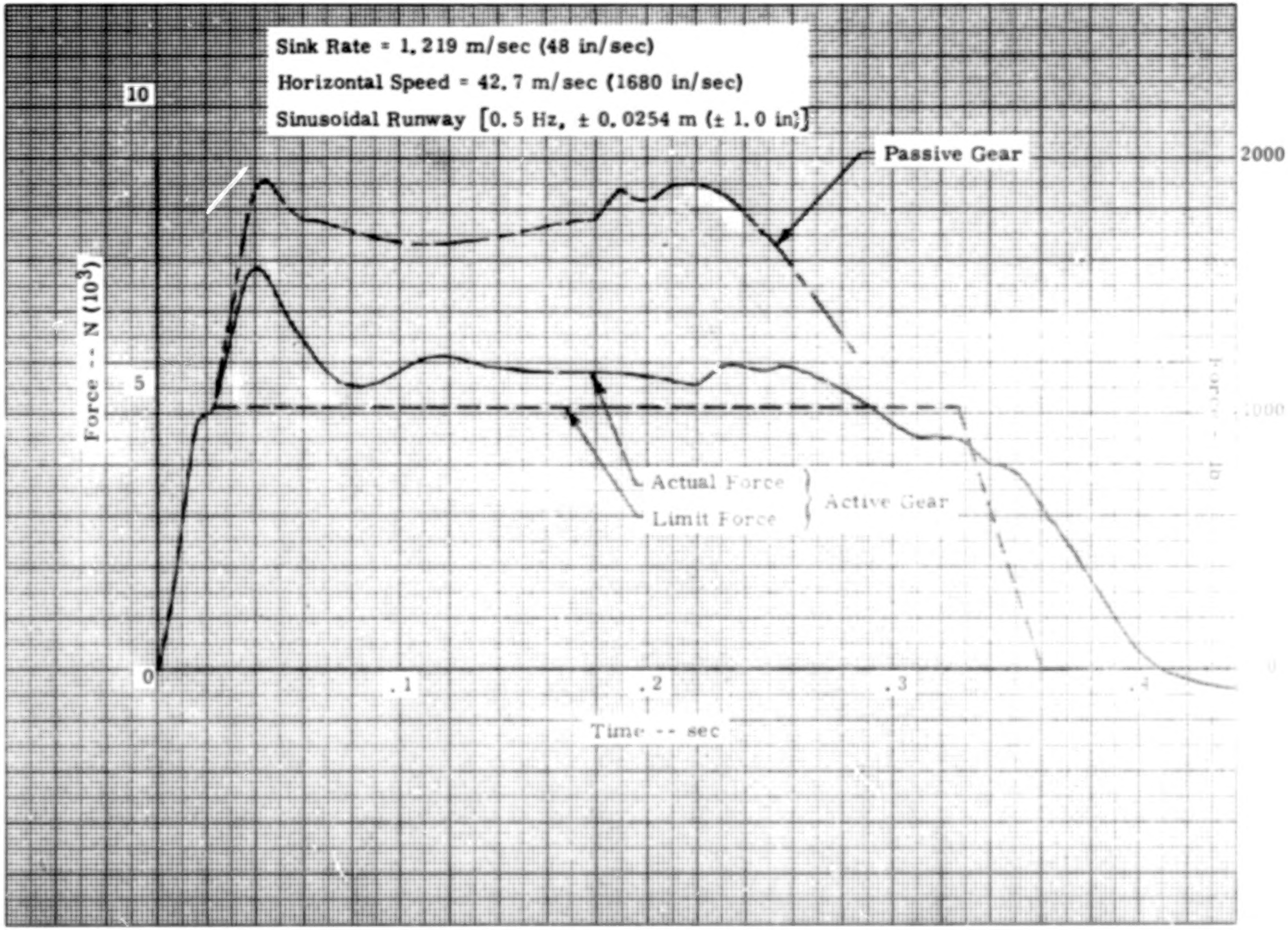

Figure 29. - Wing/gear force transient, case 3.

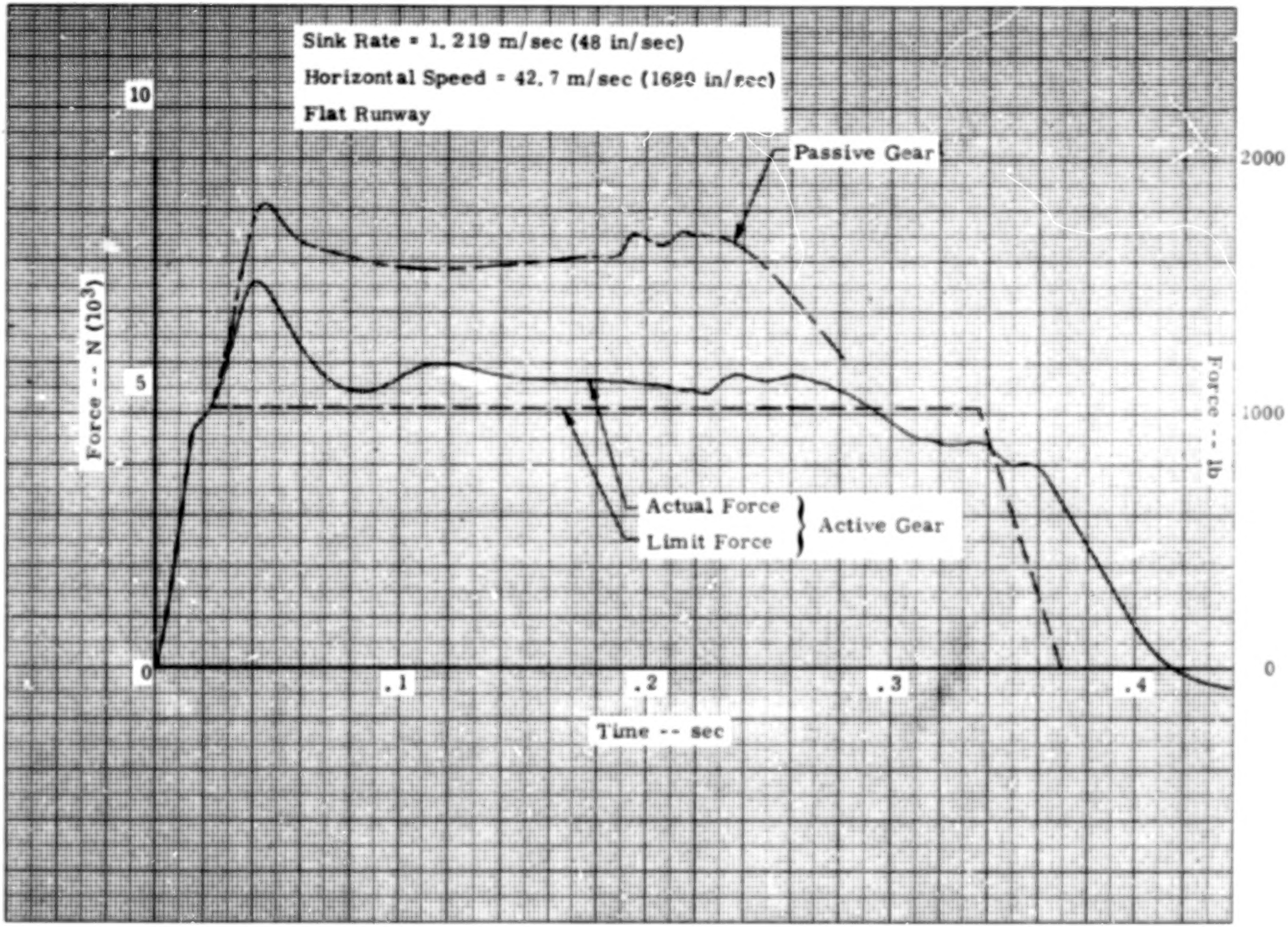

Figure 30. - Wing/gear force transient, case 4.

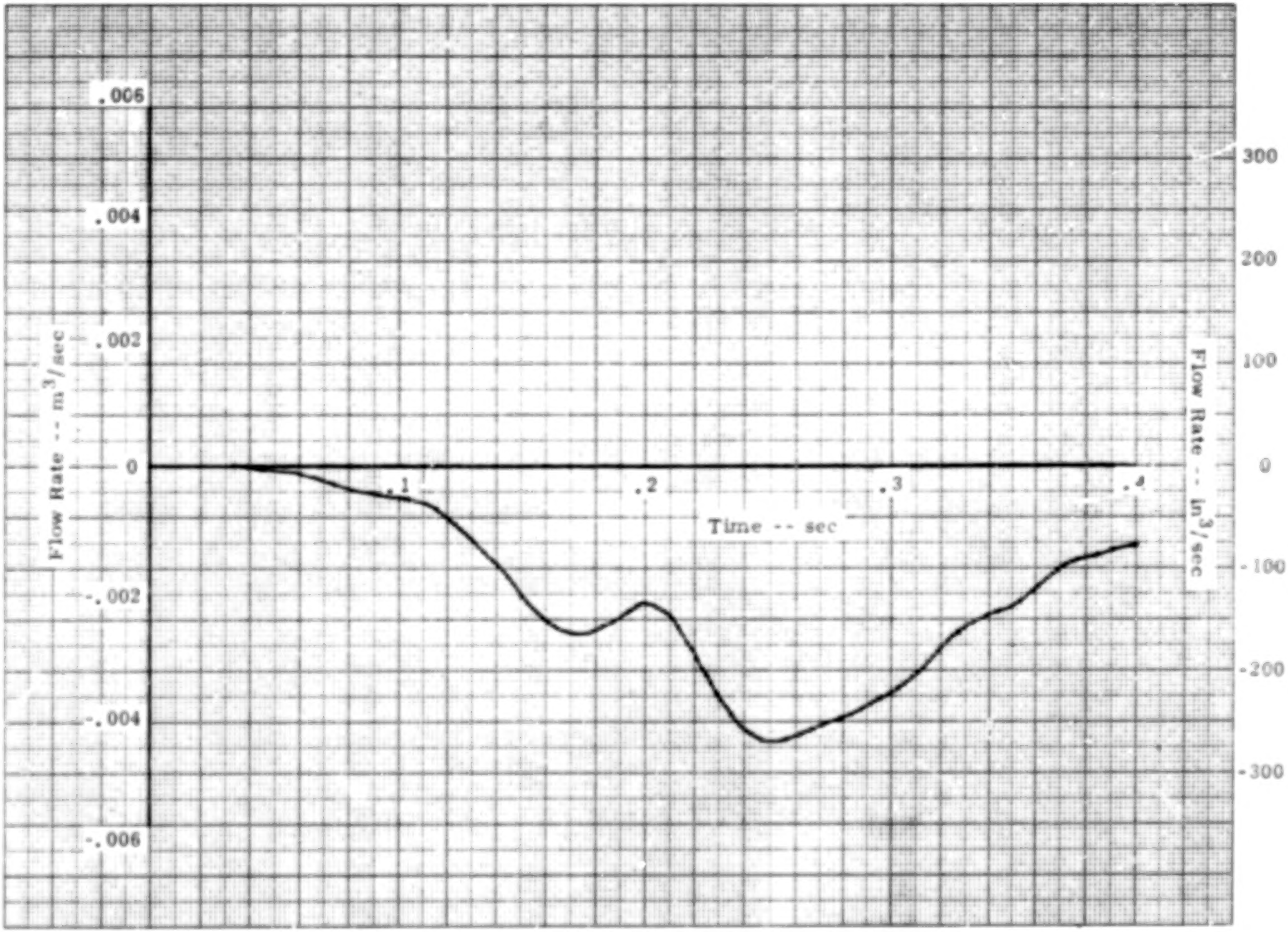

Figure 31. - Servovalve flow rate, case A.

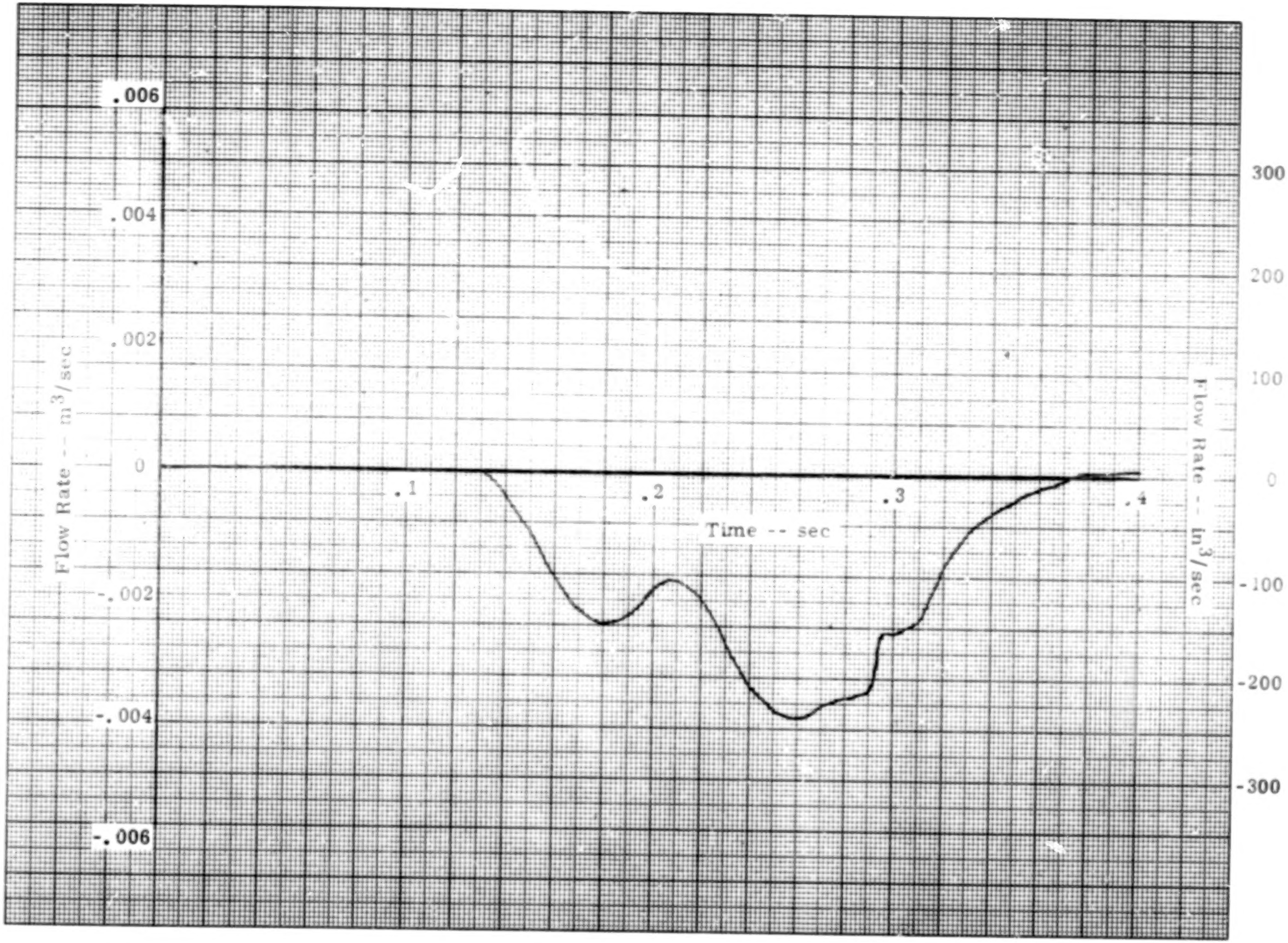

Figure 32. - Servovalve flow rate, case B.

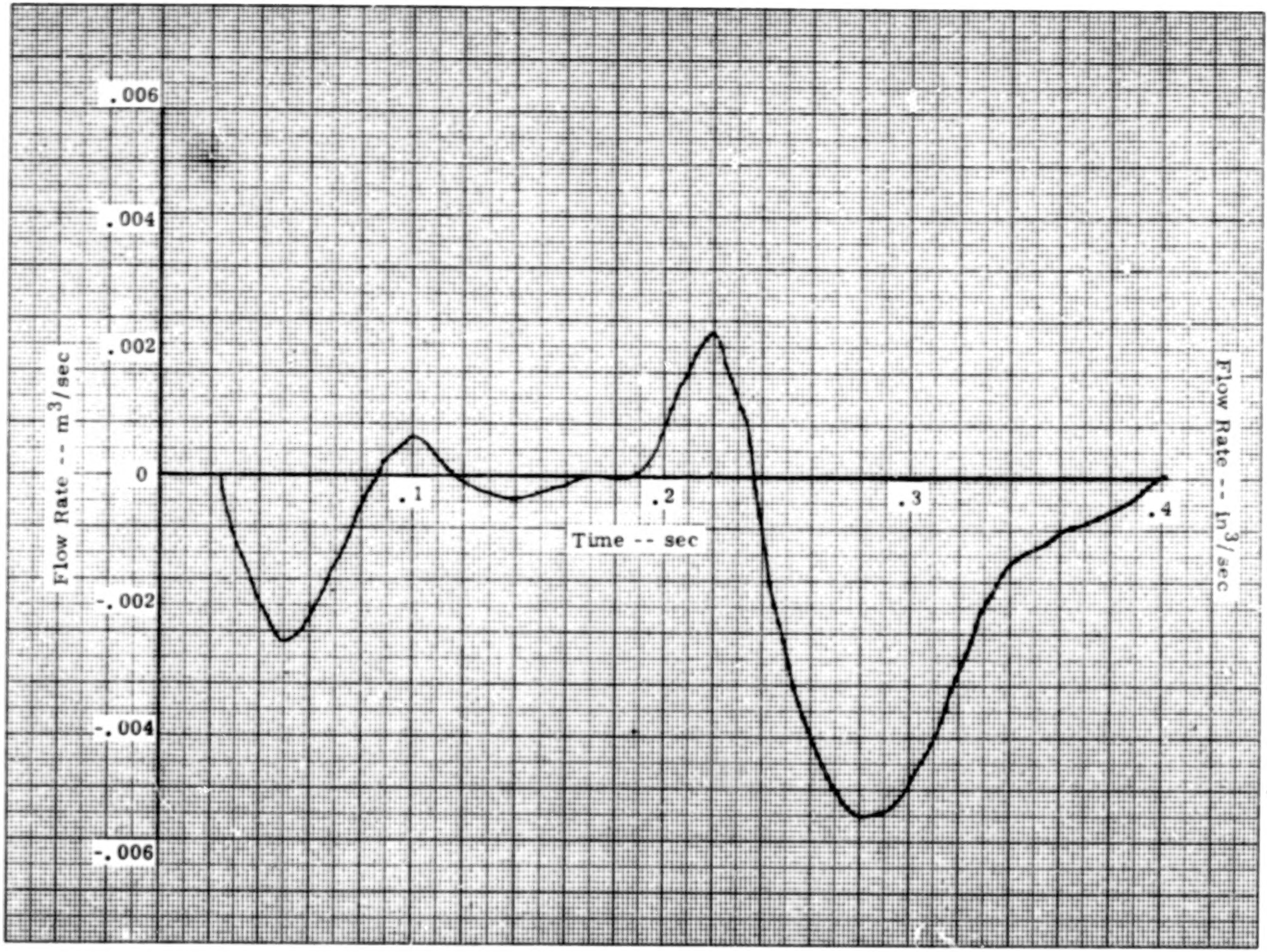

Figure 33. - Servovalve flow rate, case 1.

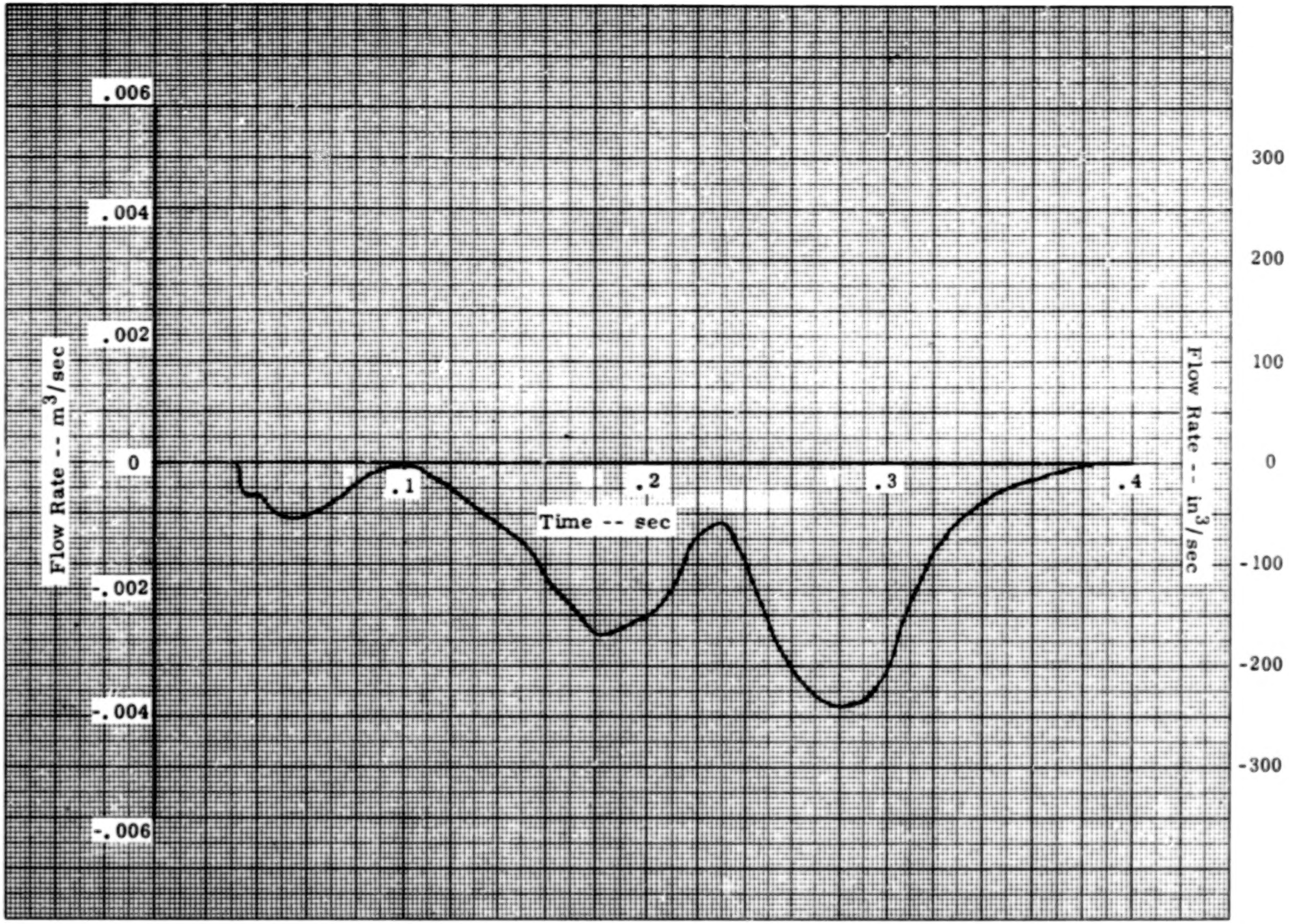

Figure 34. - Servovalve flow rate, case 2.

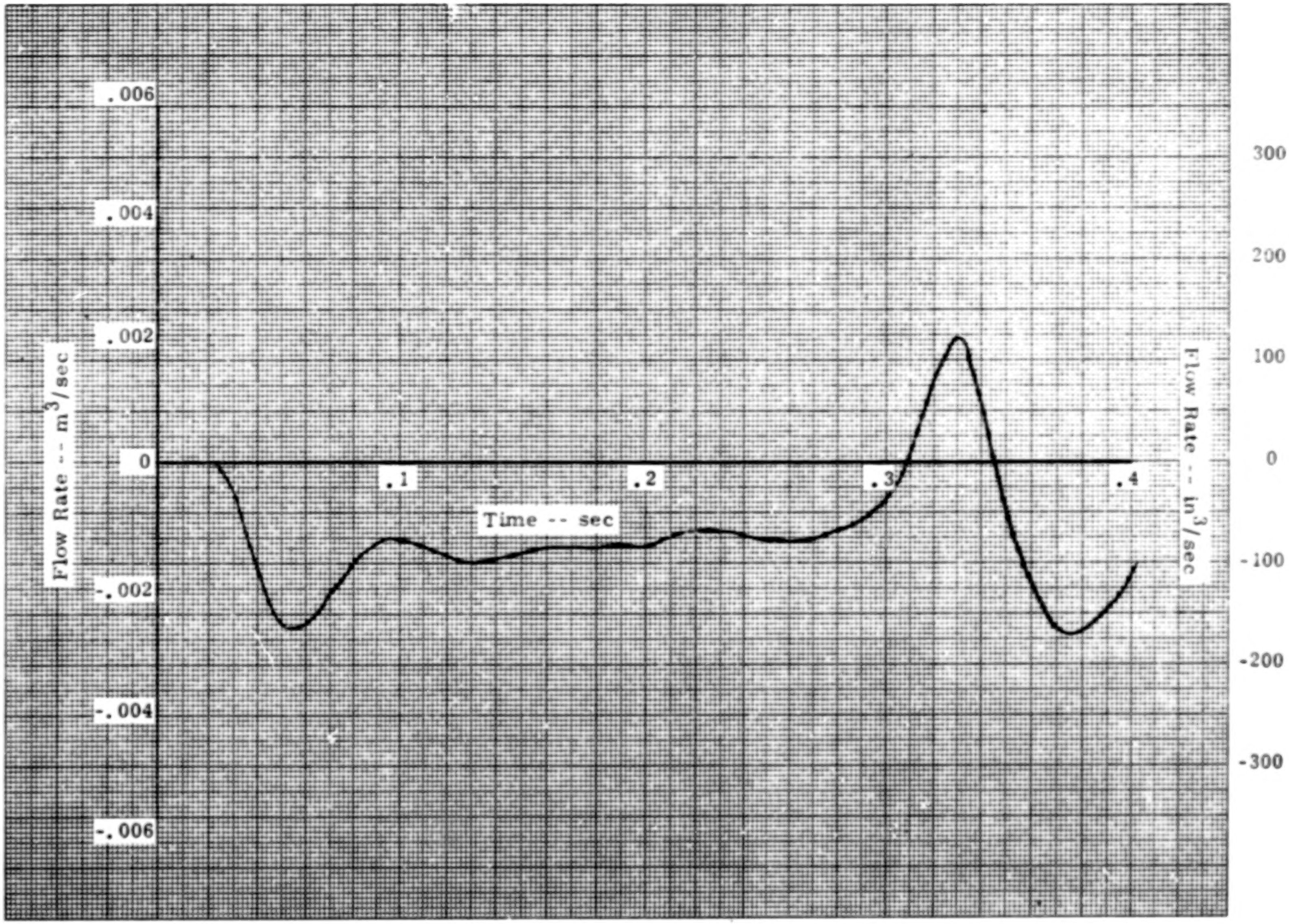

Figure 35. - Servovalve flow rate, case 3.

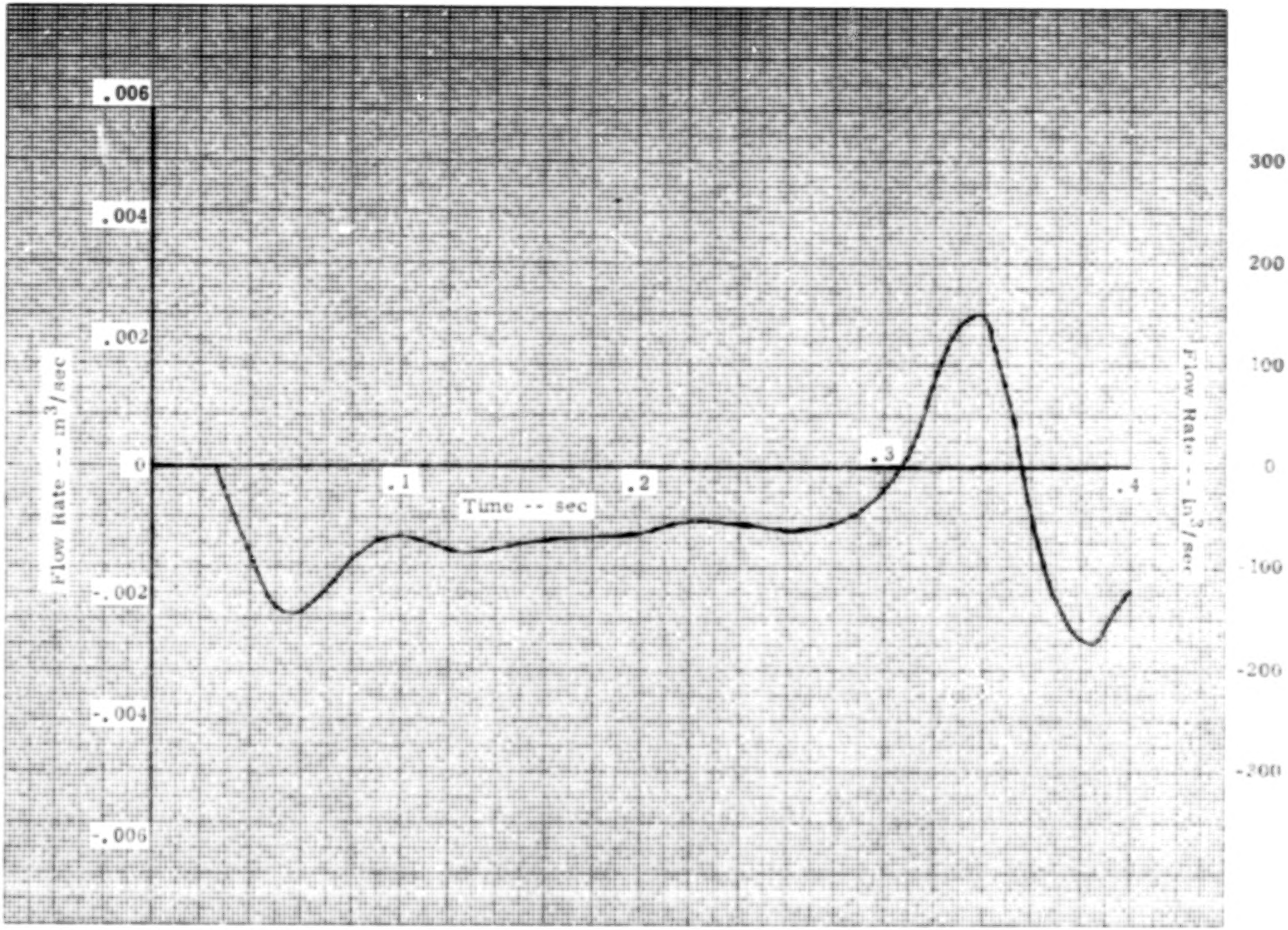

Figure 36. - Servovalve flow rate, case 4.

CONTROLLER FUNCTIONAL DESCRIPTION

Associated Equipment

The following NASA-supplied equipment is used in conjunction with the electronic controller.

(1) Accelerometer - range ± 3 g's, measures wing/gear interface force.

(2) Accelerometer - range ± 25 g's, measures hub acceleration.

(3) Potentiometer - range 0-0.305 m (0-12 in.), measures strut deflection.

(4) Pressure transducer hydraulic - range 0-3.45 (10^4) kPa (0-5000 lb/in^2), measures the gear hydraulic pressure.

(5) Pressure transducer, pneumatic - range 0-1.38 (10^4) kPa (0-2000 lb/in^2), measures the gear pneumatic pressure.

(6) Servovalve - max. flow 0.757 m^3/min @ 6895 kPa (200 gal/min. @ 1000 lb/in^2).

(7) Servovalve Electronic controller - provides the signal to drive the servovalve.

(8) Hydraulic power unit.

(9) Modified landing gear.

Interface

The interface of input/output signals is shown schematically in Figure 37. Primary inputs and outputs are those required by the controller to perform its function. Secondary inputs and outputs are provided for testing, status indication and parameter monitoring, but play no part in the basic function of the controller. The primary inputs are shown in Table II, secondary inputs in Table III and the outputs are in Table IV.

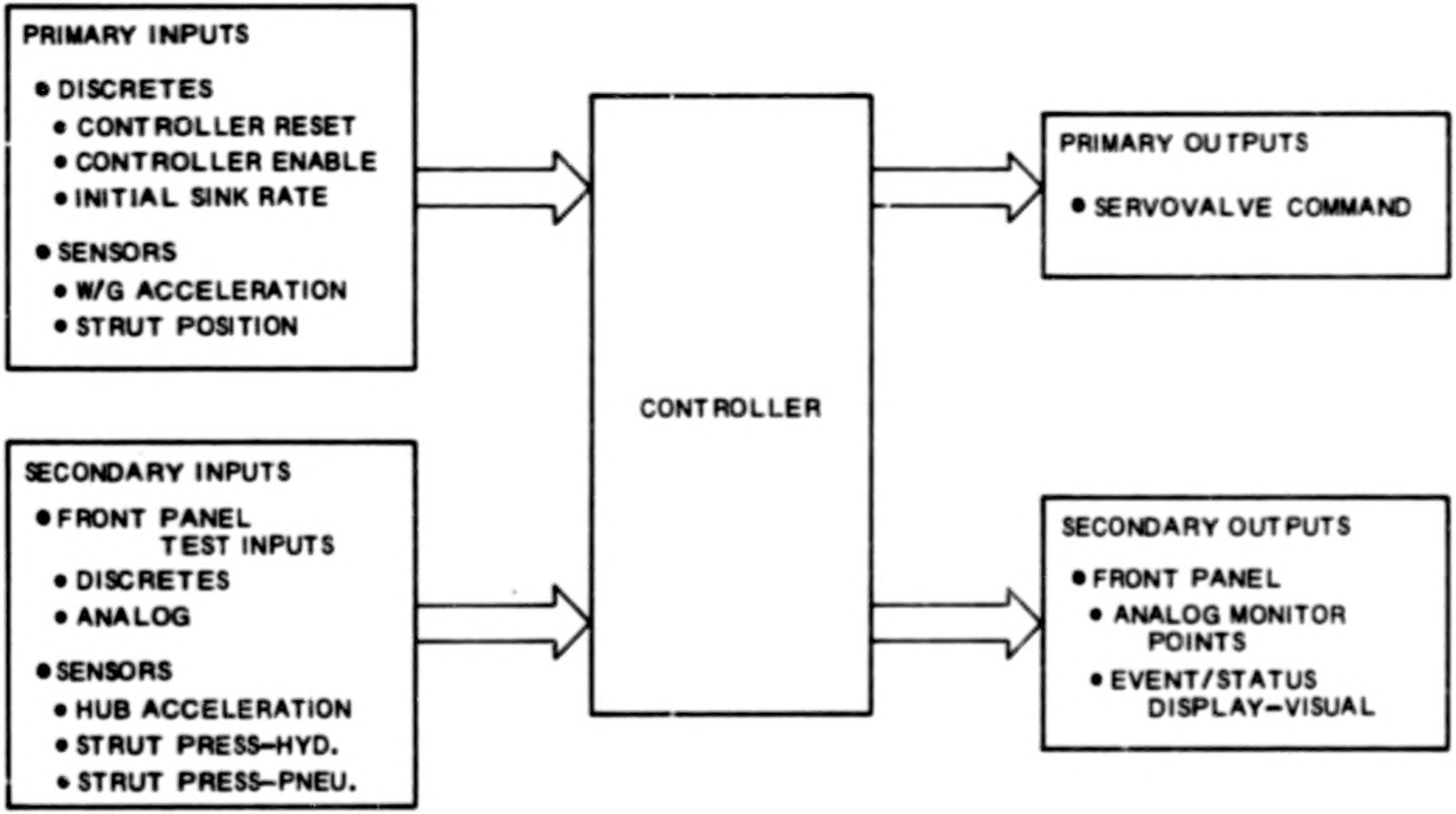
PRIMARY INPUTS
• DISCRETES
• CONTROLLER RESET
• CONTROLLER ENABLE
• INITIAL SINK RATE
• SENSORS
• W/G ACCELERATION
• STRUT POSITION
SECONDARY INPUTS
• FRONT PANEL TEST INPUTS
• DISCRETES
• ANALOG
• SENSORS
• HUB ACCELERATION
• STRUT PRESS–HYD.
• STRUT PRESS–PNEU.
CONTROLLER
PRIMARY OUTPUTS
• SERVOVALVE COMMAND
SECONDARY OUTPUTS
• FRONT PANEL
• ANALOG MONITOR POINTS
• EVENT/STATUS DISPLAY–VISUAL

Figure 37. - Input/Output Signal Schematic.

BLANK PAGE

BLANK PAGE

TABLE II. - PRIMARY INPUT SIGNAL SPECIFICATIONS

PARAMETER	UNITS	TYPE	SIGNAL RANGE
Wing/Gear Acceleration	g's	Analog	± 3g
Strut Position	m (in)	Analog	0 to 0.229 m (0 to 9 in)
Initial Sink Rate	m/sec (in/sec)	Digital	0 to 2.54 m/sec (0 to 100 in/sec)
Controller Reset	V	Logic Level	(*)
Controller Enable	V	Logic Level	(*)

(*) Logic 1 = 0 ± 0.5 V.
Logic 0 = 2.4 to 5V.

TABLE III. - SECONDARY INPUT SPECIFICATIONS

PARAMETER	UNITS	TYPE	SIGNAL RANGE	SCALE FACTOR
Hub Acceleration	g's	Analog	± 25 g	0.2 V/g
Strut Pressure - Hydraulic	kPa (lb/in^2)	Analog	0 to 2.07 (10^4) kPa (0 to 3000 lb/in^2)	6.418 (10^{-4}) m V/kPa (0.004425 mV/lb/in^2)
Strut Pressure - Pneumatic	kPa (lb/in^2)	Analog	0 to 1.384 (10^4) kPa (0 to 2000 lb/in^2)	6.418 (10^{-4}) m V/kPa (0.004425 mV/lb/in^2)
Limit Force Command	N (lb)	Analog	± 7.94 (10^4) N (± 17 860 lb)	1.26 (10^{-4}) V/N (0.00056 V/lb)
Wing/Gear Acceleration	g's	Analog	± 3 g	1.8 g
Wing/Gear Velocity	m/sec (in/sec)	Analog	0 to 2.54 m/sec (0 to 100 in/sec)	0.0393 V/m/sec (0.1 V/in/sec)
Strut Position	m (in)	Analog	0 to 0.229 m (0 to 9 in)	39.37 V/m (1 V/in)
Servoloop Enable	V	Logic Level	(*)	--
Integrator Enable	V	Logic Level	(*)	--

(*) Logic 1 = 0 ± 0.5 V.
Logic 0 = +2.4 to +5 V.

TABLE IV. - OUTPUT SPECIFICATIONS

PARAMETER	UNITS	TYPE	FRONT PANEL SOURCE		SIGNAL RANGE	SCALE FACTOR
			Jack	Visual Display		
Servovalve Command	V	Analog	X		± 10 V	1.0 V/(V Force Error)
Wing/Gear Acceleration	g's	Analog	X		± 3 g	1.8 V/g
Hub Acceleration	g's	Analog	X		± 25 g	0.2 V/g
Strut Position		Analog	X		0 to 22.9 cm (0 to 9 in)	39.37 V/m (1.0 V/in)
Strut Position Error		Analog	X		0 to 22.9 cm (0 to 9 in)	39.37 V/m (1.0 V/in)
Strut Pressure-Hydraulic	kPa (lb/in^2)	Analog	X		0 to $2.07\ (10^4)$ kPa (0 to 3000 lb/in^2)	$6.48\ (10^{-4})$ mV/kPa (0.004425 $mV/lb/in^2$)
Strut Pressure-Pneumatic	kPa (lb/in^2)	Analog	X		0 to $1.38\ (10^4)$ kPa (0 to 2000 lb/in^2)	$6.48\ (10^{-4})$ mV/kPa (0.004425 $mV/lb/in^2$)
Force Error	N (lb)	Analog	X		± 79.4 kN (± 17 860 lb)	$1.26\ (10^{-4})$ V/N (0.00056 V/lb)
Limit Force Command	N (lb)	Analog	X		± 79.4 kN (± 17 860 lb)	$1.26\ (10^{-4})$ V/N (0.00056 V/lb)
Wing/Gear Velocity	m/sec (in/sec)	Analog Logic	X		0 to 2.54 m/sec (0 to 100 in/sec)	0.03937 V/m/sec (0.1 V/in/sec)
Servoloop Enable	--	Logic Level	X		--	--
Integrator Enable	--	Logic Level	X		--	--
Controller Reset	--	Visual		X	--	--
Controller Enable	--	Visual		X	--	--
Takeoff Mode	--	Visual		X	--	--
Landing Mode	--	Visual		X	--	--

Performance Characteristics

The controller monitors the sensor data; and then, by performing computations of energy relationships and signal conditioning, provides an output signal which is the input command to the servovalve.

The controller has three basic functions which are: (1) operating-mode determination, (2) limit-force command determination, and (3) control-law implementation.

Operating-Mode Determination

When the controller is enabled, it automatically determines the operating mode — landing or takeoff.

Landing Mode

The controller selects the landing mode if the controller-enable signal has been received and the strut position signal indicates full extension. The landing mode is divided into several phases, each imposing a different functional command on the controller. These are: (1) pre-touchdown, (2) active control initiation, (3) transition, and (4) rollout.

Pre-touchdown. - During the pre-touchdown phase, the controller provides a bias signal to the servovalve to maintain the strut hydraulic pressure equal to the design charging pressure. This is accomplished by a pressure control loop in which the hydraulic pressure is the feedback signal. It also receives a signal from an external source which is representative of the aircraft sink rate prior to touchdown. In addition, it monitors the strut deflection. The servoloop is not enabled and the gear remains in a passive state.

Active Control Initiation. - Active control is initiated when the energy relationships indicate that the work potential of the strut exceeds the kinetic energy of the aircraft. Upon such occurrence, the controller causes the following to occur.

(1) The servoloop is enabled.

(2) An output is generated to the servovalve controller proportional to the force error as modified by the control laws.

(3) Energy computations are discontinued.

(4) A constant limit force is maintained.

(5) The strut pressure loop is opened.

(6) The servovalve bias is removed.

(7) The transition velocity is computed and continuously compared to the actual wing gear velocity to determine the start of transition.

Transition. - Transition to the rollout phase commences when the wing gear velocity equals the transition velocity. During transition, the controller linearly decreases the limit force command to zero and maintains active control.

Rollout. - The rollout phase commences when the limit force command during transition reaches zero. Active control is maintained and the controller remains in this mode until receipt of a reset signal (push button on the front panel).

Takeoff Mode

The controller selects the takeoff mode when: (1) a controller-enable signal has been received, and (2) the strut potentiometer signal indicates that the strut is at 0.005 m (0.2 in) less-than-full extension. At takeoff, the controller status is the same as in the rollout phase of the landing mode.

Limit-Force Command Determination

During the period prior to control initiation, the limit force is zero. (Since the servoloop is disabled during this time, the limit-force command has no effect). During the active control phase, the limit-force command is equal to the wing gear force which was present at the instant when active control was initiated. As indicated above, the limit-force command is linearly decreased to zero during the transition phase and maintained at zero throughout the rollout phase.

Control Law Implementation

The controller implements the control laws as shown in Figure 38. The transfer functions are listed in Table V.

Controller Design

Functional Sections

The controller consists of a digital section, an analog section and a power supply section as shown in Figure 39.

Digital Section. - The digital section includes a general-purpose stored-program digital computer (microprocessor) and its associated input/output devices as shown in Figure 40. The digital section accepts three analog and three discrete inputs and provides one analog and two discrete outputs. The analog inputs are applied through an analog multiplexer and A/D converter. The multiplexer is controlled by the computer software. The operating range of all inputs is 0 to +10 V.

The controller reset input is generated by a push button switch on the front panel. This input is normally in a logic "0" state. Depression of the

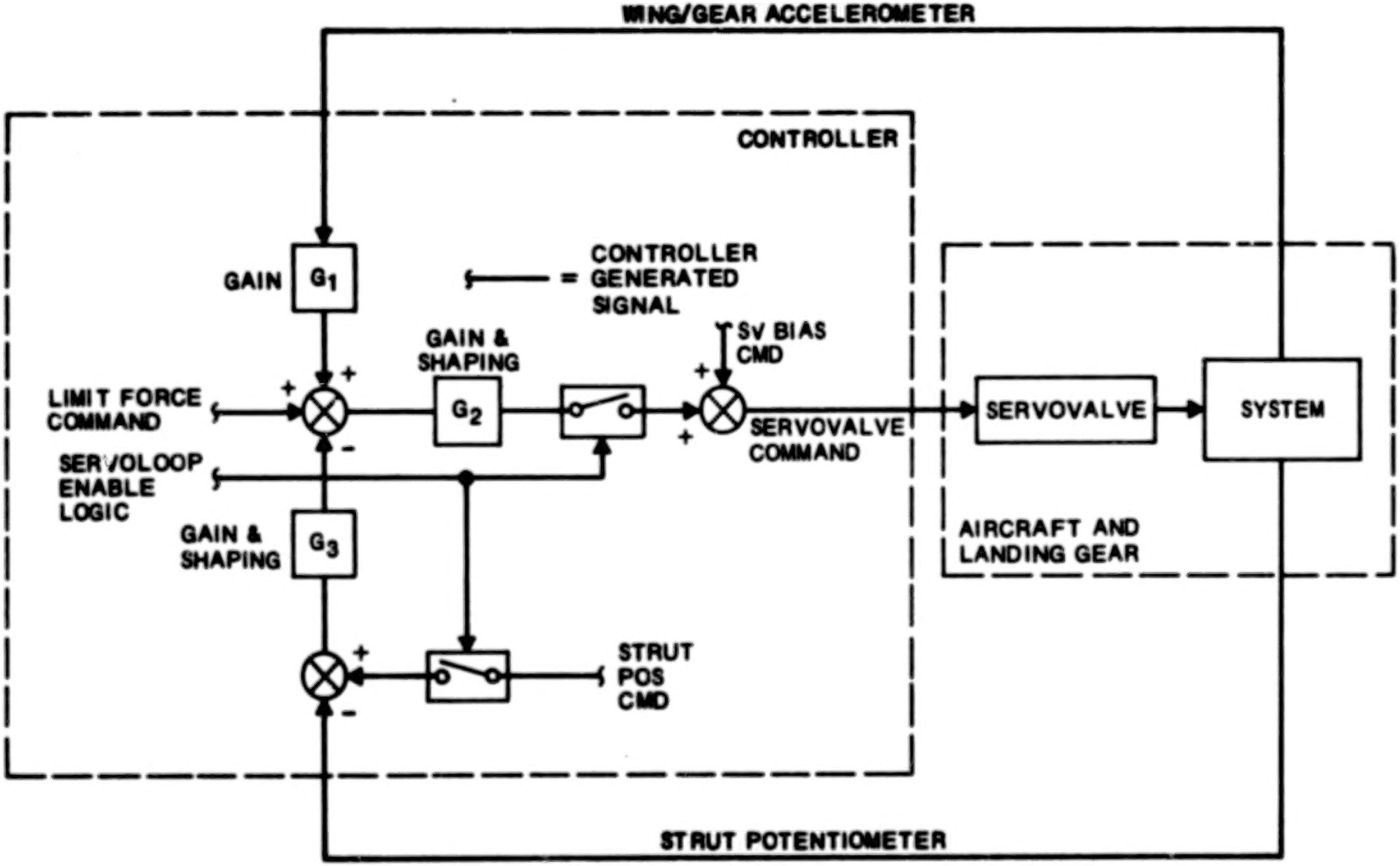
WING/GEAR ACCELEROMETER
CONTROLLER
GAIN
G_1
= CONTROLLER GENERATED SIGNAL
GAIN & SHAPING
G_2
Sv BIAS CMD
LIMIT FORCE COMMAND
+
+
-
+
+
SERVOVALVE COMMAND
SERVOVALVE
SYSTEM
SERVOLOOP ENABLE LOGIC
GAIN & SHAPING
G_3
AIRCRAFT AND LANDING GEAR
STRUT POS CMD
+
-
STRUT POTENTIOMETER

Figure 38. - Control Law Functional Schematic

TABLE V. - CONTROL LAW TRANSFER FUNCTIONS

SYMBOL (REF. FIGURE 3.2-6)	TRANSFER FUNCTION	PARAMETER VALUES
G_1	K_{WG}	K_{WG} = 1.0 V/V
G_2	$\frac{(S^2 + 2\zeta_2\omega_1 S + \omega_1^2)(T_1S + 1)(T_3S + 1)K_A}{(S^2 + 2\zeta_1\omega_1 S + \omega_1^2)(T_2S + 1)(T_4S + 1)}$	T_1 = 0.0281 sec T_2 = 0.0141 sec T_3 = 0.001 sec T_4 = 0.0001 sec ω_1 = 251.3 rad/sec ζ_2 = 0.1 ζ_1 = 5.1 K_A = 1.0 V/V nominal (variable from 50% to 200% of nominal)
G_3	$\frac{K_F}{T_F S + 1}$	K_F = 196.9V/M (5.0V/in.) T_F = 0.1 sec

BLANK PAGE

BLANK PAGE

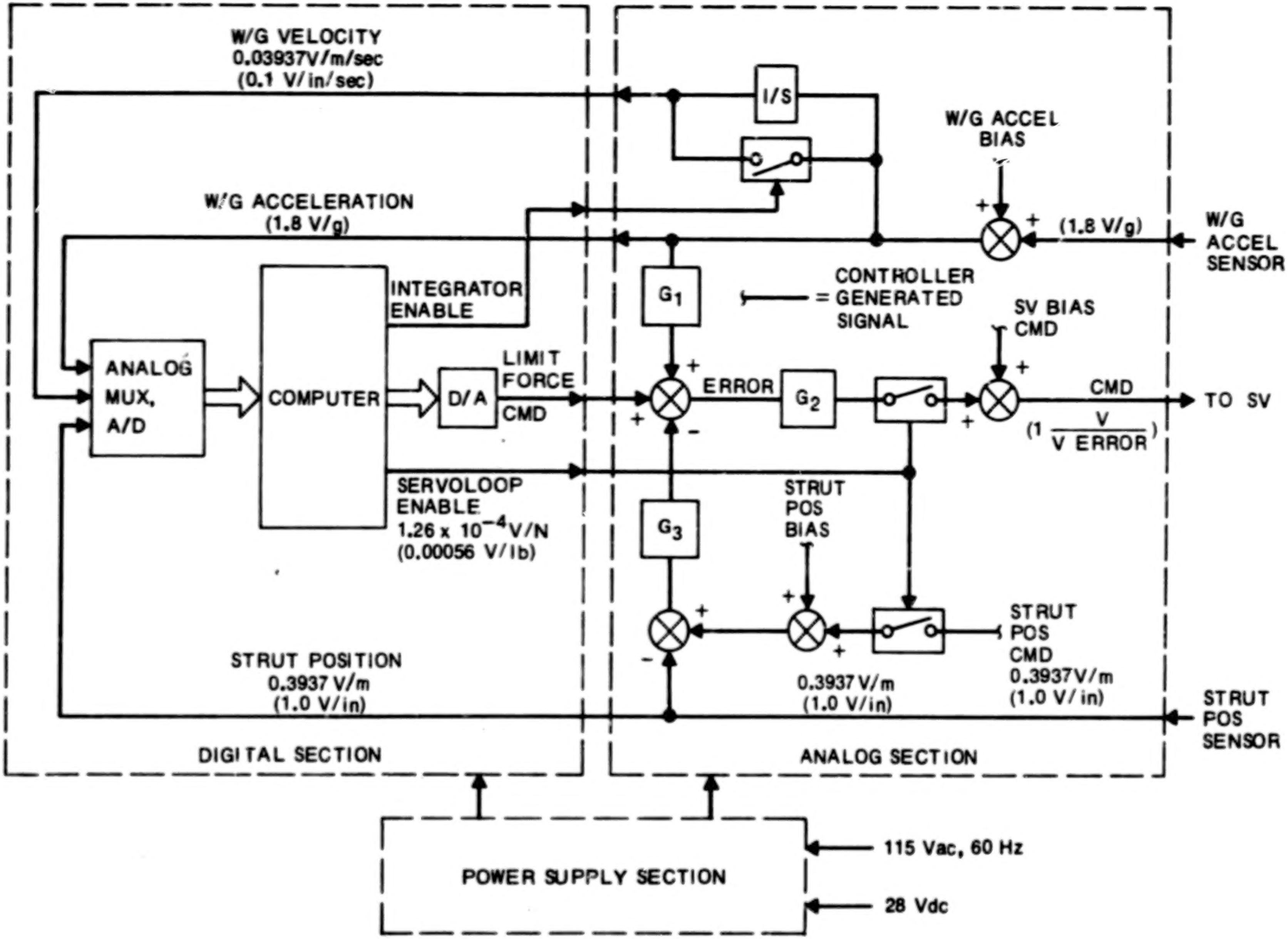
W/G VELOCITY
0.03937V/m/sec
(0.1 V/in/sec)
I/S
W/G ACCEL
BIAS
W/G ACCELERATION
(1.8 V/g)
(1.8 V/g)
W/G
ACCEL
SENSOR
INTEGRATOR
ENABLE
G1
CONTROLLER
= GENERATED
SIGNAL
SV BIAS
CMD
ANALOG
MUX,
A/D
COMPUTER
D/A
LIMIT
FORCE
CMD
ERROR
G2
CMD
TO SV
(1 V / V ERROR)
SERVOLOOP
ENABLE
1.26 x 10^-4 V/N
(0.00056 V/lb)
STRUT
POS
BIAS
G3
STRUT
POS
CMD
0.3937V/m
(1.0 V/in)
STRUT POSITION
0.3937 V/m
(1.0 V/in)
0.3937 V/m
(1.0 V/in)
STRUT
POS
SENSOR
DIGITAL SECTION
ANALOG SECTION
POWER SUPPLY SECTION
115 Vac, 60 Hz
28 Vdc

Figure 39. - Controller Functional Schematic

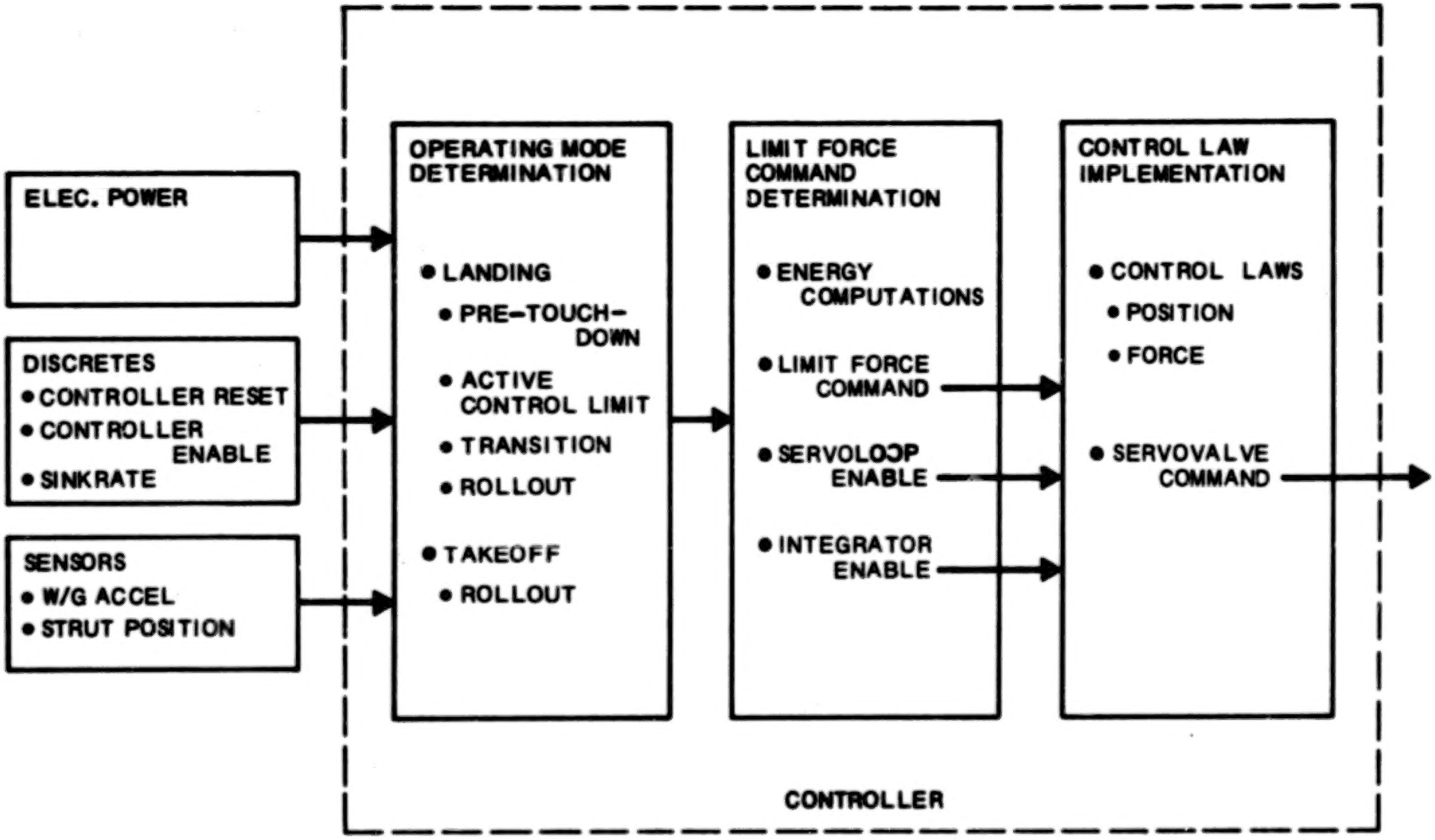
ELEC. POWER
DISCRETES
• CONTROLLER RESET
• CONTROLLER ENABLE
• SINKRATE
SENSORS
• W/G ACCEL
• STRUT POSITION
OPERATING MODE DETERMINATION
• LANDING
• PRE-TOUCH-DOWN
• ACTIVE CONTROL LIMIT
• TRANSITION
• ROLLOUT
• TAKEOFF
• ROLLOUT
LIMIT FORCE COMMAND DETERMINATION
• ENERGY COMPUTATIONS
• LIMIT FORCE COMMAND
• SERVOLOOP ENABLE
• INTEGRATOR ENABLE
CONTROL LAW IMPLEMENTATION
• CONTROL LAWS
• POSITION
• FORCE
• SERVOVALVE COMMAND
CONTROLLER

Figure 40. - Basic Functional Requirements

button changes the state to "1" which causes the controller to reset the computer. (The computer goes to step 0000 of memory).

The controller is enabled by a logic level input. Provision is made so that this input can be generated by a panel-mounted push button switch or a microswitch mounted on the gear. Both switches are connected in series. Therefore, if the controller is to be enabled by the panel switch only, then the microswitch input should be short-circuited. In any event, this signal is normally in a "0" state, and upon actuation the state becomes "1" which causes the computer to enable the controller.

Initial sink rate is an additional analog input to the multiplexer. This input is generated by an external source which is a velocity sensor or a d c signal which simulates the sink rate.

The outputs from the controller are the limit-force command (analog) signal, servoloop-enable (discrete) signal, and integrator-enable (discrete) signal.

The limit-force command is an output from the digital section by means of a digital-to-analog converter. The servoloop-enable signal is a logic level signal. A logic level "1" causes a switch to close and completes the path between the limit-force command and the output to the servovalve controller. The integrator-enable signal is also a logic-level signal. A level "0" causes a switch which is connected across the integrator, to open, thus allowing integration to occur. The integrator is used to generate wing/gear velocity from wing/gear acceleration and the input sink rate.

The computer software is illustrated in flow diagram form in Figure 41 and a detailed listing is provided as Appendix A.

Analog Section. - The function of the analog section is shown schematically in Figure 42. A detailed schematic drawing, wiring diagrams and assembly drawings, as well as a complete functional description can be found in Appendix B. The analog section accepts the primary and secondary

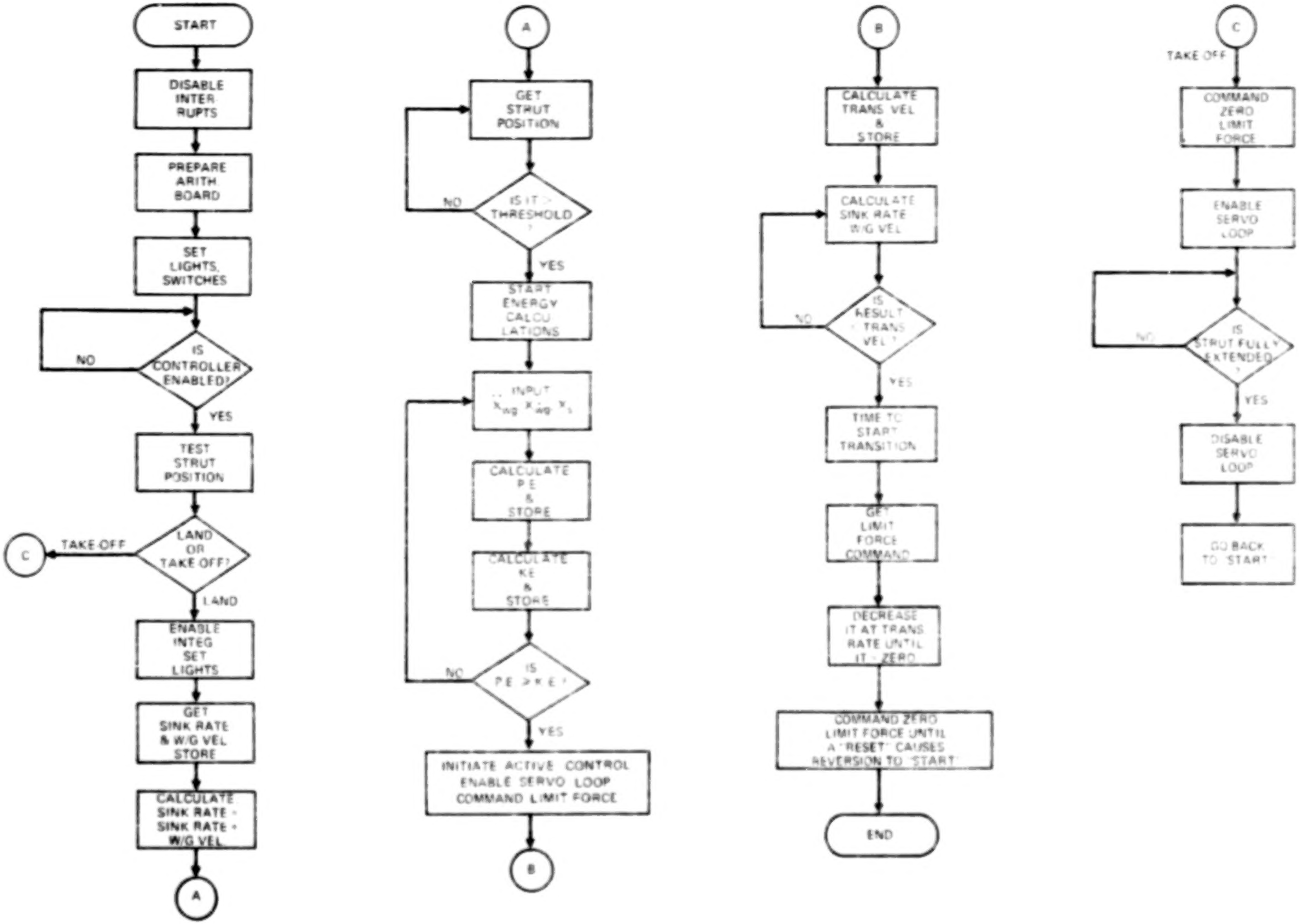
START
DISABLE INTER RUPTS
PREPARE ARITH BOARD
SET LIGHTS, SWITCHES
NO
IS CONTROLLER ENABLED?
YES
TEST STRUT POSITION
C
TAKE OFF
LAND OR TAKE OFF?
LAND
ENABLE INTEG SET LIGHTS
GET SINK RATE & W/G VEL STORE
CALCULATE SINK RATE - SINK RATE + W/G VEL
A
A
GET STRUT POSITION
NO
IS IT > THRESHOLD ?
YES
START ENERGY CALCU LATIONS
INPUT $\ddot{X}_{wg}$ $\dot{X}_{wg}$ X_s
CALCULATE P.E. & STORE
CALCULATE K.E. & STORE
NO
IS P.E. ≥ K.E.?
YES
INITIATE ACTIVE CONTROL ENABLE SERVO LOOP COMMAND LIMIT FORCE
B
B
CALCULATE TRANS. VEL & STORE
CALCULATE SINK RATE W/G VEL
NO
IS RESULT < TRANS VEL ?
YES
TIME TO START TRANSITION
GET LIMIT FORCE COMMAND
DECREASE IT AT TRANS RATE UNTIL IT = ZERO
COMMAND ZERO LIMIT FORCE UNTIL A "RESET" CAUSES REVERSION TO "START"
END
C
TAKE OFF
COMMAND ZERO LIMIT FORCE
ENABLE SERVO LOOP
NO
IS STRUT FULLY EXTENDED ?
YES
DISABLE SERVO LOOP
GO BACK TO "START"

Figure 41. - Software Flow Chart

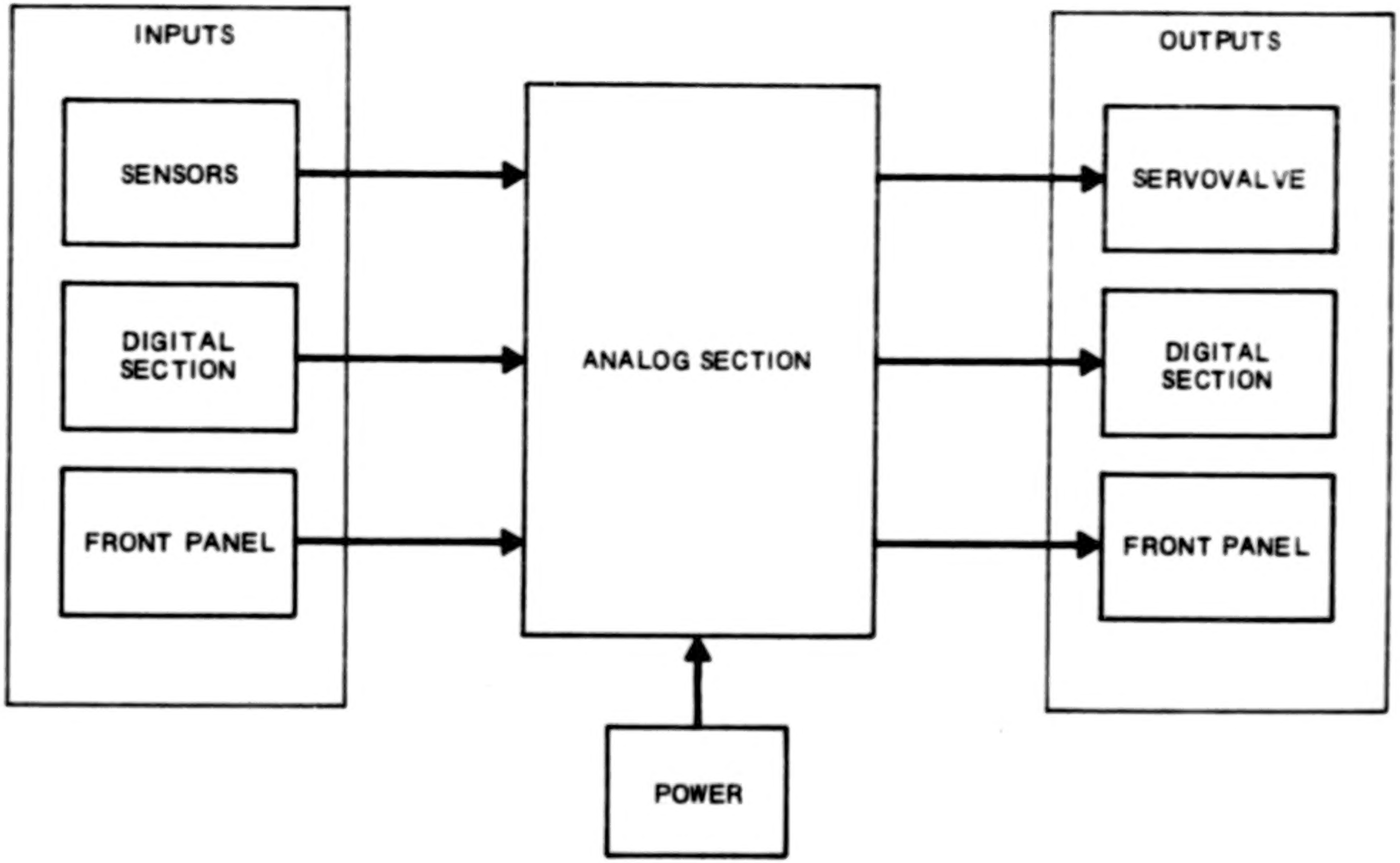
INPUTS
SENSORS
DIGITAL SECTION
FRONT PANEL
ANALOG SECTION
POWER
OUTPUTS
SERVOVALVE
DIGITAL SECTION
FRONT PANEL

Figure 42. - Analog Section Schematic

inputs, implements the required control laws and provides the output signal to the servovalve controller. It accepts signals from, and supplies signals to, the digital section.

Provisions are included to apply test signals to the controller by means of jacks on the front panel. These are shown in Figure 43. Buffered outputs are also provided on the front panel so that signals of interest can be monitored or recorded. These are shown in Figure 44.

The inputs to the analog section from the digital section are the limit-force command, servoloop-enable and integrator-enable signals, while the outputs from the analog section to the digital section are the wing/gear velocity, wing/gear acceleration and strut position signals. As previously stated, the wing/gear velocity is derived by integrating the wing/gear acceleration.

In addition, the analog section accepts inputs from the following sensors.

(1) Wing/gear accelerometer.
(2) Hub accelerometer.
(3) Strut position potentiometer.
(4) Strut hydraulic pressure transducer.
(5) Strut pneumatic pressure transducer.

These signals are applied by means of connectors on the rear panel.

Several other signals are applied to the analog section by means of controls on the front panel. These are:

(1) Servovalve bias command - to determine the static operating level of the servovalve.

(2) Strut position command - to determine static strut extension.

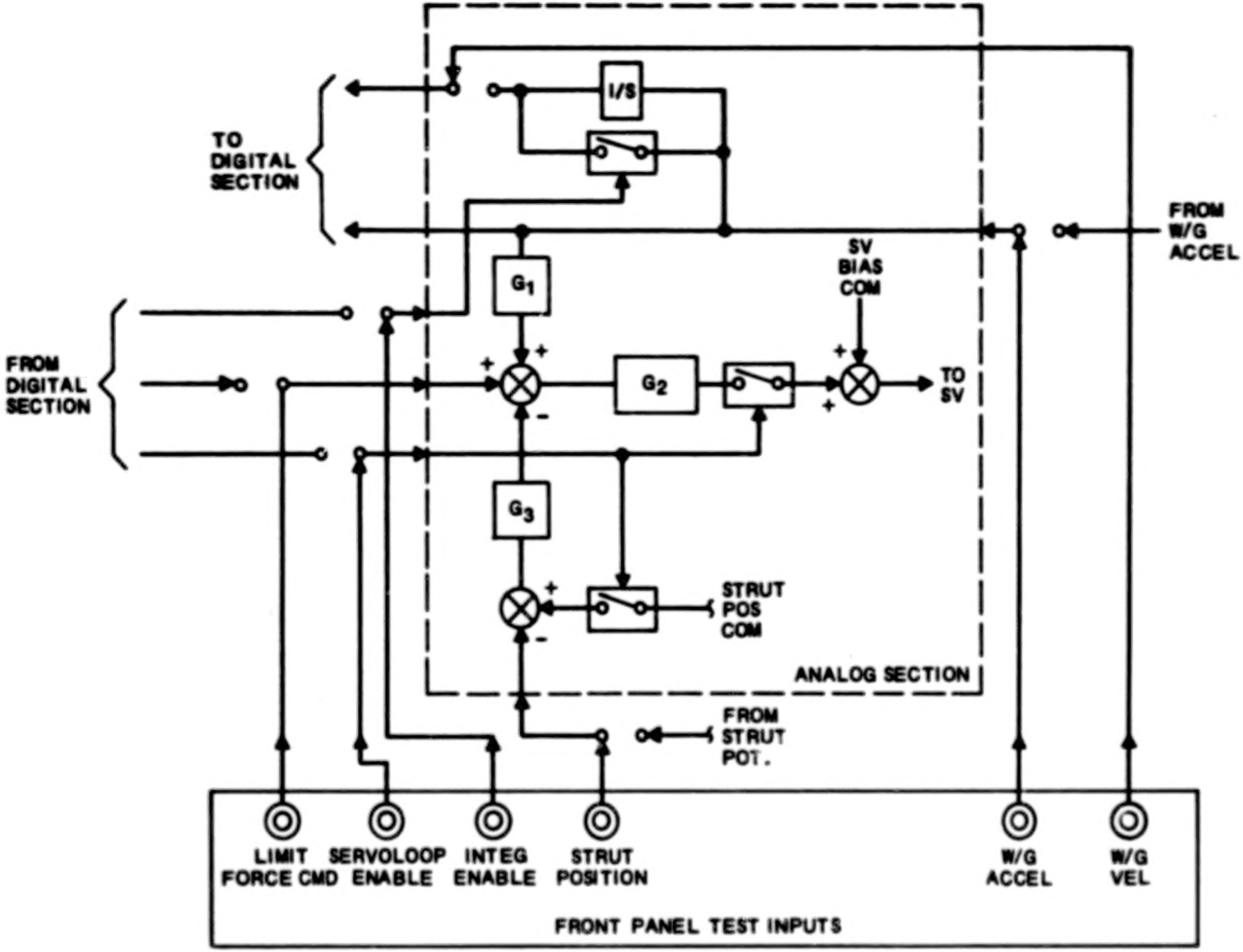
TO
DIGITAL
SECTION
I/S
FROM
W/G
ACCEL
G_1
SV
BIAS
COM
FROM
DIGITAL
SECTION
+
+
G_2
+
TO
SV
+
-
G_3
+
STRUT
POS
COM
-
ANALOG SECTION
FROM
STRUT
POT.
LIMIT
FORCE CMD
SERVOLOOP
ENABLE
INTEG
ENABLE
STRUT
POSITION
W/G
ACCEL
W/G
VEL
FRONT PANEL TEST INPUTS

Figure 43. - Analog Section - Front Panel Inputs

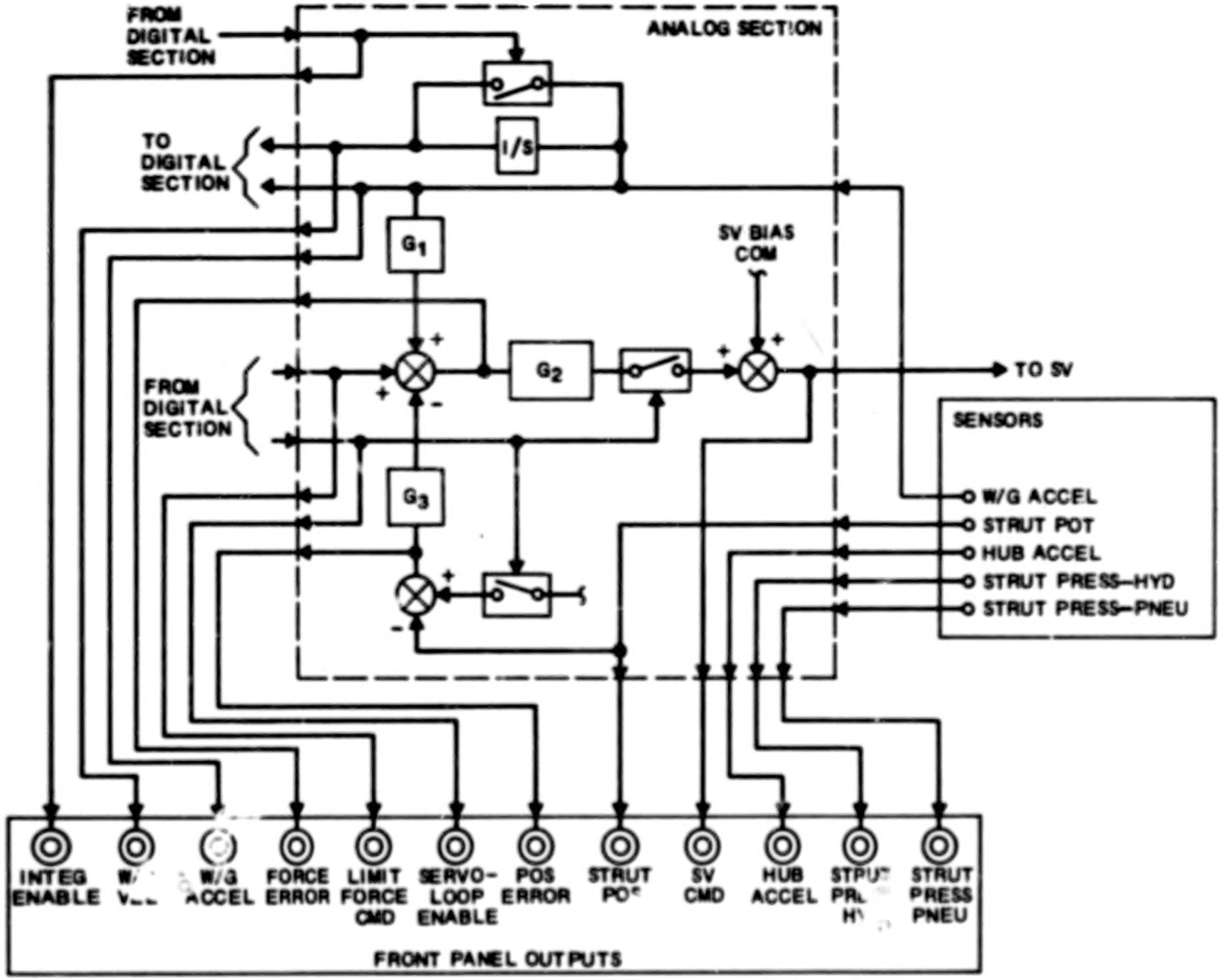
FROM DIGITAL SECTION
ANALOG SECTION
I/S
TO DIGITAL SECTION
G1
SV BIAS COM
FROM DIGITAL SECTION
G2
TO SV
SENSORS
W/G ACCEL
STRUT POT
HUB ACCEL
STRUT PRESS—HYD
STRUT PRESS—PNEU
G3
INTEG ENABLE
W/G VEL
W/G ACCEL
FORCE ERROR
LIMIT FORCE CMD
SERVO-LOOP ENABLE
POS ERROR
STRUT POS
SV CMD
HUB ACCEL
STRUT PRESS HYD
STRUT PRESS PNEU
FRONT PANEL OUTPUTS

Figure 44. - Analog Section - Front Panel Outputs

TEST

Test Fixture

The test fixture used for the ACLG is a pivoted, variable-inertia beam originally designed to test the S-1C main engine vectoring servoactuators. The fixture is shown in Figures 45 and 46. Configured for the ACLG test program, the beam, added weights, landing gear, associated mounting components and miscellaneous hardware, represents a total calculated rotational inertia of 1426 kg - m^2 (1050 slug-ft^2). The landing gear is rigidly attached at a distance of 1.02 m (3.33 ft) from the beam pivot which produces a vertical translational inertia equivalent to a mass of 1388 kg (3060 lb). This value is about 5% below the targeted simulation value of 1458 kg (3215 lb) in order to allow for the weight of components which were added (hoses, fittings, instrumentation, etc.).

Motion is imparted to the beam by means of a hydraulic cylinder attached (through a load cell) to the beam at a distance of 0.305 m (1 ft) from the beam pivot and on the opposite side of the pivot from the landing gear. The cylinder is controlled by a 0.00189-m^3/sec (30-gal/min) electrohydraulic servovalve and its associated electronics. An LVDT is used for position indication and position loop closure.

Since the gear is rigidly mounted to the beam, it traverses the same angle as the beam. The angle of the gear at touchdown is about 4° forward of vertical. After touchdown, it passes through vertical and reaches an extreme of approximately 11° aft of vertical, depending on the test condition. These angles were chosen on the basis of gear geometry and the gear forces and deflections predicted by the analytical simulation. They represent an optimum mounting configuration, the basis of which is to make the strut frictional forces the same percentage of the total axial force on the gear at both touchdown and maximum force condition.

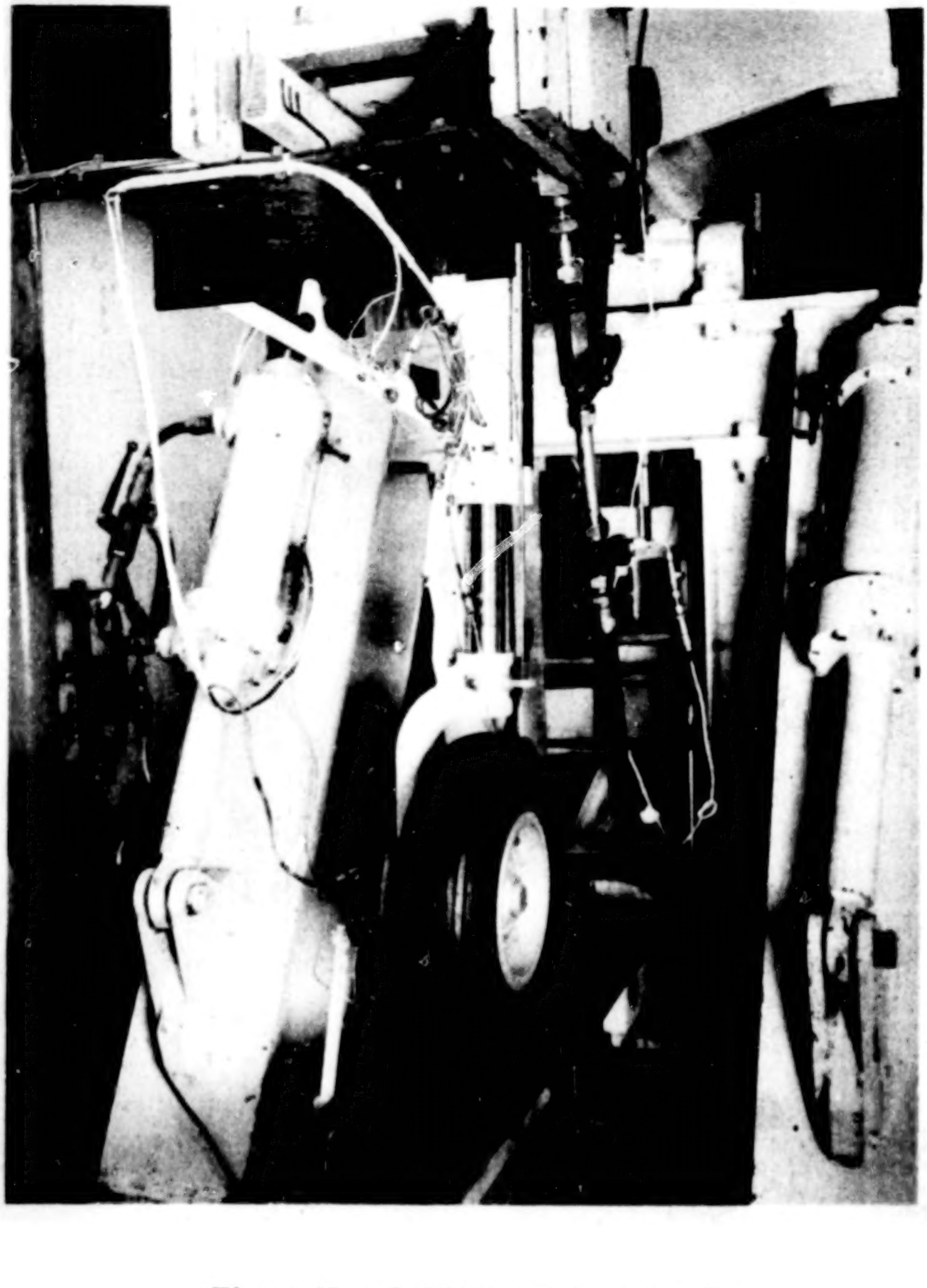

Figure 45. - S-1C Test Fixture, Landing Gear Installed (View 1)

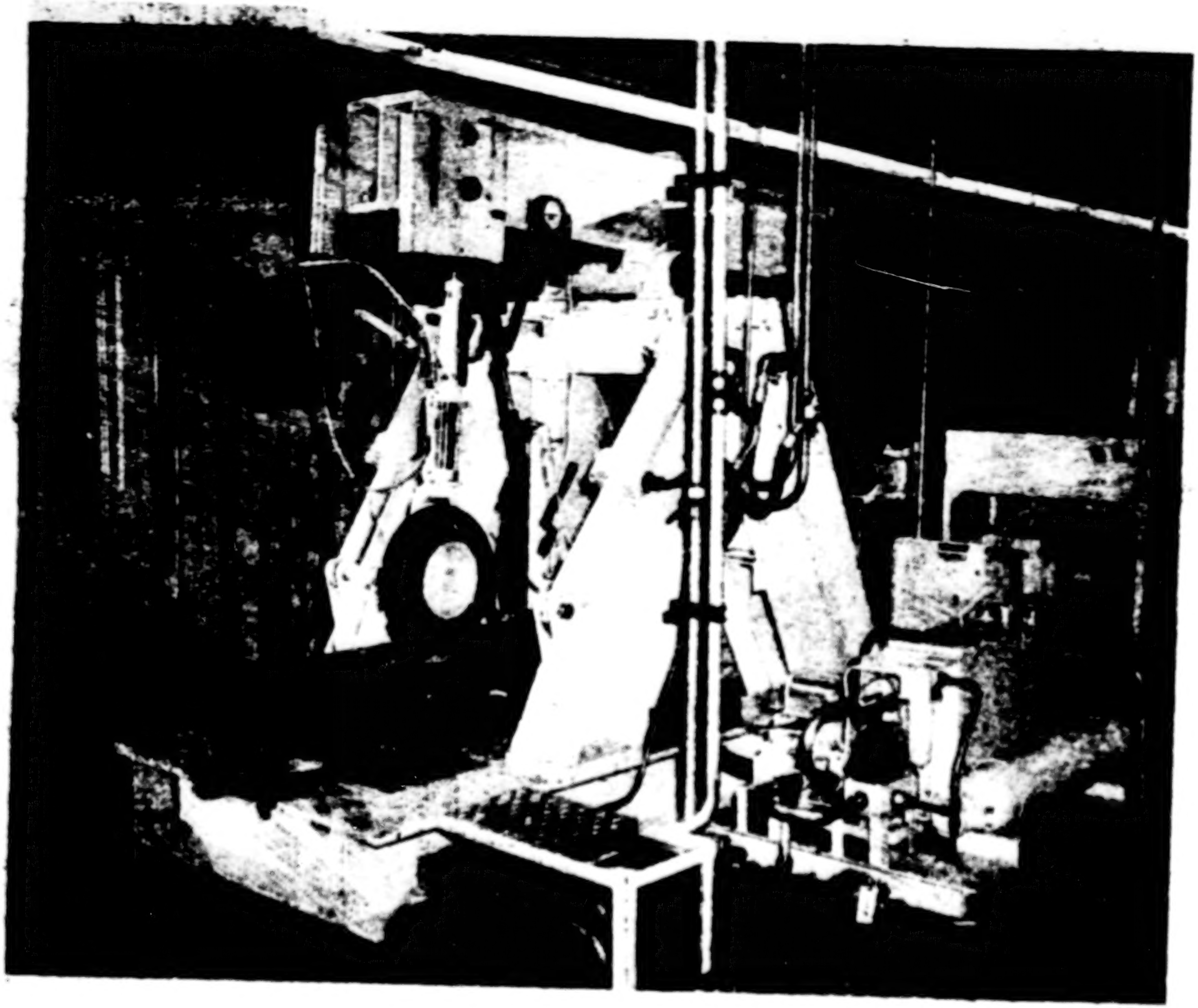

Figure 46. - S-1C Test Fixture, Landing Gear Installed (View 2)

The loading system operates in three modes as follows:

(1) Pre-test gear positioning: The cylinder is in a closed position loop, using the LVDT for feedback to "cock" the beam and gear to a pre-test position as determined by a command potentiometer.

(2) Sink speed generation: The LVDT is disconnected so that the cylinder is an open-loop configuration. A preset velocity potentiometer then provides a signal to the servovalve, thereby commanding a flow rate from the cylinder corresponding to the required sink speed.

(3) Programmed force: At touchdown, a microswitch is activated which connects the load cell and places the cylinder in a closed force loop to control the force during the interval from touchdown to the end of the test. The force program is provided by a ramp generator which begins with a 4315 N (970 lb) upward force at the gear [14 370 N (3230 lb) of tension at the load cylinder] which cancels the beam unbalance of 4315 N (970 lb) and simulates the condition of lift = weight. After 0.4 sec, the force ramps linearly to provide a downward force on the gear of 2180 N (490 lb) [7250 N (1630 lb) of compression at the load cylinder] which adds to the beam unbalance at this point of 4982 N (1120 lb) (due to the fact that the beam c.g. is above its pivot point) to produce a total downward force of 7161 N (1610 lb), which is equivalent to half of the aircraft weight per gear. The force is then held constant at this level throughout the remainder of the test.

Test Conditions

Tests were conducted under the following conditions.

Condition	Sink Speed m/sec (ft/sec)	Fully-extended Gear Pressure kPa (lb/in^2)	Mode
1.	0.305 (1)	1048 (152)	Passive
2.	0.914 (3)	1048 (152)	Passive
3.	1.524 (5)	1048 (152)	Passive
4.	0.305 (1)	1048 (152)	Active
5.	0.914 (3)	1048 (152)	Active
6.	1.524 (5)	1048 (152)	Active
7.	0.305 (1)	1931 (280)	Passive
8.	0.914 (3)	1931 (280)	Passive
9.	1.524 (5)	1931 (280)	Passive
10.	0.305 (1)	1931 (280)	Active
11.	0.914 (3)	1931 (280)	Active
12.	1.524 (5)	1931 (280)	Active

Test Procedure

The procedure for conducting the drop tests is given in Appendix C.

Test Results

The peak forces produced and percentage reduction due to active control are presented in Table VI. Comparative plots of force, strut deflection, and pressure are shown in Figures 47 through 64. The oscillograph recordings from which those plots were constructed are included as Appendix D.

TABLE VI. - PEAK FORCES AND PERCENTAGE REDUCTION

Condition No.	Sink Speed m/sec (ft/sec)	Static Strut Pressure kPa (lb/in^2)	Force at first peak N (lb)		% Reduction	Force at second peak or at 0.1 sec after touchdown N (lb)		% Reduction
			Passive	Active		Passive	Active	
1, 4	0. 305 (1)	1048 (152)	4 226 (950)	4 226 (950)	0	5 004 (1125)	4 448 (1000)	11. 1
2, 5	0. 914 (3)	1048 (152)	8 674 (1950)	7 784 (1750)	10.3	8 007 (1800)	6 005 (1350)	25. 0
3, 6	1. 524 (5)	1048 (152)	11 120 (2500)	9 564 (2150)	14. 0	10 900 (2450)	10 900 (2450)	0
7, 10	0. 305 (1)	1931 (280)	1 335 (300)	445 (100)	66. 7	4 893 (1100)	4 448 (1000)	9. 1
8, 11	0. 914 (3)	1931 (280)	11 340 (2550)	10 450 (2350)	7. 8	11 570 (2600)	8 007 (1800)	30. 8
9,12	1. 524 (5)	1931 (280)	16 240 (3650)	16 240 (3650)	0	16 680 (3750)	11 790 (2650)	29. 3

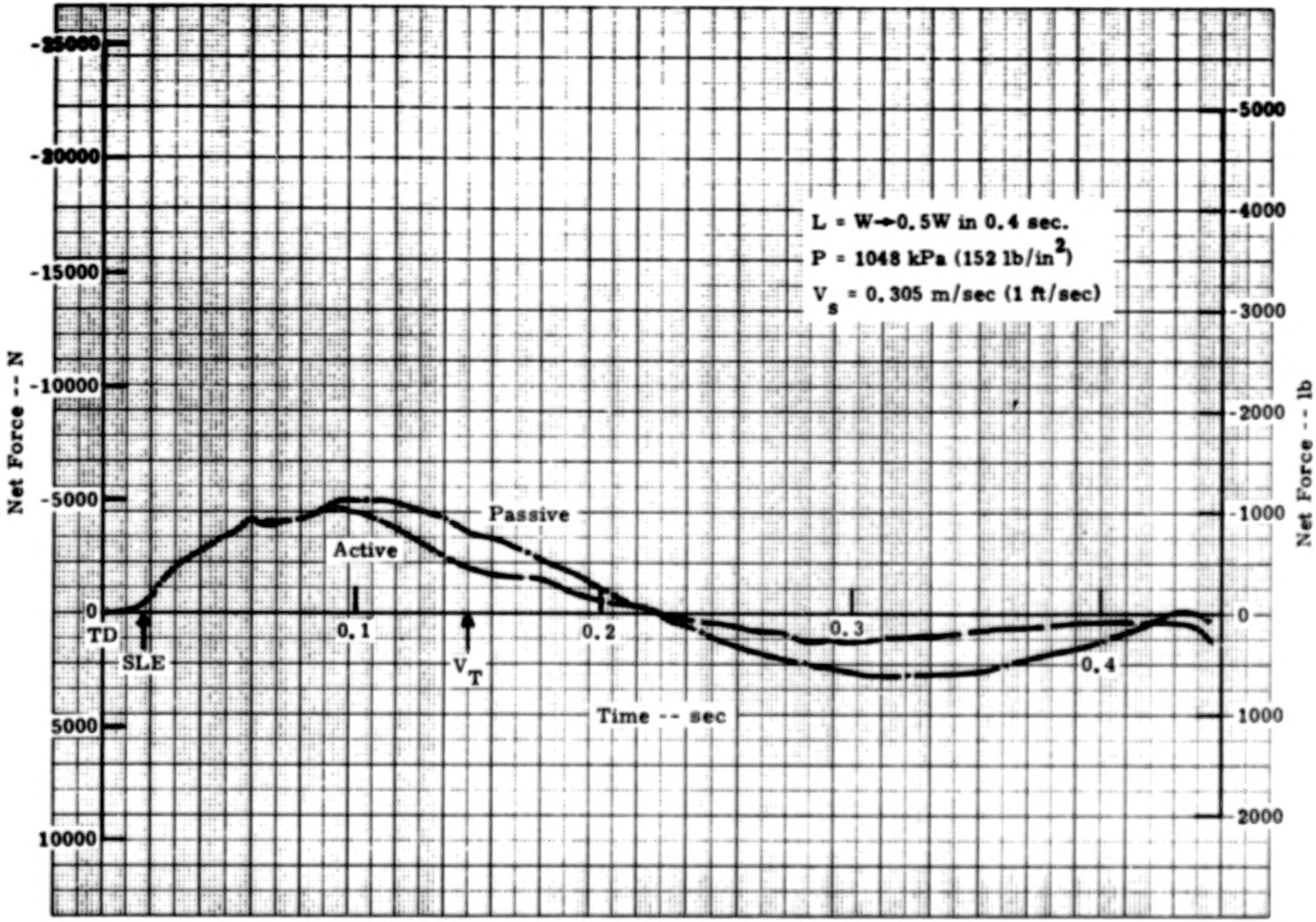

Figure 47. Net Force, Conditions 1, 4
(From W/G Accel #1)

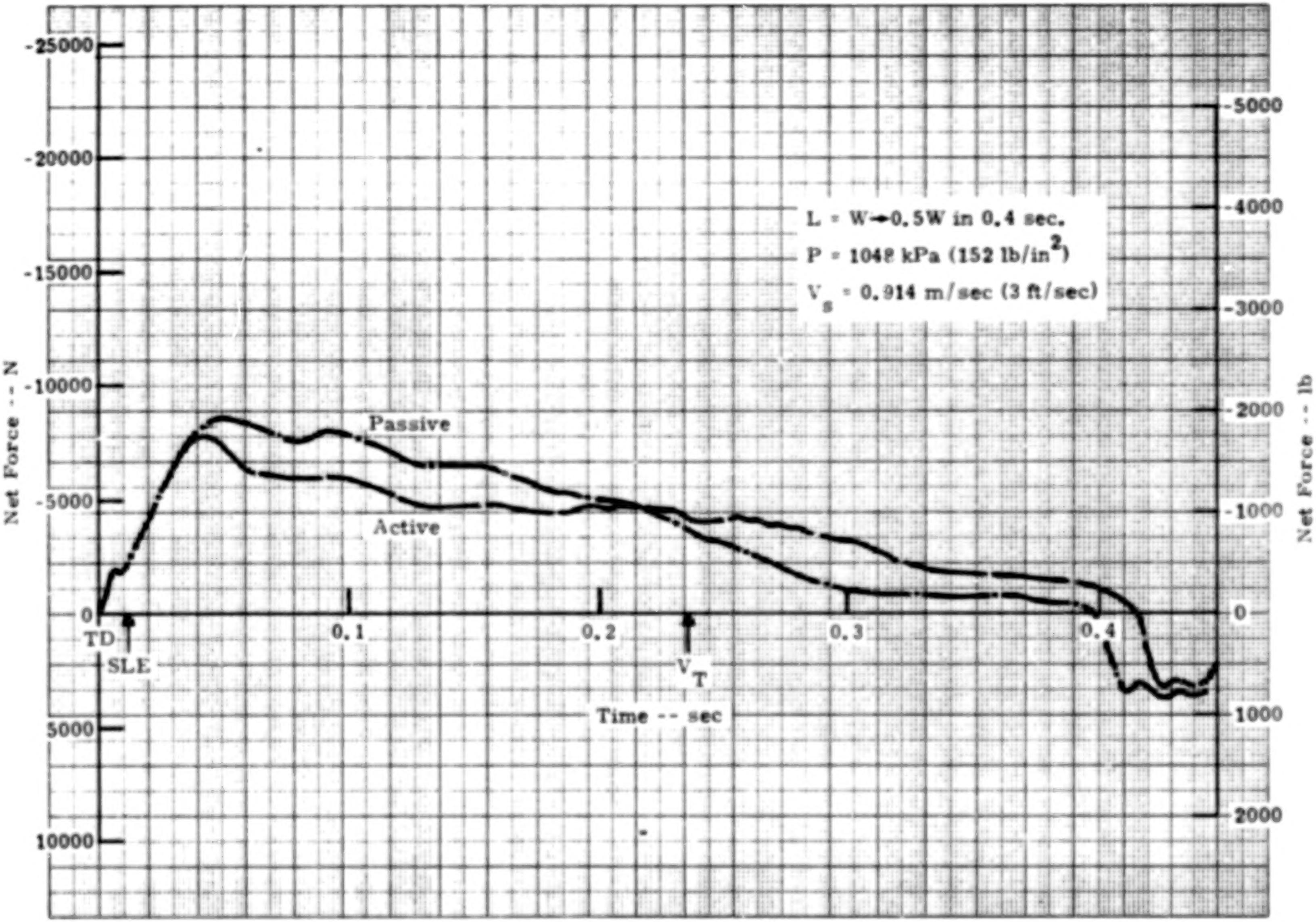

Figure 48. Net Force, Conditions 2, 5
(From W/G Accel #1)

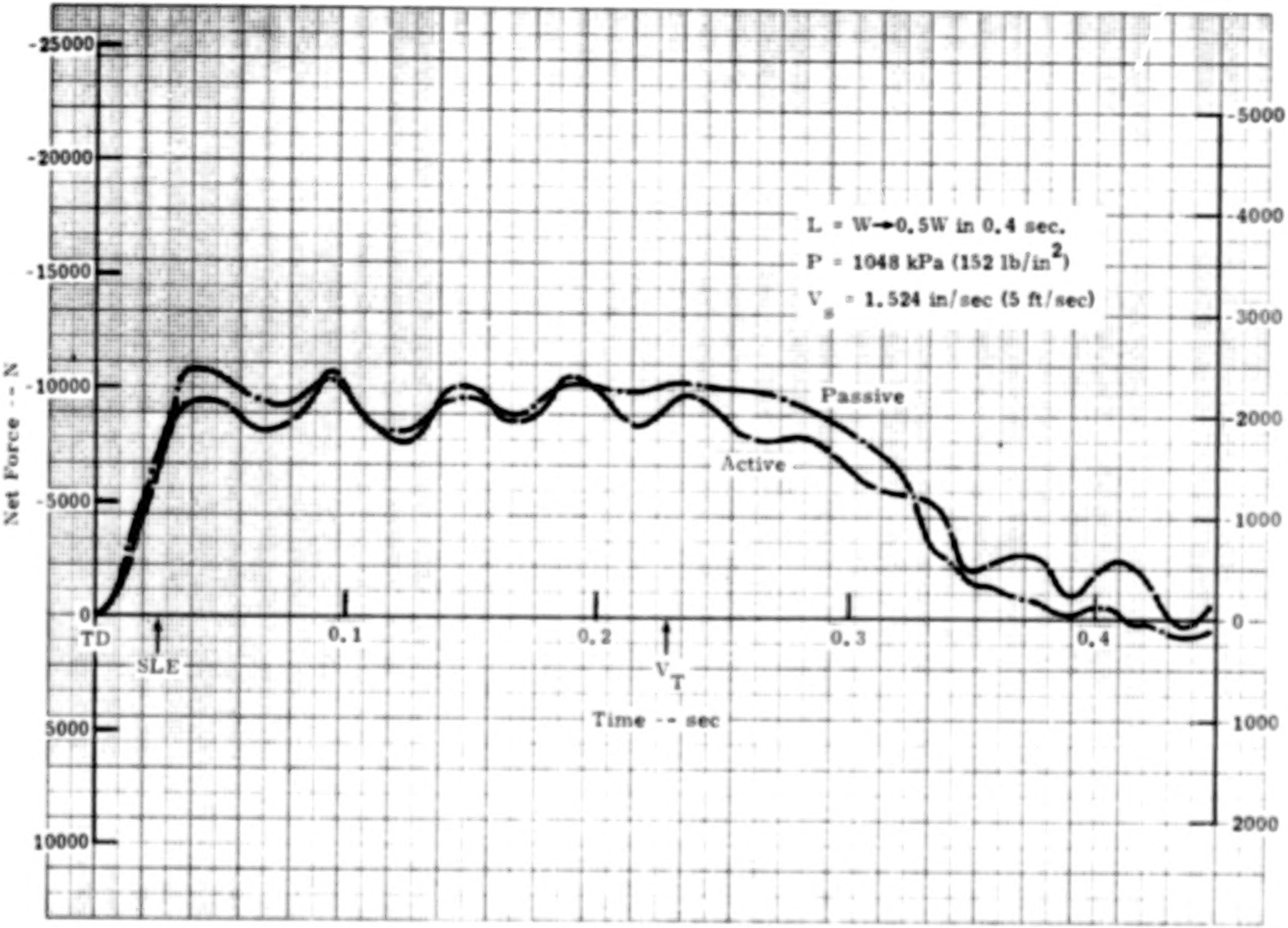

Figure 49. Net Force, Conditions 3, 6
(From W/G Accel #1)

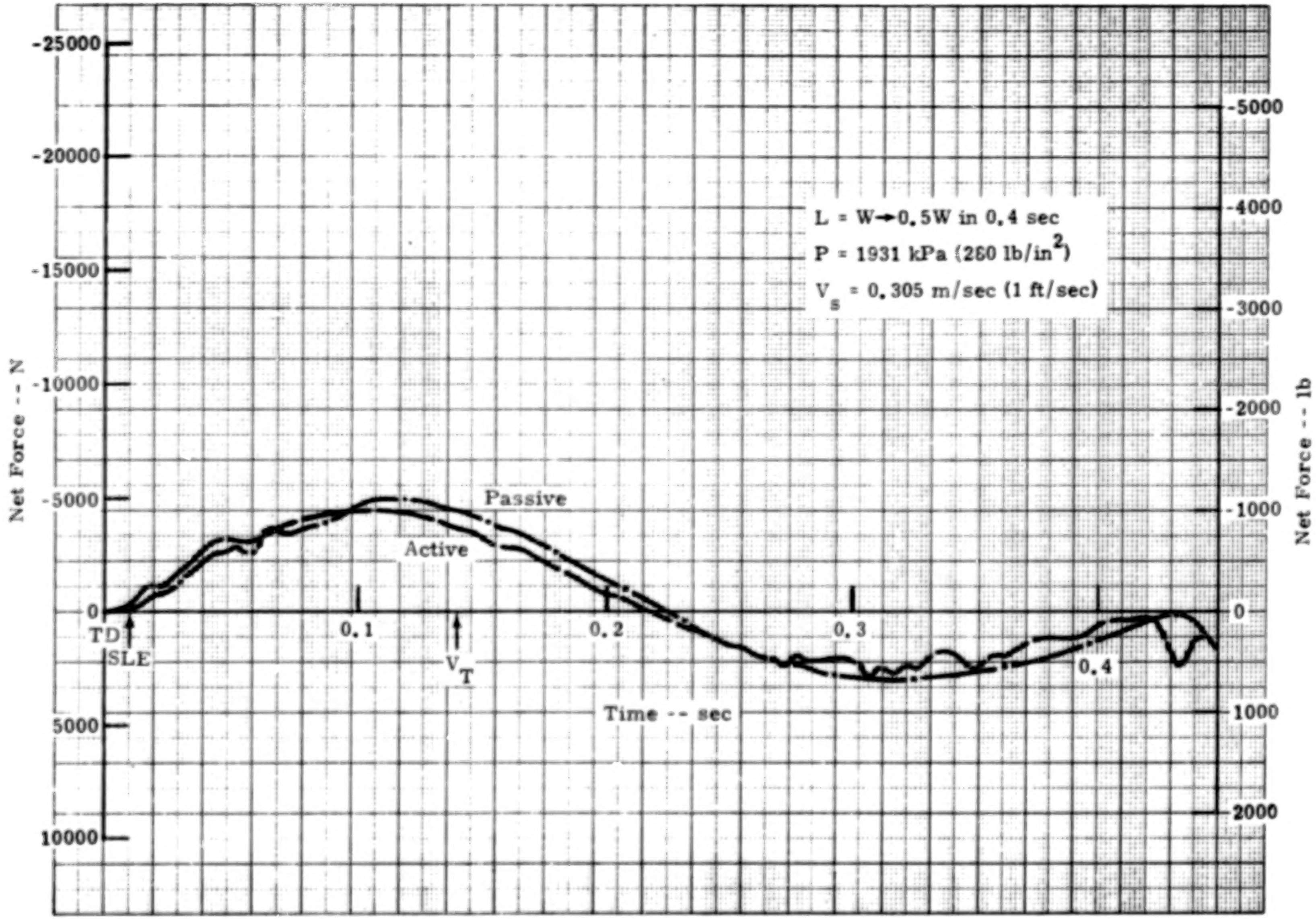

Figure 50. Net Force, Conditions 7, 10
(From W/G Accel #1)

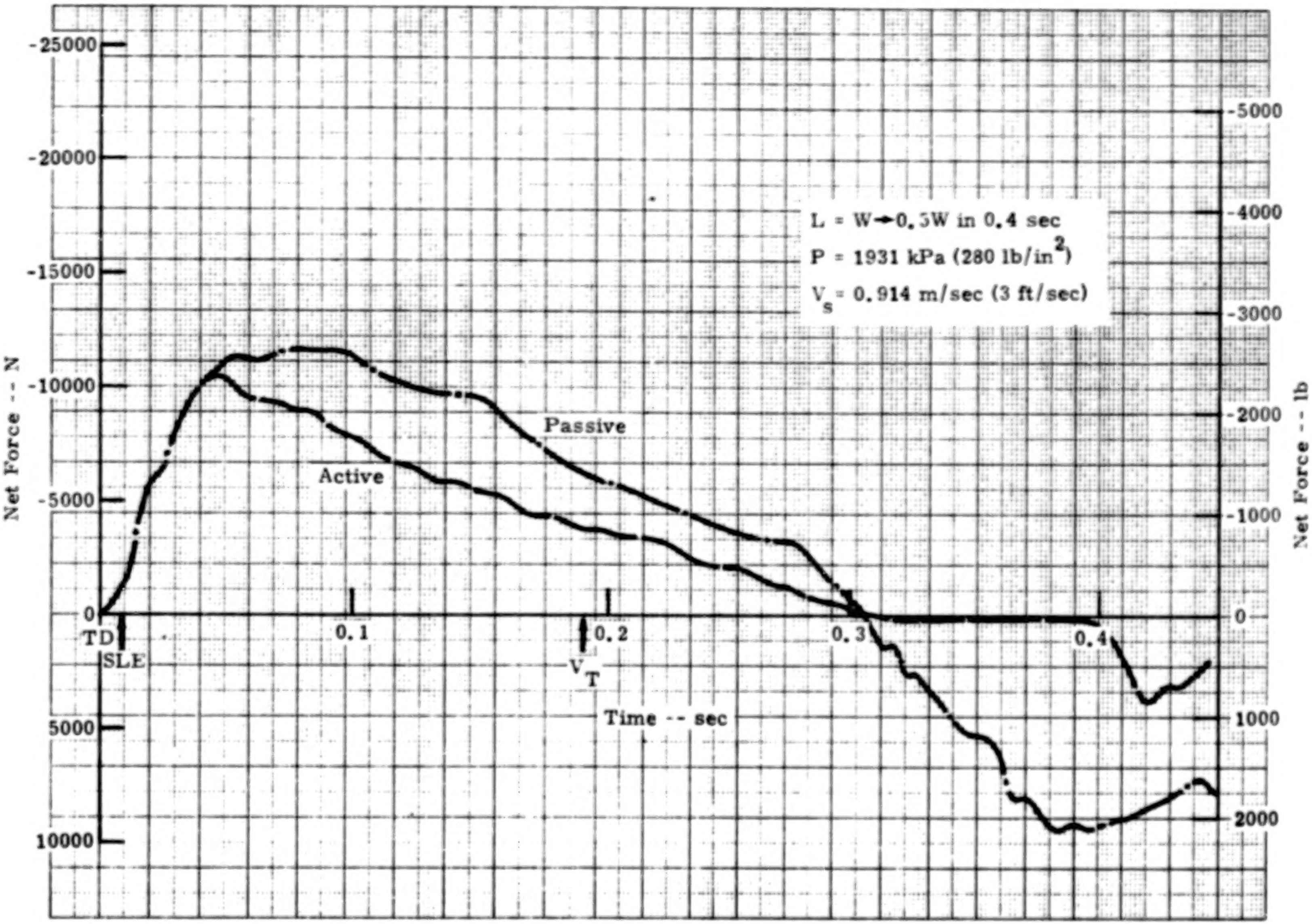

Figure 51. Net Force, Conditions 8, 11
(From W/G Accel #1)

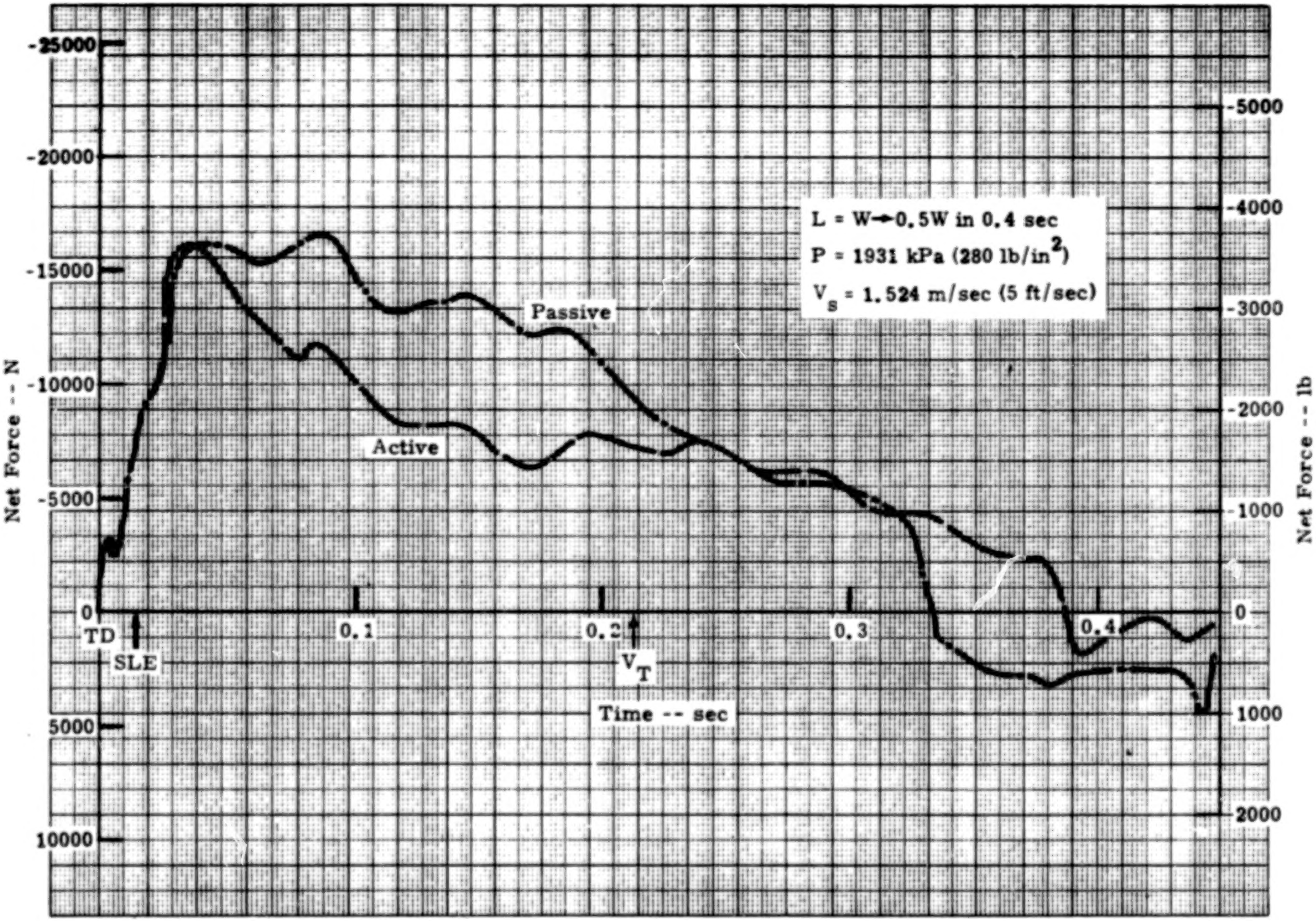

Figure 52. Net Force, Conditions 9, 12
(From W/G Accel #1)

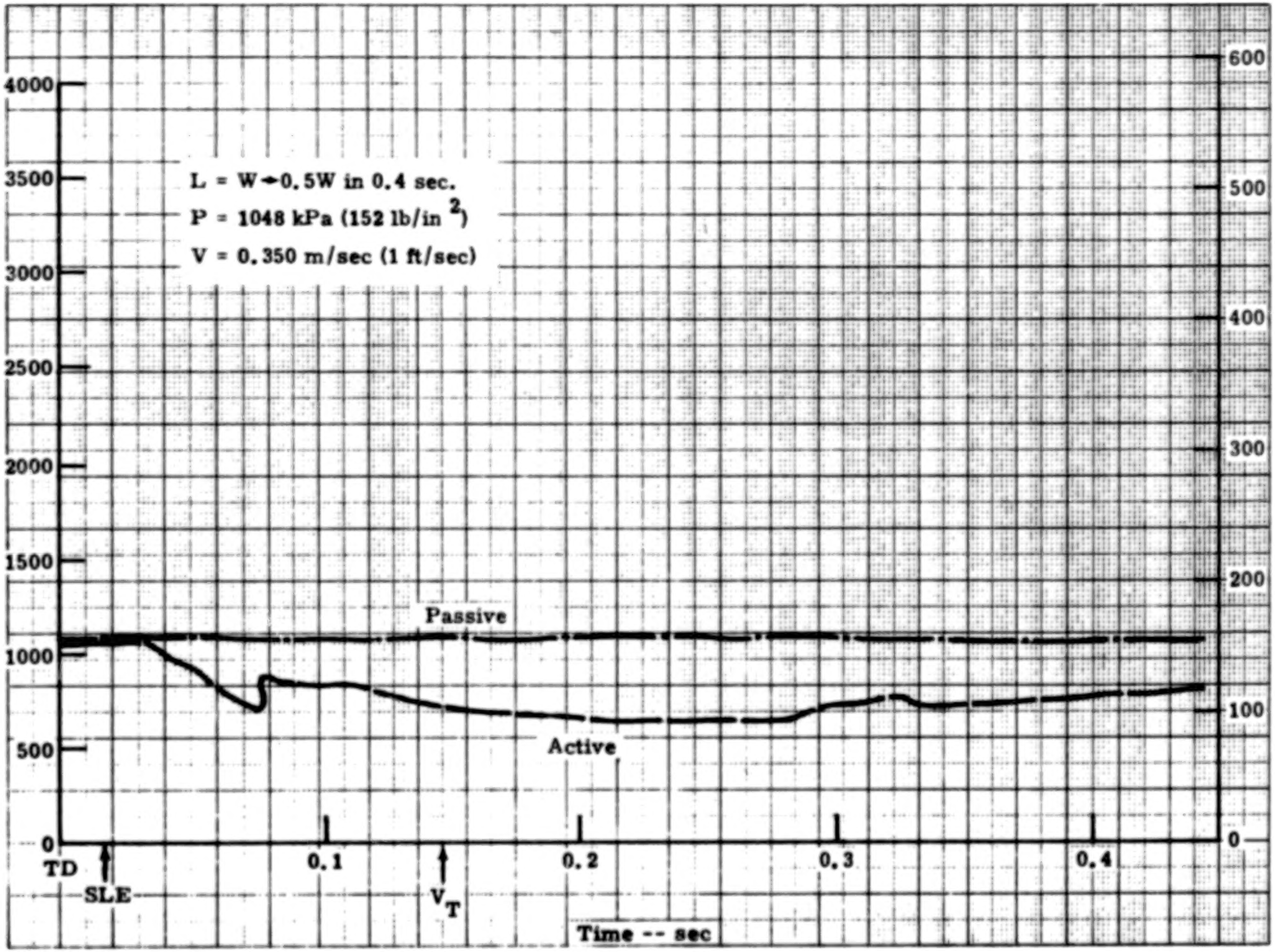

Figure 53. Gear Hydraulic Pressure, Conditions 1, 4

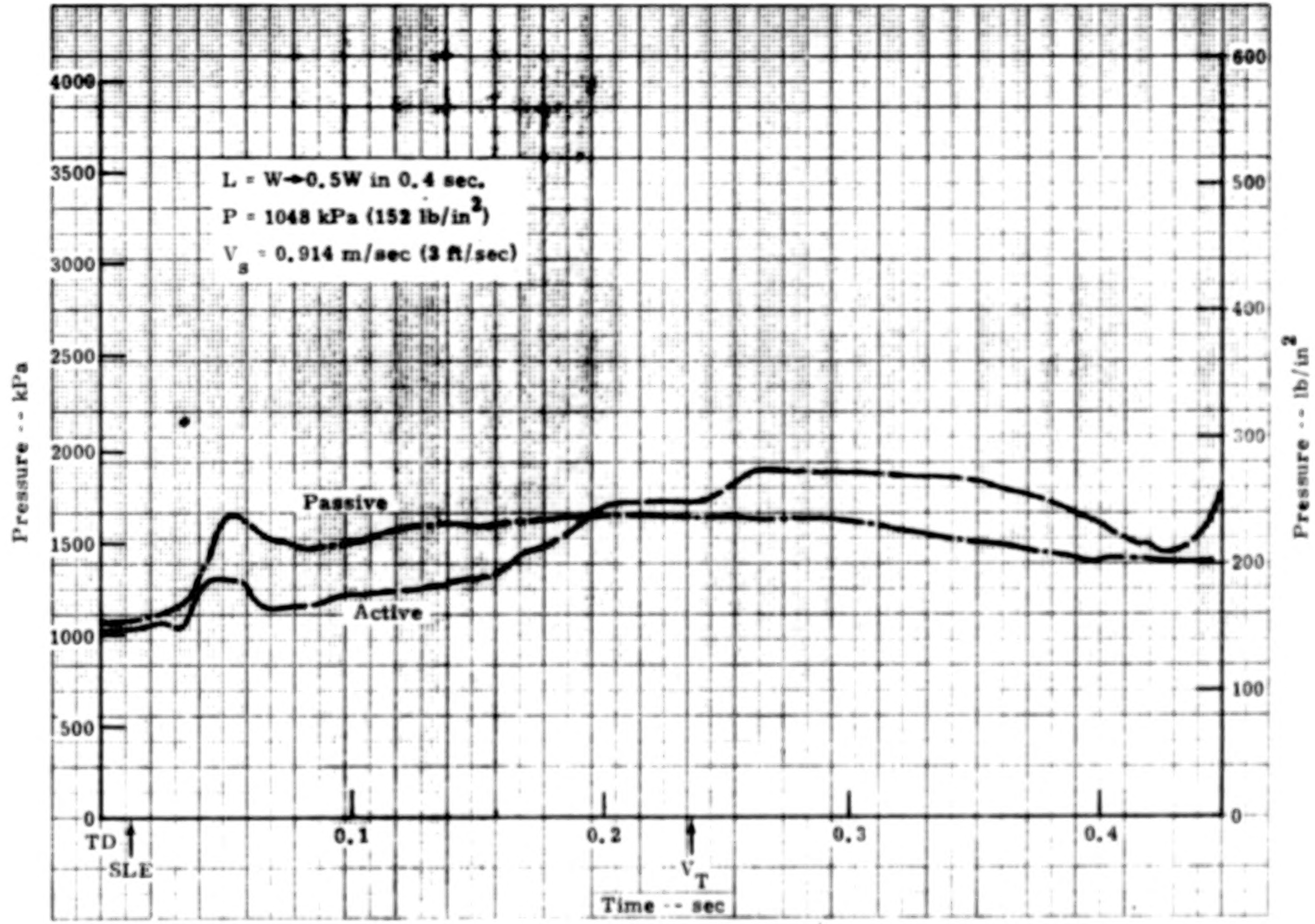

Figure 54. Gear Hydraulic Pressure, Conditions 2, 5

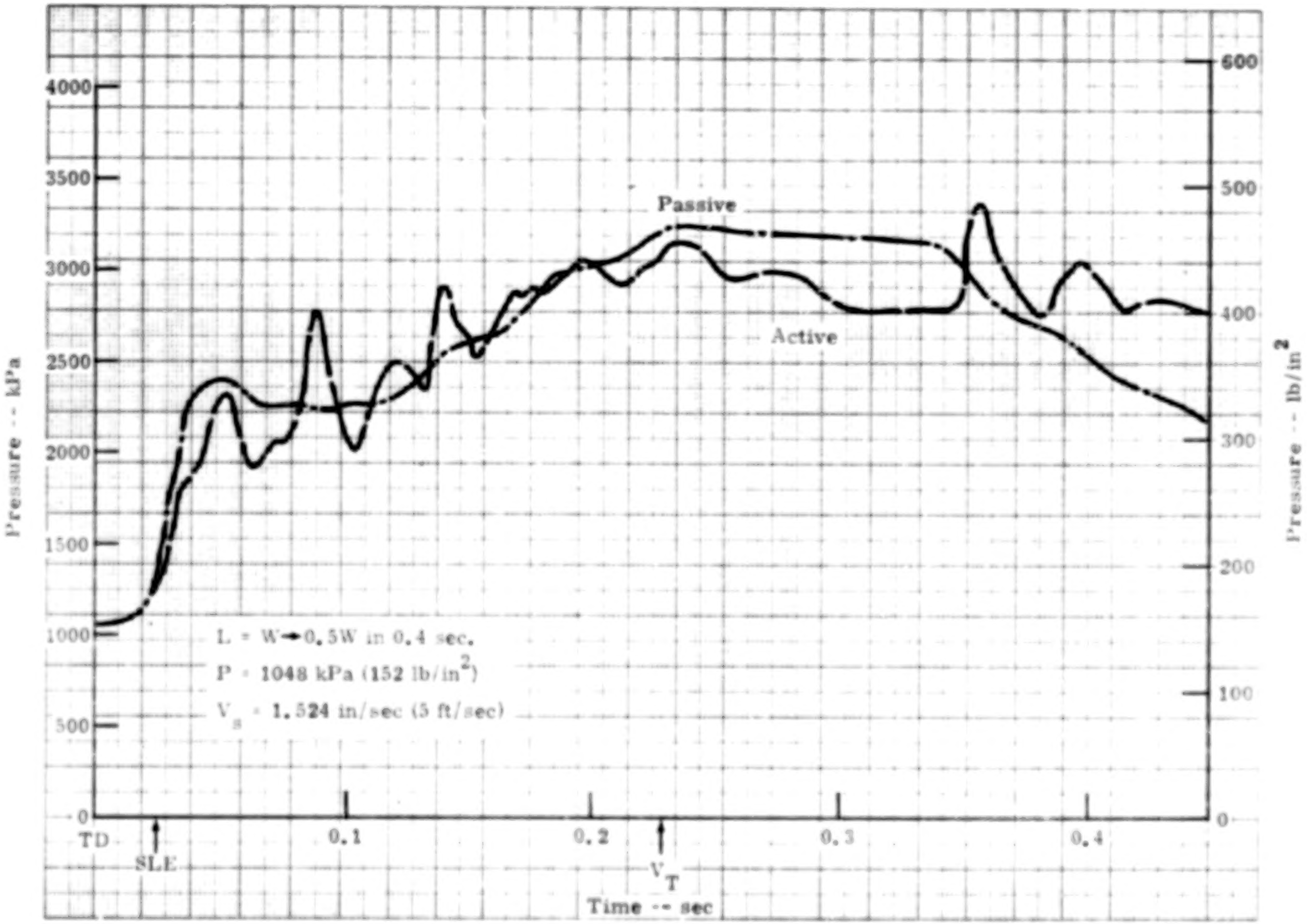

Figure 55. Gear Hydraulic Pressure, Conditions 3, 6

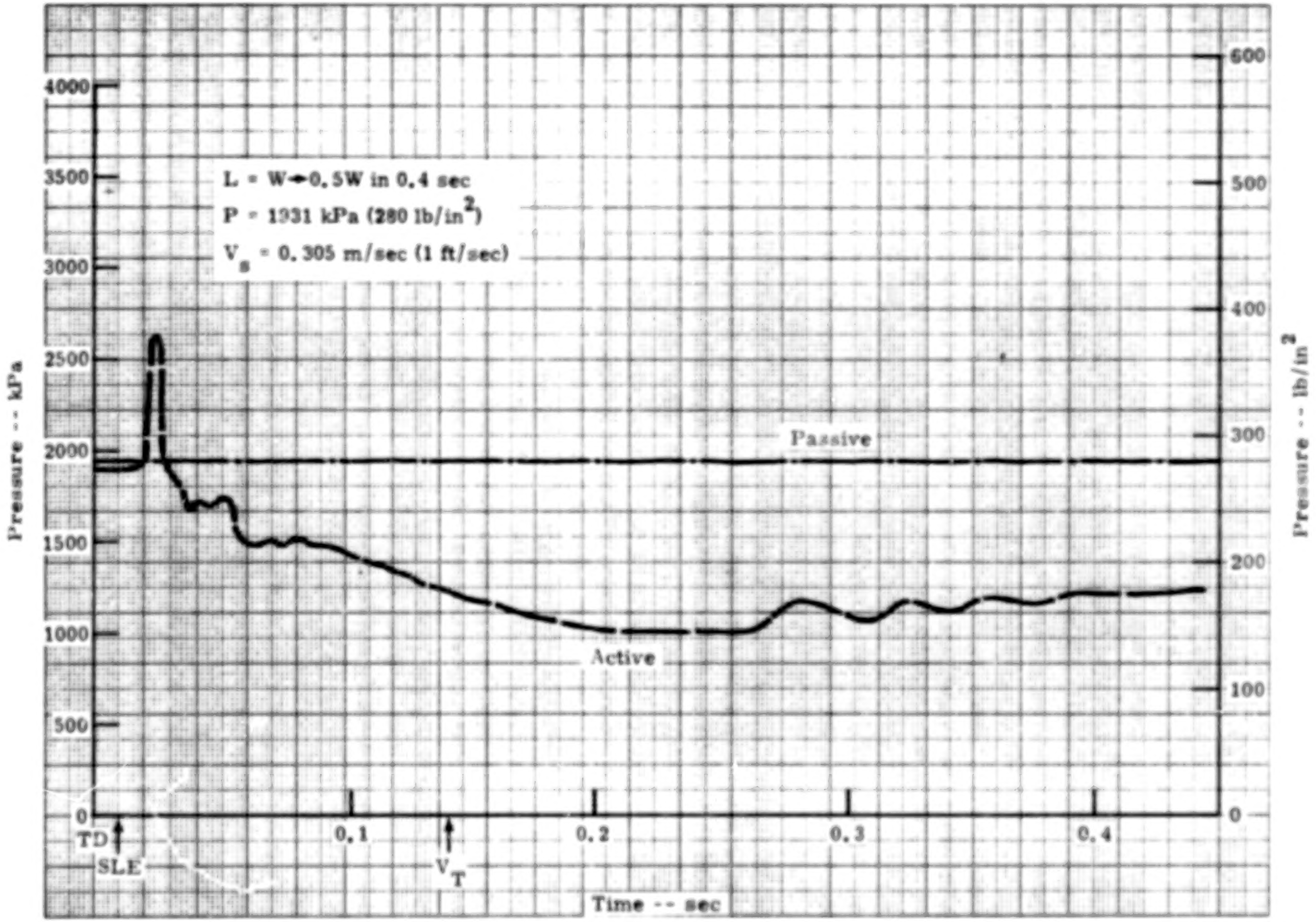

Figure 56. Gear Hydraulic Pressure, Conditions 7, 10

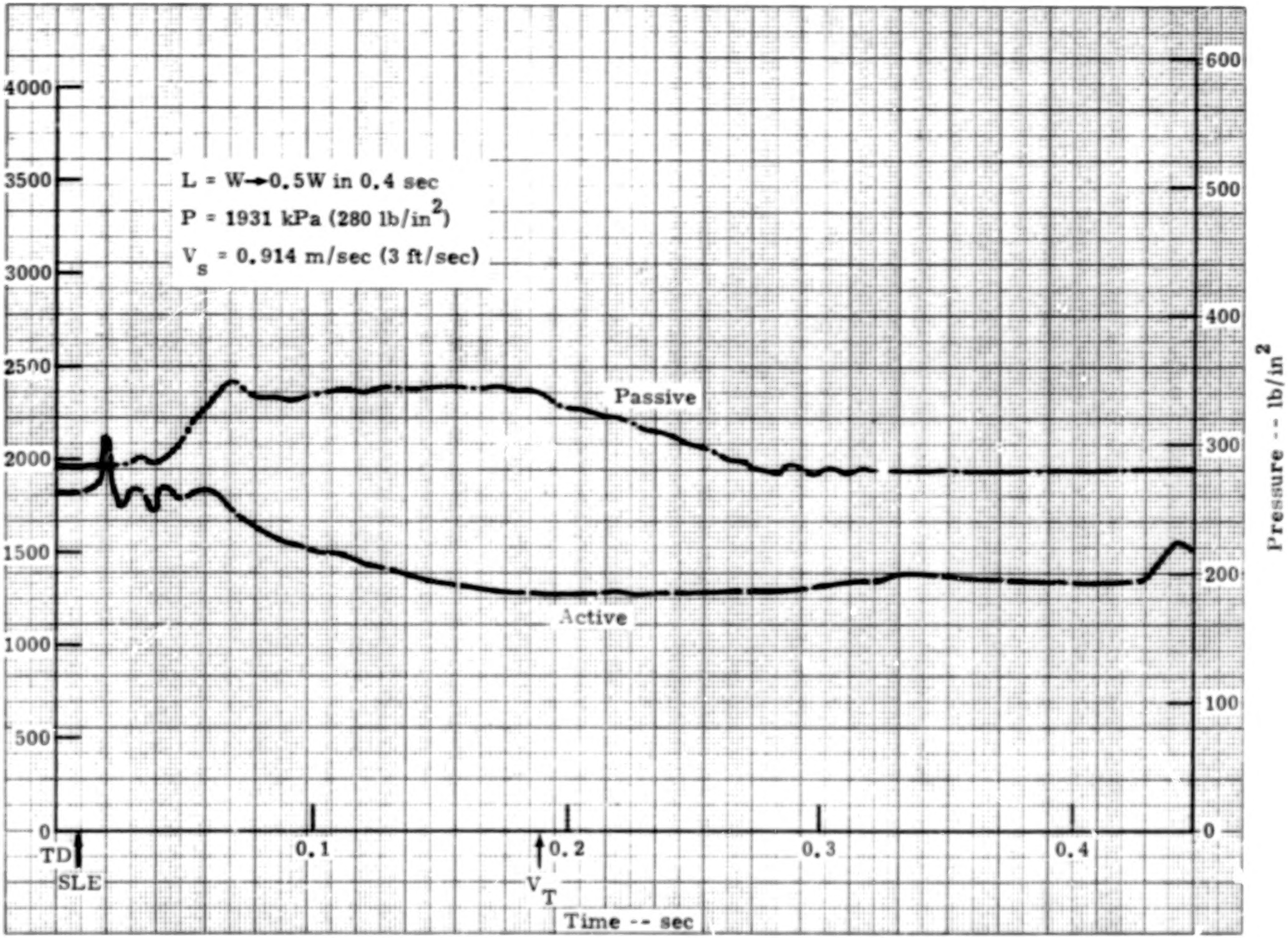

Figure 57. Gear Hydraulic Pressure, Conditions 8, 11

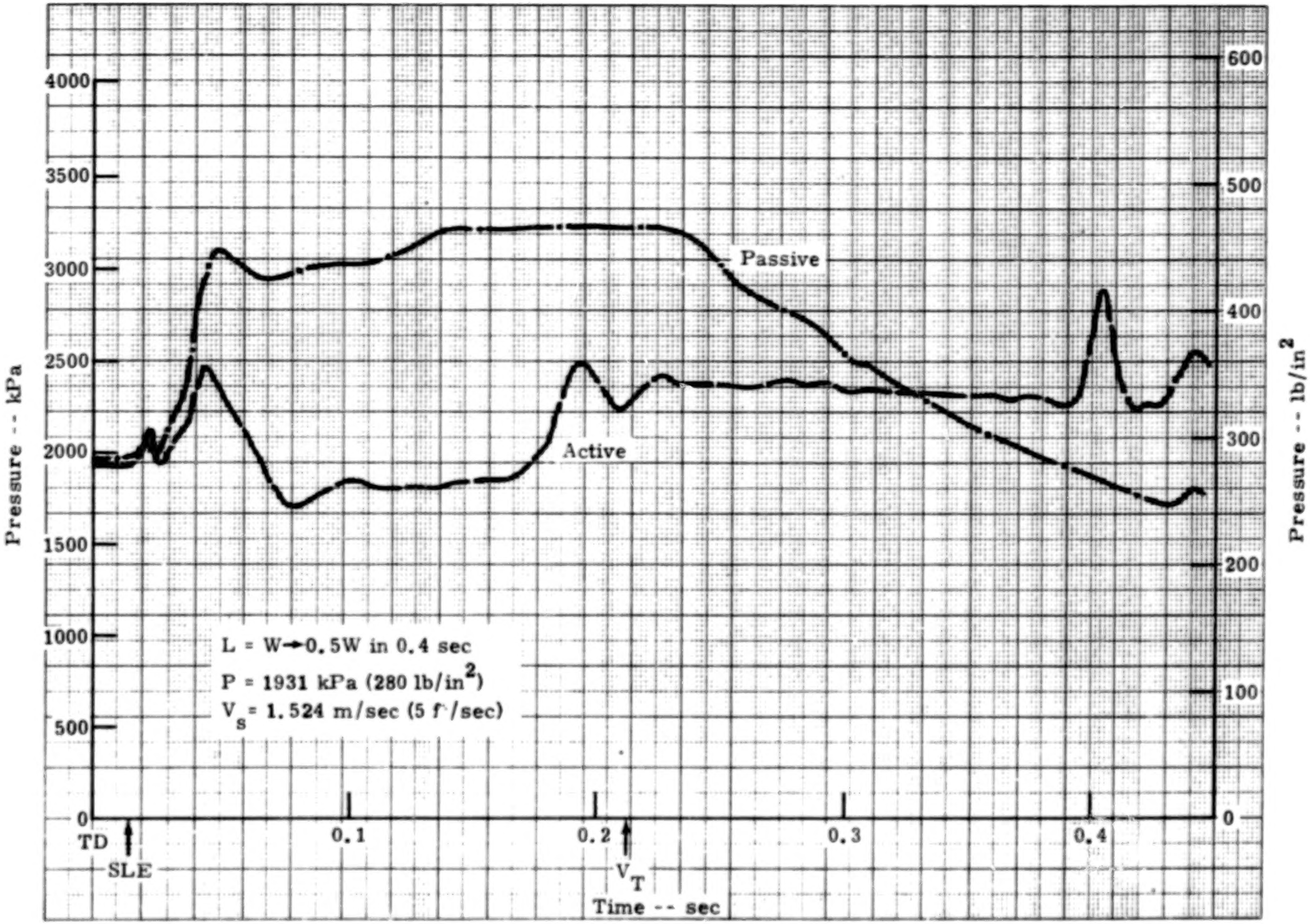

Figure 58. Gear Hydraulic Pressure, Conditions 9, 12

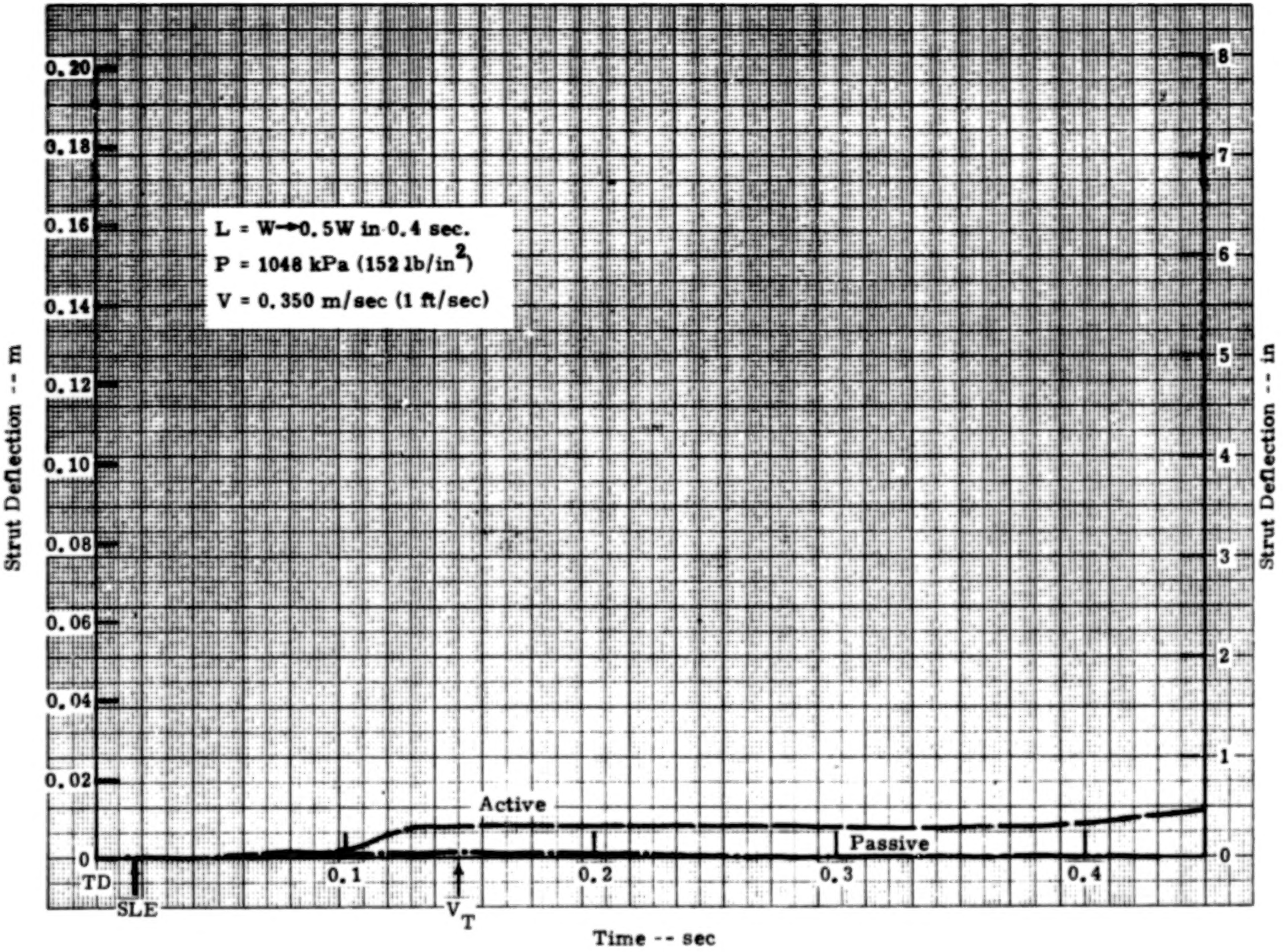

Figure 59. Strut Deflection, Conditions 1, 4

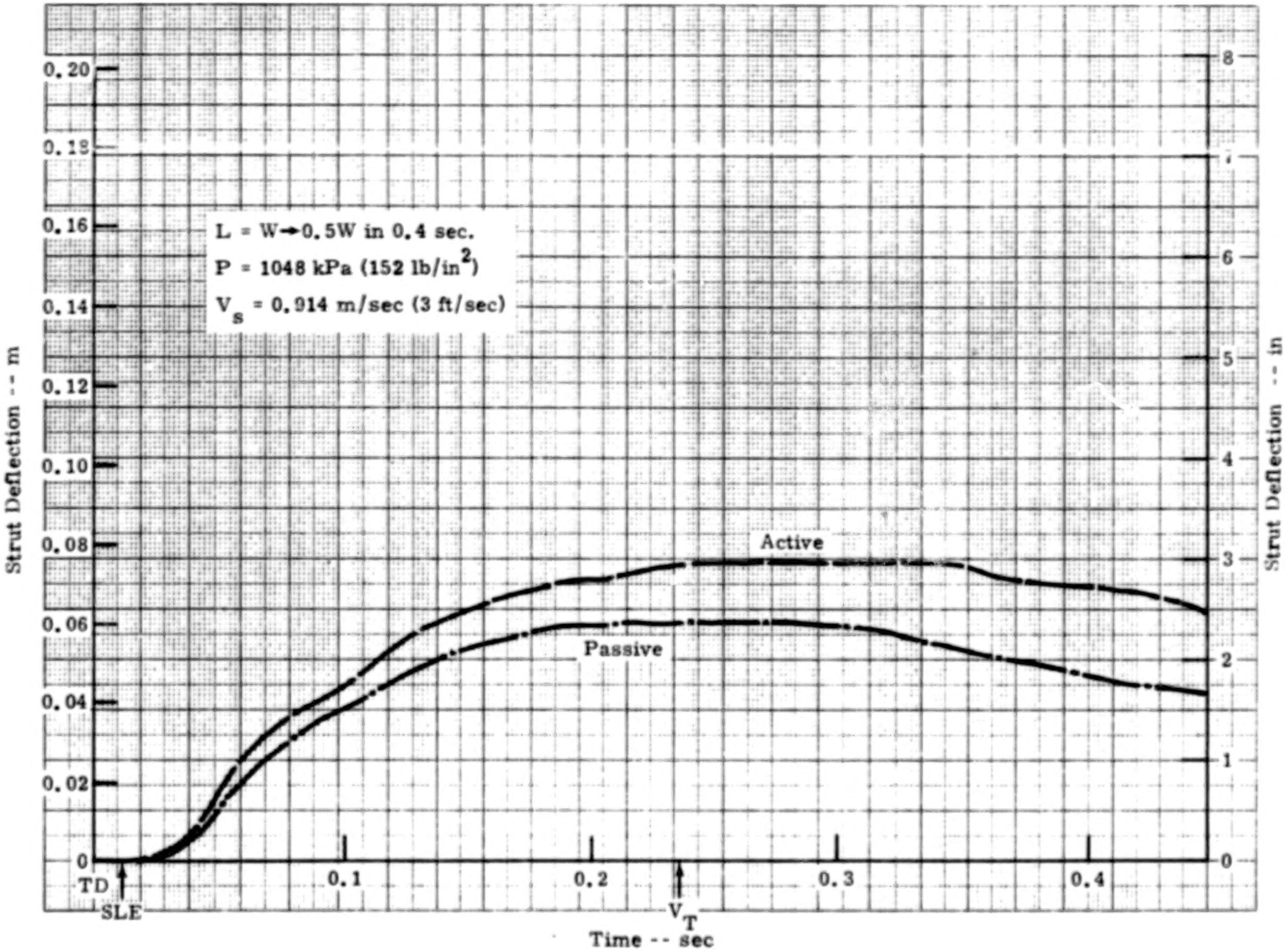

Figure 60. Strut Deflection, Conditions 2, 5

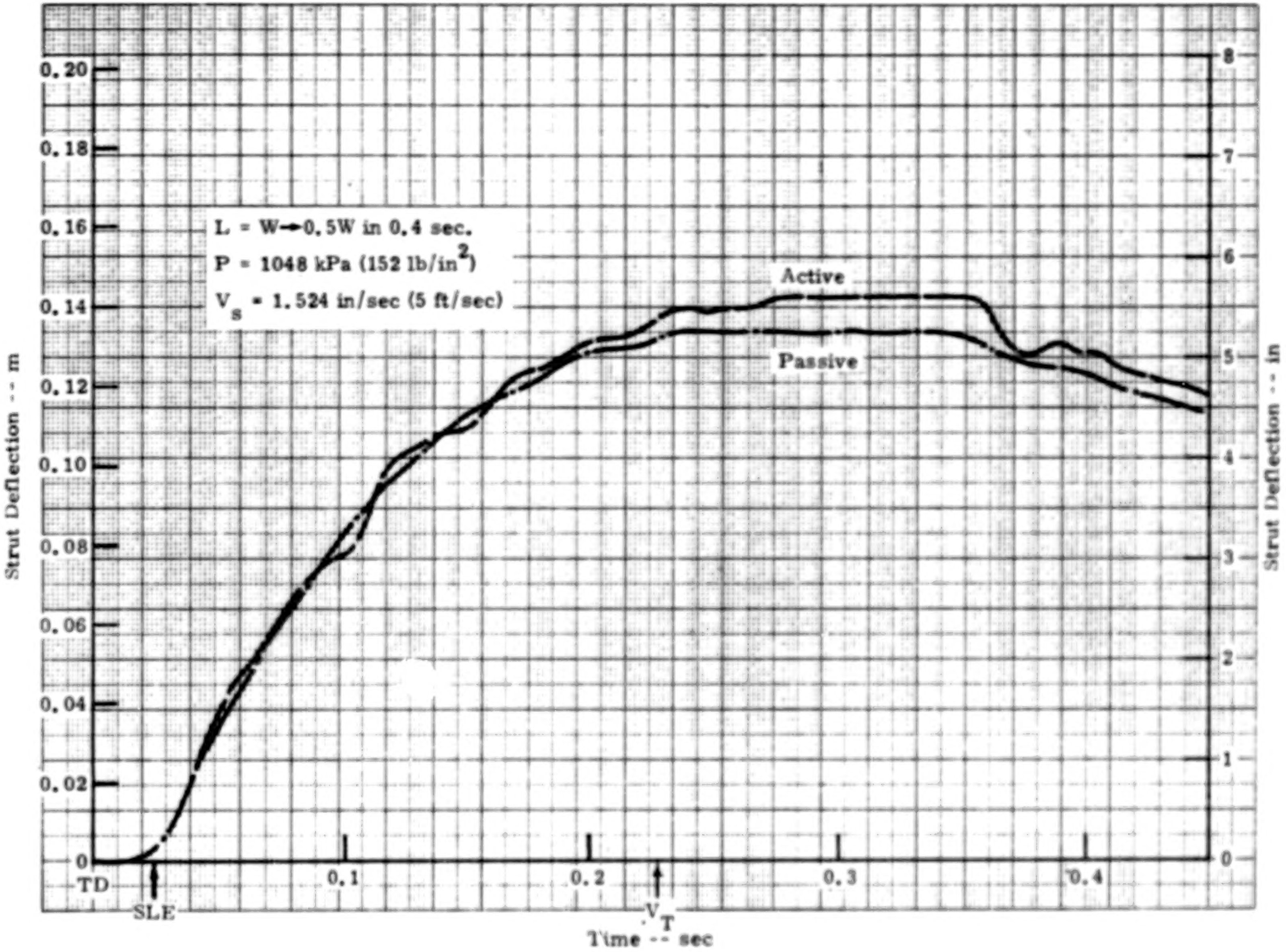

Figure 61. Strut Deflection, Conditions 3, 6

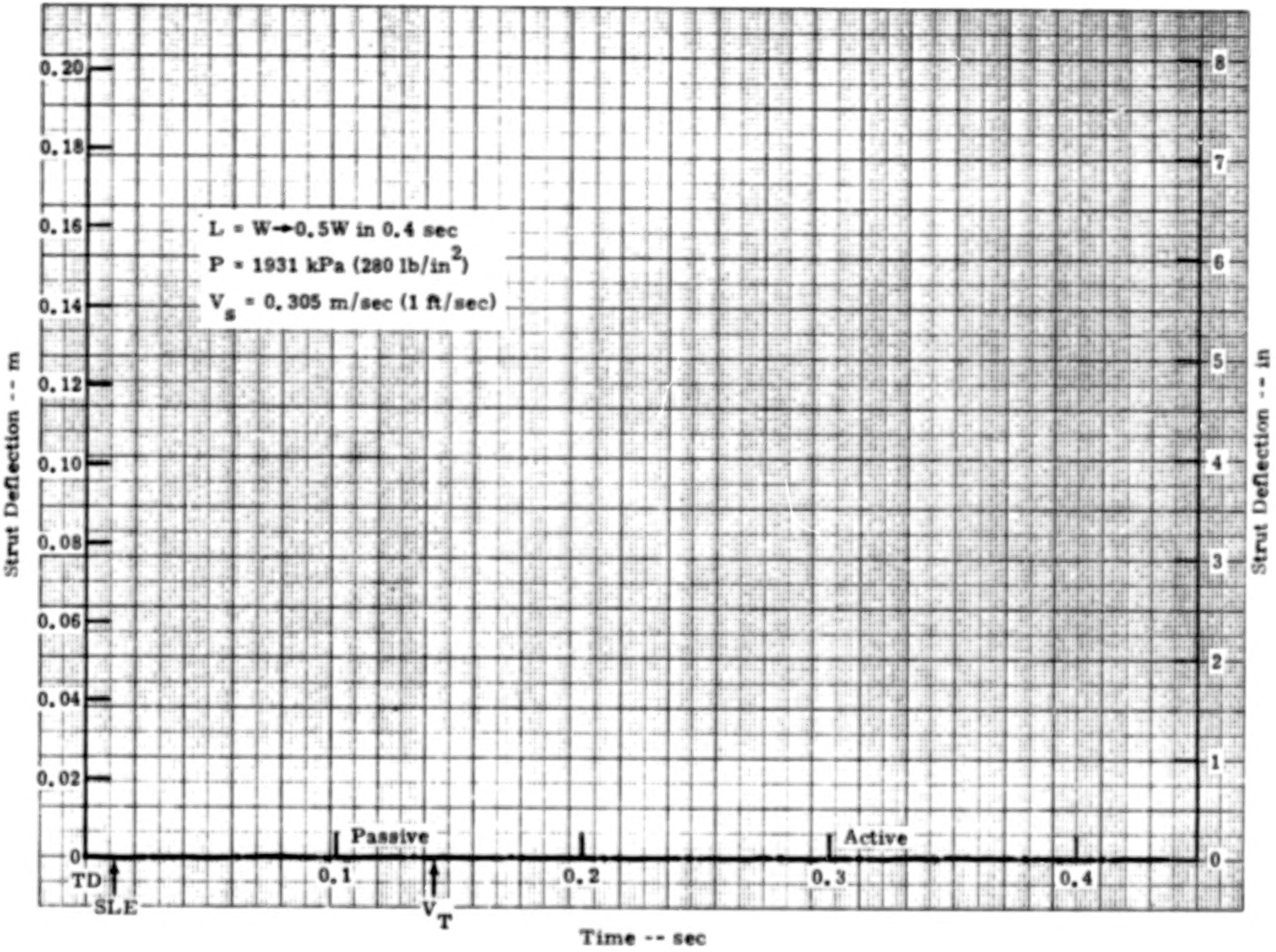

Figure 62. Strut Deflection, Conditions 7, 10

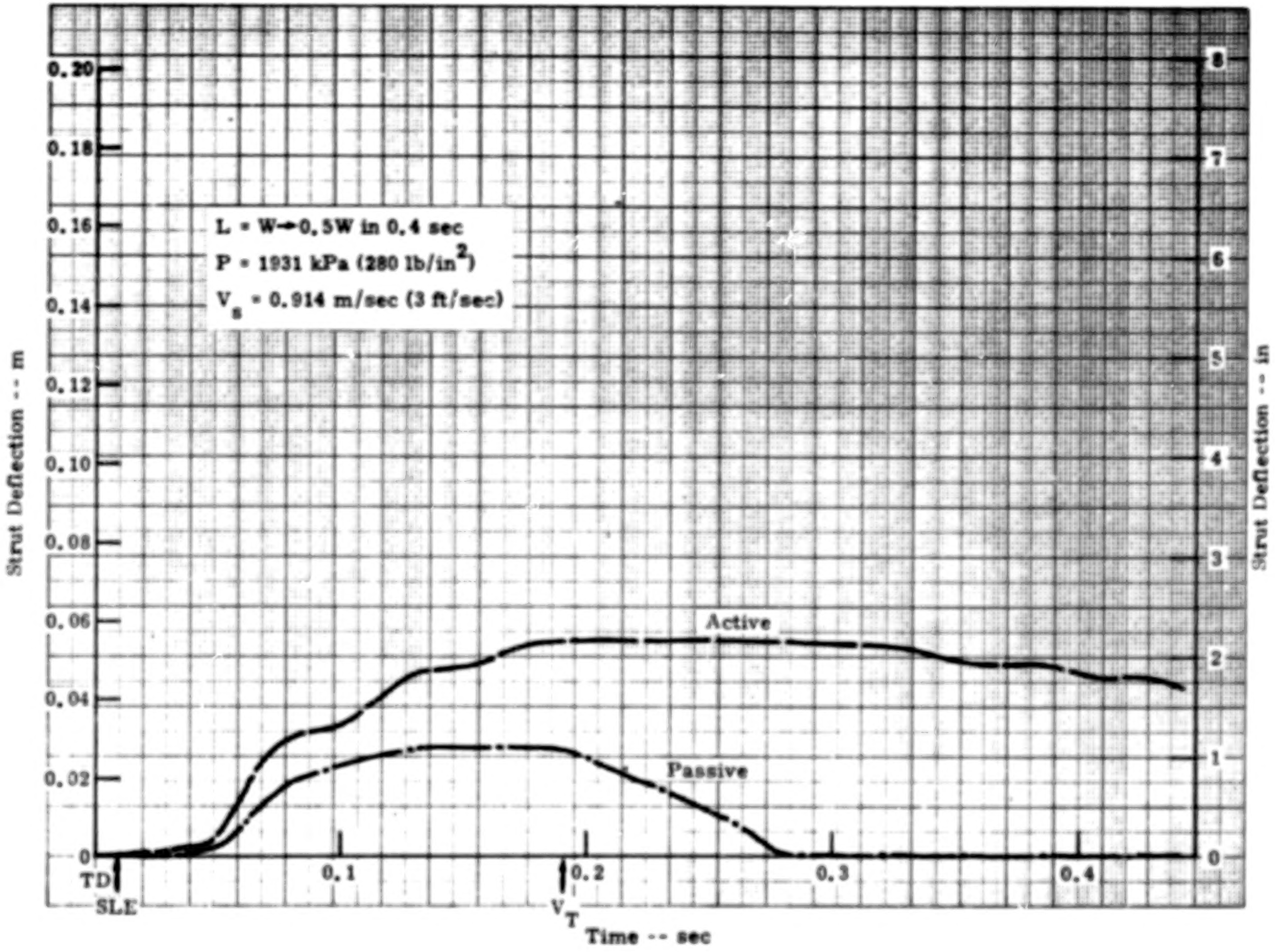

Figure 63. Strut Deflection, Conditions 8, 11

///

CONTENTS

Page

SUMMARY 1 1/A14

INTRODUCTION 1 1/A14

SYMBOLS 3 1/B2

ANALYSIS 8 1/B7
  Nonlinear Math Model for Vertical Drops 8 1/B7
    Equations of Motion 10 1/B9
    Pressure, Flow, and Volume Relationship 14 1/B14
    Servovalve Dynamics 16 1/C2
  Linear Math Model for Vertical Drops 18 1/C5
  Energy Considerations 27 1/D1
  Stability Analysis 39 1/E2

ANALYTICAL RESULTS 51 1/F11
  Vertical Drop Cases 53 1/F14
  Land and Roll Cases 53 1/F14

CONTROLLER FUNCTIONAL DESCRIPTION 71 2/B11
  Associated Equipment 71 2/B11
  Interface 71 2/B11
  Performance Characteristics 76 2/C7
  Operating-Mode Determination 76 2/C7
    Landing Mode 76 2/C7
    Takeoff Mode 77 2/C8
  Limit-Force Command Determination 78 2/C9
  Control Law Implementation 78 2/C9
  Controller Design 78 2/C9
    Functional Sections 78 2/C9

CONTENTS (Contd.)

Page

TEST 89 2/E1
  Test Fixture 89 2/E1
  Test Conditions 93 2/E6
  Test Results 93 2/E6

CONCLUSIONS 114 3/A9

APPENDIX

A Microprocessor Program Listing 115 3/A10
B Electronic Controller Detailed Description 131 3/B12
C Test Procedure 142 3/C11
D Oscillograph Recordings 148 3/D4

FIGURES

1 Illustration of variables used in nonlinear simulation of simplified vertical drop case 9 1/B8
2 Free body diagram of airplane mass 11 1/B10
3 Free body diagram of upper shock strut 11 1/B10
4 Free body diagram of lower shock strut 11 1/B10
5 Dynamic response of servovalve, ±10% input signal . . . 17 1/C3
6 Illustration of "Equivalent" system for the linear math model 22 1/C9
7 Block diagram of linear math model 26 1/C13
8 Comparison of linear model and nonlinear model results, open loop, no compensation, no position feedback 28 1/D2
9 Various energy terms versus time, from the simplified nonlinear vertical drop simulation 33 1/D8
10 Illustration of the variation of limit force versus time and the various phases of operation following impact . . . 35 1/D11
11 Block diagram of linear system without compensation . . 40 1/E3

CONTENTS (Contd.)

Page

FIGURES

12 Nyquist plot of F_{wg}/F_{lim} with force loop opened, no position feedback, no compensation 41 1/E5

13 Electronic compensation network and its characteristics . . 42 1/E7

14 Nyquist plot of F_{wg}/F_{lim} with force loop opened, no position feedback, with compensation 43 1/E9

15 Nyquist plot of F_{wg}/F_{lim} with force loop opened, position loop closed, with compensation 45 1/E12

16 Nyquist plot of X_s/X_c with position loop opened, force loop closed, with compensation 46 1/F1

17 Frequency response of F_{wg}/F_{lim} with force and position loops closed, with compensation 47 1/F3

18 Frequency response of X_s/X_c with force and position loops closed, with compensation 48 1/F5

19 Nyquist plot of F_{wg}/F_{lim} with force loop opened, position loop closed, with compensation. 49 1/F7

20 Nyquist plot of F_{wg}/F_{lim} with force loop opened, position loop closed, with compensation. 50 1/F9

21 Wing/gear force transient, case A 54 1/G1

22 Wing/gear force transient, case B 55 1/G3

23 Strut position transient, case B 56 1/G5

24 Wing/gear force transient, case 1 . . . . 57 1/G7

25 Strut pressures, case 1 . . . . 58 1/G9

26 Strut position transient, case 1 . . . . 59 1/G11

27 Wing/gear force transient, case 2 . . . . 60 1/G13

28 Strut position transient, case 2 . . . . 61 2/A6

29 Wing/gear force transient, case 3 . . . . 63 2/A9

30 Wing/gear force transient, case 4 . . . . 64 2/A11

31 Servovalve flow rate, case A 65 2/A13

32 Servovalve flow rate, case B 66 2/B1

CONTENTS (Contd.)

Page

FIGURES

33 Servovalve flow rate, case 1 . . . . 67 2/B3
34 Servovalve flow rate, case 2 . . . . 68 2/B5
35 Servovalve flow rate, case 3 . . . . 69 2/B7
36 Servovalve flow rate, case 4 . . . . 70 2/B9
37 Input/Output Signal Schematic 72 2/B10
38 Control Law Functional Schematic 79 2/C10
39 Controller Functional Schematic 81 2/D1
40 Basic Functional Requirements 82 2/D3
41 Software Flow Chart 84 2/D6
42 Analog Section Schematic 85 2/D8
43 Analog Section - Front Panel Inputs 87 2/D11
44 Analog Section - Front Panel Outputs 88 2/D13
45 S-1C Test Fixture, Landing Gear Installed (View 1) . . . 90 2/E2
46 S-1C Test Fixture, Landing Gear Installed (View 2) . . . 91 2/E3
47 Net Force, Conditions 1, 4 (From W/G Accel #1) 95 2/E9
48 Net Force, Conditions 2, 5 (From W/G Accel #1) 96 2/E11
49 Net Force, Conditions 3, 6 (From W/G Accel #1) 97 2/E13
50 Net Force, Conditions 7, 10 (From W/G Accel #1) 98 2/F1
51 Net Force, Conditions 8, 11 (From W/G Accel #1) 99 2/F3
52 Net Force, Conditions 9, 12 (From W/G Accel #1) 100 2/F5
53 Gear Hydraulic Pressure, Conditions 1, 4 . . . . 101 2/F7
54 Gear Hydraulic Pressure, Conditions 2, 5 . . . . 102 2/F9
55 Gear Hydraulic Pressure, Conditions 3, 6 . . . . 103 2/F11
56 Gear Hydraulic Pressure, Conditions 7, 10 . . . . 104 2/F12
57 Gear Hydraulic Pressure, Conditions 8, 11 . . . . 105 2/G1
58 Gear Hydraulic Pressure, Conditions 9, 12 . . . . 106 2/G3

CONTENTS (Contd.)

Page

FIGURES

59 Strut Deflection, Conditions 1, 4 . . . . 107 2/G5

60 Strut Deflection, Conditions 2, 5 . . . . 108 2/G7

61 Strut Deflection, Conditions 3, 6 . . . . 109 2/G9

62 Strut Deflection, Conditions 7, 10 . . . . 110 2/G11

63 Strut Deflection, Conditions 8, 11 . . . . 111 2/G13

64 Strut Deflection, Conditions 9, 12 . . . . 112 3/A6

TABLES

I SUMMARY OF ACTIVE CONTROL LANDING CASES SIMULATED ON THE COMPUTER 52 1/F12

II PRIMARY INPUT SIGNAL SPECIFICATIONS 73 2/C1

III SECONDARY INPUT SPECIFICATIONS 74 2/C3

IV OUTPUT SPECIFICATIONS 75 2/C5

V CONTROL LAW TRANSFER FUNCTIONS. 80 2/C12

VI PEAK FORCES AND PERCENTAGE REDUCTION 94 2/E7

REFERENCES. 161 3/F1

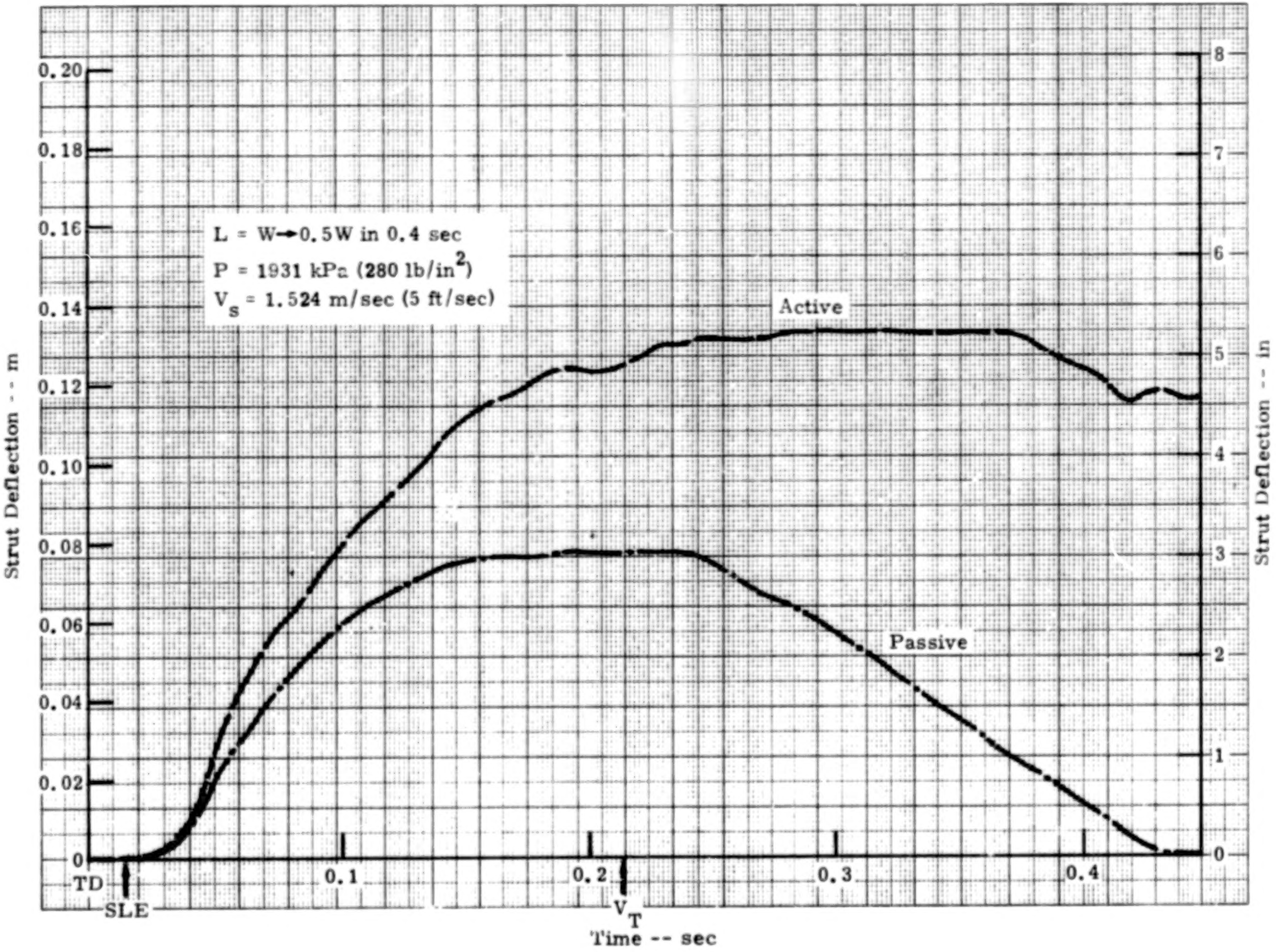

Figure 64. Strut Deflection, Conditions 9, 12

The apparent lack of reduction at the second peak under conditions 3 and 6 is due to the fact that a resonance at approximately 20 Hz is evident at these conditions, which masks the performance of the gear both passively and when actively controlled. Reference 2 indicates that a resonance of 20 Hz is apparent in the fore and aft direction when the gear is dropped on an inclined surface. This resonance can be suppressed by inclusion of appropriate compensation networks in the controller.

CONCLUSIONS

This report has presented the analysis of an active control landing gear, the detailed design of an electronic controller to produce the active control, and the results of tests of the complete system. The results indicate that the force reduction varies from 9 to 31% depending on the aircraft sink speed and the static gear pressure.

It is apparent that the effectiveness of the controller is highly dependent on the dynamic compensation employed; and, such compensation must be optimized for the particular aircraft landing gear system in which the controller is used. The compensation must be such that the dynamic response of the controller is quite high to control the impact force while still providing stable operation.

Appendix A

MICROPROCESSOR PROGRAM LISTING

Assembled at 0000

```
 ASSM 0000 8000
CW    0082
EB    00EB
PORT5 00E9
PORT6 00EA
OUT1  0040
OUT2  00A1
OUT3  0090
OUT4  0091
OUT5  0092
OUT6  0093
IOBAS 00A0
MBASE 8000
MLOW  0000
MHIGH 0080
MSTAT 00A1
MFLAG 00A7
MBIAS 007F
BASE  F700
SCA   F700
FCR   F701
LCHAN F702
CLR   F703
ADDAT F704
DAC0  F708
DAC1  F70A
MUX0  0001
MUX1  0000
MUX2  0002
MUX3  0003
XMAX  09B9
XTHR  003B
TV0   0085
TV1   00C8
TV2   002F
TVEXP 0036
STACK 3FFF
RAM   3F80
ACCEL 8000
FLIM  3F80
WBVEL 3F84
STRUT 3F86
SINK  3F88
BXTHR 3F8A
BXMAX 3F8C
```

```
PE    3F8E
TRANS 3F92
START 0000
L1    001E
L8    004B
L9    0088
L10   0096
L11   0099
L4    00DE
L5    0116
L6    0123
L?    0127
L7    0131
IN3   0143
M1    014C
M2    0165
IN1   0174
M3    017B
SUB2  0189
SHL   0190
MATH  0195
WAIT  0197
PGA   01AC
R2    01B6
0000             0010 *
0000             0020 *  DEFINE CONSTANTS
0000             0030 *
0000             0040 *            I/O PORTS
0000             0050 CW     EQU   82H        ; GROUP 2 CONTROL WORD
0000             0060 EB     EQU   0EBH       ; GROUP 2 CONTROL WORD ADDR.
0000             0070 PORT5  EQU   0E9H       ; PORT 3 ADDR
0000             0080 PORT6  EQU   0EAH       ; PORT 6 ADDR
0000             0090 *
0000             0100 *      PORT 6 OUTPUTS    CTLR   CTLR  T/O  LAND
0000             0110 *                         ENA   RESET LAMP LAMP INT.ENA SL.ENA
0000             0120 OUT1   EQU   40H        ; OFF   ON    OFF  OFF    DIS    DIS
0000             0130 OUT2   EQU   0A1H       ; ON    OFF   ON   OFF    DIS    ENA
0000             0140 OUT3   EQU   90H        ; ON    OFF   OFF  ON     DIS    DIS
0000             0150 OUT4   EQU   91H        ; ON    OFF   OFF  ON     DIS    ENA
0000             0160 OUT5   EQU   92H        ; ON    OFF   OFF  ON     ENA    DIS
0000             0170 OUT6   EQU   93H        ; ON    OFF   OFF  ON     ENA    ENA
0000             0180 *
0000             0190 *      MATH BOARD- SC 310 PARAMETERS
0000             0200 IOBAS  EQU   0A0H       ; I/O BASE ADDR
0000             0210 MBASE  EQU   8000H      ; MEMORY BASE ADDR
0000             0220 MLOW   EQU   00H        ; LS BYTE MEMORY BASE ADDR
0000             0230 MHIGH  EQU   80H        ; MS BYTE MEMORY BASE ADDR
0000             0240 MSTAT  EQU   0A1H       ; STATUS BYTE
0000             0250 MFLAG  EQU   0A7H       ; FLAG BYTE
0000             0260 MBIAS  EQU   7FH        ; FLOATING POINT EXPONENT BIAS
0000             0270 *
```

```
0000            0280 *      ANALOG I/O BOARD- SBC 732 PARAMETERS
0000            0290 BASE   EQU   0F700H      ; MEMORY BASE ADDRESS
0000            0300 SCA    EQU   BASE+0      ; A/D COMMAND-STATUS REGISTER
0000            0310 FCR    EQU   BASE+1      ; MUX ADDR AND GAIN REGISTER
0000            0320 LCHAN  EQU   BASE+2      ; LAST CHANNEL REGISTER
0000            0330 CLR    EQU   BASE+3      ; CLEAR INTERRUPTS
0000            0340 ADDAT  EQU   BASE+4      ; A/D DATA REGISTER
0000            0350 DAC0   EQU   BASE+8      ; DAC0 OUTPUT
0000            0360 DAC1   EQU   BASE+10     ; DAC1 OUTPUT
0000            0370 MUX0   EQU   01          ; A/D GAIN=1, POINT MUX TO W/G ACCEL
0000            0380 MUX1   EQU   00          ; A/D GAIN=1, POINT MUX TO W/G VEL
0000            0390 MUX2   EQU   02          ; A/D GAIN=1, POINT MUX TO STRUT POS
0000            0400 MUX3   EQU   03          ; A/D GAIN=1, POINT MUX TO SINK RATE
0000            0410 *
0000            0420 *      STRUT PARAMETERS
0000            0430 XMAX   EQU   09B9H       ; MAX STROKE= 8.5 IN. = 6.078 VOLTS
0000            0440 XTHR   EQU   003BH       ; THRESHOLD= 0.2 IN. = 0.143 VOLTS
0000            0450 *
0000            0460 *      TRANSITION VELOCITY SCALE FACTOR
0000            0470 *      =0.00004191 DECIMAL
0000            0480 *      =1.0101111110010001000010l * 2**-15 BINARY
0000            0490 TV0    EQU   85H         ; LS BYTE (M)
0000            0500 TV1    EQU   0CBH        ; LS BYTE+1 (M+1)
0000            0510 TV2    EQU   2FH         ; MS BYTE (M+2)
0000            0520 TVEXP  EQU   36H         ; EXPONENT (M+3)
0000            0530 *
0000            0540 *      RAM MEMORY ASSIGNMENTS
0000            0550 STACK  EQU   3FFFH       ; INITIAL STACK POINTER
0000            0560 RAM    EQU   3F80H       ; START OF RAM SCRATCH AREA
0000            0570 ACCEL  EQU   MBASE       ; W/G ACCEL
0000            0580 FLIM   EQU   RAM         ; LIMIT FORCE COMMAND
0000            0590 WGVEL  EQU   RAM+4       ; W/G VELOCITY
0000            0600 STRUT  EQU   RAM+6       ; STRUT POSITION
0000            0610 SINK   EQU   RAM+8       ; INITIAL SINK RATE
0000            0620 BXTHR  EQU   RAM+10      ; STRUT THRESHOLD * 16
0000            0630 BXMAX  EQU   RAM+12      ; MAX STRUT STROKE * 16
0000            0640 PE     EQU   RAM+14      ; POTENTIAL ENERGY- 4 BYTES
0000            0650 TRANS  EQU   RAM+18      ; TRANSITION VELOCITY- 4 BYTES
0000            0660 *
0000            0670 * START OF MAIN PROGRAM
0000            0680 *
0000 F3         0690 START DI              ;DISABLE INTERRUPTS
0001 21 FF 3F   0700       LXI   H,STACK ;INIT STACK POINTER
0004 F9         0710       SPHL
0005            0720 *                      CONFIGURE I/O PORTS
0005 3E 82      0730       MVI   A,CW
0007 D3 EB      0740       OUT   EB
0009            0750 *                      INIT MATH BOARD
0009 3E 00      0760       MVI   A,MLOW  ;SET MEMORY BASE ADDR
000B D3 A1      0770       OUT   MSTAT
000D 3E 80      0780       MVI   A,MHIGH
```

```
000F D3 A2        0790          OUT    MSTAT+1
0011 21 38 00     0800          LXI    H,XTHR  ;MULT STRUT THRESHOLD BY 16
0014 CD 90 01     0810          CALL   SHL     ;FOR LATER USE
0017 22 BA 3F     0820          SHLD   BXTHR
001A 3E 40        0830          MVI    A,OUT1  ;SET LIGHTS, SWITCHES
001C D3 EA        0840          OUT    PORT6
001E DB E9        0850 L1       IN     PORT5   ;CONTROLLER ENABLED?
0020 1F           0860          RAR
0021 D2 1E 00     0870          JNC    L1      ;NO, KEEP LOOKING
0024              0880 *
0024              0890 *                 CONTROLLER HAS BEEN ENABLED
0024              0900 *
0024 3E 02        0910          MVI    A,MUX2  ;YES, GET STRUT POSITION FOR
0026 CD 74 01     0920          CALL   IN1     ;LANDING/TAKEOFF DETERMINATION
0029 2A BA 3F     0930          LHLD   BXTHR   ;GET STRUT THRESHOLD
002C EB           0940          XCHG           ;PUT IN DE
002D 2A B6 3F     0950          LHLD   STRUT   ;LOAD HL WITH STRUT POSN
0030 CD B9 01     0960          CALL   SUB2    ;CALC: THRESHOLD - STRUT
0033 DA 27 01     0970          JC     L2      ;TAKING OFF
0036              0980 *
0036              0990 *                  LANDING, MAKE PREPARATIONS
0036              1000 *
0036 3E 03        1010          MVI    A,MUX3  ;GET INITIAL SINK RATE
0038 CD 74 01     1020          CALL   IN1
003B 22 B8 3F     1030          SHLD   SINK    ;STORE IT
003E 21 B9 09     1040          LXI    H,XMAX  ;MULT XMAX BY 16 TO SHIFT INTO UPPER 12 BITS
0041 CD 90 01     1050          CALL   SHL
0044 22 BC 3F     1060          SHLD   BXMAX   ;STORE IT
0047              1070 *
0047              1080 *                 ENABLE INTEGRATOR, START
0047              1090 *                 ENERGY CALCULATIONS.
0047              1100 *
0047 3E 92        1110          MVI    A,OUT5  ;ENABLE INT
0049 D3 EA        1120          OUT    PORT6
004B CD 43 01     1130 L8       CALL   IN3     ;GET ACCEL, W/G VEL, STRUT POSN FROM A/D
004E EB           1140          XCHG           ;CALC POTENTIAL ENERGY. SAVE HL IN DE
004F 2A BC 3F     1150          LHLD BXMAX     ;GET MAX STROKE
0052 EB           1160          XCHG           ;PUT IN DE
0053 7B           1170          MOV    A,E     ;CALC: XMAX - STRUT POSN
0054 95           1180          SUB    L
0055 6F           1190          MOV    L,A
0056 7A           1200          MOV    A,D
0057 9C           1210          SBB    H
0058 67           1220          MOV    H,A
0059 22 04 80     1230          SHLD   MBASE+4 ;STORE IN MATH BOARD
005C              1240 *                 ACCEL IS ALREADY IN MATH BOARD AT MBASE+0,1
005C AF           1250          XRA    A       ;MULTIPLY
005D CD 95 01     1260          CALL   MATH    ;NOW HAVE PE AS A 32-BIT WORD
0060 2A 00 80     1270          LHLD   MBASE   ;SAVE IT IN RAM
0063 22 BE 3F     1280          SHLD   PE
0066 2A 02 80     1290          LHLD   MBASE+2
```

MICROFILMED FROM
BEST AVAILABLE COPY

```
0069 22 90 3F    1300        SHLD  PE+2
006C 2A 88 3F    1310        LHLD  SINK     ;CALC KINETIC ENERGY
006F EB          1320        XCHG
0070 2A 84 3F    1330        LHLD  WGVEL
0073 CD 89 01    1340        CALL  SUB2     ;CALC: SINK RATE - W/G VEL
0076 22 00 80    1350        SHLD  MBASE    ;LOAD INTO MATH BOARD,TWO PLACES
0079 22 04 80    1360        SHLD  MBASE+4
007C AF          1370        XRA   A        ;MULT
007D CD 95 01    1380        CALL  MATH     ;NOW HAVE KE AT MBASE+0,1,2,3
0080             1390 *                      DO A BYTE-BY-BYTE COMPARISON TO TEST IF
0080             1400 *                      PE GREATER THAN KE.  DO NOT BOTHER TO TEST
0080             1410 *                      LS BYTE, IT HAS NO USEFUL DATA.
0080 06 03       1420        MVI   B,3      ;SET A BYTE COUNTER
0082 21 91 3F    1430        LXI   H,PE+3   ;POINT HL TO PE MSB
0085 11 03 80    1440        LXI D,MBASE+3  ;POINT DE TO KE MSB
0088 1A          1450 L9     LDAX  D        ;PE GREATER THAN KE?
0089 BE          1460        CMP   M
008A C2 96 00    1470        JNZ   L10
008D 1B          1480        DCX   D        ;TRY ANOTHER BYTE
008E 2B          1490        DCX   H
008F 05          1500        DCR   B        ;TESTED 3 BYTES?
0090 C2 88 00    1510        JNZ   L9       ;NO, LOOP BACK
0093 C3 99 00    1520        JMP   L11
0096 D2 4B 00    1530 L10    JNC   L8       ;GO GET NEW INPUTS, TRY AGAIN
0099             1540 *
0099             1550 *                      TIME TO INITIATE ACTIVE CONTROL
0099             1560 *
0099 2A 80 3F    1570 L11    LHLD  FLIM     ;ISSUE LIMIT FORCE COMMAND
009C 22 08 F7    1580        SHLD  DAC0
009F 3E 93       1590        MVI   A,OUT6   ;ENABLE SERVOLOOP
00A1 D3 EA       1600        OUT   PORT6
00A3             1610 *
00A3             1620 * GEAR IS NOW UNDER ACTIVE CONTROL
00A3             1630 *
00A3             1640 *                     CALC TRANSITION VELOCITY
00A3 2A 80 3F    1650        LHLD  FLIM     ;GET LIMIT FORCE CMD (FLI)
00A6 22 00 80    1660        SHLD  MBASE    ;LOAD INTO MATH BOARD
00A9 21 00 00    1670        LXI   H,0
00AC 22 02 80    1680        SHLD  MBASE+2
00AF 3E 08       1690        MVI   A,8      ;CONVERT TO FLOATING POINT
00B1 CD 95 01    1700        CALL  MATH
00B4 3E 06       1710        MVI   A,6      ;SQUARE IT
00B6 CD 95 01    1720        CALL  MATH
00B9 3E 85       1730        MVI   A,TV0    ;LOAD TRANSITION VELOCITY SCALE
00BB 32 04 80    1740        STA   MBASE+4  ;FACTOR INTO MATH BOARD
00BE 3E C8       1750        MVI   A,TV1
00C0 32 05 80    1760        STA   MBASE+5
00C3 3E 2F       1770        MVI   A,TV2
00C5 32 06 80    1780        STA   MBASE+6
00C8 3E 36       1790        MVI   A,TVEXP
00CA 32 07 80    1800        STA   MBASE+7
```

```
00CD 3E 02        1810        MVI   A,2      ;MULT BY FLI**2
00CF CD 95 01     1820        CALL  MATH
00D2 2A 00 80     1830        LHLD  MBASE    ;STORE TRANS VEL
00D5 22 92 3F     1840        SHLD  TRANS
00D8 2A 02 80     1850        LHLD  MBASE+2
00DB 22 94 3F     1860        SHLD  TRANS+2
00DE              1870 * NOW HAVE TRANSITION VEL STORED AS FLOATING POINT, 32-BIT #
00DE              1880 * SO START COMPARING THIS AGAINST (SINK RATE - W/G VEL)
00DE              1890 * FOR DETERMINING START OF TRANSITION.
00DE 2A 88 3F     1900 L4     LHLD  SINK     ;GET SINK RATE
00E1 EB           1910        XCHG           ;SAVE IN DE
00E2 3E 00        1920        MVI   A,MUX1   ;GET W/G VELOCITY
00E4 CD 74 01     1930        CALL  IN1
00E7 CD 89 01     1940        CALL  SUB2     ;CALC: SINK RATE - W/G VEL
00EA 22 00 80     1950        SHLD  MBASE    ;CONVERT TO FLOATING POINT
00ED 21 00 00     1960        LXI   H,0
00F0 22 02 80     1970        SHLD  MBASE+2
00F3 3E 08        1980        MVI   A,8
00F5 CD 95 01     1990        CALL  MATH     ;ITS NOW IN MBASE+0,1,2,3
00F8 2A 92 3F     2000        LHLD  TRANS    ;LOAD TRANS VEL INTO MATH BOARD
00FB 22 04 80     2010        SHLD  MBASE+4
00FE 2A 94 3F     2020        LHLD  TRANS+2
0101 22 06 80     2030        SHLD  MBASE+6
0104 3E 0A        2040        MVI   A,0AH    ;COMPARE AGAINST (SINK-W/G VEL)
0106 CD 95 01     2050        CALL  MATH
0109 DB A1        2060        IN    MSTAT    ;GET STATUS, MASK 'LESS THAN' BIT
010B E6 20        2070        ANI   20H      ;IS (SINK-W/G VEL) .LT. TRANS VEL?
010D CA DE 00     2080        JZ    L4       ;NO, CONTINUE LOOPING
0110              2090 *                      YES, TIME TO START TRANSITION
0110              2100 * TRANSITION PHASE
0110              2110 *
0110 2A 80 3F     2120        LHLD  FLIM     ;LOAD LIMIT FORCE COMMAND
0113 11 FD FF     2130        LXI   D,-3     ;SET RAMP RATE
0116 22 08 F7     2140 L5     SHLD  DAC0     ;OUTPUT CMD TO DAC
0119 19           2150        DAD   D        ;DECREASE LIMIT FORCE CMD
011A DA 16 01     2160        JC    L5       ;LOOP UNTIL CMD = 0
011D 21 00 00     2170        LXI   H,0      ;SET LIMIT FORCE CMD EXACTLY = 0
0120 22 08 F7     2180        SHLD  DAC0
0123 00           2190 L6     NOP            ;STAY IN A LOOP UNTIL A RESET OCCURS
0124 C3 23 01     2200        JMP   L6
0127              2210 *
0127              2220 * TAKEOFF MODE
0127              2230 *
0127 21 00 00     2240 L2     LXI   H,0      ;COMMAND A ZERO LIMIT FORCE
012A 22 08 F7     2250        SHLD  DAC0
012D 3E A1        2260        MVI   A,OUT2   ;ENABLE SERVO LOOP, LEAVE ENABLED
012F D3 EA        2270        OUT   PORT6    ;UNTIL STRUT POSITION LESS THAN THRESHOLD
0131 3E 02        2280 L7     MVI   A,MUX2   ;GET STRUT POSITION
0133 CD 74 01     2290        CALL  IN1
0136 EB           2300        XCHG           ;PUT IN DE
0137 2A 8A 3F     2310        LHLD  BXTHR    ;LOAD HL WITH THRESHOLD
```

```
013A CD 89 01      2320        CALL  SUB2    ;CALC: STRUT - THRESHOLD
013D D2 31 01      2330        JNC   L7      ;LOOP UNTIL STRUT EXTENDED FULLY
0140 C3 00 00      2340        JMP   START   ;HAVE LIFTOFF, TURN OFF CONTROLLER
0143               2350 *
0143               2360 * ROUTINE TO INPUT AND STORE DATA FROM
0143               2370 * THREE MUX CHANNELS
0143               2380 *
0143 3E 01         2390 IN3    MVI   A,MUX0  ;POINT MUX TO W/G ACCEL
0145 21 01 F7      2400        LXI   H,FCR   ;POINT HL TO MUX/GAIN REGISTER
0148 77            2410        MOV   M,A     ;LOAD REGISTER
0149 2B            2420        DCX   H       ;POINT HL TO CMD/STATUS REGISTER
014A 36 01         2430        MVI   M,01    ;START CONVERSION
014C 7E            2440 M1     MOV   A,M     ;READ STATUS
014D 07            2450        RLC           ;DONE?
014E D2 4C 01      2460        JNC   M1      ;NO, KEEP LOOPING
0151 36 00         2470        MVI   M,0     ;YES, RESET CONVERSION ENABLE
0153 2A 04 F7      2480        LHLD  ADDAT   ;GET DATA
0156 22 00 80      2490        SHLD  ACCEL   ;STO W/G ACCEL IN MATH BOARD,
0159 22 80 3F      2500        SHLD  FLIM    ;ALSO IN RAM
015C 3E 00         2510        MVI   A,MUX1  ;REPEAT FOR W/G VELOCITY
015E 21 01 F7      2520        LXI   H,FCR
0161 77            2530        MOV   M,A
0162 2B            2540        DCX   H
0163 36 01         2550        MVI   M,01
0165 7E            2560 M2     MOV   A,M
0166 07            2570        RLC
0167 D2 65 01      2580        JNC   M2
016A 36 00         2590        MVI   M,0
016C 2A 04 F7      2600        LHLD  ADDAT
016F 22 84 3F      2610        SHLD  WGVEL   ;STORE W/G VEL
0172 3E 02         2620        MVI   A,MUX2  ;REPEAT FOR STRUT POSITION
0174 21 01 F7      2630 IN1    LXI   H,FCR
0177 77            2640        MOV   M,A
0178 2B            2650        DCX   H
0179 36 01         2660        MVI   M,01
017B 7E            2670 M3     MOV   A,M
017C 07            2680        RLC
017D D2 7B 01      2690        JNC   M3
0180 36 00         2700        MVI   M,0
0182 2A 04 F7      2710        LHLD  ADDAT
0185 22 86 3F      2720        SHLD  STRUT
0188 C9            2730        RET
0189               2740 *
0189               2750 * DOUBLE PRECISION SUBTRACT ROUTINE
0189               2760 *  HL=DE-HL
0189 7B            2770 SUB2   MOV   A,E
018A 95            2780        SUB   L
018B 6F            2790        MOV   L,A
018C 7A            2800        MOV   A,D
018D 9C            2810        SBB   H
018E 67            2820        MOV   H,A
```

```
01BF C9         2830        RET
0190            2840 *
0190            2850 * ROUTINE TO SHIFT VALUE IN HL LEFT 4 PLACES.
0190            2860 *
0190 29         2870 SHL    DAD    H
0191 29         2880        DAD    H
0192 29         2890        DAD    H
0193 29         2900        DAD    H
0194 C9         2910        RET
0195            2920 *
0195            2930 * ROUTINE TO ACTIVATE MATH BOARD AND WAIT FOR RESULT.
0195            2940 * ACCUM HAS OPCODE.
0195            2950 *
0195 D3 A0      2960 MATH   OUT    IOBAS   ;COMMAND MATH BOARD TO START
0197 DB A7      2970 WAIT   IN     IOBAS+7 ;GET FLAG BYTE
0199 E6 01      2980        ANI    01      ;CHECK BUSY BIT
019B C2 97 01   2990        JNZ    WAIT    ;STAY IN LOOP UNTIL NOT BUSY
019E C9         3000        RET
019F            3010 *
019F            3020 *
019F            3030 * SPECIAL CHECK-OUT ROUTINES
019F            3040 *
019F            3050 *   ROUTINE TO INPUT A VALUE FROM A/D, STORE IN RAM.
019F            3060 *
019F F3         3070        DI
01A0 3E 00      3080        MVI    A,00    ;SELECT CHAN 0
01A2 CD 74 01   3090        CALL   IN1
01A5 CF         3100        RST    1
01A6 00         3110        NOP
01A7 00         3120        NOP
01A8            3130 * ROUTINE TO DO PGA TEST ON A/D
01A8 F3         3140        DI
01A9 21 01 F7   3150        LXI    H,FCR
01AC 36 00      3160 PGA    MVI    M,00
01AE 36 C0      3170        MVI    M,0C0H
01B0 C3 AC 01   3180        JMP    PGA
01B3 00         3190        NOP
01B4            3200 *   ROUTINE TO OUTPUT A VALUE TO DAC0, DAC1.
01B4 F3         3210        DI
01B5 00         3220        NOP
01B6 21 00 00   3230 R2     LXI    H,0
01B9 22 08 F7   3240        SHLD   DAC0
01BC 22 0A F7   3250        SHLD   DAC1
01BF 00         3260        NOP
01C0 00         3270        NOP
01C1 00         3280        NOP
01C2 C3 B6 01   3290        JMP    R2
?
```

Assembled at 3D10

```
 ASSM 3D10 8D10
CW    0082
EB    00EB
PORT5 00E9
PORT6 00EA
OUT1  0040
OUT2  00A1
OUT3  0090
OUT4  0091
OUT5  0092
OUT6  0093
IOBAS 00A0
MBASE 8000
MLOW  0000
MHIGH 0080
MSTAT 00A1
MFLAG 00A7
MBIAS 007F
BASE  F700
SCA   F700
FCR   F701
LCHAN F702
CLR   F703
ADDAT F704
DAC0  F708
DAC1  F70A
MUX0  0001
MUX1  0000
MUX2  0002
MUX3  0003
XMAX  09B9
XTHR  0038
TV0   0085
TV1   00C8
TV2   002F
TVEXP 0036
STACK 3FFF
RAM   3F80
ACCEL 8000
FLIM  3F80
WGVEL 3F84
STRUT 3F86
SINK  3F88
BXTHR 3F8A
BXMAX 3F8C
PE    3F8E
TRANS 3F92
START 3D10
L1    3D2E
L8    3D5B
L9    3D98
```

```
L10   3DA6
L11   3DA9
L4    3DEE
L5    3E26
L6    3E33
L2    3E37
L7    3E41
IN3   3E53
M1    3E5C
M2    3E75
IN1   3E84
M3    3E8B
SUB2  3E99
SHL   3EA0
MATH  3EA5
WAIT  3EA7
PGA   3EBC
R2    3EC6
3D10            0010 *
3D10            0020 *  DEFINE CONSTANTS
3D10            0030 *
3D10            0040 *            I/O PORTS
3D10            0050 CW     EQU   82H        ; GROUP 2 CONTROL WORD
3D10            0060 EB     EQU   0EBH       ; GROUP 2 CONTROL WORD ADDR.
3D10            0070 PORT5  EQU   0E9H       ; PORT 5 ADDR
3D10            0080 PORT6  EQU   0EAH       ; PORT 6 ADDR
3D10            0090 *
3D10            0100 *      PORT 6 OUTPUTS    CTLR  CTLR  T/O  LAND
3D10            0110 *                         ENA  RESET LAMP LAMP INT.ENA SL.ENA
3D10            0120 OUT1   EQU   40H        ; OFF  ON    OFF  OFF    DIS    DIS
3D10            0130 OUT2   EQU   0A1H       ; ON   OFF   ON   OFF    DIS    ENA
3D10            0140 OUT3   EQU   90H        ; ON   OFF   OFF  ON     DIS    DIS
3D10            0150 OUT4   EQU   91H        ; ON   OFF   OFF  ON     DIS    ENA
3D10            0160 OUT5   EQU   92H        ; ON   OFF   OFF  ON     ENA    DIS
3D10            0170 OUT6   EQU   93H        ; ON   OFF   OFF  ON     ENA    ENA
3D10            0180 *
3D10            0190 *      MATH BOARD- SC 310 PARAMETERS
3D10            0200 IOBAS  EQU   0A0H       ; I/O BASE ADDR
3D10            0210 MBASE  EQU   8000H      ; MEMORY BASE ADDR
3D10            0220 MLOW   EQU   00H        ; LS BYTE MEMORY BASE ADDR
3D10            0230 MHIGH  EQU   80H        ; MS BYTE MEMORY BASE ADDR
3D10            0240 MSTAT  EQU   0A1H       ; STATUS BYTE
3D10            0250 MFLAG  EQU   0A7H       ; FLAG BYTE
3D10            0260 MBIAS  EQU   7FH        ; FLOATING POINT EXPONENT BIAS
3D10            0270 *
3D10            0280 *      ANALOG I/O BOARD- SBC 732 PARAMETERS
3D10            0290 BASE   EQU   0F700H     ; MEMORY BASE ADDRESS
3D10            0300 SCA    EQU   BASE+0     ; A/D COMMAND-STATUS REGISTER
3D10            0310 FCR    EQU   BASE+1     ; MUX ADDR AND GAIN REGISTER
3D10            0320 LCHAN  EQU   BASE+2     ; LAST CHANNEL REGISTER
3D10            0330 CLR    EQU   BASE+3     ; CLEAR INTERRUPTS
```

```
3D10            0340 ADDAT  EQU   BASE+4     ; A/D DATA REGISTER
3D10            0350 DAC0   EQU   BASE+8     ; DAC0 OUTPUT
3D10            0360 DAC1   EQU   BASE+10    ; DAC1 OUTPUT
3D10            0370 MUX0   EQU   01         ; A/D GAIN=1, POINT MUX TO W/G ACCEL
3D10            0380 MUX1   EQU   00         ; A/D GAIN=1, POINT MUX TO W/G VEL
3D10            0390 MUX2   EQU   02         ; A/D GAIN=1, POINT MUX TO STRUT POS
3D10            0400 MUX3   EQU   03         ; A/D GAIN=1, POINT MUX TO SINK RATE
3D10            0410 *
3D10            0420 *      STRUT PARAMETERS
3D10            0430 XMAX   EQU   09B9H      ; MAX STROKE= 8.5 IN. = 6.078 VOLTS
3D10            0440 XTHR   EQU   0038H      ; THRESHOLD= 0.2 IN. = 0.143 VOLTS
3D10            0450 *
3D10            0460 *      TRANSITION VELOCITY SCALE FACTOR
3D10            0470 *      =0.00004191 DECIMAL
3D10            0480 *      =1.01011111100100010000101 * 2**-15 BINARY
3D10            0490 TV0    EQU   85H        ; LS BYTE (M)
3D10            0500 TV1    EQU   0C8H       ; LS BYTE+1 (M+1)
3D10            0510 TV2    EQU   2FH        ; MS BYTE (M+2)
3D10            0520 TVEXP  EQU   36H        ; EXPONENT (M+3)
3D10            0530 *
3D10            0540 *      RAM MEMORY ASSIGNMENTS
3D10            0550 STACK  EQU   3FFFH      ; INITIAL STACK POINTER
3D10            0560 RAM    EQU   3F80H      ; START OF RAM SCRATCH AREA
3D10            0570 ACCEL  EQU   MBASE      ; W/G ACCEL
3D10            0580 FLIM   EQU   RAM        ; LIMIT FORCE COMMAND
3D10            0590 WGVEL  EQU   RAM+4      ; W/G VELOCITY
3D10            0600 STRUT  EQU   RAM+6      ; STRUT POSITION
3D10            0610 SINK   EQU   RAM+8      ; INITIAL SINK RATE
3D10            0620 BXTHR  EQU   RAM+10     ; STRUT THRESHOLD * 16
3D10            0630 BXMAX  EQU   RAM+12     ; MAX STRUT STROKE * 16
3D10            0640 PE     EQU   RAM+14     ; POTENTIAL ENERGY- 4 BYTES
3D10            0650 TRANS  EQU   RAM+18     ; TRANSITION VELOCITY- 4 BYTES
3D10            0660 *
3D10            0670 * START OF MAIN PROGRAM
3D10            0680 *
3D10 F3         0690 START DI          ;DISABLE INTERRUPTS
3D11 21 FF 3F   0700       LXI   H,STACK ;INIT STACK POINTER
3D14 F9         0710       SPHL
3D15            0720 *                    CONFIGURE I/O PORTS
3D15 3E 82      0730       MVI   A,CW
3D17 D3 EB      0740       OUT   EB
3D19            0750 *                    INIT MATH BOARD
3D19 3E 00      0760       MVI   A,MLOW  ;SET MEMORY BASE ADDR
3D1B D3 A1      0770       OUT   MSTAT
3D1D 3E 80      0780       MVI   A,MHIGH
3D1F D3 A2      0790       OUT   MSTAT+1
3D21 21 38 00   0800       LXI   H,XTHR  ;MULT STRUT THRESHOLD BY 16
3D24 CD A0 3E   0810       CALL  SHL     ;FOR LATER USE
3D27 22 8A 3F   0820       SHLD  BXTHR
3D2A 3E 40      0830       MVI   A,OUT1  ;SET LIGHTS, SWITCHES
3D2C D3 EA      0840       OUT   PORT6
```

```
3D2E DB E9      0850 L1     IN    PORT5    ;CONTROLLER ENABLED?
3D30 1F         0860        RAR
3D31 D2 2E 3D   0870        JNC   L1       ;NO, KEEP LOOKING
3D34            0880 *
3D34            0890 *                      CONTROLLER HAS BEEN ENABLED
3D34            0900 *
3D34 3E 02      0910        MVI   A,MUX2   ;YES, GET STRUT POSITION FOR
3D36 CD 84 3E   0920        CALL  IN1      ;LANDING/TAKEOFF DETERMINATION
3D39 2A 8A 3F   0930        LHLD  BXTHR    ;GET STRUT THRESHOLD
3D3C EB         0940        XCHG           ;PUT IN DE
3D3D 2A 86 3F   0950        LHLD  STRUT    ;LOAD HL WITH STRUT POSN
3D40 CD 99 3E   0960        CALL  SUB2     ;CALC: THRESHOLD - STRUT
3D43 DA 37 3E   0970        JC    L2       ;TAKING OFF
3D46            0980 *
3D46            0990 *                       LANDING, MAKE PREPARATIONS
3D46            1000 *
3D46 3E 03      1010        MVI   A,MUX3   ;GET INITIAL SINK RATE
3D48 CD 84 3E   1020        CALL  IN1
3D4B 22 88 3F   1030        SHLD  SINK     ;STORE IT
3D4E 21 B9 09   1040        LXI   H,XMAX   ;MULT XMAX BY 16 TO SHIFT INTO UPPER 12 BITS
3D51 CD A0 3E   1050        CALL  SHL
3D54 22 8C 3F   1060        SHLD  BXMAX    ;STORE IT
3D57            1070 *
3D57            1080 *                     ENABLE INTEGRATOR, START
3D57            1090 *                     ENERGY CALCULATIONS.
3D57            1100 *
3D57 3E 92      1110        MVI   A,OUT5   ;ENABLE INT
3D59 D3 EA      1120        OUT   PORT6
3D5B CD 53 3E   1130 L8     CALL  IN3      ;GET ACCEL, W/G VEL, STRUT POSN FROM A/D
3D5E EB         1140        XCHG           ;CALC POTENTIAL ENERGY. SAVE HL IN DE
3D5F 2A 8C 3F   1150        LHLD BXMAX     ;GET MAX STROKE
3D62 EB         1160        XCHG           ;PUT IN DE
3D63 7B         1170        MOV   A,E      ;CALC: XMAX - STRUT POSN
3D64 95         1180        SUB   L
3D65 6F         1190        MOV   L,A
3D66 7A         1200        MOV   A,D
3D67 9C         1210        SBB   H
3D68 67         1220        MOV   H,A
3D69 22 04 80   1230        SHLD  MBASE+4 ;STORE IN MATH BOARD
3D6C            1240 *                     ACCEL IS ALREADY IN MATH BOARD AT MBASE+0,1
3D6C AF         1250        XRA   A        ;MULTIPLY
3D6D CD A5 3E   1260        CALL  MATH     ;NOW HAVE PE AS A 32-BIT WORD
3D70 2A 00 80   1270        LHLD  MBASE    ;SAVE IT IN RAM
3D73 22 8E 3F   1280        SHLD  PE
3D76 2A 02 80   1290        LHLD  MBASE+2
3D79 22 90 3F   1300        SHLD  PE+2
3D7C 2A 88 3F   1310        LHLD  SINK     ;CALC KINETIC ENERGY
3D7F EB         1320        XCHG
3D80 2A 84 3F   1330        LHLD  WGVEL
3D83 CD 99 3E   1340        CALL  SUB2     ;CALC: SINK RATE - W/G VEL
3D86 22 00 80   1350        SHLD  MBASE    ;LOAD INTO MATH BOARD,TWO PLACES
```

```
3DB9 22 04 80     1360        SHLD  MBASE+4
3D8C AF           1370        XRA   A       ;MULT
3D8D CD A5 3E     1380        CALL  MATH    ;NOW HAVE KE AT MBASE+0,1,2,3
3D90              1390 *                     DO A BYTE-BY-BYTE COMPARISON TO TEST IF
3D90              1400 *                     PE GREATER THAN KE.  DO NOT BOTHER TO TEST
3D90              1410 *                     LS BYTE, IT HAS NO USEFUL DATA.
3D90 06 03        1420        MVI   B,3     ;SET A BYTE COUNTER
3D92 21 91 3F     1430        LXI   H,PE+3  ;POINT HL TO PE MSB
3D95 11 03 80     1440        LXI D,MBASE+3 ;POINT DE TO KE MSB
3D98 1A           1450 L9     LDAX  D       ;PE GREATER THAN KE?
3D99 BE           1460        CMP   M
3D9A C2 A6 3D     1470        JNZ   L10
3D9D 1B           1480        DCX   D       ;TRY ANOTHER BYTE
3D9E 2B           1490        DCX   H
3D9F 05           1500        DCR   B       ;TESTED 3 BYTES?
3DA0 C2 98 3D     1510        JNZ   L9      ;NO, LOOP BACK
3DA3 C3 A9 3D     1520        JMP   L11
3DA6 D2 5B 3D     1530 L10    JNC   L8      ;GO GET NEW INPUTS, TRY AGAIN
3DA9              1540 *
3DA9              1550 *                     TIME TO INITIATE ACTIVE CONTROL
3DA9              1560 *
3DA9 2A 80 3F     1570 L11    LHLD  FLIM    ;ISSUE LIMIT FORCE COMMAND
3DAC 22 08 F7     1580        SHLD  DAC0
3DAF 3E 93        1590        MVI   A,OUT6  ;ENABLE SERVOLOOP
3DB1 D3 EA        1600        OUT   PORT6
3DB3              1610 *
3DB3              1620 * GEAR IS NOW UNDER ACTIVE CONTROL
3DB3              1630 *
3DB3              1640 *                    CALC TRANSITION VELOCITY
3DB3 2A 80 3F     1650        LHLD  FLIM    ;GET LIMIT FORCE CMD (FLI)
3DB6 22 00 80     1660        SHLD  MBASE   ;LOAD INTO MATH BOARD
3DB9 21 00 00     1670        LXI   H,0
3DBC 22 02 80     1680        SHLD  MBASE+2
3DBF 3E 08        1690        MVI   A,8     ;CONVERT TO FLOATING POINT
3DC1 CD A5 3E     1700        CALL  MATH
3DC4 3E 06        1710        MVI   A,6     ;SQUARE IT
3DC6 CD A5 3E     1720        CALL  MATH
3DC9 3E 85        1730        MVI   A,TV0   ;LOAD TRANSITION VELOCITY SCALE
3DCB 32 04 80     1740        STA   MBASE+4 ;FACTOR INTO MATH BOARD
3DCE 3E C8        1750        MVI   A,TV1
3DD0 32 05 80     1760        STA   MBASE+5
3DD3 3E 2F        1770        MVI   A,TV2
3DD5 32 06 80     1780        STA   MBASE+6
3DD8 3E 36        1790        MVI   A,TVEXP
3DDA 32 07 80     1800        STA   MBASE+7
3DDD 3E 02        1810        MVI   A,2     ;MULT BY FLI**2
3DDF CD A5 3E     1820        CALL  MATH
3DE2 2A 00 80     1830        LHLD  MBASE   ;STORE TRANS VEL
3DE5 22 92 3F     1840        SHLD  TRANS
3DE8 2A 02 80     1850        LHLD  MBASE+2
3DEB 22 94 3F     1860        SHLD  TRANS+2
```

```
3DEE                1870 * NOW HAVE TRANSITION VEL STORED AS FLOATING POINT, 32-BIT *
3DEE                1880 * SO START COMPARING THIS AGAINST (SINK RATE - W/G VEL)
3DEE                1890 * FOR DETERMINING START OF TRANSITION.
3DEE 2A 88 3F       1900 L4     LHLD   SINK     ;GET SINK RATE
3DF1 EB             1910        XCHG            ;SAVE IN DE
3DF2 3E 00          1920        MVI    A,MUX1   ;GET W/G VELOCITY
3DF4 CD 84 3E       1930        CALL   IN1
3DF7 CD 99 3E       1940        CALL   SUB2     ;CALC: SINK RATE - W/G VEL
3DFA 22 00 80       1950        SHLD   MBASE    ;CONVERT TO FLOATING POINT
3DFD 21 00 00       1960        LXI    H,0
3E00 22 02 80       1970        SHLD   MBASE+2
3E03 3E 08          1980        MVI    A,8
3E05 CD A5 3E       1990        CALL   MATH     ;ITS NOW IN MBASE+0,1,2,3
3E08 2A 92 3F       2000        LHLD   TRANS    ;LOAD TRANS VEL INTO MATH BOARD
3E0B 22 04 80       2010        SHLD   MBASE+4
3E0E 2A 94 3F       2020        LHLD   TRANS+2
3E11 22 06 80       2030        SHLD   MBASE+6
3E14 3E 0A          2040        MVI    A,0AH    ;COMPARE AGAINST (SINK-W/G VEL)
3E16 CD A5 3E       2050        CALL   MATH
3E19 DB A1          2060        IN     MSTAT    ;GET STATUS, MASK 'LESS THAN' BIT
3E1B E6 20          2070        ANI    20H      ;IS (SINK-W/G VEL) .LT. TRANS VEL?
3E1D CA EE 3D       2080        JZ     L4       ;NO, CONTINUE LOOPING
3E20                2090 *                       YES, TIME TO START TRANSITION
3E20                2100 * TRANSITION PHASE
3E20                2110 *
3E20 2A 80 3F       2120        LHLD   FLIM     ;LOAD LIMIT FORCE COMMAND
3E23 11 FD FF       2130        LXI    D,-3     ;SET RAMP RATE
3E26 22 08 F7       2140 L5     SHLD   DAC0     ;OUTPUT CMD TO DAC
3E29 19             2150        DAD    D        ;DECREASE LIMIT FORCE CMD
3E2A DA 26 3E       2160        JC     L5       ;LOOP UNTIL CMD = 0
3E2D 21 00 00       2170        LXI    H,0      ;SET LIMIT FORCE CMD EXACTLY = 0
3E30 22 08 F7       2180        SHLD   DAC0
3E33 00             2190 L6     NOP             ;STAY IN A LOOP UNTIL A RESET OCCURS
3E34 C3 33 3E       2200        JMP    L6
3E37                2210 *
3E37                2220 * TAKEOFF MODE
3E37                2230 *
3E37 21 00 00       2240 L2     LXI    H,0      ;COMMAND A ZERO LIMIT FORCE
3E3A 22 08 F7       2250        SHLD   DAC0
3E3D 3E A1          2260        MVI    A,OUT2   ;ENABLE SERVO LOOP, LEAVE ENABLED
3E3F D3 EA          2270        OUT    PORT6    ;UNTIL STRUT POSITION LESS THAN THRESHOLD
3E41 3E 02          2280 L7     MVI    A,MUX2   ;GET STRUT POSITION
3E43 CD 84 3E       2290        CALL   IN1
3E46 EB             2300        XCHG            ;PUT IN DE
3E47 2A 8A 3F       2310        LHLD   BXTHR    ;LOAD HL WITH THRESHOLD
3E4A CD 99 3E       2320        CALL   SUB2     ;CALC: STRUT - THRESHOLD
3E4D D2 41 3E       2330        JNC    L7       ;LOOP UNTIL STRUT EXTENDED FULLY
3E50 C3 10 3D       2340        JMP    START    ;HAVE LIFTOFF, TURN OFF CONTROLLER
3E53                2350 *
3E53                2360 * ROUTINE TO INPUT AND STORE DATA FROM
3E53                2370 * THREE MUX CHANNELS
```

```
3E53                2380 *
3E53 3E 01          2390 IN3   MVI   A,MUX0  ;POINT MUX TO W/G ACCEL
3E55 21 01 F7       2400       LXI   H,FCR   ;POINT HL TO MUX/GAIN REGISTER
3E58 77             2410       MOV   M,A     ;LOAD REGISTER
3E59 2B             2420       DCX   H       ;POINT HL TO CMD/STATUS REGISTER
3E5A 36 01          2430       MVI   M,01    ;START CONVERSION
3E5C 7E             2440 M1    MOV   A,M     ;READ STATUS
3E5D 07             2450       RLC           ;DONE?
3E5E D2 5C 3E       2460       JNC   M1      ;NO, KEEP LOOPING
3E61 36 00          2470       MVI   M,0     ;YES, RESET CONVERSION ENABLE
3E63 2A 04 F7       2480       LHLD  ADDAT   ;GET DATA
3E66 22 00 80       2490       SHLD  ACCEL   ;STO W/G ACCEL IN MATH BOARD,
3E69 22 80 3F       2500       SHLD  FLIM    ;ALSO IN RAM
3E6C 3E 00          2510       MVI   A,MUX1  ;REPEAT FOR W/G VELOCITY
3E6E 21 01 F7       2520       LXI   H,FCR
3E71 77             2530       MOV   M,A
3E72 2B             2540       DCX   H
3E73 36 01          2550       MVI   M,01
3E75 7E             2560 M2    MOV   A,M
3E76 07             2570       RLC
3E77 D2 75 3E       2580       JNC   M2
3E7A 36 00          2590       MVI   M,0
3E7C 2A 04 F7       2600       LHLD  ADDAT
3E7F 22 84 3F       2610       SHLD  WGVEL    ;STORE W/G VEL
3E82 3E 02          2620       MVI   A,MUX2  ;REPEAT FOR STRUT POSITION
3E84 21 01 F7       2630 IN1   LXI   H,FCR
3E87 77             2640       MOV   M,A
3E88 2B             2650       DCX   H
3E89 36 01          2660       MVI   M,01
3E8B 7E             2670 M3    MOV   A,M
3E8C 07             2680       RLC
3E8D D2 8B 3E       2690       JNC   M3
3E90 36 00          2700       MVI   M,0
3E92 2A 04 F7       2710       LHLD  ADDAT
3E95 22 86 3F       2720       SHLD  STRUT
3E98 C9             2730       RET
3E99                2740 *
3E99                2750 * DOUBLE PRECISION SUBTRACT ROUTINE
3E99                2760 *  HL=DE-HL
3E99 7B             2770 SUB2  MOV   A,E
3E9A 95             2780       SUB   L
3E9B 6F             2790       MOV   L,A
3E9C 7A             2800       MOV   A,D
3E9D 9C             2810       SBB   H
3E9E 67             2820       MOV   H,A
3E9F C9             2830       RET
3EA0                2840 *
3EA0                2850 * ROUTINE TO SHIFT VALUE IN HL LEFT 4 PLACES.
3EA0                2860 *
3EA0 29             2870 SHL   DAD   H
3EA1 29             2880       DAD   H
```

```
3EA2 29         2890        DAD   H
3EA3 29         2900        DAD   H
3EA4 C9         2910        RET
3EA5            2920 *
3EA5            2930 * ROUTINE TO ACTIVATE MATH BOARD AND WAIT FOR RESULT.
3EA5            2940 * ACCUM HAS OPCODE.
3EA5            2950 *
3EA5 D3 A0      2960 MATH   OUT   IOBAS   ;COMMAND MATH BOARD TO START
3EA7 DB A7      2970 WAIT   IN    IOBAS+7 ;GET FLAG BYTE
3EA9 E6 01      2980        ANI   01      ;CHECK BUSY BIT
3EAB C2 A7 3E   2990        JNZ   WAIT    ;STAY IN LOOP UNTIL NOT BUSY
3EAE C9         3000        RET
3EAF            3010 *
3EAF            3020 *
3EAF            3030 * SPECIAL CHECK-OUT ROUTINES
3EAF            3040 *
3EAF            3050 *   ROUTINE TO INPUT A VALUE FROM A/D, STORE IN RAM.
3EAF            3060 *
3EAF F3         3070        DI
3EB0 3E 00      3080        MVI   A,00    ;SELECT CHAN 0
3EB2 CD 84 3E   3090        CALL  IN1
3EB5 CF         3100        RST   1
3EB6 00         3110        NOP
3EB7 00         3120        NOP
3EB8            3130 * ROUTINE TO DO PGA TEST ON A/D
3EB8 F3         3140        DI
3EB9 21 01 F7   3150        LXI   H,FCR
3EBC 36 00      3160 PGA    MVI   M,00
3EBE 36 C0      3170        MVI   M,0C0H
3EC0 C3 BC 3E   3180        JMP   PGA
3EC3 00         3190        NOP
3EC4            3200 *   ROUTINE TO OUTPUT A VALUE TO DAC0, DAC1.
3EC4 F3         3210        DI
3EC5 00         3220        NOP
3EC6 21 00 00   3230 R2     LXI   H,0
3EC9 22 08 F7   3240        SHLD  DAC0
3ECC 22 0A F7   3250        SHLD  DAC1
3ECF 00         3260        NOP
3ED0 00         3270        NOP
3ED1 00         3280        NOP
3ED2 C3 C6 3E   3290        JMP   R2
?
```

Appendix B

ELECTRONIC CONTROLLER DETAILED DESCRIPTION

GENERAL CONSTRUCTION

The controller consists of four boards, together with + and - 5V dc power supplies, control switches, and test jacks. The four boards perform the following functions.

(1) Central Processing Unit (CPU) Board: The CPU board is part of the computer and performs the basic digital computations as well as the logical computations which determine the operating mode of the controller.

(2) Arithmetic Board: The arithmetic board performs, in digital form, the required multiplication and division functions associated with energy and transition velocity.

(3) Linear (Analog) Board: The linear board provides the control laws and functions associated with the force and position loops. It also computes the wing/gear velocity by integrating the wing/gear acceleration. In addition, it incorporates the switching circuitry which is actuated by signals from the CPU.

(4) Analog-to-Digital (A/D) and Digital-to-Analog (D/A) Board: This controller board converts the sensed and computed analog quantities to digital form so that the digital computations can be performed to determine the commanded limit force, and converts the limit force to analog form so that it can be used as the input to the force loop.

The physical location of the units is shown in Figure B-1 and the functional interrelationship (block diagram form) is shown in Figure B-2.

As received from the factory, the A/D board is configured to operate over the range of -10 to +10 V. All of the analog signals in the controller lie between 0 and +10 V. Therefore, to achieve maximum accuracy, the A/D board was reconfigured to operate in this range in accordance with the manual's jumpering instructions. The board is sent to NASA in this configuration.

1. Analog Board
2. A/D and D/A Board
3. CPU Board
4. Arithmetic Board

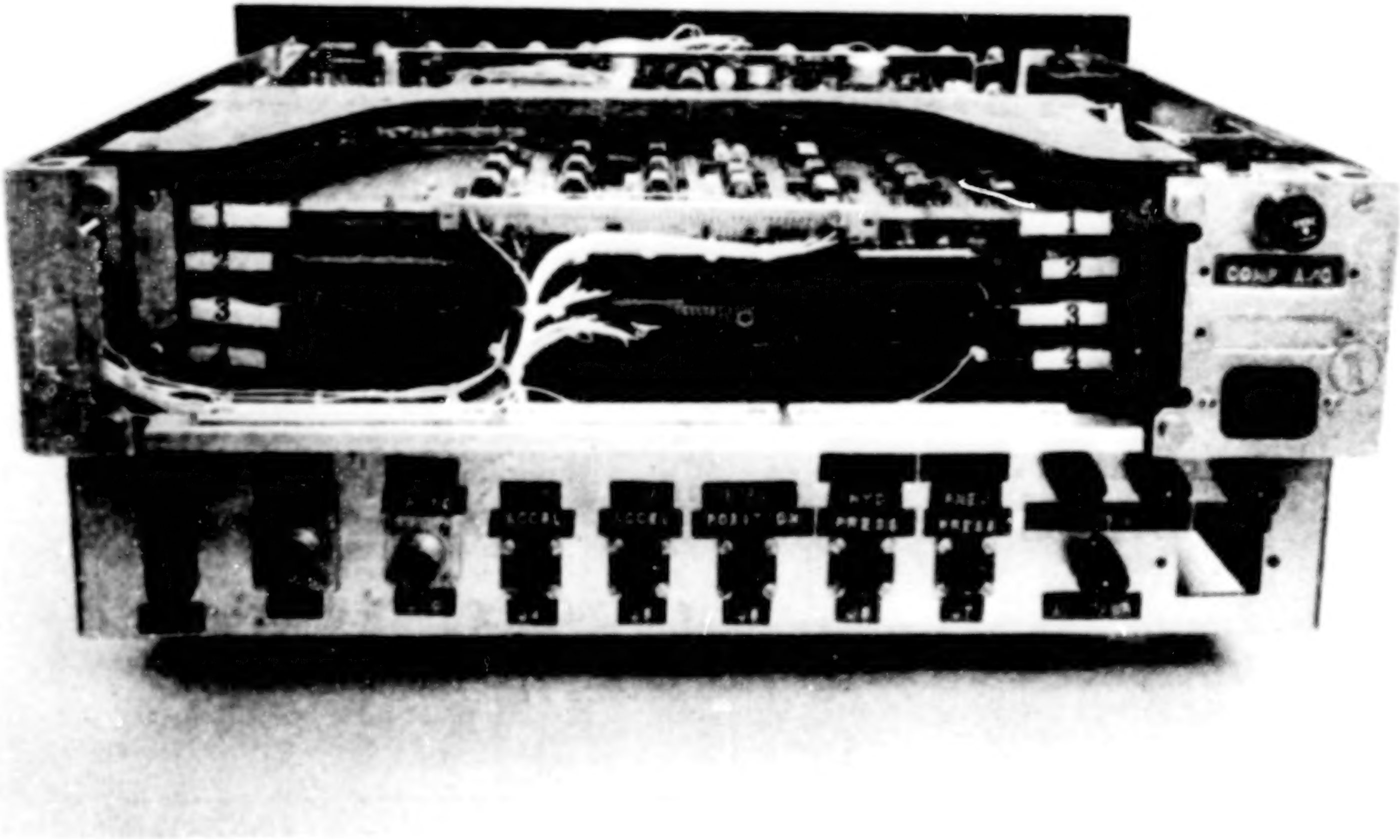
2
3
4
2
3
4
COMP A/C
1
ACCEL
ACCEL
HYD PRESS
PNEU PRESS

Figure B-1. - Landing Gear Controller (Rear View)

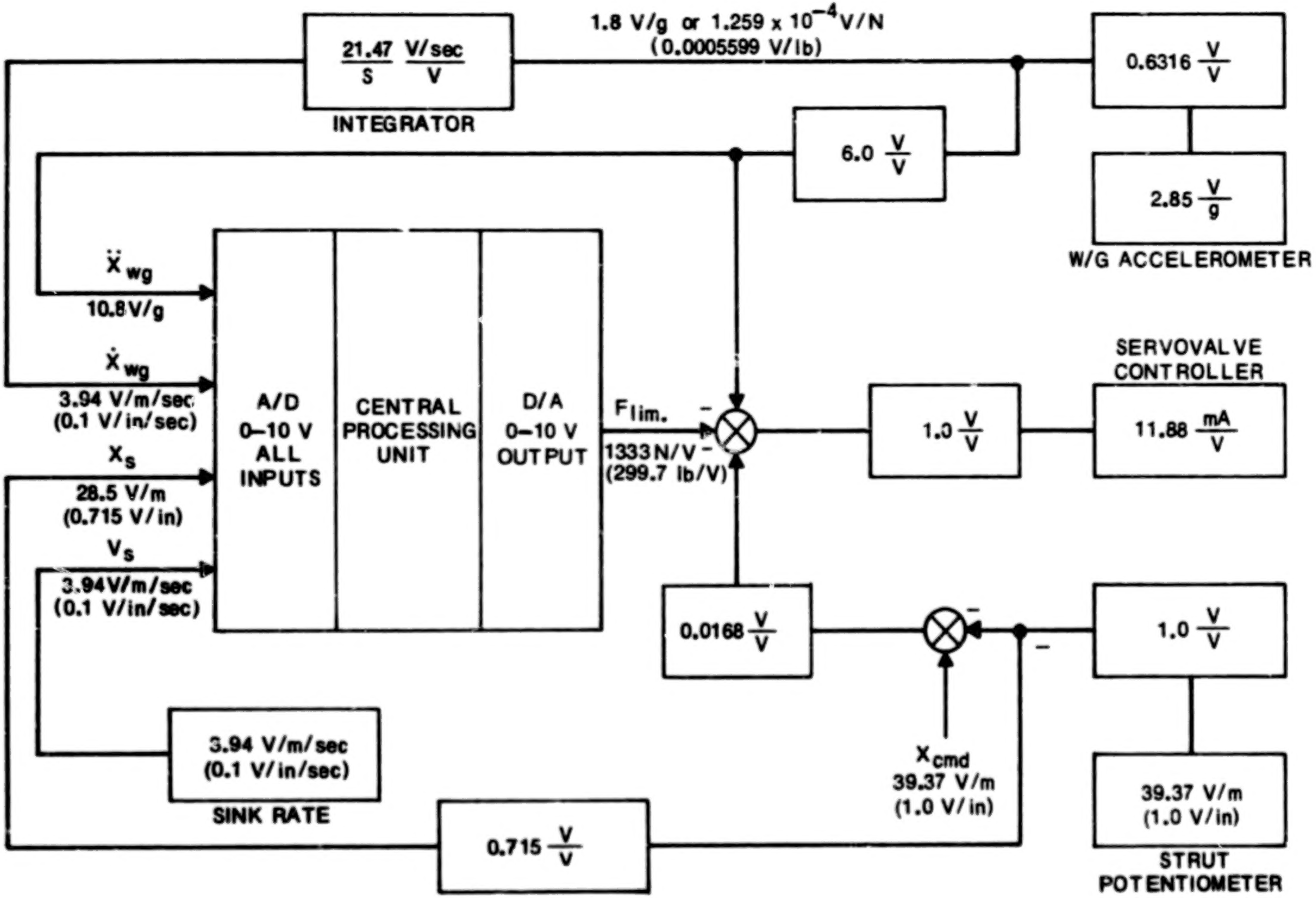

21.47/S V/sec/V
INTEGRATOR
1.8 V/g or 1.259 x 10^-4 V/N
(0.0005599 V/lb)
0.6316 V/V
2.85 V/g
W/G ACCELEROMETER
6.0 V/V
Ẍwg
10.8 V/g
Ẋwg
3.94 V/m/sec
(0.1 V/in/sec)
Xs
28.5 V/m
(0.715 V/in)
Vs
3.94 V/m/sec
(0.1 V/in/sec)
A/D
0–10 V
ALL
INPUTS
CENTRAL
PROCESSING
UNIT
D/A
0–10 V
OUTPUT
Flim.
1333 N/V
(299.7 lb/V)
–
–
SERVOVALVE
CONTROLLER
1.0 V/V
11.88 mA/V
0.0168 V/V
–
–
1.0 V/V
39.37 V/m
(1.0 V/in)
STRUT
POTENTIOMETER
Xcmd
39.37 V/m
(1.0 V/in)
3.94 V/m/sec
(0.1 V/in/sec)
SINK RATE
0.715 V/V

Figure B-2. - Controller Static Gains and Scale Factors

CONTROL LAWS

The control laws implemented in the controller are presented below in Figure B-3. (Refer to SYMBOLS, Page 3, Report Proper.)

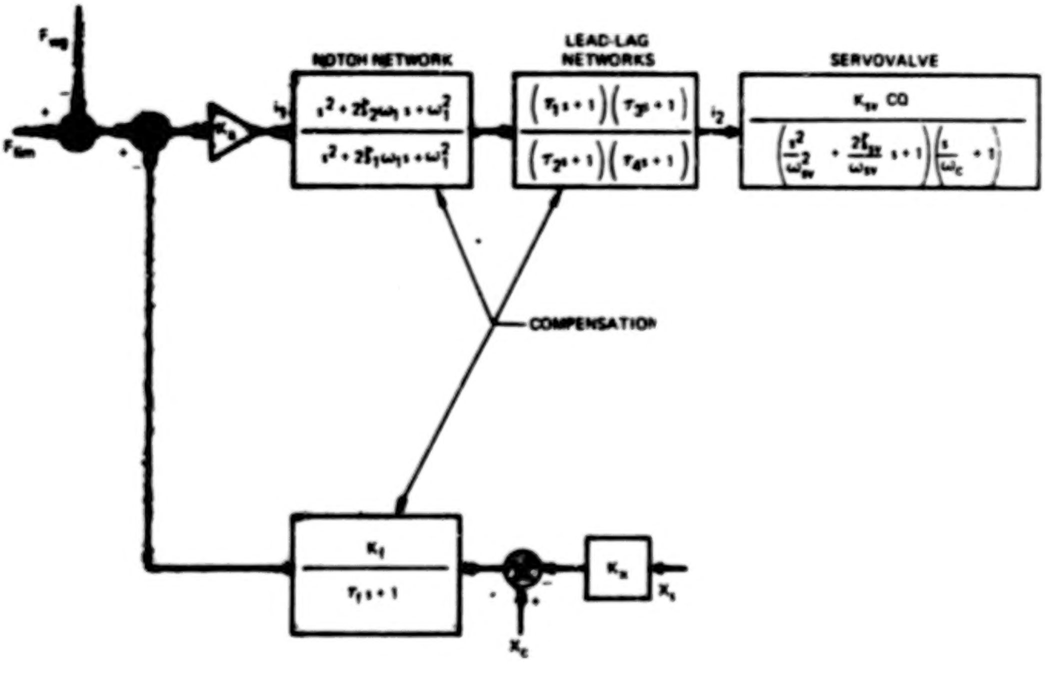
F_{eq}
F_{sim}
K_a
i_1
NOTCH NETWORK
$\frac{s^2 + 2\zeta_2\omega_1 s + \omega_1^2}{s^2 + 2\zeta_1\omega_1 s + \omega_1^2}$
LEAD-LAG NETWORKS
$\frac{(\tau_1 s + 1)(\tau_3 s + 1)}{(\tau_2 s + 1)(\tau_4 s + 1)}$
i_2
SERVOVALVE
$\frac{K_{sv}\ CQ}{\left(\frac{s^2}{\omega_{sv}^2} + \frac{2\zeta_{sv}}{\omega_{sv}} s + 1\right)\left(\frac{s}{\omega_c} + 1\right)}$
COMPENSATION
$\frac{K_f}{\tau_f s + 1}$
K_x
x_s
x_c

Figure B-3. Controller Control Laws

As shown in this figure, the force loop compensation consists of a notch filter with a center frequency of 251.3 rad/sec and two lead-lag networks, 0.0281S + 1/0.0141S + 1 and 0.001S + 1/0.0001S + 1. The position loop, which insures that the strut returns to its static position, incorporates a simple lag network: Kf/0.1S+1.

GAINS AND SCALING-LINEAR

The static gains and scale factors of the controller are shown in Figure B-2. These gains and scale factors were chosen to be compatible with the maximum values of the system parameters and the 10-V maximum of the microprocessor.

The digital scaling is accomplished as follows:

(1) **W/G acceleration ($\ddot{X}_{wg}$)**

$X_{\ddot{w}g}$ = 6 (1.8) V/g · 409.5 bit/V = 4423 bit/g, or 0.000226 g/bit

(2) **W/G velocity ($\ddot{X}_{wg}$)**

$X_{\dot{w}g}$ = 3.937 V/m/sec · 409.5 bit/V = 1612 bit/m/sec (40.95 bit/in/sec)

or 6.203 (10^{-4}) m/sec/bit (0.02442 in/sec/bit)

(3) **Strut displacement (X_s)**

X_s = 0.715 · 39.37 V/m · 409.5 bit/V = 1.153 (10^4) bit/m (292.8 bit/in)

or 8.673 (10^{-5}) m/bit (0.003415 in/bit)

(4) **Strut velocity (V_s)**

V_s = 3.937 V/m/sec · 409.5 bit/V = 1612 bit/m/sec (40.95 bit/in/sec)

or 6.203 (10^{-4}) m/sec/bit (0.02442 in/sec/bit)

(5) **Work potential of the strut (WP)**

$WP = F_{wg} \cdot (X_{s\,max} - X_s) = M\ddot{X}_{wg} (X_{s\,max} - X_s)$

If $\ddot{X}_{wg}$ = 1g and X_s = 0.0254 m (1 in)

$WP = M_g = W$ = 363.3 N · m (3215 in · lb)

In digital terms,

WP = 6 (1.8) V · 409.5 bit/V · 0.715V · 409.5 bit/V

= 1.2949 (10^{-6}) bits

Therefore, the scale factor of WP is:

$$\frac{1.2949\ (10^{6})\ \text{bits}}{363.3\ \text{N} \cdot \text{m}} = 3564\ \text{bit/N} \cdot \text{m; or } 2.806\ (10^{-4})\ \text{N} \cdot \text{m/bit}$$

(402.7 bit/in · lb, or 0.002483 in · lb/bit)

(6) Kinetic energy (KE)

$KE = 1/2 \cdot W/g\,(V_{TOT})^2$ where $V_{TOT} = \dot{X}_{wg\ touchdown} + \int_0^t \dot{X}_{wg}\,\Delta t$

If V = 0.0254 m/sec (1 in/sec)

KE = 0.4706 N · m (4.1645 in · lb)

In digital terms,

$KE = 0.1\ V\ (409.5\ bit/V)^2 = 1676.9\ bits$

Therefore, the scale factor of KE is

1676.9/0.4706 = 3564 bit/N · m, or 2.806 (10^{-4}) N · m/bit

(402.7 bit/in · lb, or 0.002483 in · lb/bit)

Which is the same scale factor as that for WP, and the two terms can be compared directly.

(7) Decrease of limit force command (F_{LI}) during the transition from impact phase to rollout phase:

The scale factor of F_{LI} is 1.324 (10^4)N (2977 lb) for 10 V; and, 10 V corresponds to 4095 digital bits. Therefore, the digital scale factor for F_{LI} is 4095/1.324 (10^4)N; or 0.3094 bit/N (1.376 bit/lb). During transition, F_{LI} is decreased at a rate of 1.379 (10^5) N/sec (31 000 lb/sec), or digitally at 1.379 (10^5) 0.3094 = 42 642 bit/sec.

(8) Transition Velocity:

From Figure 3.2.3 of the system specification:

$$V_T = \frac{F_{LI}^2}{2\,(W/g)\,R}$$

where W = aircraft weight per gear and R is the limit force transition rate.

The scale factor of V_T is determined as follows:

$W/g = 1459\ N \cdot sec^2/m$

Then 1 Newton of F_{LI} produces

$$\frac{(1)^2}{2\,(1459)\,(1.379 \cdot 10^5)} = 2.486\,(10^{-9})\ m/sec\ of\ V_T$$

Digitally, the scale factor for F_{LI} (from the previous section) is 0.3094 bit/N (1.3755 bit/lb) Then, the scale factor for V_T / F_{LI} =

$(0.3094)^2 = 0.0956$ bit/N (1.892 bit/lb) of F_{LI}

Therefore, the scale factor for V_T is:

$$\frac{0.0956}{2.486(10^{-9})} = 3.845\ (10^7)\ \text{bit/m/sec}\ (977\ 000\ \text{bit/in/sec})$$

This scaling must be matched to the scaling of V_{TOT}; that is,

$\int X_{wg} dt + V_s$.

The scaling of $V_{TOT} = \dfrac{0.1V}{0.0254\ \text{m/sec}} \times \dfrac{409.5\ \text{bit}}{V}$

$\doteq$ 1612 bit/m/sec (40.95 bit/in/sec)

To provide this scaling for V_T it must be multiplied by $1612/3.845\ (10^7)$ = 0.00004191 using the arithmetic board. This is accomplished as follows:

0.00004191 DECIMAL (D) =

.00000000000000101011111100100010000101 BINARY (B)

or $1.01011111100100010000101 \times 2^{-15}$ (B)

The exponent is -15 (D)

The bias in the arithmetic board is

07F HEXIDECIMAL (H) or 127 (D)

Therefore, the number must be applied to the arithmetic board with a bias of 127-15 = 112 (D). In addition, a factor must be applied due to the fact that the numbers from the A/D converter are stored in the most significant 12 bits out of 16 so that the number for V_{TOT} is a factor of 16 too high. The transition velocity (V_T) is a function of $F_{LI}{}^2$, and is a factor of $(16)^2$ too high. The net result is that the number for V_T is too high by a factor of 16. It must therefore be reduced by a factor of 16 or 2^4.

Therefore, the exponent of the applied number is 112-4 or 108 (D) = 6C (H) = 01101100 (B).

A sign bit ("0" for positive) must precede the exponent. The format of the applied number, is:

$$\underbrace{\overbrace{0}^{\text{Sign}}\overbrace{0110110}^{\text{Exp.}}}_{M+3}\overbrace{\underbrace{00101111}_{M+2}\underbrace{11001000}_{M+1}\underbrace{10000101}_{M}}^{\text{Fraction}}$$

Therefore, if this number starts at location M, the contents of memory are:

M	85(H)
M+1	C8(H)
M+2	2F(H)
M+3	36(H)

LINEAR CIRCUIT DESCRIPTION

The linear circuit is shown in HR drawing 88000080-201. Power for the linear components is obtained from two auxiliary power supplies which provide +15 Vdc and -15 Vdc. The signal from the wing/gear accelerometer is applied to a differential pair of amplifiers, U22 and U23. This approach was taken in order to minimize the noise on the low-level signal. The output of the differential pair is applied to U4 and the output of U4 is biased by potentiometer R6 to provide a 1-g offset level. The biased signal is applied to U3 and then to U5 which has a gain of 6 and the output of which is the wing/gear interface force which is applied to the microprocessor. The acceleration signal is available at J13 on the front panel.

The acceleration signal from U3 is also applied through potentiometer R2 to integrator U2, the output of which is the wing/gear velocity signal and is applied to the microprocessor. R2 provides a means of adjusting the integrator gain. The integrator is enabled by analog switch U1A which removes the short circuit across the capacitor upon receiving an enable signal from the microprocessor. The wing/gear velocity signal is available at J12 on the front panel. Switch S7 is provided on the front panel in order to allow a simulated wing/gear signal to be applied to the microprocessor for test purposes. The simulated test signal is applied to J25 on the front panel.

The commanded limit force is algebraically summed with the wing/gear force by means of R22 and R23 to produce the force error which is then amplified by U6 and U7. The limit force command signal is available at J15 on the front panel. Switch 5 allows a simulated limit force command signal (applied at J23 on the front panel) to be used for test purposes. R15, in the feedback path of U7, allows the forward loop gain of the system to be adjusted as required.

The output of U7 is applied to the notch network (bridged T) which is composed of R16, R17, C2 and C3, and the output of which is applied to U8. The output of U8 is applied to U9, which provides one of the lead-lag functions, and then through U10 to U11, which provides the other lead-lag function, and the output of which is applied to U12. The signal from U12 passes through one path of dual analog switch U1 and then to U14, the output of which is the servovalve command signal, and is applied to the servovalve controller. This signal is available at J19. U1 closes the forward loop path upon receipt of an enable signal from the microprocessor. R31 on the front panel provides a means of biasing the servovalve.

The strut position is set by R41 on the front panel. The signal from this potentiometer passes through U17 and U16 (when the servoloop is enabled) and is algebraically summed, at U15, with the signal from the strut potentiometer, after it has passed through U19 and U18. The output of U15 is the strut position loop error. It passes through U21 and is applied to the force loop at U6. The strut position command signal is available at TP1, the strut position signal is available at J18 and the strut position error signal is available at J17, all on the front panel. The controller is enabled and reset by means of switches on the front panel which are provided for this purpose. In addition, the strut hydraulic pressure signal and pneumatic pressure signal are available at J21 and J22 respectively on the front panel.

The signals for the controller are applied at the rear of the unit. These are:

J2 - 28 Vdc
J4 - W/G acceleration
J5 - Hub acceleration
J6 - Strut position
J7 - Strut pneumatic pressure
J8 - Strut hydraulic pressure
J9 - Servovalve command

In order to set and maintain the initial hydraulic pressure in the gear an auxiliary pressure loop is used prior to enabling of the servoloop. To accomplish this, the pressure signal is amplified by amplifiers U24, U25, U28, U30 and U32, the output of which is added to the servoloop command signal through switch U33. When the servoloop is disabled, the switch is closed and allows the pressure signal to close the loop. The pressure is then controlled by a servovalve bias signal. When the servoloop is enabled the switch is opened and the pressure is free to vary in response to the loop command signal.

DIGITAL SOFTWARE

The digital software program is listed in Appendix B. Appended to this listing are routines for testing the arithmetic board and A/D board.

The program is in the C. P. U. twice; that is, the C. P. U. contains two PROM's, each containing the entire program. One PROM is at location 0000 and is the one normally used. No special procedures are required to use it. When power is applied the computer starts at this location, and once the Controller Enable signal is received it assumes control of the process.

The second PROM is intended for test and program changes if required. It is located at address 0800 in program memory but is programmed to start at address 3D10 in RAM. To use it, the first PROM must be replaced by the monitor ROM (at 0000) and then the program can be controlled by a standard teletypewriter connected to the proper socket on the rear of the CPU board. The contents of locations 0800 to 09F9 are moved to new locations starting at 3D10 with a teletype input: M0800, 09F9, 3D10 RETURN. Then, any input desired can be applied to the computer by means of the teletype -- for testing or for program changes. To operate in this mode an input is required -- G3D10 RETURN -- before any test.

If permanent program changes are required the PROM must be "burned" to contain the new program..

Appendix C

TEST PROCEDURE

GEAR CHARGING PROCEDURE

(1) With the gear vertical, and the dead weight of the beam as a static load, bleed any accumulated gas from the hydraulic port of the gear until hydraulic fluid escapes from the port.

(2) Bleed gas or hydraulic fluid from the pneumatic charge port of the gear until the gear is fully compressed.

(3) Recheck the hydraulic port for any additional accumulated gas.

(4) If hydraulic fluid does not emerge from both gear ports in the fully compressed condition then fluid must be added. One method of accomplishing this is as follows:

(a) Turn on the controller 28-Vdc supply and electronics.

(b) Press the controller "RESET" button. This applies a positive bias command (pressure bias) to the servovalve.

(c) Turn on the gear hydraulic supply pump. Momentarily raise the pressure by means of the main relief valve to approximately 4140 kPa (600 lb/in^2), and then reduce this pressure to about 690 kPa (100 lb/in^2).

(d) Slowly open the gear isolation valve (see Figure C-1). This should apply hydraulic pressure to the gear and bleed gas at both the hydraulic and pneumatic ports of the gear until hydraulic fluid escapes from both.

(e) Close the gear isolation valve.

(f) Turn off the gear hydraulic supply pump.

(g) If the gear has extended during this procedure repeat steps 1, 2 and 3.

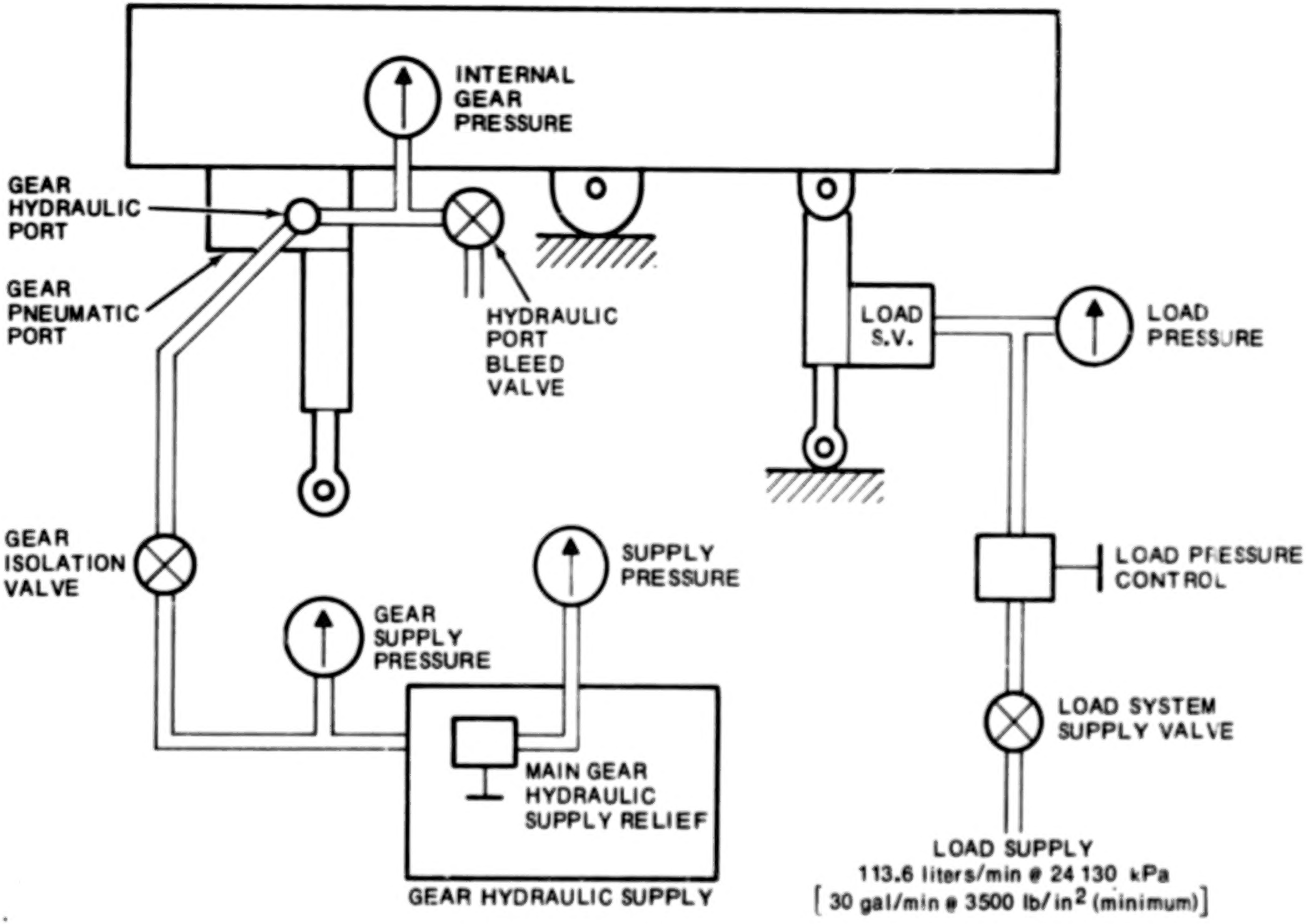
INTERNAL GEAR PRESSURE
GEAR HYDRAULIC PORT
GEAR PNEUMATIC PORT
HYDRAULIC PORT BLEED VALVE
LOAD S.V.
LOAD PRESSURE
GEAR ISOLATION VALVE
SUPPLY PRESSURE
GEAR SUPPLY PRESSURE
LOAD PRESSURE CONTROL
LOAD SYSTEM SUPPLY VALVE
MAIN GEAR HYDRAULIC SUPPLY RELIEF
GEAR HYDRAULIC SUPPLY
LOAD SUPPLY
113.6 liters/min @ 24 130 kPa
[30 gal/min @ 3500 lb/in2 (minimum)]

Figure C-1. - Gear Charging Schematic

(5) Connect a nitrogen charging system to the pneumatic charge port and apply the desired pre-charge pressure.

NOTE: The gear has a working pressure rating of 3450 kPa (500 lb/in^2). Therefore, caution should be exercised to avoid exceeding the proof pressure of 5170 kPa (750 lb/in^2).

(6) Until the strut is fully extended and is stabilized at the desired charge pressure, slowly lift the upper gear using the load system.

(7) Close the pneumatic charge port and remove the charging system.

PASSIVE GEAR TEST PROCEDURE

(1) Turn on the load system electronics and allow 30 minutes for warm-up.

(2) Turn on the load hydraulic supply system. Be sure minimum capacities are 114 liter/min (30 gal/min) and 2.413(10^4) kPa (3500 lb/in^2).

(3) Move the mode switch on the load controller to "POSITION".

(4) Open the load system supply valve and slowly raise the load system pressure to 1.45 (10^4) kPa (2100 lb/in^2). If the position command potentiometer has been preset to maximum drop height, the beam will move to its retract stop, thereby raising the gear.

(5) If the position command potentiometer has not been pre-set, then slowly adjust it to position the beam against the retract stop and check to see if the gear charge pressure is at the desired value.

(6) Set the recorder to monitor the required parameters and set the channel gains.

(7) Momentarily move the reset/operate switch on the load controller to "RESET" and then return it to "OPERATE".

(8) Raise the load system pressure to 2.069 (10^4) kPa (3000 lb/in^2).

(9) Start the recorder and move the mode switch to "VELOCITY/ LOAD" to drop the gear.

(10) After the drop, reduce the load system pressure to 2100 lb/in^2 and move the mode switch to "POSITION".

(11) For further testing repeat steps 6 through 9.

(12) When testing is concluded, reduce the load system pressure to minimum and close the load system supply valve.

ACTIVE GEAR TEST PROCEDURE

(1) Turn on all load system, controller, and servovalve controller electronics. Allow 30 minutes for warm-up.

(2) Follow the procedures of steps 2 through 7 of "Passive Gear Test Procedure".

(3) Place the gear controller in the "RESET" state.

(4) With the gear isolation valve closed, turn on the gear hydraulic supply pump and adjust its main relief valve to provide 6895 kPa (1000 lb/in^2) as read on the supply pressure gage.

(5) Adjust the "BIAS" control on the servovalve controller to produce approximately the same gear supply pressure as the gear charge pressure.

(6) Slowly open the gear isolation valve while observing the pressure in the gear. The gear internal pressure must not fall more than 345 kPa (50 lb/in^2) below its pre-set charge pressure. Otherwise, the gas may be forced into the hydraulic side of the gear and necessitate recharging in accordance with the first section, "Gear Charging Procedure".

(7) Readjust the "BIAS" control on the servovalve controller to obtain the desired gear internal charge pressure, as read by the gear hydraulic pressure transducer.

(8) Confirm that the "S. V. CMD. BIAS" control on the gear controller is set to the proper value for the gear charge pressure.

(9) Set the sink speed value by means of the "SINK SPEED" control.

(10) Set the load "VELOCITY" command potentiometer for the desired sink speed.

(11) Momentarily move the reset operate switch on the load controller to "RESET" and then return it to "OPERATE".

(12) Raise the gear supply pressure to 2.069 (10^4) kPa (3000 lb/in^2) and recheck the gear internal pressure. If necessary, readjust the servovalve controller "BIAS" control for the desired gear pressure.

NOTE: To prevent overheating do not operate the gear hydraulic supply at 2.069 (10^4) kPa (3000 lb/in^2) until immediately prior to the drop.

(13) Raise the load system pressure to 2.069 kPa (3000 lb/in^2).

(14) Start the recorder and move the load mode switch to "VELOCITY LOAD" to drop the gear.

(15) After the drop, reduce the gear supply pressure to 6900 kPa (1000 lb/in^2).

(16) Reduce the load system pressure to 1.45 (10^4) kPa (2100 lb/in^2).

(17) Close the gear isolation valve.

(18) Raise the gear by moving the mode switch on the load controller to "POSITION".

(19) Return the gear controller to the "RESET" mode.

(20) Slowly open the gear isolation valve. The gear internal pressure should return to the pre-set charge value. For further testing repeat steps 9 through 19. Otherwise proceed to step 21.

(21) Reduce the load pressure slowly to minimum allowing the gear to settle gently, and close the load system supply valve.

(22) Turn off all electronics except the recorder. Wait about two minutes (to allow capacitors to discharge) and run a short record for channel zero references.

Appendix D

OSCILLOGRAPH RECORDINGS

Key to Recordings

Channel	Parameter	Sensitivity	Zero Position (with respect to reference line)
1	W/G Velocity	0.25 m/sec/cm (0.25 in/sec/in)	16.76 cm (6.6 in)
2	Net Force (Accelerometer #1)	2224 N/cm (1270 lb/in)	7.62 cm (3.0 in)
3	Servovalve Spool Pos.	0.05 cm/cm (0.05 in/in)	15.24 cm (6.0 in)
4	Limit Force Command	876 N/cm (500 lb/in)	2.54 cm (1.01 in)
5	Net Force (filtered (Accelerometer #2)	2224 N/cm (1270 lb/in)	10.19 cm (4.01 in)
6	Strut Position	0.0127 m/in (1.27 in/in)	19.71 cm (7.76 in)
7	Servovalve Command	1.97 ma/cm (5 ma/in)	9.17 cm (3.61 in)
8	Gear Hydraulic Pressure	277 kPa/cm (102 lb/in^{2}in)	19.81 cm (7.8 in)
9	Gear Pneumatic Pressure	277 kPa/cm (102 lb/in^2/in)	19.30 cm (7.6 in)
10	Lift Force Command	1.97 V/cm (5 V/in)	18.26 cm (7.19 in)
11	Lift Simulator Position	0.05 m/cm (5 in/in)	12.70 cm (5.0 in)
12	Lift Force	8756 N/cm (5000 lb/in)	17.78 cm (7.0 in)

Reference Line

HR RUN 712-9 1048 kPa (152 lb/in^2), 0.305 m/sec (1 ft/sec), Passive

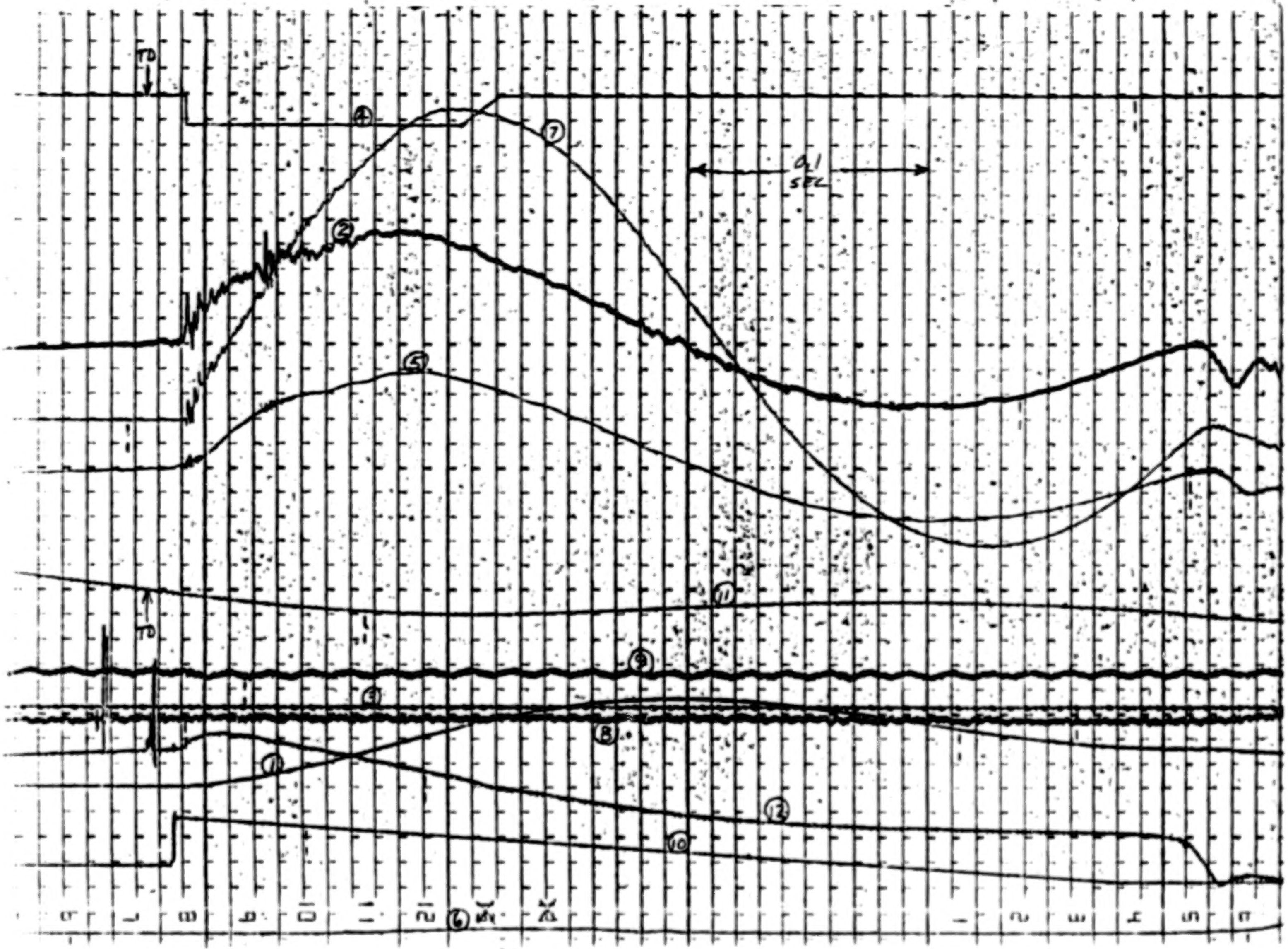

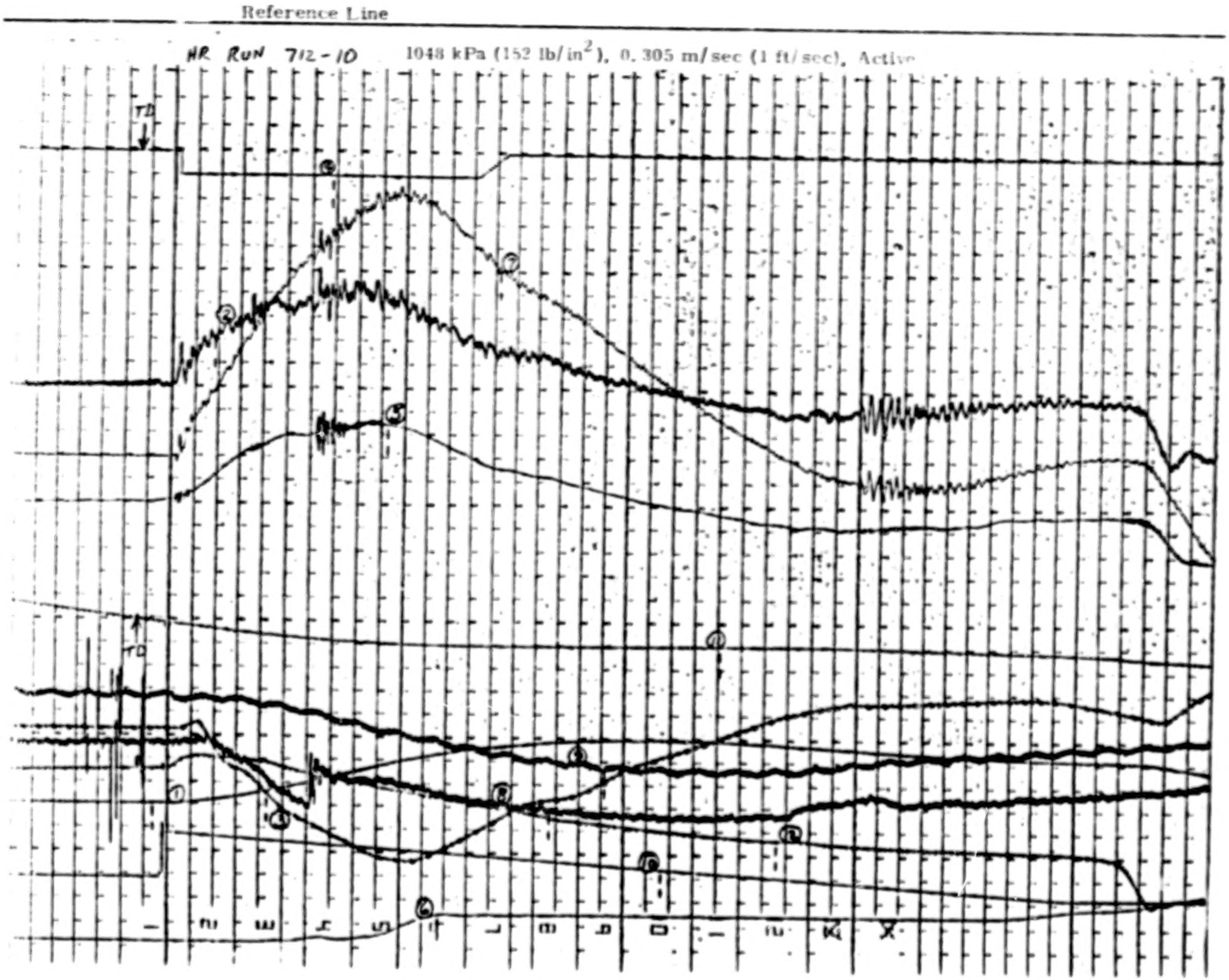

1048 kPa (152 lb/in^2), 0.305 m/sec (1 ft/sec), Active

Reference Line

HR RUN 712-1 , 1048 kPa (152 lb/in^2), 0.914 m/sec (3 ft/sec), Passive

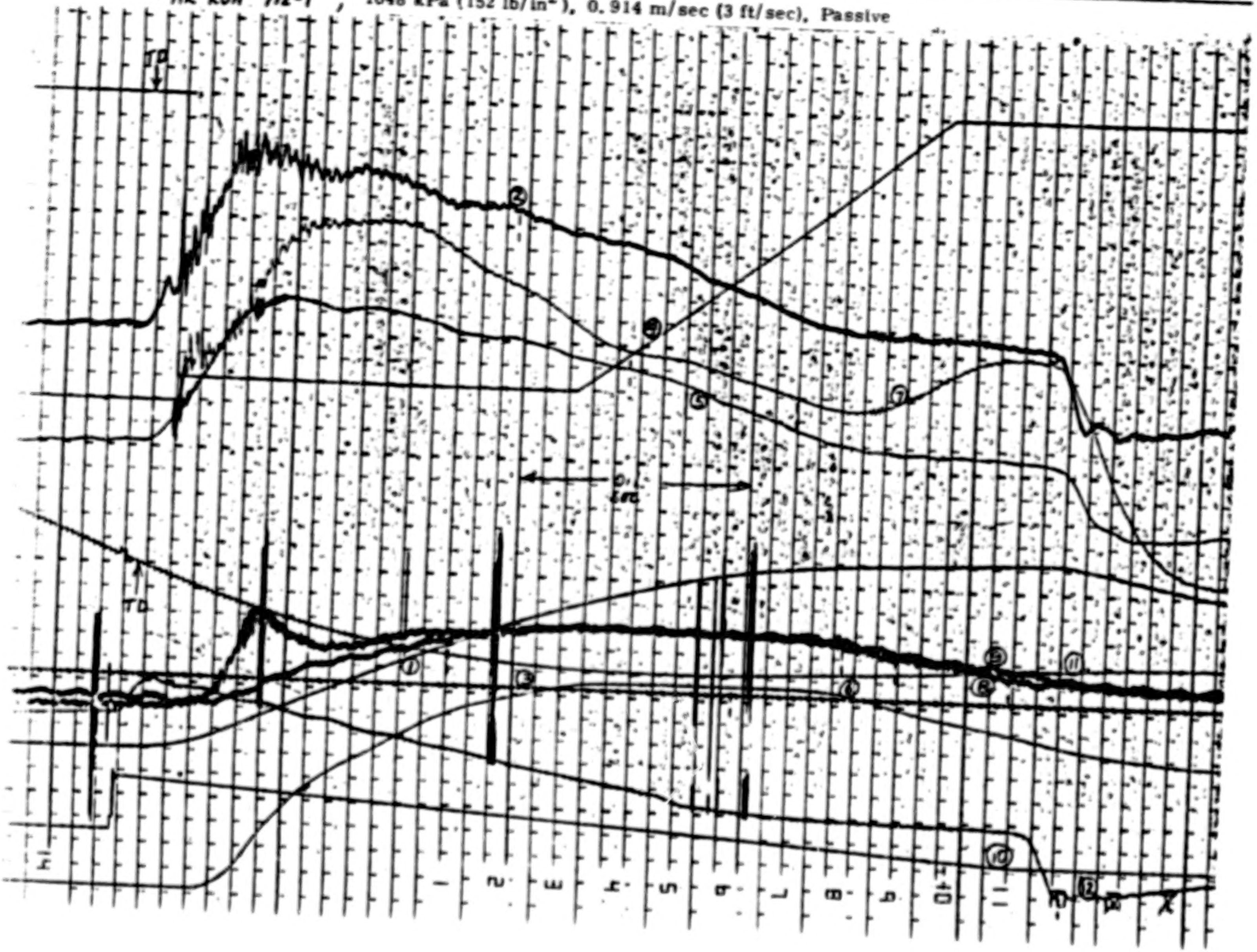

MICROFILMED FROM
BEST AVAILABLE COPY

Reference Line

HR RUN 7/2-2 1048 kPa (152 lb/in^2), 0.914 m/sec (3 ft/sec), Active

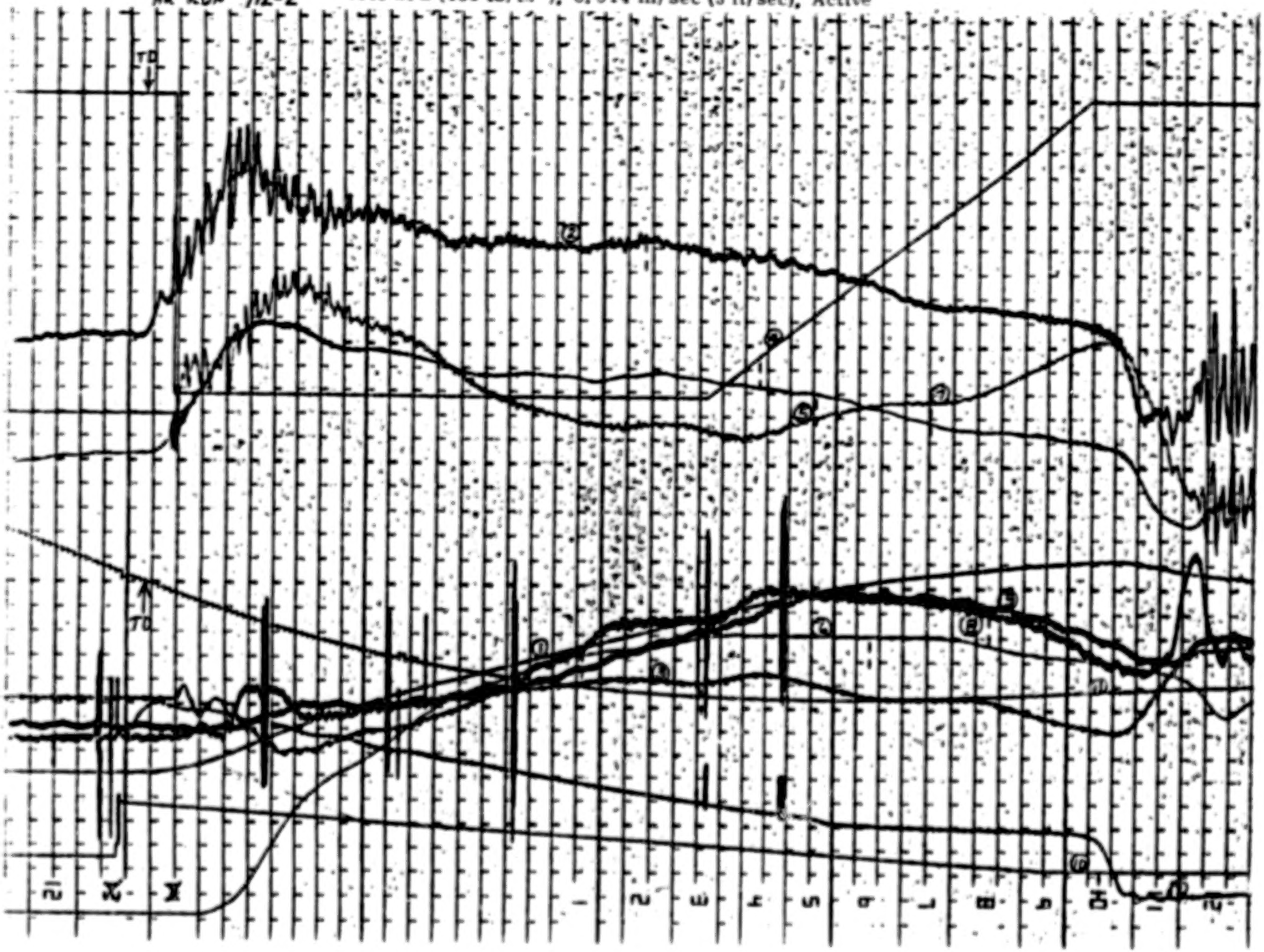

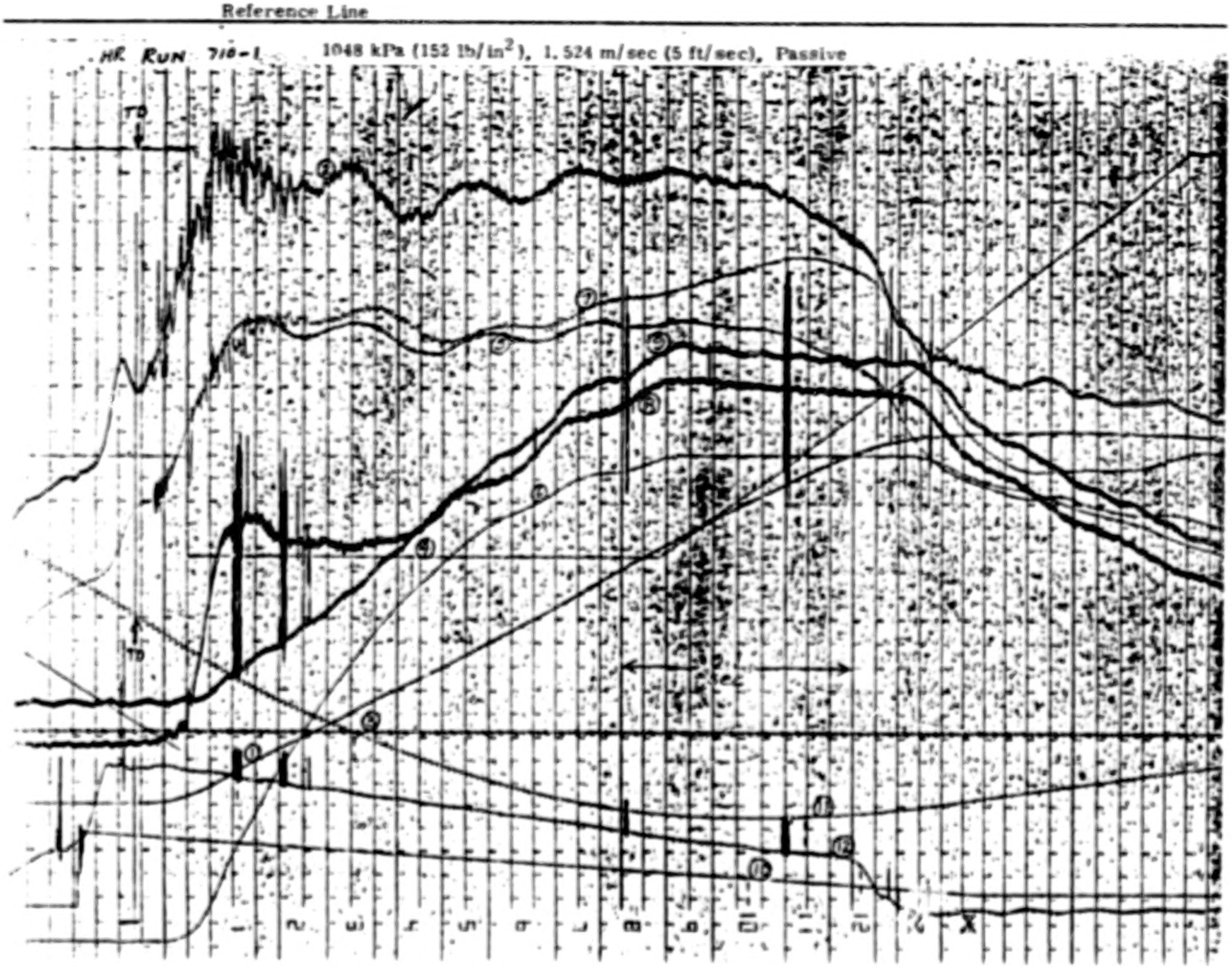

HR RUN 710-1 1048 kPa (152 lb/in^2), 1.524 m/sec (5 ft/sec), Passive

MICROFILMED FROM
BEST AVAILABLE COPY

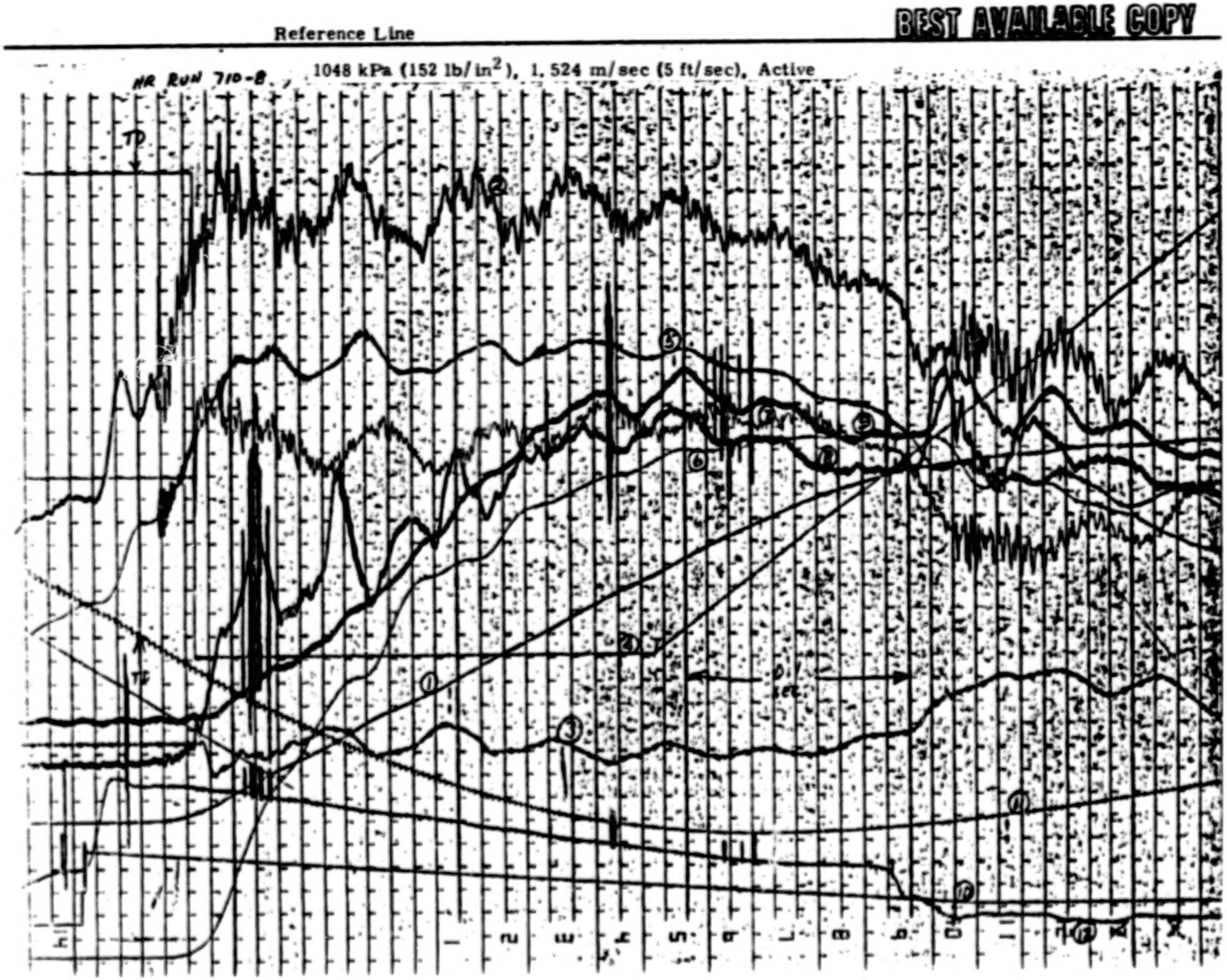

HR RUN 710-8, 1048 kPa (152 lb/in^2), 1,524 m/sec (5 ft/sec), Active

Reference Line

HR RUN 713-1   1930 kPa (280 lb/in^2), 0.305 m/sec (1 ft/sec), Passive

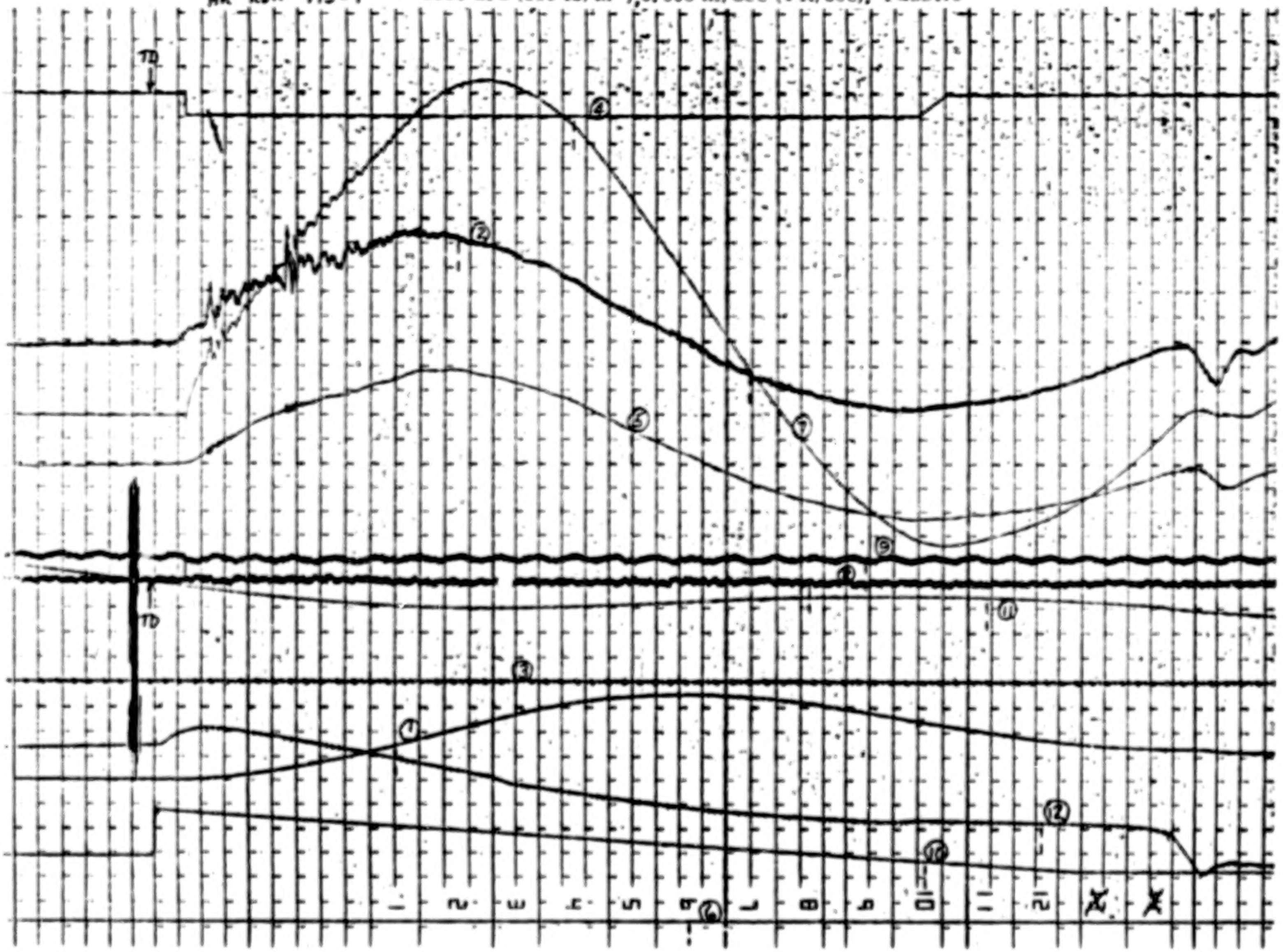

1930 kPa (280 lb/in²), 0.305 m/sec (1 ft/sec), Active

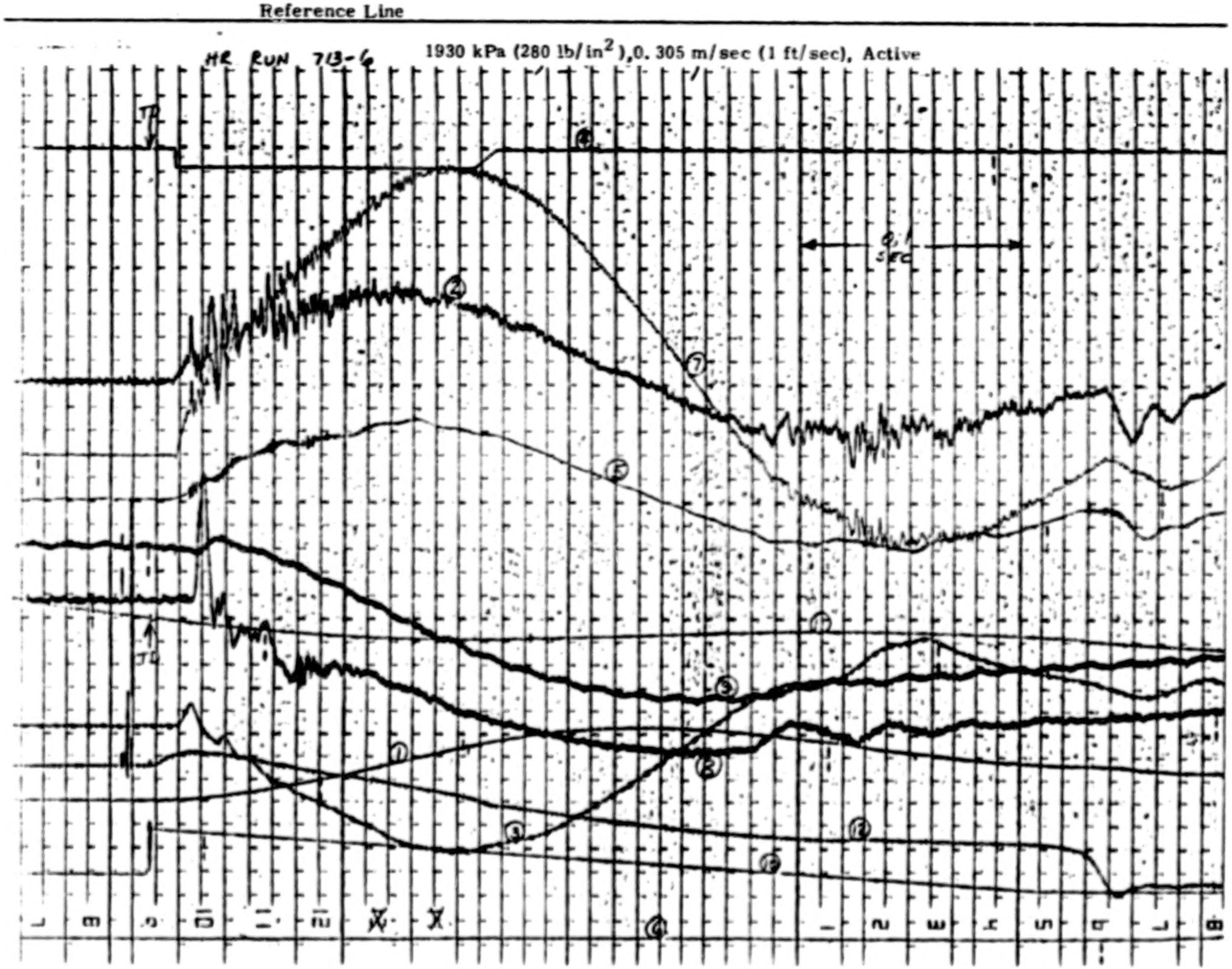

HR RUN 714-2

1930 kPa (280 lb/in^2), 0.914 m/sec (3 ft/sec), Passive

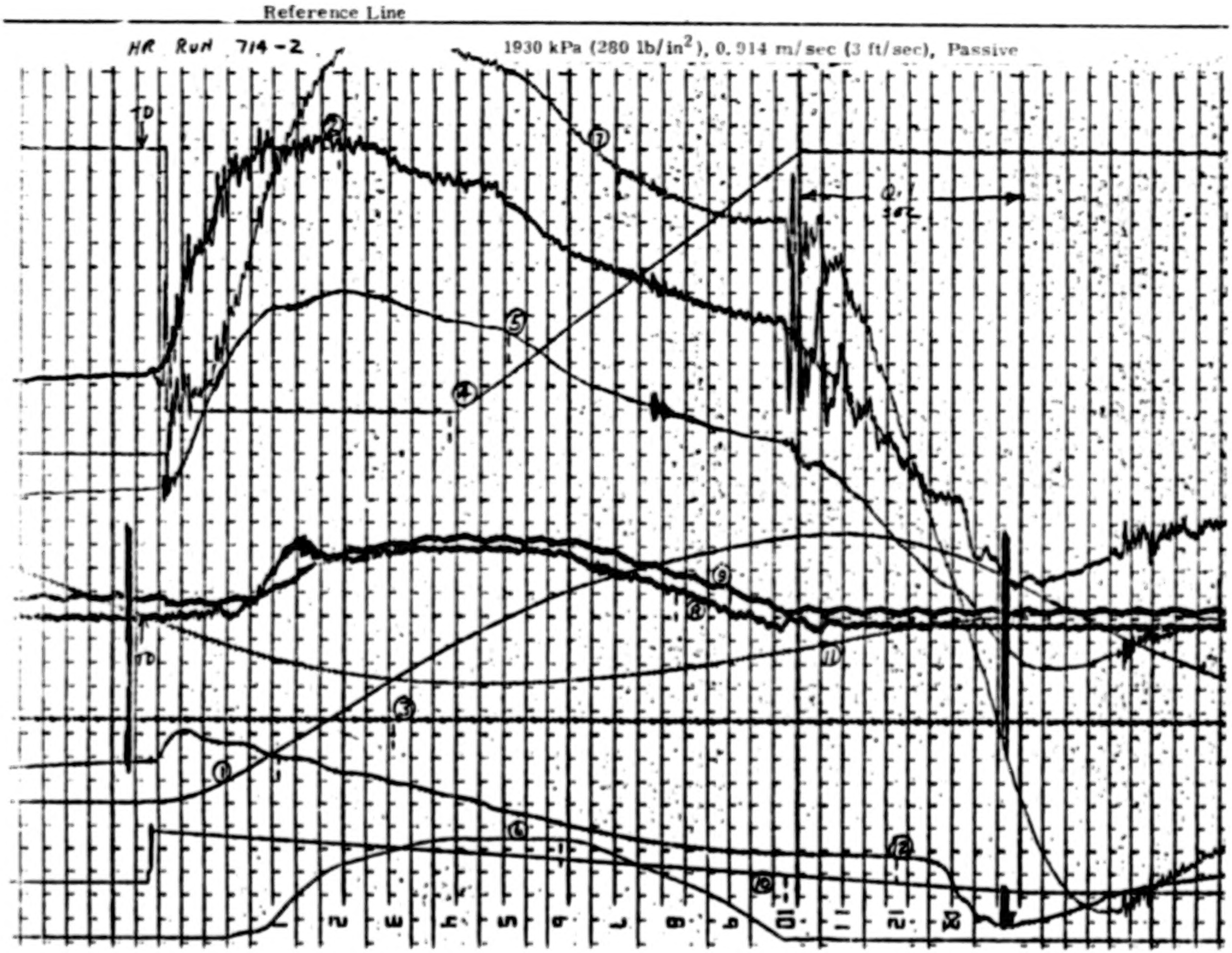

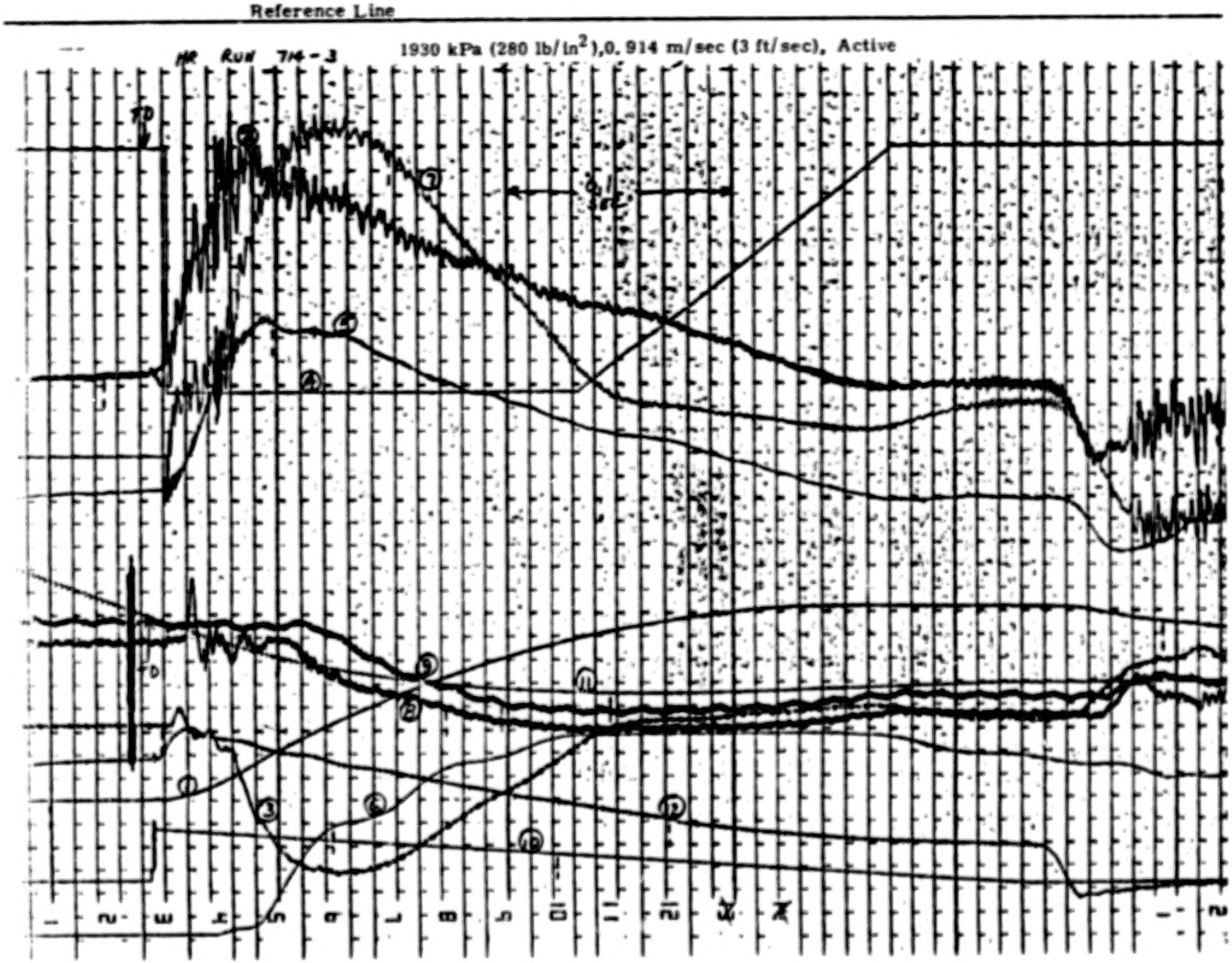

1930 kPa (280 lb/in²), 0.914 m/sec (3 ft/sec), Active

Reference Line

HR RUN 714-6, 1930 kPa (280 lb/in²), 1.524 m/sec (5 ft/sec), Passive

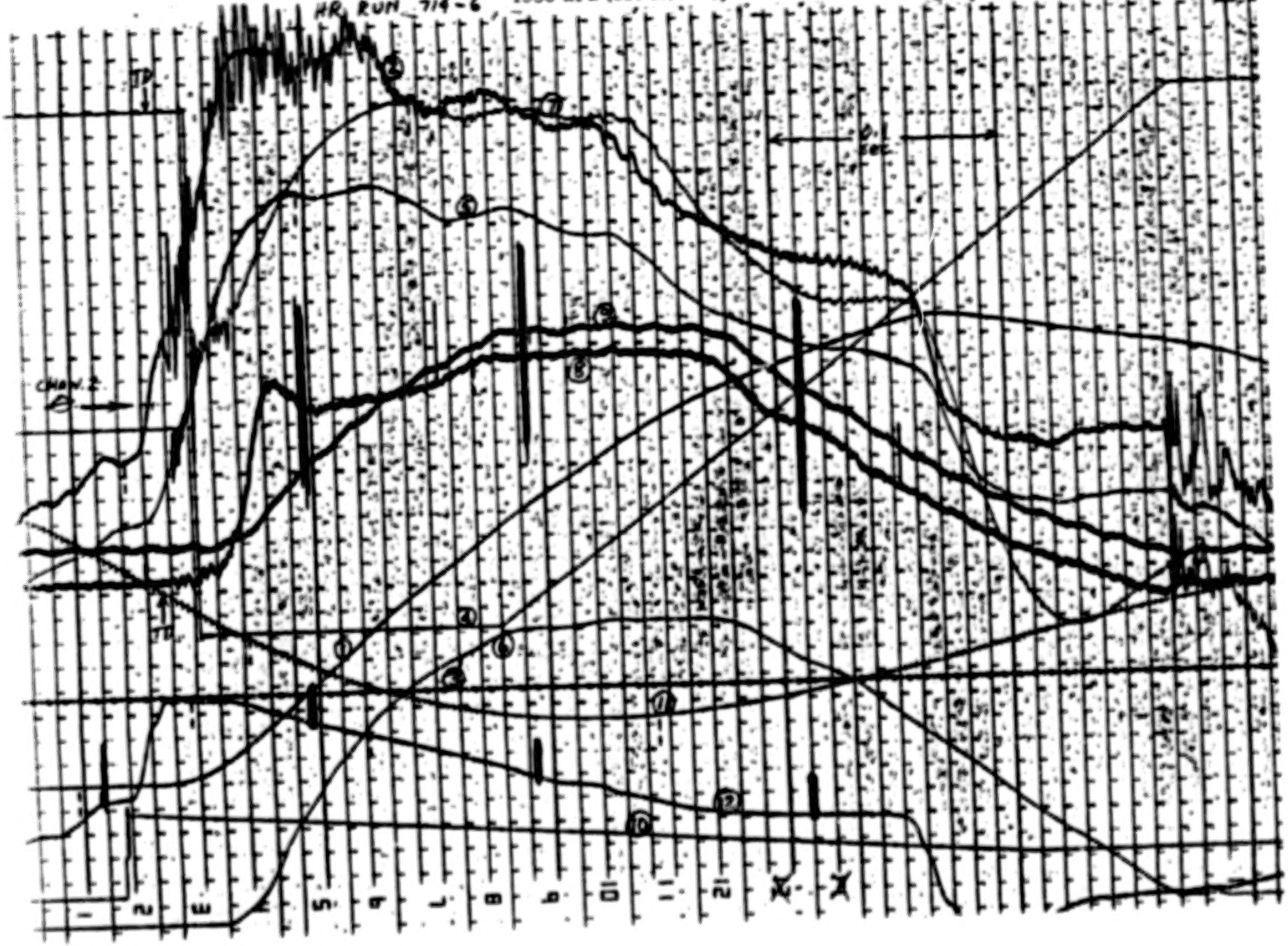

157

MICROFILMED FROM
BEST AVAILABLE COPY

Reference Line

HR Run 7M-8 1930 kPa (280 lb/in^2), 1.524 m/sec (5 ft/sec), Active

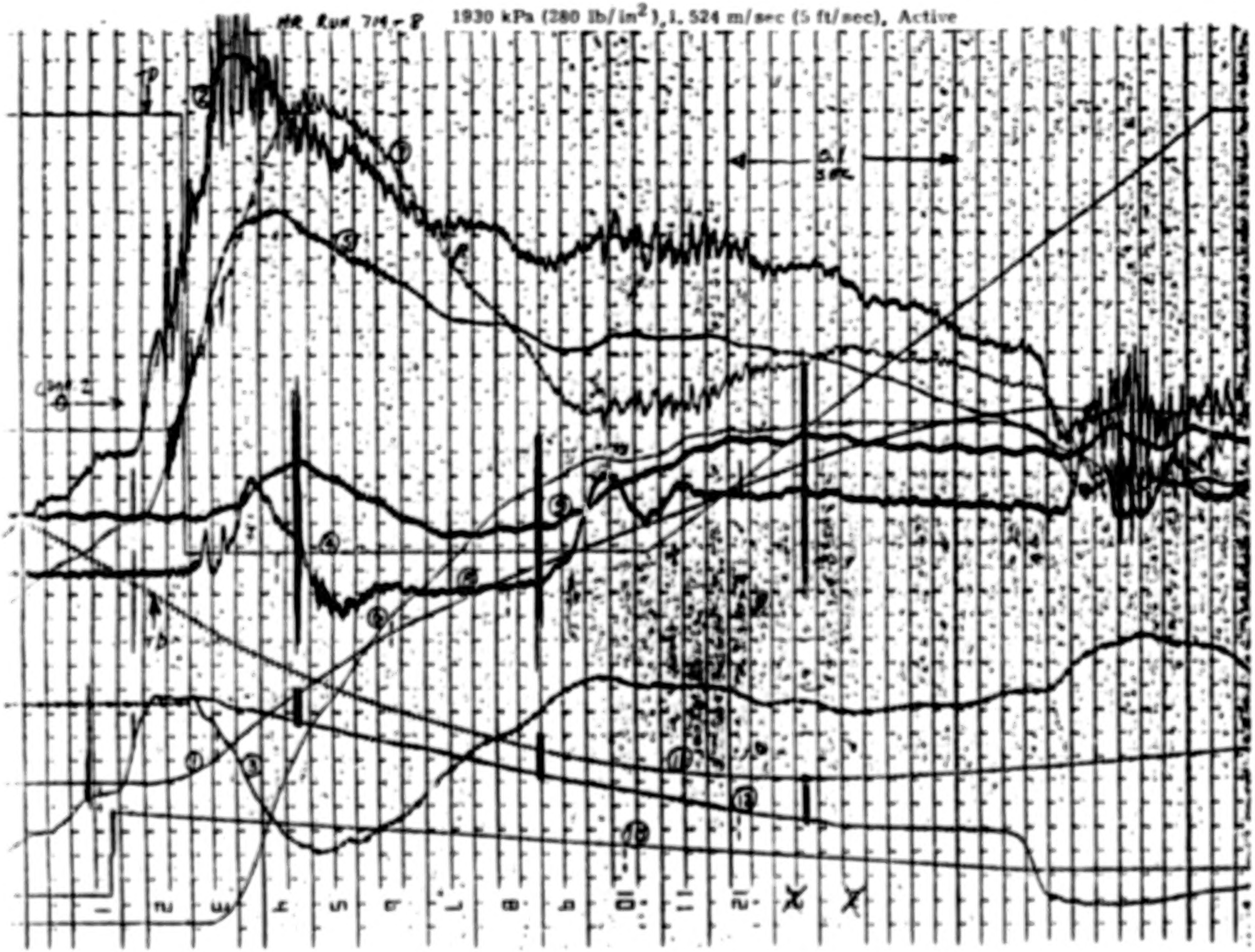

REFERENCES

1. McGehee, John R.; and Carden, Huey D.: A Mathematical Model of an Active Control Landing Gear for Load Control During Impact and Roll-Out. NASA TN D-8080, 1976.

2. Fasanella, Edwin L.; McGehee, John R.; and Pappas, M. Susan.: Experimental and Analytical Determination of Characteristics Affecting Light Aircraft Landing-Gear Dynamics. NASA TM X-3561, 1977.

1. Report No. NASA CR-3113	2. Government Accession No.	3. Recipient's Catalog No.

4. Title and Subtitle An Electronic Control for an Electrohydraulic Active Control Aircraft Landing Gear	5. Report Date April 1979 6. Performing Organization Code
7. Author(s) Irving Ross and Ralph Edson	8. Performing Organization Report No.
	10. Work Unit No.
9. Performing Organization Name and Address Hydraulic Research Textron Valencia, California 91355	11. Contract or Grant No. NAS1-14459
12. Sponsoring Agency Name and Address National Aeronautics and Space Administration Washington, DC 20546	13. Type of Report and Period Covered Contractor Report 14. Sponsoring Agency Code

15. Supplementary Notes

Langley technical monitor: John R. McGehee
Final Report

16. Abstract

Hydraulic Research, under NASA Contract NAS1-14459, has developed, designed, fabricated and tested an electronic controller for an electro-hydraulic active control aircraft landing gear. Drop tests of a modified gear from a 2722 kg (6000 lbm) class of airplane were conducted to illustrate controller performance. The results of this effort indicate that the active gear effects a force reduction, relative to that of the passive gear, from 9 to 31 percent depending on the aircraft sink speed and the static gear pressure.

17. Key Words (Suggested by Author(s)) Aircraft landing gear Electronic controls Active controls Landing loads	18. Distribution Statement Unclassified-Unlimited Subject Category 05

19. Security Classif. (of this report) UNCLASSIFIED	20. Security Classif. (of this page) UNCLASSIFIED	21. No. of Pages 167	22. Price* $8.00

* For sale by the National Technical Information Service, Springfield, Virginia 22161

167

END

June 12, 1981